Partitioning biotic and abiotic components of soil CO_2 fluxes using subsurface CO_2 dynamics and stable carbon isotopes, Taylor Valley, Antarctica

---

A thesis

submitted in partial fulfilment

of the requirements for the Degree of

Doctor of Philosophy

at

Lincoln University

by

Fiona L. Shanhun

Lincoln University

2013

Abstract of a thesis submitted in partial fulfilment of the requirements for the Degree of Doctor of Philosophy

Partitioning biotic and abiotic components of soil CO_2 fluxes using subsurface CO_2 dynamics and stable carbon isotopes, Taylor Valley, Antarctica

by

Fiona L. Shanhun

To date, surface CO_2 fluxes in soils of the McMurdo Dry Valleys in Antarctica have been assumed to represent heterotrophic respiration. Important aspects of soil ecosystem function have been inferred on the basis of this assumption.

This study used high-resolution measurements of CO_2 concentration, and, for the first time, the stable C isotopic composition of surface CO_2 fluxes and subsurface CO_2 profiles to: 1) link surface and subsurface CO_2 dynamics, 2) test whether abiotic mechanisms of CO_2 production and consumption can explain diel variability in surface CO_2 flux rates, and 3) partition biotic and abiotic components of surface CO_2 fluxes at two sites with contrasting organic C levels in soils of Taylor Valley.

In the 2008/09 austral summer, surface CO_2 flux rates and subsurface CO_2 concentration and $\delta^{13}C_{CO2}$ profiles were measured at the warmest and coolest times of the day at two sites with contrasting soil organic C contents. Site A, located near a small lake, can be considered a "biological hotspot", with the lake providing a contemporary organic C source via algal growth and subsequent wind-dispersal onto nearby soils. Site B had no contemporary lacustrine-derived organic C supply, and soil organic C levels were typical of the low levels in Dry Valley soils. A physical model, describing the temperature-driven dissolution and exsolution of CO_2 according to Henry's Law, and incorporating empirical data from field measurements of soil moisture content, pH, and temperature changes, showed that an abiotic mechanism of CO_2 uptake and release could explain changes in subsoil CO_2 concentrations. However, the twice-daily sampling regime did not resolve diel changes or rates of change in surface CO_2 fluxes and subsurface CO_2 concentration and $\delta^{13}C_{CO2}$ profiles.

During the 2009/10 austral summer, a 48-h time-series of surface CO_2 fluxes and subsurface CO_2 concentration and $\delta^{13}C_{CO2}$ profiles were measured simultaneously at Sites A and B, at 4-hourly intervals. The increased sampling resolution revealed dynamic changes in subsurface soil CO_2

concentration and $\delta^{13}C_{CO2}$ profiles as soil temperatures varied throughout the diel cycle. At Site B, highly depleted surface CO_2 fluxes were explained by dynamic fractionation effects, and could not be attributed to biological respiration. Short-lived (4 h) periods of steady-state efflux and influx showed CO_2 production (exsolution) and consumption (dissolution) of relatively enriched (−5.2‰) and depleted CO_2 (−11.4‰), respectively. This is consistent with the kinetic fractionation expected as a result of preferential exsolution of $^{13}CO_2$ and dissolution of $^{12}CO_2$.

At Site A, static chambers were unreliable for determining surface CO_2 flux rates. Nonetheless, variation in subsurface CO_2 concentration and $\delta^{13}C_{CO2}$ profiles was consistent with heterotrophic respiration dominating soil CO_2 production. Unexpectedly, the highest rates of CO_2 production occurred during cooler periods of the day, possibly as a result of cooling-induced condensation providing biota with water sufficient to stimulate their activity.

An abiotic contribution to Dry Valley soil CO_2 fluxes must be considered in future studies of Dry Valley ecosystem activity and C cycling. Measures of surface CO_2 flux at single points in time do not necessarily capture a solely biological signal.

Keywords: McMurdo Dry Valleys, soil respiration, Antarctic soils, organic C, dynamic fractionation, CO_2 fluxes.

Glossary of terms

$\delta^{13}C$	^{13}C isotopic composition
$\delta^{13}C_{CO2}$	^{13}C isotopic composition of CO_2 (this can be soil CO_2, or CO_2 sampled from a headspace chamber)
$\delta^{13}C_{\Delta CO2}$	^{13}C isotopic composition of the net surface CO_2 flux
$\Delta T/\Delta t$	rate of change in soil temperature
C_T	total dissolved CO_2
D_e	effective diffusivity of CO_2 in soil
Site A	representative of a “biological hotspot”; has a contemporary source of organic C
Site B	representative of “typical” Dry Valley soils; has no contemporary organic C source

Acknowledgements

It has been a great privilege to work in the Dry Valleys of Victoria Land: the magic and unpredictability of Antarctica always makes for challenging, memorable and rewarding experiences. Many individuals have helped ensure the success of the field work, and others have provided excellent advice during the laboratory and write-up phases of this work.

Firstly, I thank my supervisor Tim Clough for his critical evaluation and thought-provoking feedback. It is unfortunate that Tim was not able to visit the field area, and I hope that one day that may be possible as part of another project. Thanks also to my associate supervisor, Carol Smith, who was always enthusiastic about the research, and contributed to the successful field season in 2008/09, not only in terms of research, but also with her sense of humour and camp culinary skills. Peter Almond is thanked for his invaluable feedback, and for guiding me through the mathematically-demanding aspects of this study. Peter also contributed to all aspects of the field work in both 2008/09 and 2009/10. His commitment to carrying gear and taking gas samples at unearthly hours was outstanding, and his efforts also extended to the creation of "polygon scones" and legendary lamb roasts. My supervisors must collectively be thanked greatly for their encouragement and suggestions, and for patiently understanding my need to return to Antarctica during the summer of 2011/12 to work on a different research project investigating factors controlling biodiversity in the Prince Charles Mountains, Mac. Robertson Land.

Jim Bockheim's knowledge of Taylor Valley and soils of the Transantarctic Mountains, as well as his enthusiasm and assistance, was greatly appreciated in the 2008/09 field season. André Eger and Vicky Nall provided outstanding field assistance in the 2009/10 summer – assisting with gas sampling at all hours, and always ensuring a healthy mix of melodies were transmitted during the "Drive Time" radio shows. All of the field work and associated logistics was made possible by the excellent logistical support provided by Antarctica New Zealand. Shulamit Gordon, Paul Woodgate, Simon Trotter, Rod Strachan, and the Scott Base summer staff of 2008/09 and 2009/10 are particularly thanked for their role in ensuring all logistical aspects of the project ran smoothly. Thanks also to Rob McPhail and his mechanics for our safe and enjoyable flights to and from the field sites.

Staff of the Department of Soil and Physical Sciences also made major contributions to the project, for which I am very grateful. Amanda Clifford and Leanne Hassall ensured the timely arrival of all necessary equipment, and Neil Smith spent long hours helping with programming and testing the data loggers. Leanne is especially thanked for her wise counsel and valued friendship. Roger Cresswell's help with gas sampling preparations and analyses was invaluable. Roger worked tirelessly to ensure the mass spec was running well, with assistance from Manjula Premaratne. Lynne Clucas

and Joy Jiao patiently analysed and re-analysed many samples. Thanks also to Rob Sherlock and the late Graeme Buchan for the opportunities afforded to me during my time as a PhD student, as well as for their support and encouragement, and many helpful discussions about my work. Janet Bertram, Amal Torky and Jim Moir are also thanked for their support and encouragement. Thank you also to my friends and fellow students in the Department for their good company – particularly André Eger, Vicky Nall, Brendon Malcolm, Nimlesh Balaine, Pranoy Pal and Jen Owens.

Thanks also to Barry Thornton and his team at the Macaulay Land Use Research Institute in Aberdeen, Scotland for making me very welcome in their laboratory, and for their careful analysis of many gas samples.

Thank you to Megan Balks for her support throughout my PhD. Megan is always a cheery voice down the end of the phone, and I am very grateful for her helpful suggestions and advice, as well as for sparking my Antarctic research adventures by giving me the opportunity to visit Wright Valley as a Masters student nine years ago. Jenny Webster-Brown also gave helpful suggestions and advice. Ed Gregorich shared his knowledge of gas sampling methods he had used in the Dry Valleys, and John Hunt gave advice on chamber design.

Operational support for the project was provided by the Lincoln University Research Fund. I am extremely grateful for financial assistance from Helicopters New Zealand, the William Machin Trust, Freemasons New Zealand, the Kate Sheppard Memorial Trust and Kathryn Claridge of Lincoln Physiotherapy.

Thank you to my dear friends Michele Frey, Jodi Antunovich and Charlotte Fletcher for your wonderful support and encouragement, and for giving me so many reasons to smile.

To my partner, Peter: thank you so much for your patience, support, understanding and love. Finally, to my Mum and Dad, and my brother David: I cannot thank you enough for your love, advice and encouragement. You taught me to dream, and have always supported me and encouraged me to make and take opportunities.

Table of Contents

List of Tables

List of Figures

Chapter 1

Introduction

1.1 Background

The McMurdo Dry Valleys are the largest of the ice-free areas in Antarctica, and comprise low-complexity polar desert ecosystems within one of the most inhospitable environments on Earth. Dry Valley terrestrial ecosystems exist under conditions considered to be biologically extreme: liquid water is scarce, winds can be strong, there are large diel and seasonal variations in temperature, and extremes in solar radiation which range from 0-h daylight during the dark winter months, to 24-h daylight during the austral summer. Soils are generally saline, and contain low levels of carbon (C) and nitrogen (N). However, despite these largely unfavourable conditions for life, biological communities are widely distributed throughout the Dry Valleys.

The harsh conditions under which Dry Valley biological communities exist dictate that ecosystems are relatively simple, thus providing a unique opportunity to test theories of trophic interactions and factors controlling community structure and function (Wall and Virginia, 1999). The advent of modern molecular genetic sequencing techniques has also enabled questions about how environmental factors influence biodiversity and ecosystem functioning to be addressed. As small changes in environmental conditions can have profound effects on Dry Valley ecosystems (Fountain et al., 1999), such studies are often predicated on providing a better understanding of the distribution, diversity and activity of biota in order to facilitate predictions about how community structure and function will be affected by future environmental change. One such measure of biological activity is soil respiration.

Previous studies of soil respiration in the Dry Valleys have provided insight into the physical controls on soil carbon dioxide (CO_2) flux rates (Parsons et al., 2004), and the effects of simulated climate change on C cycling (Ball et al., 2009). In addition, soil respiration rates have been used to calculate the turnover time of the soil organic C pool (Burkins et al., 2001; Elberling et al., 2006), and to provide a basis for comparing ecosystem function between sites (Barrett et al., 2006b). Long-term records of soil respiration rates have been proposed as potentially providing one of the most sensitive indicators of ecosystem response to environmental change (Barrett et al., 2006c).

Recent studies of Dry Valley soil CO_2 fluxes have identified that surface CO_2 flux rates follow diel variations, with positive fluxes measured during warmer parts of the day, and negative fluxes measured during cooler periods (Parsons et al., 2004; Ball et al., 2009). The negative CO_2 fluxes have

no biological explanation, and, as changes in soil temperature have been shown to account for almost half of the variation in CO_2 flux rate (Ball et al., 2009), it has been suggested that Henry's Law-controlled dissolution of CO_2 in soil water may account for the diel variability observed (Parsons et al., 2004; Ball et al., 2009). The potential abiotic contribution to soil CO_2 fluxes (via exsolution of CO_2 as soil temperatures increase) means that surface CO_2 flux rates cannot be assumed to solely represent biological CO_2 production.

An abiotic contribution to soil CO_2 fluxes has potentially profound implications for the interpretation of Dry Valley CO_2 fluxes, particularly in terms of quantifying biological activity and rates of C cycling. A significant abiotic contribution to soil CO_2 fluxes would mean that previous measurements of soil respiration rate are overestimates of the rate of biological CO_2 production, and hence turnover times calculated from such fluxes would be underestimates. Furthermore, as any abiotic component is likely to vary according to local site conditions, using surface CO_2 flux rates as a means of comparing ecosystem activity between sites may not provide an accurate representation of differences in biotic CO_2 production. Single measures of soil CO_2 flux rate may comprise both biotic and abiotic components, thus to capture an absolute biological signal would require repeated measurements over sufficiently long timescales so as to integrate any cyclical abiotic effects. Further research is needed to partition the biotic and abiotic components of soil CO_2 fluxes, from which biotic and abiotic rates of CO_2 production can be quantified.

1.2 Aim and objectives

This study aimed to characterise and quantify the detailed variations in surface CO_2 flux rates and subsurface CO_2 concentration and ^{13}C isotopic composition ($\delta^{13}C_{CO2}$) profiles at two sites with contrasting organic C inputs. This research builds on previous work on Dry Valley soil CO_2 fluxes by using high-resolution measurements of surface CO_2 flux rate and, for the first time, subsurface CO_2 concentration and $\delta^{13}C_{CO2}$ profiles in order to link surface and subsurface soil CO_2 dynamics, and to discriminate between biotic and abiotic sources of CO_2.

The study comprised both field and laboratory work in order to achieve the following objectives:

- To test whether abiotic mechanisms of CO_2 production and consumption can explain observed diel variability in surface CO_2 flux rates (Chapter 3);
- To determine the relative importance of abiotic factors on soil CO_2 production and consumption at a site with low levels of organic C, which is representative of "typical" Dry Valley soils (Chapter 4);

- To partition the biotic and abiotic components of surface CO_2 fluxes at a site with relatively high levels of organic C, characteristic of a biological "hotspot" (Chapter 5).

1.3 Field work

The results presented in this thesis are based on field work carried out during the 2008/09 and 2009/10 austral summers. The main campsite from which this work was undertaken was located ~ 800 m east of Howard Glacier, in eastern Taylor Valley (Figure 1.1).

Figure 1.1 Field camp beside Spaulding Pond, eastern Taylor Valley. Howard Glacier is on the left hand side of the photograph (taken 27 December 2009).

1.4 Thesis structure

The research is presented in three main results chapters which follow a literature review (Chapter 2) that provides the background to and rationale for the study. The first results chapter (Chapter 3) is written as a manuscript, and has been published in *Soil Biology and Biochemistry*. Correspondence prompted by this paper is to be published as a Letter to the Editor (Elberling et al., 2013), along with the subsequent response, in *Soil Biology and Biochemistry*. The published paper, together with the comment and response, are included as Appendix A. Following some alterations to the style in which results are described, the second and third results chapters (Chapters 4 and 5) will also be submitted to *Soil Biology and Biochemistry*. A synthesis and summary of findings is presented in Chapter 6.

1.5 Publications and conference presentations resulting from this thesis

1.5.1 Peer-reviewed journal articles to date

Shanhun, F.L., Almond, P.C., Clough, T.J., Smith, C.M.S., 2012. Abiotic processes dominate CO_2 fluxes in Antarctic soils. Soil Biology & Biochemistry, 53: 99−111. doi:10.1016/j.soilbio.2012.04.027.

This article resulted in a Letter to the Editor (Elberling et al., 2013; Appendix A) and a reply as follows:

Shanhun, F.L., Almond, P.C., Clough, T.J., Smith, C.M.S., 2013. Reply to Elberling et al.'s (2013) comments on "Abiotic processes dominate CO_2 fluxes in Antarctic soils" (Soil Biol. Biochem. 53, 99−111). Soil Biology & Biochemistry, *In Press*, http://dx.doi.org/10.1016/j.soilbio.2013.10.039.

1.5.2 Selected conference presentations

Shanhun, F., Almond, P., Clough, T., Smith, C., 2013. Diel variation in the biotic and abiotic components of soil CO_2 fluxes. XIth SCAR Biology Symposium, Barcelona, Spain. 15−19 July 2013.

Shanhun, F., Almond, P., Clough, T., Smith, C., 2011. Abiotic processes dominate soil CO_2 fluxes in Taylor Valley. 2011 Annual Antarctic Conference, University of Waikato, Hamilton. 4−6 July 2011.

Shanhun, F.L., Almond, P.C., Clough, T.J., Smith, C.M.S., Bockheim, J.G., 2009. Isotopic composition of soil CO_2 in Antarctica: Implications for a pedogenic carbonate paleotemperature proxy. 2009 Lincoln University Postgraduate Conference. 31 August – 1 September 2009.

Shanhun, F.L., Almond, P.C., Clough, T.J., Smith, C.M.S., Bockheim, J.G., 2009. Reconstructing past temperatures in ice-free areas: Development of a pedogenic carbonate proxy. 2009 Annual Antarctic Conference, University of Auckland. 1−3 July 2009.

Chapter 2

Literature review

2.1 Introduction

The McMurdo Dry Valleys are the largest contiguous ice-free area in Antarctica, and are home to organisms that can withstand conditions that are considered to be biologically extreme: strong winds, low moisture availability, low nutrient availability, high salinity, large daily and seasonal variations in temperature, and extremes in solar radiation that range from total darkness during the winter months, to 24-h daylight during the austral summer. The low-complexity ecosystems found within the McMurdo Dry Valleys provide a unique natural laboratory for answering fundamental questions about the survival, distribution, and activity of biological communities in the absence of vascular plants. These ecosystems provide an opportunity to study abiotic controls on ecosystem structure and function, as well as their sensitivity to changes in environmental conditions (Fountain et al., 1999; Wall and Virginia, 1999). Consequently, the McMurdo Dry Valleys are an important indicator environment from which predictions of future change can be made.

Recent research has focused on understanding the factors controlling the distribution and diversity of biota throughout the Dry Valleys and beyond (Lee et al., 2012; Magalhães et al., 2012; Stomeo et al., 2012; Van Horn et al., 2013), and previous studies have aimed to quantify rates of soil respiration, with such rates being used to inform calculations of soil organic carbon (C) turnover time (Burkins et al., 2001; Barrett et al., 2006a; Elberling et al., 2006), and to compare ecosystem function between sites (Barrett et al., 2006b). These previous studies were predicated on the assumption that, as in temperate environments, surface carbon dioxide (CO_2) fluxes are representative of biological CO_2 production. However, as abiotic factors largely control biological distribution, diversity and activity in the Dry Valleys (Barrett et al., 2004; Hogg et al., 2006; Lee et al., 2012; Magalhães et al., 2012; Stomeo et al., 2012; Van Horn et al., 2013), this assumption may not necessarily apply to dry valley ecosystems, and needs to be tested. Furthermore, recent studies investigating Dry Valley soil CO_2 fluxes at regular intervals over several diel cycles have identified negative CO_2 flux rates (Parsons et al., 2004; Ball et al., 2009), with the rate of change in soil temperature, rather than variation in absolute temperature, accounting for almost half of the variability in surface CO_2 flux rates (Ball et al., 2009). Since negative CO_2 flux rates have no biological explanation, it has been suggested that Henry's Law-controlled dissolution and exsolution of CO_2 may account for the diel variability in surface CO_2 flux rates (Parsons et al., 2004; Ball et al., 2009). This hypothesis is, as yet, untested, and forms the basis for the research presented in this study.

This review examines literature pertinent to measurement and interpretation of soil CO_2 fluxes, and provides a basis for understanding CO_2 dynamics in Dry Valley ecosystems.

2.2 Soil CO_2 dynamics and effects on carbon isotopic composition

This thesis examines the rate and C isotopic composition ($\delta^{13}C_{CO2}$) of soil CO_2 fluxes and depth profiles of CO_2 concentration and $\delta^{13}C_{CO2}$ in a polar desert environment. A short section on soil gas sampling and factors affecting the isotopic composition of soil CO_2 is presented here to provide the necessary background to understand the results presented in Chapters 3, 4, and 5. More detailed discussion of the current knowledge of soil CO_2 fluxes in the McMurdo Dry Valleys follows in section 2.3.5.

2.2.1 CO_2 sampling using headspace chambers

Surface CO_2 flux rates are typically determined via the use of headspace chambers. Such chambers can be manually sampled, where gas samples are extracted from the chamber and injected into a vial for later analysis, or coupled to automated flux measurement instruments. As static chambers were employed in this study, this review is limited to their design and potential limitations. Further discussion of additional chamber types and their limitations, as derived from a comprehensive modelling study, can be found in Creelman et al. (2013).

Static chamber design and limitations

Static chambers, which accumulate CO_2 in a sealed headspace above the soil surface, enable calculation of surface CO_2 flux rates based on a time-series of changes in CO_2 concentration. Such chambers are closed, thus representing a non-steady-state measurement technique, as they change the natural dynamics of CO_2 diffusion into the free atmosphere. Consequently, any increase (or decrease) in CO_2 concentration within the headspace chamber creates a feedback effect, which distorts the subsurface soil CO_2 concentration gradient (Healy et al., 1996; Conen and Smith, 2000). This leads to increased storage of gas within the profile (Conen and Smith, 2000), and lateral diffusion of CO_2 (Creelman et al., 2013), both of which cause underestimation of the true surface CO_2 flux rate. The underestimation of surface CO_2 flux rates calculated using static chamber methods can be up to 35% (Rayment, 2000; Pumpanen et al., 2004), although individual site factors and sampling design have a large influence on the likely errors in measurement.

The feedback effect of static chambers on subsurface CO_2 concentration gradients is most pronounced in dry, porous soils with high gas diffusivity (Davidson et al., 2002; Nickerson and Risk, 2009b; Creelman et al., 2013), although chamber height and CO_2 production rate (Healy et al., 1996; Conen and Smith, 2000), depth of insertion (Davidson et al., 2002; Creelman et al., 2013), and

duration of deployment (Davidson et al., 2002; Creelman et al., 2013) are all factors that can moderate the degree of distortion of the subsurface concentration gradient and associated lateral diffusion. As the soils in the study area are characteristically dry and porous, they are highly susceptible to lateral diffusion and associated underestimation of surface CO_2 flux rates if CO_2 concentrations in surface chambers increase substantially. Even if CO_2 production rates in dry, porous soils are low and do not cause substantial accumulation of CO_2 in headspace chambers, flux rates may still be underestimated owing to the relatively large volume of gas that can be stored in the soil beneath the chamber (Rayment, 2000).

2.2.2 Isotopic fractionation

The stable isotopes of C, ^{12}C and ^{13}C, constitute 98.89% and 1.11% of the C atoms on Earth, respectively (Fry, 2006). The partitioning (or "fractionation") of the two stable isotopes of C, on the basis of differences in their mass in response to physical or biochemical processes, enables them to be used as a natural tracer. For example, isotopic fractionation in biological systems, such as that which occurs during photosynthesis, enables the ^{13}C isotopic composition ($\delta^{13}C$) of plant tissue or of respired CO_2 to be used to determine the photosynthetic pathway used in assimilating C. Different types of fractionation may occur, and these are discussed below in the context of soil CO_2 dynamics.

Notation and nomenclature

As absolute isotopic ratios are often small and difficult to measure directly, the isotopic ratios (δ) of measured samples are reported in units of per mil (‰), relative to an international standard:

$$\delta_{sample} = \left(\frac{R_{sample} - R_{standard}}{R_{standard}}\right) \times 1000 \quad (2.1)$$

where R_{sample} and $R_{standard}$ are the ratios of heavy to light isotopes in the sample and standard, respectively.

Consistent with other literature (e.g. Cerling et al., 1991), 'soil-respired CO_2' represents the flux of CO_2 passing through a soil, whereas 'soil CO_2' refers to the CO_2 at any given depth within the soil. Soil-respired CO_2 has an isotopic composition ($\delta^{13}C_{CO2}$) that reflects the net production of CO_2, but the $\delta^{13}C_{CO2}$ of soil CO_2 reflects a mixture between atmospheric CO_2 and any CO_2 produced within the soil, and is not constant with depth (Cerling, 1984). In most systems, soil-respired CO_2 is of biological origin, arising from microbial metabolism of C compounds and root respiration (Cerling, 1984), but in environments where soil-respired CO_2 fluxes are low, net surface fluxes may also include a significant component of CO_2 produced as a result of abiotic processes (e.g. Parsons et al., 2004; Ball et al., 2009).

Equilibrium fractionation

Equilibrium fractionation is the mass-dependent partitioning of isotopes among various species or compounds in a system at chemical (and thermodynamic) equilibrium. As such, the forward and backward reaction rates of any particular isotope are identical (Kendall and Caldwell, 1998), and the distribution of isotopes between compounds is temperature dependent (Craig, 1953). The temperature-dependent fractionation of isotopes provides a means by which records of past temperatures can be constructed, as the degree of fractionation can be used to determine the temperature at which a persistent compound formed.

Kinetic fractionation

Kinetic fractionation is the mass-dependent partitioning of isotopes resulting from incomplete or unidirectional processes (Mook, 2000; Hoefs, 2009). Kinetic fractionation is associated with the diffusive transport of gases, and arises from the different diffusivities of different isotopes. During diffusion of CO_2, the isotopically lighter $^{12}CO_2$ molecule moves faster than the heavier $^{13}CO_2$ molecule, with the difference in the diffusivities of the $^{12}CO_2$ and $^{13}CO_2$ isotopologues causing a transport-related fractionation. The diffusion coefficients of $^{12}CO_2$ and $^{13}CO_2$ differ by 4.4‰ (Craig, 1953), as given by:

$$\frac{D(^{12}CO_2)}{D(^{13}CO_2)} = \left(\frac{M(^{12}CO_2) + M_{air}}{M(^{12}CO_2)\,M_{air}}\,\frac{M(^{13}CO_2)\,M_{air}}{M(^{13}CO_2) + M_{air}}\right)^{\frac{1}{2}} = 1.0044 \tag{2.2}$$

where $D(^{12}CO_2)$ and $D(^{13}CO_2)$ are the diffusion coefficients for $^{12}CO_2$ and $^{13}CO_2$, respectively, and $M(^{12}CO_2)$, $M(^{13}CO_2)$ and M_{air} are the atomic masses of $^{12}CO_2$, $^{13}CO_2$ and average air, respectively. This relationship dictates that, in diffusion-driven natural systems, the $\delta^{13}C_{CO2}$ of soil CO_2 must be at least 4.4‰ enriched relative to soil-respired CO_2 (Cerling et al., 1991).

In a steady-state system, the transport-related fractionation during diffusion is referred to as kinetic fractionation. For example, in a soil environment with a constant soil respiration rate at a given $\delta^{13}C_{CO2}$ value, and a constant atmospheric boundary value, the $\delta^{13}C_{CO2}$ of soil CO_2 will be at least 4.4‰ enriched with respect to the $\delta^{13}C_{CO2}$ of soil-respired CO_2 (Cerling et al., 1991; c.f. error in Midwood and Millard, 2011). This is because the lighter $^{12}CO_2$ isotopes move through the soil faster than the heavier $^{13}CO_2$ isotopes, resulting in a surface flux that is more depleted than the soil CO_2. In a system at steady-state, the CO_2 concentration and $\delta^{13}C_{CO2}$ profiles remain constant (although the absolute values will vary with depth). Based on gradients of the individual $^{12}CO_2$ and $^{13}CO_2$ isotopologues, these profiles dictate that CO_2 is emitted from the soil surface at the rate of soil respiration and with the same $\delta^{13}C_{CO2}$ as that of the soil-respired CO_2.

The degree of isotopic enrichment of soil CO_2 also depends on the soil respiration rate (Cerling, 1984; Cerling et al., 1991). When the soil respiration rate and soil CO_2 concentration is high, the enrichment of soil CO_2 relative to soil-respired CO_2 almost exactly matches the theoretical enrichment of 4.4‰ (Cerling et al., 1991). At low soil respiration rates, the difference between the $\delta^{13}C_{CO2}$ of soil CO_2 and soil-respired CO_2 is > 4.4‰, due to the enhanced diffusion of $^{13}CO_2$ from the isotopically heavy atmosphere into the soil. Low soil respiration rates mean that the soil atmosphere is less depleted (than in a soil with a high respiration rate) due to a smaller input of isotopically light CO_2 produced by respiration.

Dynamic fractionation

Dynamic fractionation, a term coined by Nickerson and Risk (2009c), describes isotopic fractionation that occurs in non-steady-state environments. It is similar to kinetic fractionation in that it is also transport-related, but it results from transient changes in environmental variables driving changes in $^{12}CO_2$ and $^{13}CO_2$ gradients (Nickerson and Risk, 2009c), rather than just differences in the diffusivities of $^{12}CO_2$ and $^{13}CO_2$.

In non-steady-state (dynamic) systems, the theoretical kinetic fractionation of 4.4‰ is unlikely to be observed (Risk and Kellman, 2008) because the dynamic nature of the environment dictates that there is a non-infinite source or sink of gas moving towards, but never reaching, equilibrium. Instead, transient changes in environmental variables such as soil temperature and moisture content drive changes in biotic and abiotic CO_2 production rates, which alter gradients of $^{12}CO_2$ and $^{13}CO_2$. Such changes in the $^{12}CO_2$ and $^{13}CO_2$ gradients, which are amplified by the rate of change in the $^{13}CO_2$ gradient always being slower due to the low natural abundance of $^{13}CO_2$, lead to transient changes in the isotopic composition of the soil CO_2 flux (Nickerson and Risk, 2009c). For example, an increase in biological production of isotopically light CO_2 acts to steepen the $^{12}CO_2$ gradient between the soil and the atmosphere, thus driving $^{12}CO_2$ out of the profile at a proportionately greater rate than the slower moving $^{13}CO_2$, and thereby acting to produce a transiently light surface CO_2 flux. Similarly, a decrease in the rate of biological production of CO_2 will result in a decrease in the $^{12}CO_2$ gradient between the soil and the atmosphere; this results in proportionately more $^{13}CO_2$ diffusing out of the soil, thus producing a transiently heavy surface CO_2 flux.

Confounding effects: variation in CO_2 production rate

Diurnal variation in the CO_2 production rate also influences the isotopic composition of the soil CO_2 flux, as shown by Nickerson and Risk (2009c) who used a model to simulate the production and transport of $^{12}CO_2$ and $^{13}CO_2$ in a soil profile. As well as identifying the dynamic fractionation that occurs (discussed above), their model simulations showed that measured surface CO_2 flux rates are

out of phase with variations in CO_2 production rates, owing to a lagged response which is predominantly controlled by soil diffusivity.

Furthermore, variation in the isotopic composition of the surface CO_2 flux is also out of phase with variation in CO_2 production, such that measured surface flux $\delta^{13}C_{CO2}$ values are not representative of instantaneous CO_2 production, but rather CO_2 production that occurred some time before the measurement was made (Nickerson and Risk, 2009c). Soil diffusivity was again the main property controlling the time taken for $\delta^{13}C_{CO2}$ values to re-equilibrate following a change in the rate of CO_2 production, with higher diffusivities facilitating a more rapid return to equilibrium conditions. High soil diffusivity values also acted to amplify the degree of deviation from the equilibrium $\delta^{13}C_{CO2}$ value.

Nickerson and Risk's (2009c) work clearly demonstrates that dynamic fractionation is continuously present in non-steady-state systems, and requires that, for natural abundance isotope techniques to be of significant value in discriminating between different sources of CO_2, the two sources must differ isotopically by at least 1‰.

In testing both 1-D and 3-D diffusion scenarios using a model of isotopologue transport as well as experimental data from static chambers, Nickerson and Risk (2009b) found that the use of Keeling plots to determine the $\delta^{13}C_{CO2}$ of CO_2 being produced is inappropriate in diffusive environments. This is because differences in the rates of transport of $^{12}CO_2$ and $^{13}CO_2$ cause non-linearities in Keeling plots, which, when relying on linear regression in order to determine the source $\delta^{13}C_{CO2}$, is unacceptable. Furthermore, in soils with high diffusivity, the effect of non-linearities in Keeling plots is amplified (Nickerson and Risk, 2009b).

Influence of chamber methodology on $\delta^{13}C_{CO2}$ of soil-respired CO_2

Further modelling by Nickerson and Risk (2009a) identified that chamber methodology also introduces errors in determining the $\delta^{13}C_{CO2}$ of soil-respired CO_2. This applies to both steady-state and non-steady-state chambers, with the magnitude of enrichment in the $\delta^{13}C_{CO2}$ of soil-respired CO_2 (relative to the true $\delta^{13}C_{CO2}$ value of soil-respired CO_2) ranging from 1 to 4‰. In steady-state chambers, such as those that use a CO_2 sorbent in order to maintain headspace concentration at ambient atmospheric levels, lateral diffusion of CO_2 causes equilibration of the chamber CO_2 with that of soil CO_2 at the base of the collar (the lowermost edge of the chamber within the soil). However, factors such as diffusivity, collar insertion depth, and biological CO_2 production rate all influence the magnitude of the enrichment in measured $\delta^{13}C_{CO2}$ values. In non-steady-state chambers, such as static chambers in which CO_2 accumulates over time (and samples are taken at regular intervals in order to determine the $\delta^{13}C_{CO2}$ of soil-respired CO_2 using a Keeling plot approach), or purged chambers in which the headspace is initially purged, and then either a single sample is taken, which is considered to represent the $\delta^{13}C_{CO2}$ of soil-respired CO_2, or multiple samples are taken

in order to ascertain $\delta^{13}C_{CO2}$ using a Keeling plot approach, both chamber-to-soil feedbacks and lateral diffusion of CO_2 introduce errors in $\delta^{13}C_{CO2}$.

The fact that chamber-to-soil diffusive feedbacks affect $\delta^{13}C_{CO2}$ values is not surprising: increases in chamber concentration over time act to change the gradients of $^{12}CO_2$ and $^{13}CO_2$ between the soil and the chamber, thus acting to slow overall diffusion rates from the soil to the chamber, as well as exacerbating the differential diffusion rates of $^{12}CO_2$ and $^{13}CO_2$. Lateral diffusion effects also influence $\delta^{13}C_{CO2}$, with the greatest effects seen when collar lengths are short, and soil diffusivities are high (Nickerson and Risk, 2009b). As with the steady-state chambers, once lateral diffusion becomes significant, CO_2 in non-steady-state chambers begins to equilibrate with soil CO_2 at the depth to which the collar is inserted (Nickerson and Risk, 2009a). These effects highlight the importance of utilising a model of $^{12}CO_2$ and $^{13}CO_2$ transport in order to accurately interpret isotopic data.

Summary

In dynamic systems, transient changes in environmental variables drive changes in soil CO_2 production and $\delta^{13}C_{CO2}$. Consequently, surface CO_2 flux and $\delta^{13}C_{CO2}$ measurements alone are insufficient to determine the timing and magnitude of maxima and minima in soil CO_2 production. In such systems, surface CO_2 flux rates are unlikely to be accurate representations of CO_2 production rates due to lags between changes in production and measured surface fluxes. Furthermore, interpretation of the isotopic composition of the measured surface flux is complicated by lags as well as dynamic fractionation effects, with the measured $\delta^{13}C_{CO2}$ values not representing the $\delta^{13}C_{CO2}$ of CO_2 being produced in the soil at the time of surface flux measurement.

Interpretation of surface fluxes and their isotopic composition can be aided by installation of soil profile CO_2 sampling tubes. Sampling of subsurface soil CO_2 concentration and $\delta^{13}C_{CO2}$ immediately before or after surface flux sampling provides an instantaneous measure of the gradients of $^{12}CO_2$ and $^{13}CO_2$; these gradients can be used to predict surface fluxes and their $\delta^{13}C_{CO2}$. Additionally, subsurface soil CO_2 concentration and $\delta^{13}C_{CO2}$ profiles can be used to determine whether or not there are periods of steady-state production of CO_2, in which case surface flux rates and their isotopic composition would be representative of the processes happening in the soil over those periods.

Approach used

Despite the problems with the use of static chambers and fractionation effects in non-steady state environments discussed above, measurements of surface CO_2 flux rate and $\delta^{13}C_{CO2}$ were made using static chambers. This was deemed to be acceptable in this study because surface CO_2 flux rates in the Dry Valleys of Antarctica are known to be low, hence changes in $^{12}CO_2$ and $^{13}CO_2$ gradients due to accumulation of CO_2 in headspace chambers are likely to be minimal. Issues of interpretation of surface fluxes and $\delta^{13}C_{CO2}$ were countered by the installation of subsurface sampling tubes, from

which instantaneous profiles of soil CO_2 concentration and $\delta^{13}C_{CO2}$ could be used to assess periods of steady-state and predict surface flux rates and their isotopic composition, based on a simple model utilising the gradients in $^{12}CO_2$ and $^{13}CO_2$. Further details of sampling methods and modelling follow in the methods sections of Chapters 3 and 4.

2.2.3 Biological respiration

Biological respiration refers to the CO_2 released from soils as a result of CO_2 production by organisms and roots (Lloyd and Taylor, 1994) while metabolising C compounds. In the absence of moisture limitations, the rate of soil respiration increases with increasing soil temperature (Lloyd and Taylor, 1994; Fang and Moncrieff, 2001). The sensitivity of this relationship is amplified at low soil temperatures (Lloyd and Taylor, 1994; Kirschbaum, 1995), although soil respiration under low temperatures may be controlled by other mechanisms that are not yet clear (Fang and Moncrieff, 2001). Nonetheless, several confounding effects influence the relationship between soil temperature and soil respiration. These effects include biotic and abiotic conditions which differ throughout the soil profile, such as variations in: 1) soil moisture content and CO_2 diffusivity; 2) the vertical distribution of roots and microbes and their individual relationships between respiration rate and temperature; and 3) the quality and availability of soil organic matter (Subke and Bahn, 2010). Additionally, differences in the temperature dependence of soil organic C decomposition under different soil temperature regimes are likely influenced by differences in soil microbial community composition (Zhu and Cheng, 2011). Therefore, the apparent temperature influence on soil respiration should be treated cautiously, particularly in cooler environments. A greater understanding of the interactions between biotic and abiotic processes in different ecosystems is required in order to make more realistic predictions of soil CO_2 efflux under different climate scenarios (Subke and Bahn, 2010).

Carbon isotopic fractionation in the biological system

Isotopic fractionation during photosynthesis enables differentiation between various biotic influences on soil CO_2 fluxes. The major fractionation of C isotopes associated with photosynthetic fixation of atmospheric CO_2 is a two-step process (Park and Epstein, 1960; O'Leary, 1981). The first step involves preferential uptake of $^{12}CO_2$ from the atmosphere (Park and Epstein, 1960), which has a kinetic fractionation of 4.4‰ (O'Leary, 1981), owing to the differences in diffusivities between the $^{12}CO_2$ and $^{13}CO_2$ isotopologues as they pass through stomata. Subsequent fractionation that occurs within plant tissues via the different carboxylation pathways in C_3, C_4 and Crassulacean acid metabolism (CAM) plants is not relevant to understanding the mechanisms of CO_2 production explored in this study, so is not discussed here. However, the fractionations that occur during photosynthesis ultimately dictate that C_3 plants are depleted in ^{13}C relative to atmospheric CO_2, and

have average $\delta^{13}C$ values of approximately −27‰ (O'Leary, 1988). C_4 plants, which do not discriminate so strongly against $^{13}CO_2$ during photosynthesis, have average $\delta^{13}C$ values around −13‰ (O'Leary, 1988). CAM plants, which utilise C_3 pathways during the daytime and C_4 pathways at night, have $\delta^{13}C$ values intermediate between C_3 and C_4 plants, generally between −10 and −20‰ (O'Leary, 1988).

Within plants, $\delta^{13}C$ values differ slightly between plant roots and shoot tissues (Werth and Kuzyakov, 2010), hence different organic matter fractions have slight differences in their C isotopic composition. Preferential utilisation of ^{13}C-rich substrates by microorganisms, particularly in C_3 soils, acts to enrich the microbial biomass, which respires CO_2 depleted in ^{13}C relative to itself, but still enriched compared to soil organic matter (Werth and Kuzyakov, 2010). Numerous studies have reported various fractionations that either concur or disagree with this, yet others have shown no indication of isotopic fractionation during the decomposition of various substrates (Boström et al., 2007). Werth and Kuzyakov (2010) performed a comprehensive analysis of measured fractionations between soil organic matter and soil C pools, incorporating data from field and laboratory studies carried out at various sites around the world. Their analysis (for C_3 soils) yielded a mean fractionation between soil organic matter and soil microbial biomass of 1.2 ± 2.6‰, and a mean fractionation between soil organic matter and soil organic matter-derived CO_2 of 0.7 ± 2.8‰. These fractionations can be considered relatively minor in terms of their effect on soil-respired $\delta^{13}C_{CO2}$ values.

In arid environments, the fractionations associated with biological utilisation of organic matter and respiration of CO_2 are likely to be even less significant. Firstly, the activity of organisms is restricted to periods when abiotic factors (primarily soil temperature and moisture content) are suitable. Secondly, such environments tend to be characterised by low levels of soil organic matter: limited substrate availability restricts the potential for preferential decomposition of particular soil organic matter fractions. Therefore, the low substrate availability and abiotic factors which regulate soil microbial activity dictate that organisms will consume all types of soil organic matter available (Werth and Kuzyakov, 2010), and consequently, the isotopic composition of soil-respired CO_2 will be very close to that of the bulk soil organic matter pool (Dörr and Münnich, 1980).

2.2.4 Dissolution of CO_2 in water

The partitioning of CO_2 between gaseous and dissolved forms is determined by Henry's Law and the pH of the solution into which it dissolves. The Henry coefficient (K_H) expresses the relationship between CO_2 in the atmosphere (pCO_2) and dissolved gaseous CO_2 ($[CO_{2(aq)}] = [H_2CO_3]$) as $pCO_2 = K_H[CO_{2(aq)}]$. Total dissolved CO_2 (C_T) comprises the species H_2CO_3, HCO_3^- and CO_3^{2-}, as determined by the equilibrium:

$$CO_{2(g)} + H_2O_{(l)} \leftrightarrow H_2CO_{3(aq)} \leftrightarrow H^+{}_{(aq)} + HCO_3^-{}_{(aq)} \leftrightarrow 2H^+{}_{(aq)} + CO_3^{2-}{}_{(aq)}. \quad (2.3)$$

Therefore, the relationship between C_T and dissolved CO_2 is:

$$C_T = \left[CO_{2_{(aq)}}\right]\left(1 + \frac{K_{a_1}}{[H^+]} + \frac{K_{a_1}K_{a_2}}{[H^+]^2}\right). \quad (2.4)$$

The equilibrium constants for $[H^+]\,[HCO_3^-]/[H_2CO_3]$ and $[H^+]\,[CO_3^{2-}]/[HCO_3^-]$ are K_{a1} and K_{a2}, respectively (Stumm and Morgan, 1996).

The Henry coefficient is temperature dependent. As temperature increases, the solubility of CO_2 decreases, thus pCO_2 increases and $[CO_{2(aq)}]$ decreases. The total amount of dissolved inorganic C is related to pH, according to equation (2.4); as pH increases ($[H^+]$ decreases), the total amount of dissolved inorganic C (C_T) increases. The relationship between pH and the dissolved CO_2 species present is expressed in Figure 2.1.

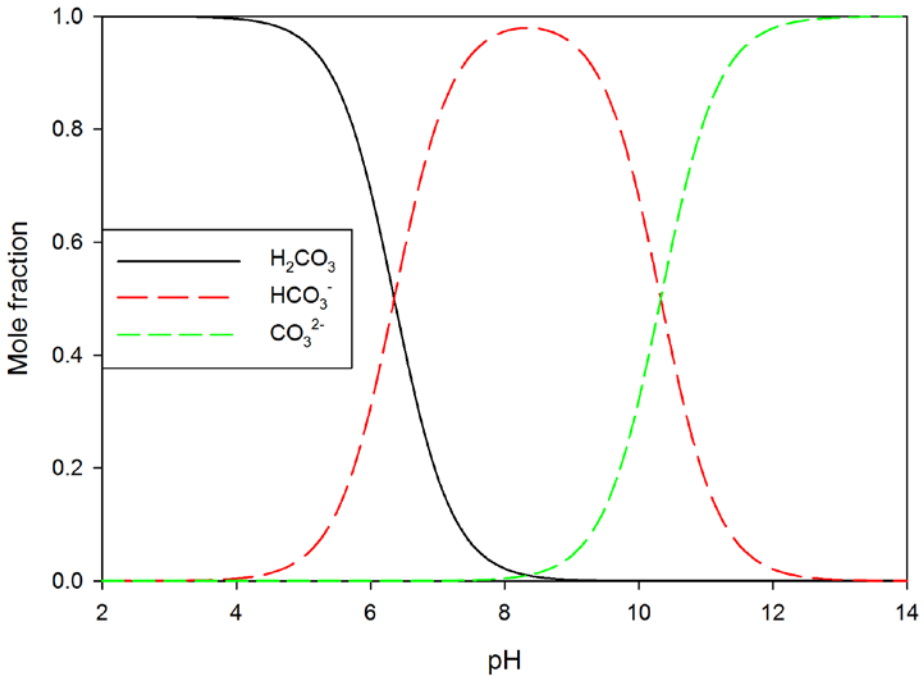

Figure 2.1 The effect of pH on the distribution of dissolved inorganic carbon species in solution.

Mechanism for abiotic CO_2 fluxes

In soils, Henry's Law-controlled dissolution and exsolution of CO_2 provides a mechanism by which abiotic CO_2 fluxes can occur, with diel variability in soil temperatures driving the dissolution and exsolution of CO_2.

2.2.5 Carbon isotopic fractionation in the carbonate system

Isotopic fractionation of C in the carbonate equilibrium system described above enables abiotic influences on soil CO_2 fluxes to be quantified. The values for the fractionations that occur as a result of dissolution of CO_2 in water are solely temperature dependent, and are derived empirically based on the dissolution of CO_2 and subsequent dissociation reactions within equation (2.3).

As shown in Figure 2.1, pH dictates which species are present. Equilibrium fractionation of CO_2 gas to $HCO_3^-{}_{(aq)}$, $CO_3^{2-}{}_{(aq)}$ and solid calcium carbonate as a result of CO_2 dissolution results in depletion of CO_2 gas relative to $HCO_3^-{}_{(aq)}$, $CO_3^{2-}{}_{(aq)}$, and solid calcium carbonate (Table 2.1; Thode et al., 1965; Mook et al., 1974; Mook, 2000). At pH values <8.3, dissolution of CO_2 will produce some H_2CO_3, which results in enrichment of CO_2 gas relative to $H_2CO_{3(aq)}$ (Vogel et al., 1970). Therefore, dissolution of CO_2 in soil water to form HCO_3^- and CO_3^{2-} (at pH values >8.3) would result in reduced soil CO_2 concentrations and depletion of the $\delta^{13}C_{CO2}$ of the soil atmosphere. Conversely, exsolution of CO_2 would increase soil CO_2 concentrations and lead to enrichment of the $\delta^{13}C_{CO2}$ of the soil atmosphere. This constitutes an important abiotic mechanism of CO_2 uptake and release, driven by temperature, which can occur in soils.

Table 2.1 Carbon isotope fractionation in the CO_2–HCO_3–CO_3–$CaCO_3$ system under equilibrium conditions. $^{13}\varepsilon_{y/x}$ represents the fractionation of compound y relative to compound x. Soil temperatures (T) shown are similar to those measured in the McMurdo Dry Valleys. g = gaseous CO_2, a = dissolved CO_2, b = dissolved HCO_3^-, c = dissolved CO_3^{2-} ions, s = solid calcium carbonate. T_K = T (°C) + 273.15 K.

T (°C)	$^{13}\varepsilon_{g/a}$ [a] (‰)	$^{13}\varepsilon_{g/b}$ [b] (‰)	$^{13}\varepsilon_{g/c}$ [c] (‰)	$^{13}\varepsilon_{g/s}$ [d] (‰)
1	1.17	−10.70	−10.06	−10.47
5	1.15	−10.20	−9.61	−10.19

[a] $^{13}\varepsilon_{g/a} = -0.19‰ + 373/T_K$ (Vogel et al., 1970).
[b] $^{13}\varepsilon_{g/b} = 23.89‰ - 9483/T_K$ (Mook et al., 1974).
[c] $^{13}\varepsilon_{g/c} = {}^{13}\varepsilon_{g/b} + {}^{13}\varepsilon_{b/c}$ (= −2.52 ‰ + 867/T_K; Thode et al., 1965).
[d] $^{13}\varepsilon_{g/s} = 9.15‰ - 5380/T_K$ (Mook, 2000).

2.3 McMurdo Dry Valleys

The McMurdo Dry Valleys are the largest ice-free region in Antarctica (4500 km^2; Levy, 2013) and comprise a polar desert landscape dominated by coarse-textured soils formed in glacial drift, interspersed with alpine glaciers, ephemeral streams, and perennially ice-covered lakes (Figure 2.2). Vascular vegetation is absent, and biota consists of microorganisms and a limited number of invertebrate species (Adams et al., 2006; Cary et al., 2010).

Figure 2.2 The polar desert landscape of the McMurdo Dry Valleys. Clockwise from top: alpine glaciers and ice-covered Lake Bonney, central Taylor Valley; polygonal patterned ground, lower Taylor Valley; ephemeral stream, lower Taylor Valley.

The Dry Valleys are predominantly comprised of three large east-west oriented valleys: Taylor Valley, Wright Valley and the Victoria Valley system. They extend from the crest of the Transantarctic Mountains to the ocean (McMurdo Sound) and range in length from 80−100 km long, and 5−10 km wide. Elevation ranges from sea level to over 2000 m in a horizontal distance of only a few kilometres (Fountain et al., 1999; Doran et al., 2002a). The ice-free nature of the valleys results from the

Transantarctic Mountains blocking much of the flow of the East Antarctic Ice Sheet toward McMurdo Sound (Clow et al., 1988). Additionally, low precipitation and high sublimation rates dictate that annual ablation rates exceed accumulation rates (Fountain et al., 1999).

The Dry Valleys are one of the most intensively studied areas in Antarctica; their relative ease of access, glacial history, and relatively simple ecosystems make them ideal for studying fundamental landscape and ecosystem processes in a polar desert environment (Wall and Virginia, 1999). The study area this thesis focuses on is located within Taylor Valley, the smallest and southernmost of the three main dry valleys. Therefore, this review focuses on the climate, hydrology, geomorphology, soils, CO_2 fluxes and ecosystem processes in Taylor Valley.

2.3.1 Climate

The McMurdo Dry Valleys are a polar desert environment, characterised by a paucity of liquid water and extreme cold conditions (Fountain et al., 1999). The austral summer provides a short opportunity for life to flourish: daylight is continuous, temperatures are relatively mild (and are predominantly controlled by diel variation in solar radiation (Clow et al., 1988)), and, for short periods, liquid water is present. In contrast, sunlight and liquid water are absent during the winter months (Fountain et al., 1999), and temperatures are controlled by the wind (Clow et al., 1988). The presence of ice within the valleys, which exists as alpine glaciers flowing down the valley walls, ice-covered lakes, and ice-cemented permafrost within the soils, provides a significant pool of water that is potentially available for melting. As such, the Dry Valleys are highly climate-sensitive environments, with small changes in summer temperature and the associated phase changes of H_2O between ice and liquid water potentially leading to extreme variations in the hydrological regime (Fountain et al., 1999; Lyons et al., 2005), with concomitant effects on soil chemistry, and moisture availability for organisms.

Annual water-equivalent precipitation is < 50 mm, with snow transported by katabatic winds supplying up to another 50 mm (water-equivalent) to the valley floor (Fountain et al., 2010). Meltwater from alpine glaciers is the dominant source of moisture for streams (Doran et al., 2002b), as in the valley floors, ablation of snow and ice exceeds accumulation throughout the year (Clow et al., 1988). The annual net radiation balance is positive (Dana et al., 1998) due to the relatively low surface albedo (Thompson et al., 1971). Snow patches are generally rapidly sublimed, and hence lost as a potential source of moisture to soils or streams (Keys, 1980).

Mean annual air temperature in Taylor Valley ranges from –14.8 to –23.1°C (Doran et al., 2002a). A strong east to west gradient in summer temperature, which is correlated with the wind regime, exists within the valleys; temperatures increase with distance inland (Doran et al., 2002a). In summer, the most frequent wind direction in the valley floors is up-valley winds (easterly sea

breezes; Thompson et al., 1971; Keys, 1980; Clow et al., 1988; Doran et al., 2002a; Nylen et al., 2004), generated as a result of differential heating of the dark coloured valley floors and the ice-covered ocean. These winds typically intensify during the day (Clow et al., 1988), becoming strongest in the afternoons and evenings when ground temperatures are warmest (Keys, 1980). The easterly winds also warm as they progress up-valley over the relatively warmer dark valley surfaces; air temperatures increase by 0.09°C per kilometre inland and cool with inland elevation at the dry adiabatic lapse rate (Doran et al., 2002a).

Westerly katabatic winds, which warm adiabatically as they descend into the valleys (Keys, 1980; Clow et al., 1988), occur more frequently in winter than in summer (Clow et al., 1988; Nylen et al., 2004). In summer, they occur infrequently (Nylen et al., 2004), and are generally limited to the mornings, when solar radiation is minimal, thus the atmosphere is more stable (Thompson et al., 1971; Clow et al., 1988). The onset and cessation of katabatic winds is generally abrupt, though the adiabatic warming of the winds, combined with the disruption they cause to temperature inversions (Thompson et al., 1971; Doran et al., 2002a; Nylen et al., 2004) acts to increase air temperatures and decrease relative humidity (Thompson et al., 1971; Clow et al., 1988; Nylen et al., 2004). Katabatics can reach speeds of 37 m s^{-1} and can increase winter air temperatures by 30°C in a few hours (Doran et al., 2002a; Nylen et al., 2004), with the warming effect of the katabatics persisting for days after the winds cease (Nylen et al., 2004).

Mean annual solar flux in the Dry Valleys ranges from 73 – 117 W m^{-2} (Doran et al., 2002a). Strong diel variability in solar radiation, further influenced by topographic shading and localised cloudiness, acts to drive diel variation in air and soil temperatures, glacial meltwater production, and stream flow.

2.3.2 Hydrology

Small changes in summer temperature and solar radiation affects the availability and distribution of liquid water, which has a significant influence on ecological function and biological diversity in the Dry Valleys (Doran et al., 2002b). Taylor Valley contains three major lakes, and many ephemeral streams and ponds (Fountain et al., 1999; Moorhead et al., 2003; Moorhead, 2007). The major lakes are perennially ice-covered, although absorption of radiation during summer causes melting at the ice-margins, forming moats around the edges of the lakes (Hendy, 2000). These moats and other ice-free ponds are zones of biological productivity during most summers; algae produced within the lakes and ponds represent a significant contemporary organic C source in the landscape (Moorhead et al., 2003; Moorhead, 2007).

Ephemeral streams, fed by glacial melt, provide a significant source of liquid water to hydrological and biological systems within the Dry Valleys. Such streams generally flow for between four and ten weeks during the austral summer (Fountain et al., 1999; McKnight et al., 1999), with flow rates markedly influenced by diel variation in solar radiation. Water tracks also provide an extensive topographically-controlled transport network that distributes meltwater from snow patches and melting of ice-cement through soils, and ultimately to lakes (Levy et al., 2011).

The variable nature of solar radiation received in the Dry Valleys produces strong daily and seasonal variations in glacier melting and stream flow (Conovitz et al., 1998; Dana et al., 1998). Hydrologic data from both Taylor and Wright Valleys highlights the significant variability in stream flow over daily, seasonal, and interannual time scales (Conovitz et al., 1998; McKnight et al., 1999; Doran et al., 2008). Such variation is predominantly a result of differences in solar intensity on source glaciers, which is primarily influenced by solar geometry and the aspect of the glaciers, but also by altitude, air temperature (Clow et al., 1988), and cloud cover (Conovitz et al., 1998; Dana et al., 1998). However, Doran et al.'s (2008) comparison of high and low stream-flow summers showed that despite solar radiation being the same for the two summers compared, increased air temperatures in the high-flow year, driven by an increased frequency of westerly winds, was the primary reason for increased meltwater production.

Discrete climate events such as the relatively warm summer of 2001/2002 can also have a significant influence on Dry Valley hydrology (Barrett et al., 2008b; Doran et al., 2008), acting to increase stream-flow and lake levels, and melting of ice-cement within soils. Melting of subsurface ice during warm summers can lead to the development of groundwater seeps (Lyons et al., 2005), and can influence water availability in surface soils for several years, even if temperatures are average or below-average in subsequent seasons (Barrett et al., 2008b). Furthermore, increased moisture supply to soils can significantly decrease soil salinity, thereby improving habitat suitability and altering soil faunal community abundance and diversity (Nielsen et al., 2012).

2.3.3 Geomorphology

The McMurdo Dry Valleys are east-west oriented deglaciated valleys. In Taylor Valley, the valley floors are covered by tills of various thicknesses, preserving evidence of ice advances from Taylor Glacier (draining the East Antarctic Ice Sheet), the Ross Sea, and local alpine glaciers. The eastern part of Taylor Valley is mantled with Ross Sea drift, deposited when a thick lobe of westward-flowing ice, grounded in McMurdo Sound, blocked the valley mouth and dammed Glacial Lake Washburn (Hall et al., 2000). The drift is predominantly comprised of sediments which were deposited via a lake-ice conveyor operating on Glacial Lake Washburn, a large proglacial lake which filled central and lower Taylor Valley to around 300 m elevation from ~12.4–23.8 ka BP (Denton et al., 1989).

Consequently, the valley floors contain lacustrine sediments, and lacustrine organic material provides evidence of shorelines delineating former lake levels. Ross Sea drift is also characterised by the presence of kenyte erratics, sourced from Ross Island (Hall et al., 2000).

In the central and upper parts of the valley, advances of Taylor Glacier are recorded by at least four drift sheets. Tills are mainly comprised of granite, granodiortie, diorite, gneiss and schist of the Precambrian Ross System, with small amounts of diabase and sandstone from the Beacon Supergroup (Pastor and Bockheim, 1980). Taylor IV drift contains several units of different age, representing at least four expansions of Taylor Glacier (Wilch et al., 1993). However, these units can be difficult to distinguish, and are referred to only as Taylor IVa and Taylor IVb (Bockheim et al., 2008), with ages of <1.50 Ma and >3.47 Ma, respectively (Wilch et al., 1993). Taylor III drift is dated as 250−340 ka, and contains reworked lacustrine carbonates (Higgins et al., 2000b). Taylor II/Bonney drift (70−130 ka; Higgins et al., 2000b) extends up to around 300 m elevation on the valley walls between Lake Bonney and Canada Glacier, and is dominantly comprised of yellowish silty meltout till and gravelly sandy waterlain till (Higgins et al., 2000a). Bonney drift also contains lacustrine carbonates, which were deposited in a proglacial lake of Taylor Glacier (Hendy et al., 1979; Higgins et al., 2000b). Moraines associated with the present advance of Taylor Glacier, which flows into the western part of the valley and is currently in its most extensive Holocene position, are referred to as Taylor I (Higgins et al., 2000a). The advances of alpine glaciers in Taylor Valley are in-phase with advances of Taylor Glacier (Hendy et al., 1979; Higgins et al., 2000a); these advances are out-of-phase with westward ice-expansion up-valley from grounded ice in the Ross Sea (Hendy et al., 1979).

2.3.4 Soils

The soil-forming environment of the McMurdo Dry Valleys is characterised by hyper-arid climatic conditions, reflecting the prevailing low temperatures, low levels of precipitation, and low humidity within the valleys. The prevailing cold temperatures act to restrict the availability of water in the landscape, and dictate that, outside the short period of relative warmth in December and January, any water present is generally frozen. However, individual site factors such as aspect, parent material (through its influence on surface albedo) and proximity to glaciers or meltwater channels are also important in determining soil moisture availability. Soils developed on northerly aspects are considerably warmer than those on southerly aspects, and soils formed from darker coloured parent materials absorb more heat from incoming radiation than those formed in lighter coloured parent materials (Campbell and Claridge, 2006).

Classification

Soils of the McMurdo Dry Valleys are classified in the Gelisol soil order of Soil Taxonomy (Bockheim, 2002), with further subdivision based on soil climatic regimes and soil properties. Soils with ice-cemented permafrost within the upper 70 cm of the profile are generally cryoturbated, and are classified in the Turbel suborder, whereas soils with dry-frozen permafrost tend to have little or no evidence of cryoturbation, and are classified as Orthels (Bockheim and McLeod, 2008; Bockheim et al., 2008). The anhydrous conditions (< 50 mm annual water equivalent precipitation) prevalent throughout the Dry Valleys dictates that most soils are in Anhy- great groups; soils adjacent to lakes or meltwater streams, or in moist coastal areas are classified in Haplo- great groups.

Soils in the eastern part of Taylor Valley are generally ice-cemented, and are mapped as Typic Haploturbels (Bockheim and McLeod, 2008; Bockheim et al., 2008). In central and upper Taylor Valley, Typic Anhyorthels (containing dry-frozen permafrost) are dominant on Taylor III drift, whereas Salic and Petrosalic Anhyorthels occur on older surfaces (Bockheim and McLeod, 2008; Bockheim et al., 2008), reflecting increased salt accumulation with soil age.

Soil morphology

Soils within the McMurdo Dry Valleys are typically overlain by a thin, gravelly desert pavement. The desert pavement often contains varnished and ventifacted clasts, with the proportion of each increasing with surface age (Bockheim, 2010). Beneath the desert pavement, soils sometimes contain a horizon with vesicular porosity, which is dominated by sand and silt-sized particles that are thought to be produced by weathering, rather than via dust deposition (Bockheim, 2010). These surficial layers typically overlie gravelly sands, with the level of oxidation generally reflecting surface age (Campbell and Claridge, 1982). Soils in the Dry Valleys contain permafrost, which is ice-cemented where there is sufficient moisture, or “dry frozen” in the absence of sufficient moisture to cause cementation (Bockheim, 1980; Bockheim, 1997; Campbell et al., 1998). The spatial distribution of ice-cemented soils varies with soil age, elevation, distance inland, climatic conditions, and proximity to potential moisture sources (Campbell and Claridge, 2006). Characteristic changes in soil morphology and surface weathering features with increasing soil age are shown in Table 2.2.

Table 2.2 Changes in soil morphology and surface weathering features with increasing weathering (Campbell and Claridge, 1975).

Weathering stage	Surface rock characteristics	Soil colour	Horizon development	Salt morphology	Soil depth
1	fresh, unstained, coarse & angular	pale olive to light grey (5Y 6/3 - 7/2)	nil	absent	very shallow, underlain by ice
2	light staining, slight rounding, some disintegration	pale brown to light brownish grey (10YR 6/3-2.5Y 6/2)	weak	few flecks	shallow, underlain by ice
3	distinct polish, staining & rounding, some cavernous weathering, some ventifacts	light yellowish brown (10 YR 5/3-2.5Y 6/4)	distinct	many flecks in upper part of profile & beneath stones	moderately deep
4	boulders much reduced by rounding, crumbling & ventifaction, strongly developed cavernous weathering; staining & polish well developed; some desert varnish	yellowish brown (10YR 5/4) in upper horizons, paler in lower horizons	very distinct	in continuous or discontinuous horizon beneath surface	deep
5	few boulders, many pebbles forming pavement, extensive crumbling, staining, rounding, pitting & polish	dark yellowish brown to yelolowish red (10YR 4/4-5YR 5/8)	very distinct	in horizon 20-30 cm beneath surface & scattered throughout profile	deep
6	weathered & crumbled bedrock, very strongly stained	strong brown to yellowish red & dark red (7.5YR 5/6-5YR 4/8 or 2.5YR 3/6)	very distinct	(as for Stage 5)	shallow to deep

Salts are a prominent feature of Antarctic soils (Claridge and Campbell, 1977; Keys and Williams, 1981; Bockheim, 1997), and occur as encrustations beneath surface clasts, disseminated salt flecks within the matrix, or salt pans (Campbell and Claridge, 1982). A morphogenetic sequence of soluble salt accumulation in cold desert soils has been defined (Bockheim, 1990; Table 2.3). This sequence enables comparisons of relative age to be made between soils with varying salt accumulations, although the influence of local climate must be carefully considered, as salts can be readily leached in areas with greater moisture availability (Toner et al., 2013). Nonetheless, salt encrustations are more common in older soils, evident as indurated pans at their maximum expression (Campbell and Claridge, 1975; Bockheim, 1990).

Table 2.3 Morphogenetic stages of accumulation of soluble salts in Cold Desert soils (Bockheim, 1990).

Salt stage	Maximum salt morphology	Electrical conductivity (dS/m)	Numerical age
0	None	<0.6	<10 ka
I	Coatings on stone bottoms	0.6-5.0	10−18 ka
II	Few flecks (<20% of surface area has flecks 1 – 2 mm in diameter)	5−18	18−90 ka
III	Many flecks (>20% of surface area has flecks 1 – 2 mm in diameter)	18−25	90−200 ka
IV	Weakly cemented pan	25−40	250−? ka
V	Strongly cemented pan	40−60	~ 1.7−2.5 Ma
VI	Indurated pan	60−100+	~ >2.5 Ma

Chemical properties

Chemical weathering processes are limited by the cold, dry climatic conditions, although oxidation of parent materials and precipitation of secondary minerals does occur (Claridge, 1965; Campbell and Claridge, 1975; Keys and Williams, 1981; Bockheim, 1997). The dominant soil-forming processes occurring are salinisation and oxidation (Bockheim, 1990).

Soil pH values range from neutral to alkaline (Bockheim, 1980), depending on the balance between acidic salts derived from atmospheric deposition, and alkaline salts derived from local marine inputs (Claridge and Campbell, 1977). Consequently, trends in soil pH are closely related to the distribution of salts. Higher pH values are measured in coastal zones where marine influxes are dominant, whereas lower pH values measured inland reflect the influence of atmospheric deposition on soil salt composition (Claridge and Campbell, 1977; Keys and Williams, 1981). Electrical conductivity, which is a proxy for saltiness, varies according to age and soil moisture regime. The dominant cation in 1:5 soil:water extracts of soils older than 18 ka is sodium (Bockheim, 1980); this further highlights the

arid nature of the soil-forming environment, with the low levels of soil moisture effectively preserving the presence of soluble salts.

Soluble salts

Salt input and migration can be considered one of the few active and enduring processes occurring in the hyperarid environment of the Dry Valleys (Bao et al., 2008). The stability of the landscape over long timescales means that analysis of salts within the soils provides opportunities to investigate processes controlling the distribution of salts in the landscape, as well as the sources of salts and their post-depositional transformations and translocations.

Salts present within soils of the McMurdo Dry Valleys are predominantly chlorides, nitrates and sulfates of sodium, potassium, calcium and magnesium (Claridge and Campbell, 1977; Keys and Williams, 1981). Early studies of the origin of these salts concluded that calcium, magnesium and potassium are largely derived from rock weathering, and sodium is predominantly of marine origin. Chlorides, nitrates and sulfates were also considered to be of marine origin, with nitrate and sulfate predominantly derived from atmospheric circulation, and chloride from local air masses (Claridge and Campbell, 1977).

More recent studies (e.g. Michalski et al., 2005; Bao and Marchant, 2006; Bao et al., 2008) have utilised stable isotope ratios of anions to quantitatively determine their origins. The oxygen isotopic composition of nitrates in soils of the Dry Valleys indicates that their source is solely atmospheric in origin, comprising roughly equal proportions of atmospheric nitrate from the troposphere, and stratospheric HNO_3 (Michalski et al., 2005). These salts are transported to Dry Valley soils either by oceanic air masses moving up-valley, or by down-valley katabatic winds picking up nitrates deposited on the polar plateau (Michalski et al., 2005). Given the general trend of increasing nitrate concentrations with distance inland and soil age (Claridge and Campbell, 1977; Keys and Williams, 1981; Bockheim, 1997), it appears that transport via katabatic winds off the polar plateau accounts for the majority of nitrate deposition in the Dry Valleys.

A study of the isotopic composition of sulfates in soils of the McMurdo Dry Valleys revealed three components contribute to the total sulfate content of soils. Sea-salt sulfate and background sulfate, derived from weathering and volcanic sources, are more abundant in coastal zones, whereas non-sea-salt sulfate, which predominantly consists of photochemically generated sulfate derived from the oxidation of dimethylsulfide, dominates in soils of the upland valleys (Bao and Marchant, 2006).

By investigating the isotopic composition of chloride, Bao et al. (2008) identified two major sources of chloride: airborne sea-salt chloride, and secondary atmospheric chloride. They also found that chloride distribution within the Dry Valleys is explained by the balance between continuous influx

from atmospheric deposition and variable outflux through leaching. Chloride influx decreases inland, as the dominant sea-salt component is transport-limited (Claridge and Campbell, 1977; Keys and Williams, 1981; Bao et al., 2008). Similarly, chloride outflux decreases inland, as soil temperatures decrease with increasing distance (and elevation) from the coast, thereby limiting moisture availability and thus potential for leaching. Interestingly, chloride concentrations were relatively low in both the coastal thaw and stable upland zones, and highest (yet highly variable) in the inland mixed zone (Bao et al., 2008). This distribution can be explained by relatively high rates of leaching in the moist coastal thaw zone, and relatively low inputs of chloride in the stable upland zone. The high concentrations measured in the inland mixed zone show that the rate of chloride influx exceeds the rate of outflux via leaching.

The leaching of chloride in relatively moist coastal zones enables the typically high soil pH values measured in coastal areas to be explained. So long as liquid moisture is present, there is effectively an unlimited supply of HCO_3^- via dissolution of CO_2 in soil solution. Na^+ from local sea-salt aerosolic deposition is relatively abundant, hence $NaHCO_3^-$ is readily formed. This reaction displaces calcium, available in relatively small quantities via rock weathering (Claridge and Campbell, 1977; Keys and Williams, 1981), calcite dissolution (Toner et al., 2013) or aerosolic dust inputs (Foley et al., 2006), which is likely to be leached with chloride ions as Ca-Mg-Cl brines (Toner et al., 2013). The presence of $NaHCO_3^-$ acts to increase soil pH to values above 8.34 (the pH that can be generated by the presence of calcium carbonate alone). In soils of the stable upland zone, chloride concentrations are low, moisture is generally absent, and consequently, soil pH values are lower.

Carbon

Soil organic C contents are very low, typically ranging between 0.01 and 0.05% (Burkins et al., 2001). Inorganic C concentrations are an order of magnitude greater than organic C concentrations, ranging from 0.02 to 0.3% (Burkins et al., 2001; Foley et al., 2006), thus constituting the largest terrestrial C pool in ice-free areas of Antarctica.

Two different models of C cycling have been proposed for the McMurdo Dry Valleys. The “legacy model” suggests that organic matter present at lower elevations in the Dry Valleys is a legacy of ancient glacial tills and lacustrine systems, and organic matter at higher elevations is a result of long-term *in situ* autotrophic activity in soils (Burkins et al., 2000). An alternative “spatial subsidies model” proposes that present lakes provide the dominant source of organic matter which is subsequently distributed around the valleys by wind (Elberling et al., 2006). This model, however, acknowledges that the two hypotheses are not mutually exclusive, with C present in Dry Valley soils perhaps being partially sourced from ancient lakes as well as receiving a modern subsidy, with the relative

proportions from each source likely influenced by valley size and the proportion of the valley occupied by lakes (Elberling et al., 2006).

Attempts to constrain the relative importance of legacy effects on C cycling in Dry Valley ecosystems have been impeded by the lack of conspicuous sources of legacy organic matter (Hopkins et al., 2009). As such, the isotopic composition of soil organic matter continues to provide a useful indication as to its origin, but cannot definitively provide an indication as to its relative age. Soils on valley floors are predominantly characterised by lacustrine-derived organic matter, reflecting either the influence of large paleolakes or contemporary lakes within the valleys, whereas soils at higher elevations tend to have organic matter signatures characteristic of endolith-derived organic matter (Burkins et al., 2000; Hopkins et al., 2009).

Current estimates of C turnover times in the McMurdo Dry Valleys derived from *in situ* soil CO_2 flux rates are between 23 and 123 years (Burkins et al., 2001; Elberling et al., 2006). Such rapid turnover times suggest that there would be no legacy C remaining in the soils. However, these estimates are based on measured CO_2 effluxes which are assumed to be biologically driven.

Biota

Despite climatic conditions appearing unfavourable for life, diverse biological communities exist in the lakes, streams and soils (Fountain et al., 1999). Such communities are adapted for survival in biologically extreme conditions including freeze-thaw cycles, high winds (Fountain et al., 1999), prolonged low temperatures, hypersalinity, total darkness during winter and exposure to high intensities of solar radiation during summer, and low levels of moisture and organic C.

Soil organisms in the Dry Valleys are limited to microorganisms and a few invertebrate species (nematodes, rotifers, tardigrades, springtails and mites; Adams et al., 2006). Springtails and mites are the largest terrestrial invertebrates, but nematodes are the most abundant invertebrates in the Dry Valleys (Freckman and Virginia, 1997; Treonis et al., 1999; Treonis and Wall, 2005). The distribution of nematodes across a wide range of soil habitats is enhanced by their ability to undergo anhydrobiosis, a survival strategy induced by desiccation (Treonis et al., 2000; Treonis and Wall, 2005).

The low-complexity ecosystems of the Dry Valleys provide opportunities to investigate factors controlling ecosystem structure and function in the absence of vascular plants. Recent studies have shown that the distribution and diversity of biota within Dry Valley terrestrial ecosystems is largely controlled by abiotic factors, with soil moisture content and salinity identified as key factors over a range of sites (Barrett et al., 2004; Smith et al., 2010; Lee et al., 2012; Magalhães et al., 2012; Stomeo et al., 2012; Van Horn et al., 2013).

2.3.5 CO_2 fluxes

Respiration

Previous studies of soil respiration in Dry Valley ecosystems have been conducted in order to quantify the turnover time of the soil organic C pool (Burkins et al., 2001; Barrett et al., 2006a; Elberling et al., 2006), and to provide a basis for comparing ecosystem functioning between sites (Barrett et al., 2006b). Surface CO_2 fluxes in the McMurdo Dry Valleys generally range from −0.1 to 0.15 μmol CO_2 m^{-2} s^{-1} (e.g. Burkins et al., 2001; Parsons et al., 2004; Elberling et al., 2006; Ball et al., 2009), although at sites with higher C and moisture contents, rates can be as high as 0.78 μmol CO_2 m^{-2} s^{-1} (Gregorich et al., 2006). Previous studies have generally focused on relating soil respiration rates to environmental variables such as soil temperature and moisture content (Parsons et al., 2004; Elberling et al., 2006; Gregorich et al., 2006) and observing responses to *in situ* (Burkins et al., 2001; Ball et al., 2009) and laboratory manipulations (Burkins et al., 2001; Treonis et al., 2002; Parsons et al., 2004; Barrett et al., 2005, 2006a; Elberling et al., 2006; Hopkins et al., 2006; Hopkins et al., 2008; Hopkins et al., 2009).

Studies of Dry Valley soil respiration have generally been predicated on the basis that, as in temperate environments, CO_2 fluxes are biologically produced, and the maximum rate of CO_2 production occurs during the warmest part of the day. However, as the diversity, abundance and activity of biota that inhabit Dry Valley soil ecosystems is comparatively low, and largely controlled by abiotic factors (Barrett et al., 2004; Lee et al., 2012; Magalhães et al., 2012; Stomeo et al., 2012; Van Horn et al., 2013), this assumption may not necessarily be valid, and therefore needs to be tested. Additionally, none of the previous measurements of soil CO_2 flux in the McMurdo Dry Valleys have identified the depths at which CO_2 production occurs, and have therefore not considered potential lags between CO_2 production rate and surface CO_2 flux.

However, studies of soil CO_2 flux rates over several diel cycles by Parsons et al. (2004) and Ball et al. (2009) found that soil CO_2 fluxes in the McMurdo Dry Valleys follow diel variations, with changes in soil temperature accounting for almost half of the variation in CO_2 flux (Ball et al., 2009). Both authors conclude that soil CO_2 flux is strongly influenced by abiotic factors, and suggest that dissolution of CO_2 in water, consistent with Henry's Law, is the likely explanation for the diel variation observed.

Discriminating between biotic and abiotic processes using stable carbon isotopes

An abiotic contribution to soil CO_2 fluxes has potentially profound implications for interpretation of the fluxes in terms of soil respiration and C cycling in the McMurdo Dry Valleys. Investigating the isotopic composition of surface CO_2 fluxes and subsurface soil CO_2 profiles is one way of determining the extent to which Henry's Law-controlled dissolution and exsolution of CO_2 can account for Parsons

et al. (2004) and Ball et al.'s (2009) observed diel variation in surface CO_2 flux rates. By using a mixing model that incorporates the isotopic composition of two end members, namely biotically and abiotically-produced CO_2, the proportion of biotic and abiotic processes that contribute to measured surface CO_2 fluxes can be quantified.

Natural abundance isotope studies of soils from the McMurdo Dry Valleys have been used to trace the provenance of organic material within the soils (e.g. Burkins et al., 2000; Hopkins et al., 2009), and in laboratory studies of organic matter decomposition (Hopkins et al., 2009), but no field studies have incorporated isotopic analyses of soil CO_2 samples. The only profile gas concentrations measured in the McMurdo Dry Valleys are from Gregorich et al.'s (2006) study of relatively moist, organic-rich lakeshore soils in Garwood Valley, where high levels of CO_2 (up to 5550 µL L^{-1}) were measured at 5 and 10 cm depth. The isotopic composition of the CO_2 was not determined.

$\delta^{13}C$ values associated with biotic CO_2 production and consumption

Biotic production and consumption of CO_2 and the abiotic dissolution/exsolution processes outlined above produce distinctive $\delta^{13}C_{CO2}$ values. Biological respiration produces $\delta^{13}C_{CO2}$ values that reflect the $\delta^{13}C$ of the source organic material (Dörr and Münnich, 1980), as respiration does not (or only to a minor extent) discriminate against ^{13}C. In soils of the McMurdo Dry Valleys, sources of soil organic C have values that range between −10 and −19‰ for lacustrine detritus and from −22 to −30.5‰ for moss and endolith-derived organic matter (Burkins et al., 2000; Hopkins et al., 2009). Any CO_2 produced by biological respiration would have a similarly depleted $\delta^{13}C_{CO2}$ value. In contrast, consumption of CO_2 via algal photosynthesis would enrich soil $\delta^{13}C_{CO2}$ values, as preferential uptake of $^{12}CO_2$ by photosynthetic organisms acts to concentrate the heavier $^{13}CO_2$ in the soil atmosphere (Park and Epstein, 1960). However, given that photosynthesis, by definition, requires light in order to occur, such processes can be readily eliminated at depths beneath the soil surface.

$\delta^{13}C$ values associated with abiotic CO_2 production and consumption

The fractionation of soil CO_2 associated with dissolution and exsolution processes suggests that any abiotically-produced CO_2 will be of substantially different isotopic composition to that of biologically-produced CO_2. This means that a 2-component mixing model should be able to be used to determine the relative proportions of biotic and abiotic processes contributing to soil CO_2 fluxes in Dry Valley soils. At pH values >9, dissolved inorganic C species are dominated by the HCO_3^- and CO_3^{2-} forms (Stumm and Morgan, 1996), and equilibrium fractionation of CO_2 gas to HCO_3^- and CO_3^{2-} results in a ~ −10‰ depletion of CO_2 gas relative to HCO_3^- or CO_3^{2-} (Thode et al., 1965; Mook et al., 1974; Table 2.1). Therefore, dissolution of CO_2 in soil water to form HCO_3^- and CO_3^{2-} (at high soil pH values and relatively low soil temperatures typical of Dry Valley soils) would result in the depletion of $\delta^{13}C_{CO2}$ in

the soil atmosphere. Conversely, exsolution of CO_2 would lead to enrichment of $\delta^{13}C_{CO2}$ in the soil atmosphere.

2.4 Research gaps

This review has established that Dry Valley soil CO_2 fluxes have the potential to be strongly influenced by abiotic factors, with Parsons et al. (2004) and Ball et al. (2009) suggesting Henry's Law-controlled dissolution and exsolution of CO_2 as a driving mechanism. However, as yet there has been no attempt to quantify the potential abiotic contribution to CO_2 fluxes in Dry Valley soils, and thereby test the assumption made in previous studies that Dry Valley soil CO_2 fluxes are biologically produced.

This study aims to characterise and quantify the detailed variations in surface CO_2 flux rates and subsurface CO_2 concentration and $\delta^{13}C_{CO2}$ profiles at two sites with contrasting organic C inputs. This research extends previous work on Dry Valley soil CO_2 fluxes by using high-resolution measurements of surface CO_2 flux rate and, for the first time, subsurface CO_2 concentration and $\delta^{13}C_{CO2}$ profiles in order to link surface and subsurface soil CO_2 dynamics, and to discriminate between biotic and abiotic sources of CO_2.

The research presented in this thesis will contribute to an improved understanding of the factors and processes governing CO_2 fluxes in Dry Valley soils by addressing the following research questions:

- Can exsolution and dissolution of CO_2 in accordance with Henry's Law account for diel variation in surface CO_2 flux rates (Chapter 3)?
- What are the environmental controls on biotic and abiotic CO_2 production in soils with contrasting organic C supplies (Chapters 4 and 5)?
- What are the relative contributions of biotic and abiotic processes to soil CO_2 fluxes in 1) a dry soil with low organic C content, which is representative of "typical" Dry Valley soils (Chapter 4), and 2) a soil with relatively high levels of organic C, which is characteristic of a biological "hotspot" (Chapter 5)?

Chapter 3

Abiotic processes dominate CO_2 fluxes in Antarctic soils

This chapter is written as a manuscript, and has been published in *Soil Biology and Biochemistry*. The citation is as follows:

Shanhun, F.L., Almond, P.C., Clough, T.J., Smith, C.M.S., 2012. Abiotic processes dominate CO_2 fluxes in Antarctic soils. Soil Biology & Biochemistry, 53: 99−111. doi:10.1016/j.soilbio.2012.04.027.

3.1 Abstract

Ecosystems within the McMurdo Dry Valleys of Antarctica are highly sensitive to environmental change. Increases in soil temperature and/or moisture content may dramatically change rates of soil respiration and soil carbon (C) turnover. Present estimates of soil respiration rates and C turnover times are based on surface carbon dioxide (CO_2) fluxes and soil organic C content. However, the assumption that surface CO_2 fluxes are purely biological in origin has not been rigorously tested. This study uses concentration and, for the first time, the stable C isotopic composition of surface soil CO_2 fluxes and subsurface CO_2 profiles to: 1) examine mechanisms of soil CO_2 uptake and release, 2) identify the location of potential CO_2 sources and sinks within the soil profile, and 3) discriminate between biotic and abiotic contributions to CO_2 fluxes in soils of Taylor Valley. Surface CO_2 fluxes and subsurface CO_2 profiles confirm that these soils take up and release CO_2 on a daily basis (during the austral summer), associated with small changes in soil temperature. Shifts in the C isotopic composition of soil CO_2 are inconsistent with biological mechanisms of CO_2 production and consumption. Instead, the isotopic shifts can be accounted for by Henry's Law dissolution and exsolution of CO_2 into a solution of high pH, driven by changes in soil temperature. The results constrain the biological component of soil CO_2 fluxes in Taylor Valley to less than 25% (and likely to be significantly less). This finding implies that previous measurements of surface soil CO_2 fluxes are overestimates of soil respiration, thus C turnover times calculated from them are underestimates. Discriminating between biotic and abiotic contributions to CO_2 fluxes in Antarctic Dry Valley soils is essential if the effects of climate change on these sensitive ecosystems are to be accurately identified.

3.2 Introduction

Predicting the impact of changes in climate conditions on Antarctic ice-free areas necessitates a detailed understanding of the rates and dynamics of processes operating in these extreme environments. Previous studies of soil respiration in Antarctic ecosystems have been conducted in order to quantify the turnover time of the soil organic carbon (C) pool (Burkins et al., 2001; Barrett et al., 2006a; Elberling et al., 2006), and to provide a basis for comparing ecosystem functioning between sites (Barrett et al., 2006b). Investigations of Antarctic soil respiration rates have also provided insight into the physical controls on soil carbon dioxide (CO_2) flux (Parsons et al., 2004) and the effects of climate variation on C cycling (Ball et al., 2009) in dry valley ecosystems. Surface CO_2 fluxes in the Dry Valleys generally range from −0.1 to 0.15 μmol CO_2 m^{-2} s^{-1} (e.g. Burkins et al., 2001; Parsons et al., 2004; Elberling et al., 2006; Ball et al., 2009), although at sites with higher C and moisture contents, rates can be as high as 0.78 μmol CO_2 m^{-2} s^{-1} (Gregorich et al., 2006). Previous studies have generally focused on relating soil respiration rates to environmental variables such as soil temperature and moisture content (Parsons et al., 2004; Elberling et al., 2006; Gregorich et al., 2006) and observing responses to *in situ* (Burkins et al., 2001; Ball et al., 2009) and laboratory manipulations (Burkins et al., 2001; Treonis et al., 2002; Parsons et al., 2004; Barrett et al., 2005, 2006a; Elberling et al., 2006; Hopkins et al., 2006; Hopkins et al., 2008; Hopkins et al., 2009).

Studies by Parsons et al. (2004) and Ball et al. (2009) found that soil CO_2 fluxes in the McMurdo Dry Valleys follow diel variations, with soil temperature accounting for almost half of the variation in CO_2 flux (Ball et al., 2009). Both authors conclude that soil CO_2 flux is strongly influenced by abiotic factors, and suggest that dissolution of CO_2 in soil water, consistent with Henry's Law, is the likely explanation for the diel variation observed. This is in contrast to many other ecosystems, where temperature predominantly influences biotic factors.

An abiotic contribution to soil CO_2 flux has potentially profound implications for interpretation of CO_2 fluxes in terms of soil respiration and C cycling in the McMurdo Dry Valleys. Present estimates of turnover times based on *in situ* soil respiration rates are between 23 – 130 years (Burkins et al., 2001; Elberling et al., 2006). Any abiotic contributions to CO_2 fluxes would mean that soil respiration rates overestimate the biological contributions, and turnover times calculated from such fluxes would be underestimates.

This chapter presents data from a study aimed to advance the mechanistic understanding of the processes governing CO_2 fluxes in Antarctic soils. Surface soil CO_2 fluxes and subsurface soil CO_2 concentration profiles were used to characterise diel soil CO_2 dynamics, and identify potential CO_2 sources and sinks within the soil profile. This enabled the hypothesis of Ball et al. (2009) and Parsons et al. (2004) to be tested by: 1) comparing measured subsurface soil CO_2 concentrations with values

simulated by a model that incorporates Henry's Law dissolution of CO_2, and 2) quantifying the biotic and abiotic components of soil CO_2 by utilising the contrasting relationships between concentration and C isotopic composition of soil CO_2 ($\delta^{13}C_{CO2}$) characteristic of biotic and abiotic processes.

3.3 Materials and Methods

3.3.1 Study area

The study was conducted during the 2008/09 austral summer at two sites in Taylor Valley, in the McMurdo Dry Valleys, Antarctica. The McMurdo Dry Valleys are the largest ice-free region in Antarctica (4500 km^2; Levy, 2013) and comprise a polar desert landscape dominated by coarse-textured soils formed in glacial drift, interspersed with alpine glaciers, ephemeral streams, and perennially ice-covered lakes. Vascular vegetation is absent, and biota consist of microorganisms and a limited number of invertebrate species (Adams et al., 2006; Cary et al., 2010). Mean annual air temperature in Taylor Valley ranges from −14.8°C to −23.1°C (Doran et al., 2002a), and annual water-equivalent precipitation is < 50 mm, with snow transported by katabatic winds supplying up to another 50 mm (water-equivalent) to the valley floor (Fountain et al., 2010).

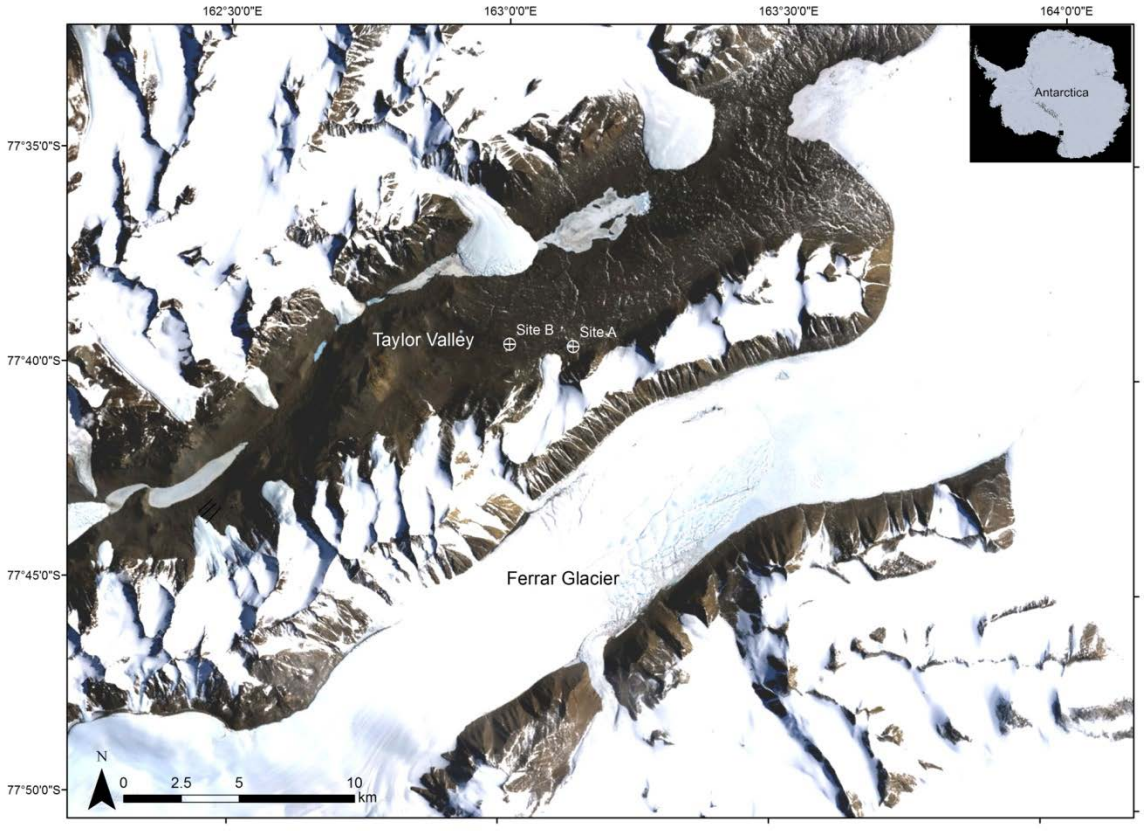

Figure 3.1 Location of Sites A and B, Taylor Valley, Antarctica.

Site A was on relatively young glacial drift (Ross Sea Drift, ~ 9 − 28 ka; Hall and Denton, 2000), adjacent to a small lake (~0.05 km^2; known as Spaulding Pond) situated 700 m east of Howard Glacier (77° 39.572'S, 163° 07.394'E; Figure 3.1). This site was selected to provide soils with relatively low salt concentrations and higher inputs of organic C. During summer, when a moat forms around the edge of the lake, algae are driven to the lake margins by winds and are eventually blown onshore, providing a local source of organic C (Figure 3.2). Soils at Site A are weakly developed, strongly cryoturbated, and contain ice-cemented permafrost within 70 cm of the soil surface (Typic Haploturbels; Bockheim et al., 2008). At the time of sampling (late December 2008), soils at Site A were ice-cemented below 35 cm depth.

Site B was on an older moraine crest (Taylor III Drift, 250 − 340 ka; Higgins et al., 2000b), approximately 1.5 km west of Howard Glacier (77° 39.540'S, 163° 00.484'E). Soils at Site B were expected to have higher salt concentrations due to their age, and lower organic C levels as there was no lake nearby to provide a local source of organic material (Figure 3.3). Soils formed in Taylor III drift are mapped as Typic Anhyorthels (Bockheim et al., 2008), which by definition should not contain ice-cemented permafrost in the upper 70 cm of the profile. However, soils at Site B had a similar morphology to those at Site A (Figure 3.4; Typic Haploturbels), and were ice-cemented below 26 cm depth. Both sites were characterised by patterned ground comprised of flat-centred polygons measuring approximately 15 x 15 m.

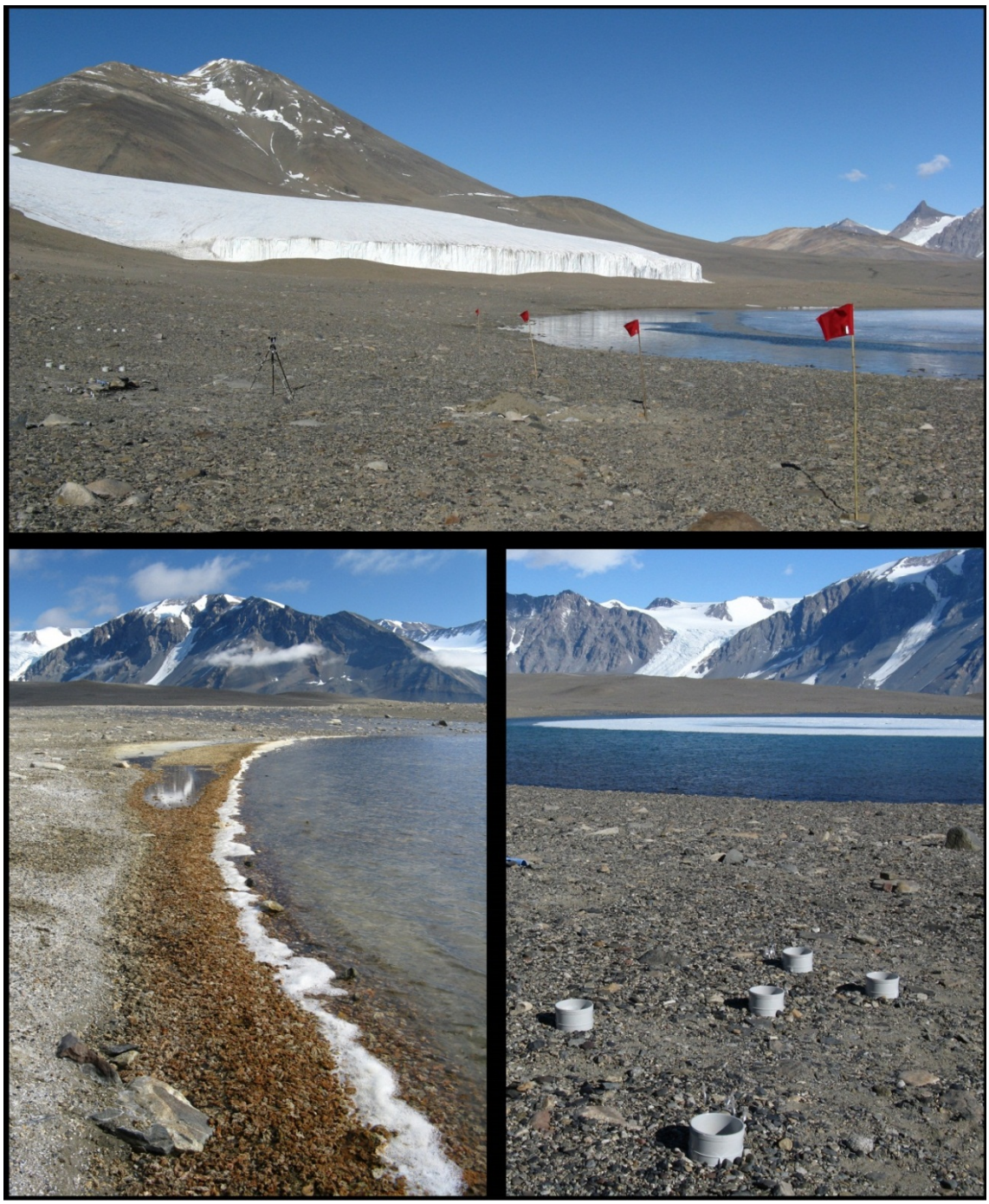

Figure 3.2 Site A, lower Taylor Valley. Clockwise from top: view west to gas sampling area and Howard Glacier; headspace chambers with Spaulding Pond in the background; algae accumulating at the edge of Spaulding Pond.

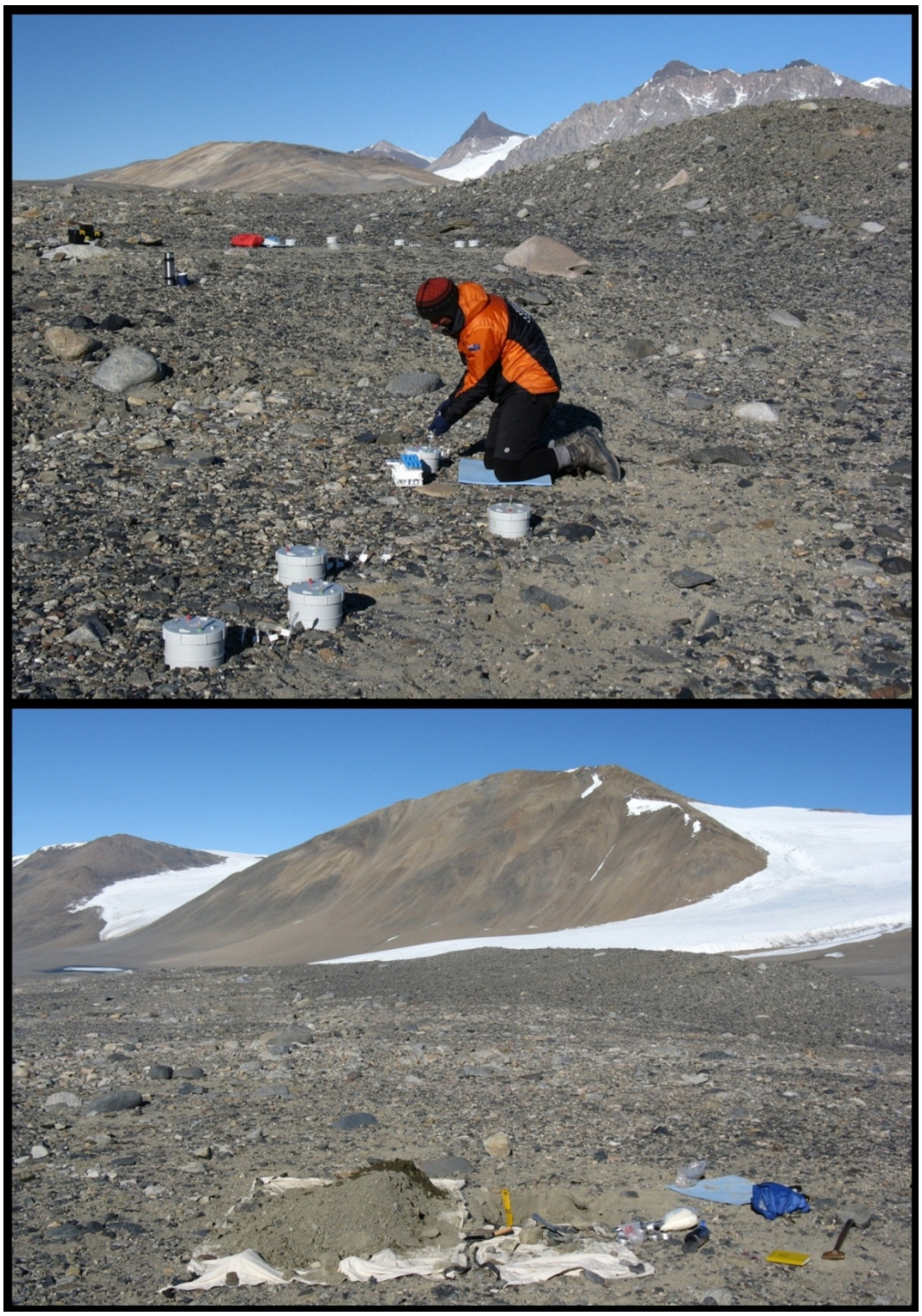

Figure 3.3 Site B, lower Taylor Valley. Top: view west showing gas sampling chambers and tubes. Bottom: view south-east showing soil pit on broad moraine crest. Site A is located next to the lake in the distance on the left hand site of the photo.

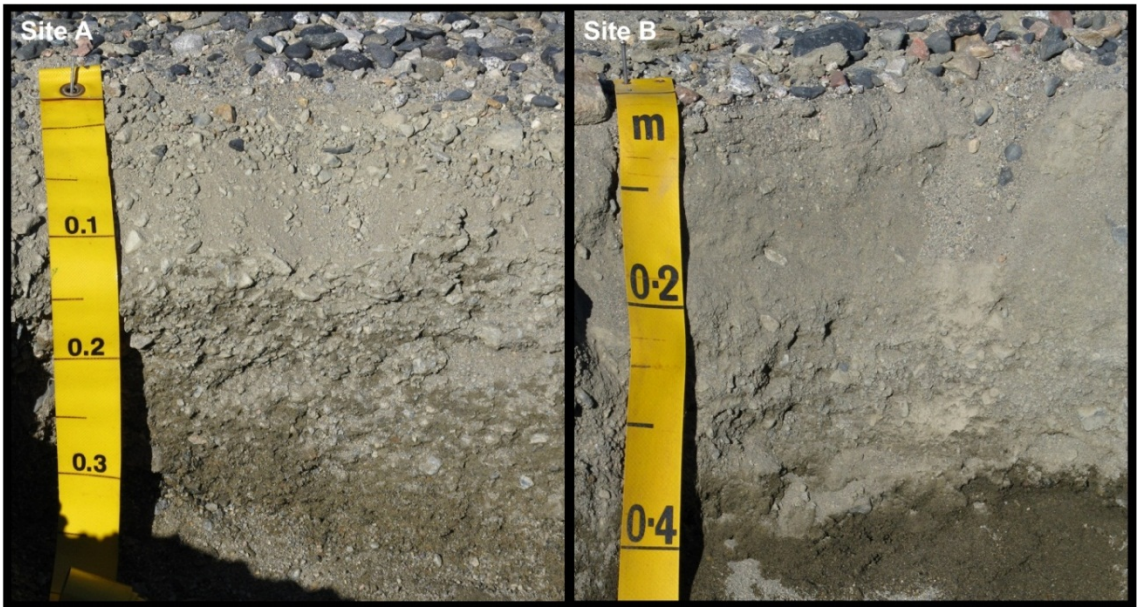

Figure 3.4 Soils (Typic Haploturbels) at Site A and Site B. At the time of sampling (late December 2008), soils at Sites A and B were ice-cemented below 35 and 26 cm, respectively. The profile shown for Site B has been deepened with a concrete breaker and is moistened from melting of ice-cemented permafrost.

3.3.2 Soil temperature and moisture content measurements

Soil temperature and moisture content at 5, 15 and 25 cm depth were measured using Hydra Probes (Hydra Probe II, Stevens Water Monitoring Systems Inc., Portland, Oregon, USA). An intermittent fault occurred in the probe installed at 5 cm depth at Site A; data from this probe are only available for one of the CO_2 sampling periods. Surface air temperature was measured 2 mm above the soil surface (CS215-L, Campbell Scientific Inc., Logan, Utah, USA). All data were recorded every 2 minutes, with 20 minute averages calculated and logged by a CR 1000 data logger (Campbell Scientific Inc., Logan, Utah, USA).

3.3.3 Soil CO_2 sampling

Soil CO_2 sampling was replicated in two adjacent polygons at each site. Within each polygon, five opaque tubes (iPLex® Novadrain uPVC access tubes – 15 cm diameter by 16 cm high; iPLEX® DWV 136.150) were pressed into the soil surface to a depth of 6 cm. An opaque uPVC lid (iPLEX® DWV 136C.150) with an internal rubber O-ring, drilled to fit a pressure release bung and an injectable septum (Baxter Interlink Injection Site Ref #2N3399K), was screwed on to the tubes immediately before surface CO_2 flux sampling. This created a chamber with a mean effective headspace of 0.0018 m^3. In order to determine soil surface CO_2 fluxes, 20 ml gas samples were taken from the headspace chambers immediately after the chamber lids were fitted and vented, with three subsequent

samples taken at 20 min intervals over a 1 h period. Surface CO_2 fluxes were calculated based on headspace CO_2 concentrations during the 1 h sampling period using the following equation:

$$n_{CO_2} = [CO_2] \frac{PV}{RTA} \quad (3.1)$$

where n_{CO2} is the number of moles of CO_2 emitted per m^2 (µmol m^{-2}), [CO_2] is headspace CO_2 concentration (µL L^{-1}), P is atmospheric pressure (101325 Pa), V is the chamber volume (m^3), R is the ideal gas constant (8.314 J K^{-1} mol^{-1}), T is air temperature (K), and A is the area covered by the chamber (0.0177 m^2). Surface CO_2 flux rates (µmol m^{-2} s^{-1}) were calculated by linear regression of surface CO_2 fluxes (µmol m^{-2}) against time over which samples were collected (s). Linear regression was also used to determine the rate of change of $\delta^{13}C_{CO2}$ (‰ min^{-1}) in the headspace chamber samples.

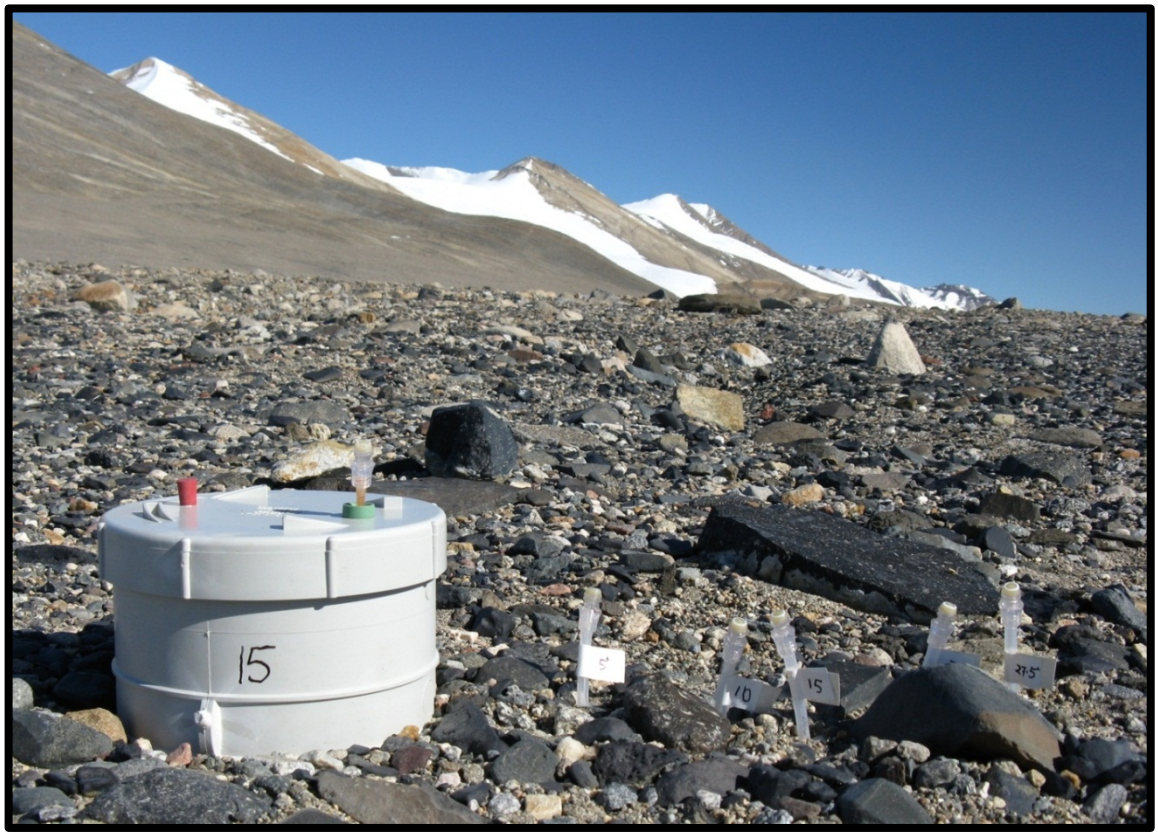

Figure 3.5 Static headspace chamber and subsurface sampling tubes, Site B, Taylor Valley.

Soil CO_2 sampling began > 96 h after installation of equipment. Gas samples were taken during the warmest and coolest periods of the day, based on surface air temperature measurements at each site, on two days in late December 2008. Site B was only sampled during one “cold” period due to an

error in determining the timing of the coldest part of the day. All CO_2 samples were taken using gas-tight syringes (BD 30 ml syringe; Ref 309650) fitted with 3-way stopcocks (Baxter 2C6201) and 26G ½" needles (BD PrecisionGlide). Samples were injected into evacuated (0 atm) 12 ml vials (Exetainers®, Labco Inc., UK) fitted with additional polytetrafluoroethylene (PTFE) septa (Supelco Analytical, USA) to maintain sample integrity (Rochette and Bertrand, 2003; Knohl et al., 2004), and stored in insulated containers prior to transport back to New Zealand. All samples were analysed for CO_2 concentration and $\delta^{13}C_{CO2}$ using a trace gas module (TGII, Sercon Ltd., Cheshire, UK) connected to a continuous flow isotope ratio mass spectrometer (Sercon Ltd., Cheshire, UK). The $\delta^{13}C$ values are expressed in parts per thousand (‰) enrichment or depletion of ^{13}C, relative to Vienna Pee Dee Belemnite (VPDB). Soil profile CO_2 samples were analysed at Lincoln University, New Zealand (within 4 months of being collected), and surface CO_2 flux samples at the University of California Davis Stable Isotope Facility, California, USA (within 8 months of being collected). Standard reference gas samples were also collected in the field following surface CO_2 flux and subsurface CO_2 sampling, and were analysed with the samples. The standards showed no sign of storage effects. The analytical precision of CO_2 concentration and $\delta^{13}C$ values was ≤5 ppm and ≤0.1‰, respectively.

3.3.4 Soil sampling, physical and chemical analyses

In polygons adjacent to CO_2 sampling sites, soil pits were dug by hand to ice cement, and deepened to a minimum of 55 cm depth using a concrete breaker to penetrate ice-cemented material. Soils were described and classified using USDA nomenclature before being sampled volumetrically (500 cm^3) at 5 cm contiguous intervals to 50 cm depth. All samples were returned to New Zealand where they were air-dried, and weighed to determine bulk density (ρ_b) before being sieved (< 2 mm). All chemical analyses were performed in duplicate on the < 2 mm fraction.

Soil pH and electrical conductivity were determined on a 1:5 soil: deionised water suspension (United States Salinity Laboratory Staff, 1954). Samples were subsequently filtered through 0.45 µm syringe filters (Advantec MFS-25) to remove suspended sediment prior to analysing for cations and anions. Cations were determined by inductively coupled plasma optical emission spectroscopy (720-ES, Varian, Melbourne, Australia) and anions by ion exchange chromatography (DX-120, Dionex, Sunnyvale, California, USA). Total C and nitrogen (N) contents of solid samples were determined on a finely ground (< 50 µm) subsample of the < 2 mm fraction. Samples were combusted at 1000°C using a Europa ANCA-GSL CN analyser connected to a continuous flow isotope ratio mass spectrometer which also determined $\delta^{13}C$ and $\delta^{15}N$ values (Sercon Ltd., Cheshire, UK). The $\delta^{13}C$ and $\delta^{15}N$ values are expressed relative to VPDB and atmospheric N_2, respectively. Two separate runs were performed in order to obtain total soil $\delta^{13}C$ and organic $\delta^{13}C$ values, and to enable calculation of soil inorganic C content. Samples analysed for total soil C, N, $\delta^{13}C$ and $\delta^{15}N$ were not subjected to any treatment.

Samples analysed for organic $\delta^{13}C$ and total organic C content were fumigated with HCl to remove all inorganic C prior to analysis. Subsamples of the finely ground fraction were put into small glass vials, moistened with deionised water, and placed in a vacuum dessicator containing a beaker with 100 ml of concentrated (12 *M*) HCl for 12 h (Harris et al., 2001). Samples were then dried at 60°C, cooled in a desiccator and capped tightly prior to being weighed into tin capsules for analysis. Soil inorganic C contents were calculated by subtracting the total C content of the HCl fumigated samples from the total C values obtained from the untreated samples.

3.3.5 Statistical analyses

Principal component analysis (PCA) was used to identify the main components influencing the variance in soil chemical properties with depth and between sites. PCA was completed using the function princomp() in R 2.11.1 (The R Foundation). Linear regression was used in Microsoft Excel® 2007 to determine surface CO_2 fluxes and the rate of change in $\delta^{13}C_{CO2}$ in surface flux samples.

3.4 Results

3.4.1 Environmental variables

At the time of sampling (late December 2008), soils at Sites A and B were ice-cemented below 35 and 26 cm, respectively, although soil temperatures during the sampling periods were very similar at both sites (Figure 3.6A and Figure 3.7A). The strongest vertical soil temperature gradients occurred during “warm” sampling periods, with soil temperatures reaching 13−14°C at 5 cm depth, and 1.3−2.6°C at 25 cm depth. During “cold” sampling periods, soil temperature gradients were lower, with temperatures ranging from ~0.5°C at 5 cm depth to ~1.6−3.6°C at 25 cm depth. The progressively greater lag in soil temperature response to surface heating with increasing depth in the profile meant that soil temperatures at 25 cm depth during the “cold” sampling period were slightly warmer than those measured during the “warm” sampling period. The rate of change in soil temperature during warm and cold sampling periods was always greatest at 5 cm depth, and decreased with depth in the soil profile.

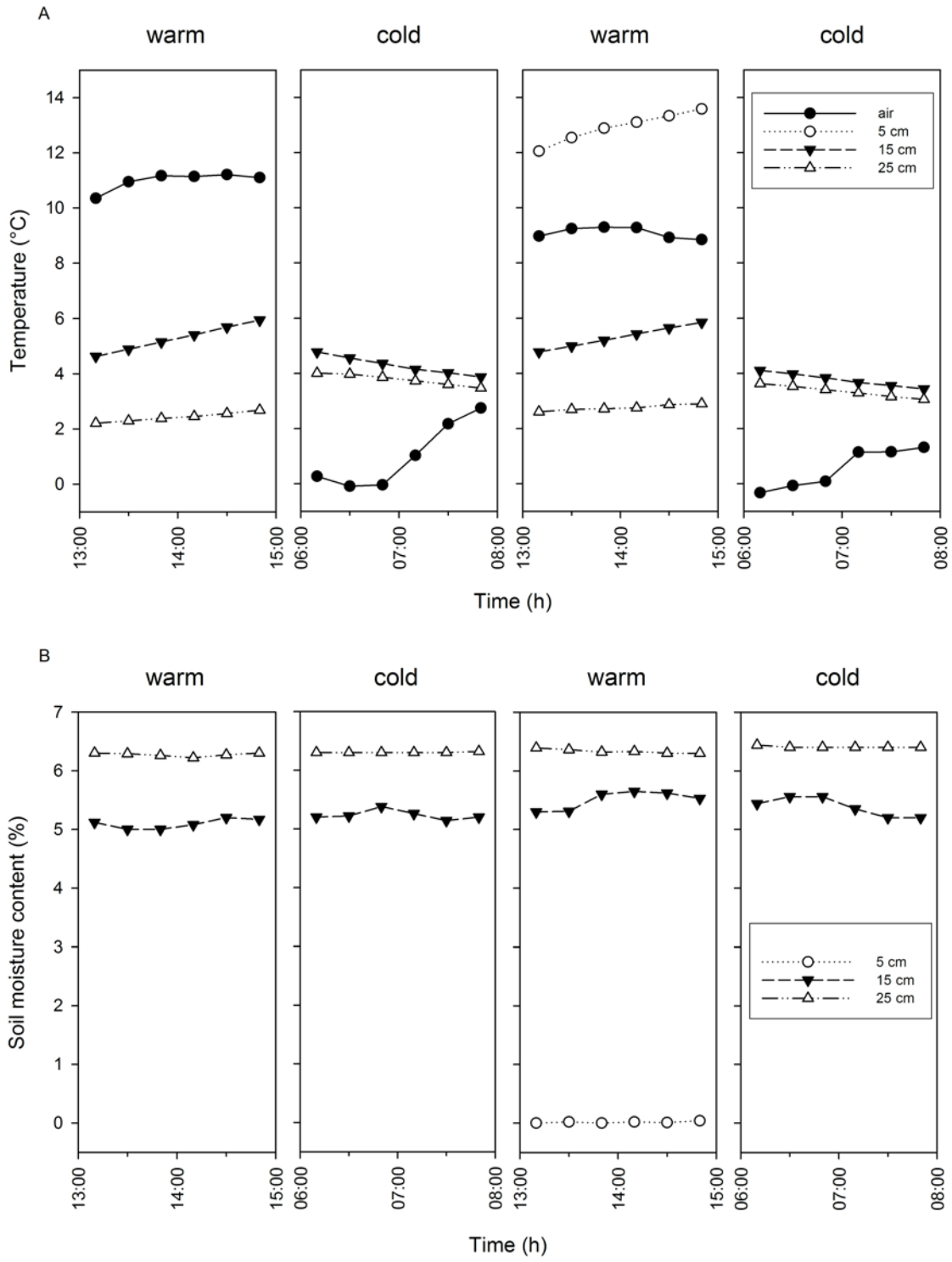

Figure 3.6 Soil temperature **(A)** and moisture content **(B)** during gas sampling periods, Site A Taylor Valley. Note: data at 5 cm depth were only recorded during one sampling period due to a faulty probe.

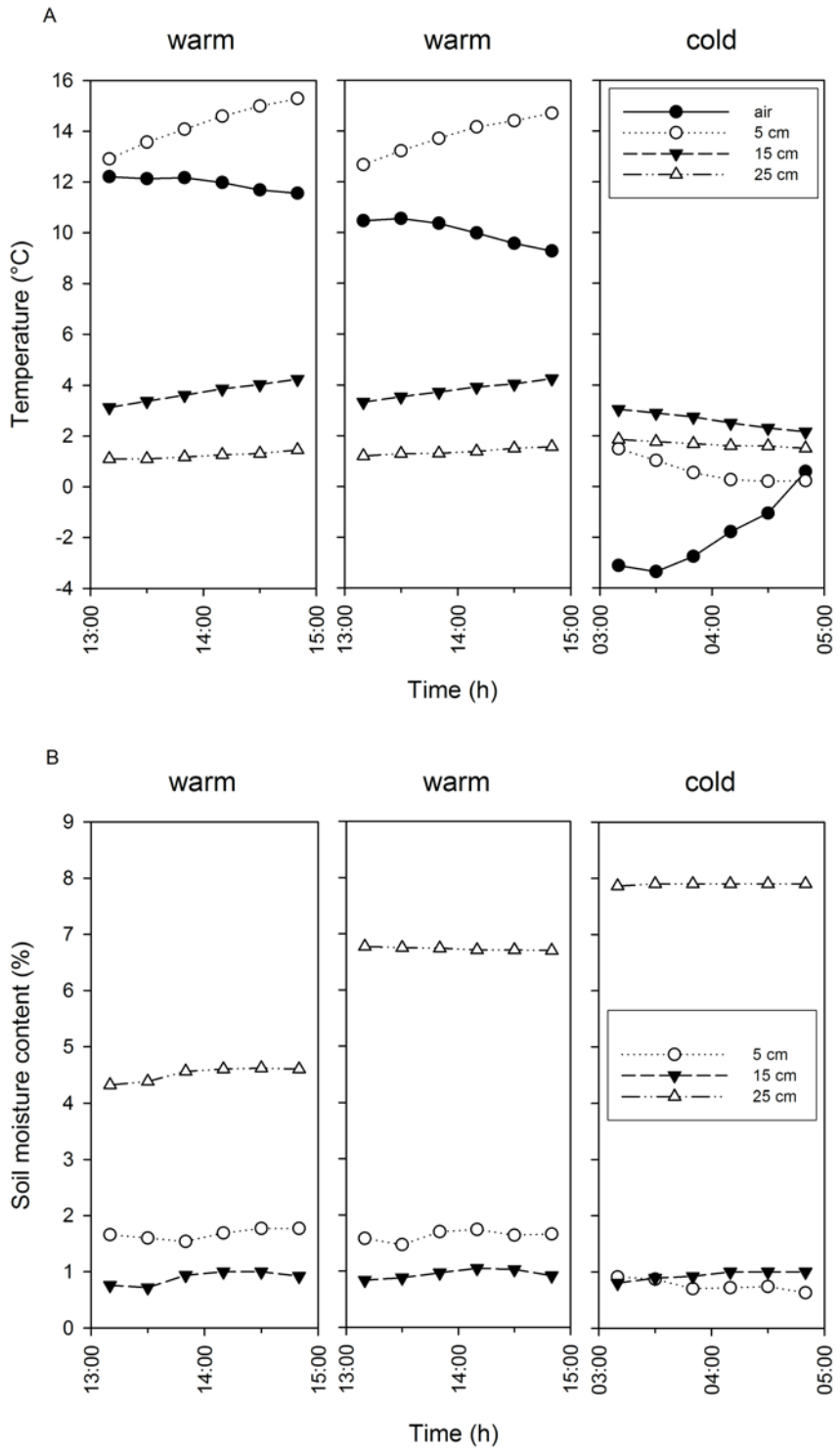

Figure 3.7 Soil temperature **(A)** and moisture content **(B)** during gas sampling periods, Site B Taylor Valley. Note: this site was only sampled during one "cold" period due to an error in determining the timing of the coldest part of the day.

Soil moisture content remained relatively constant throughout the sampling period at Site A (Figure 3.6B), with no moisture detected at 5 cm depth. Ponded water was observed on the soil surface in low-lying areas within 300 m of the sampling area, suggesting subsurface melt from ice-cemented soils on adjacent north-facing hill slopes was contributing to the relatively high moisture content

(~5%) observed at 15 cm depth at this site. Soil moisture content at 25 cm depth was around 6%. At Site B, soil moisture content at 5 cm depth was higher during warm sampling periods, whereas at 15 cm depth it remained relatively constant (~1%) (Figure 3.7B). Soil moisture content at 25 cm depth increased from 4 to 8% over the sampling period due to thawing ice-cement at the base of the profile.

3.4.2 Soil physical and chemical properties

Soil bulk density ranged from 1.5 to 2.3 g cm^{-3}. These values correspond to soil porosities ranging from 18 to 45%, assuming a particle density of 2.8 g cm^{-3} (Barrett and Froggatt, 1978) which is appropriate for the dominantly mafic igneous rocks of the study area.

Principal component analysis of soil chemical data revealed three principal components which explained 80% of the variance in the original soil chemical data. Principal component (PC) 1 represents total C, inorganic C, calcium (Ca^{2+}), magnesium (Mg^{2+}), nitrate (NO_3^-) and sulphate (SO_4^{2-}) (Supplementary Table 3.4). PC 1 can be considered a C component as it is dominated by total C and inorganic C. PC 2 represents pH, EC and sodium (Na^+), and is effectively a measure of saltiness. PC 3 represents total N, organic C, potassium (K^+), chloride (Cl^-) and sulphate, although component correlations suggest that total N and organic C are the variables best described by PC 3. Depth profiles, contrasts and similarities between the soils at each site are discussed below in terms of the major variables contributing to the three principal components.

Inorganic C (PC 1)

Inorganic C was higher at Site A than at Site B (Figure 3.8A). At Site A, inorganic C decreased from 2 mg g^{-1} to 1 mg g^{-1} in the upper 15 cm of the profile, and increased with depth below 15 cm. The maximum inorganic C content (4 mg g^{-1}) occurred in the 40–45 cm depth increment, coinciding with the approximate maximum thaw depth of the active layer. Despite inorganic C content in the upper 15 cm being the lowest in the profile at Site A, it was more than double the organic C content. Below 15 cm depth, inorganic C was always more than four times greater than organic C at the same depth. At Site B, inorganic C decreased from 2 mg g^{-1} in the top 5 cm to 0.3 mg g^{-1} between 10 and 25 cm depth. Below 25 cm depth, inorganic C increased, and was always more than five times greater than organic C at the same depth.

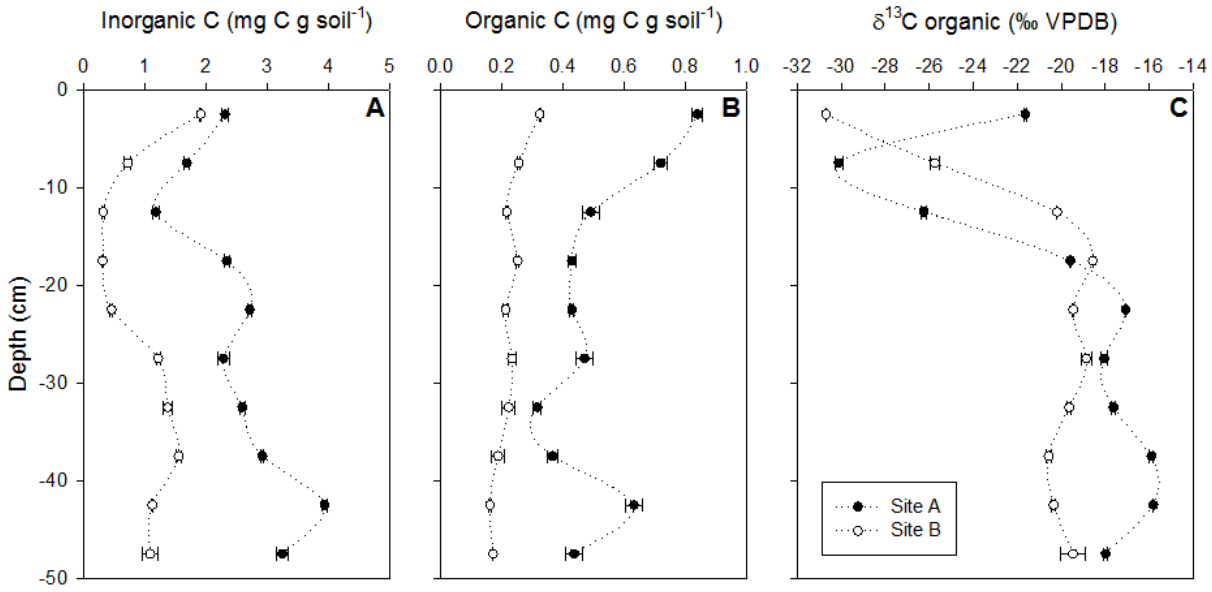

Figure 3.8 Depth profiles of **A**) soil inorganic C, **B**) soil organic C, and **C**) C isotopic composition of soil organic C at Sites A and B, Taylor Valley. Error bars are ±1 standard deviation; n = 2.

Organic C (PC 3)

Total organic C decreased with depth down the profile at Site A (Figure 3.8B), except for a secondary peak of 0.6 mg g^{-1} at 40–45 cm depth, which was only slightly lower than values measured between 0–10 cm depth. The depth of the secondary peak corresponds to the estimated maximum thaw depth of the active layer. At Site B, total organic C values were very low (0.16 – 0.32 mg g^{-1}) and decreased slightly with depth.

From 5–15 cm depth at Site A, and in the upper 10 cm of the profile at Site B, $\delta^{13}C$ values were highly depleted relative to VPDB, ranging from −25.7 to −30.7‰ (Figure 3.8C). The upper 5 cm at Site A had a comparatively enriched $\delta^{13}C$ value of −21.6‰; below 15 cm depth, values ranged from −15.8 to −19.6‰. At Site B, $\delta^{13}C$ values beneath 10 cm depth were more depleted relative to those at Site A, ranging from −18.6 to −20.6‰.

Soil pH and electrical conductivity (PC 2)

Soil pH ranged from ~ 10 in the upper part of the profile at both sites to between 8.8 and 9.4 at 45–50 cm depth (Figure 3.9A). Electrical conductivity (EC), a proxy for soil salt concentration, was higher in the upper 10 cm of the soil at Site B than at Site A (Figure 3.9B). At both sites, EC values were relatively low and constant between 10 and 40 cm depth. Between 40 and 50 cm depth, EC values at both sites increased to a level similar to that in the upper 5 cm at Site A (Figure 3.9B).

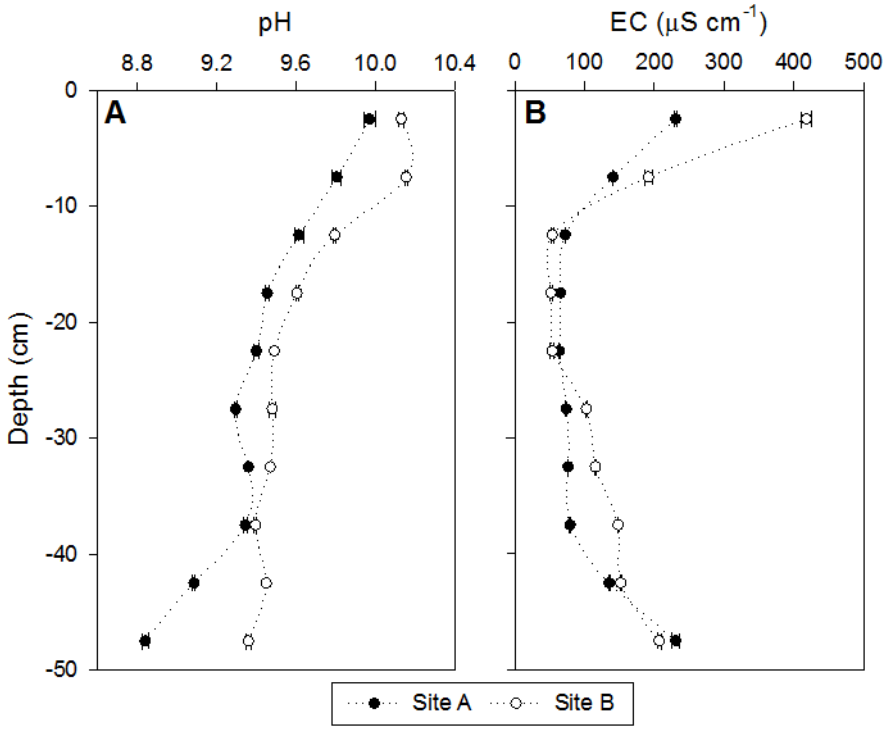

Figure 3.9 Depth profiles of **A**) soil pH, and **B**) electrical conductivity at Sites A and B, Taylor Valley. Error bars are ±1 standard deviation; n = 2.

3.4.3 CO_2 dynamics

Subsurface CO_2 profiles

Subsurface CO_2 concentrations were significantly different between warm and cold periods at both sites (Figure 3.10A). During warm periods, soil CO_2 concentrations were greater than atmospheric CO_2 concentration (383.3 µL L^{-1} at the South Pole in December 2008; Keeling et al., 2001) in the upper 10 cm of the profile at Site A, reaching a maximum of 400 µL L^{-1} at 10 cm depth. Samples taken during cold sampling periods showed soil CO_2 concentrations were substantially below that of atmospheric CO_2, the lowest being 315 µL L^{-1} at 15 cm depth at Site A. At both sites, shifts in soil CO_2 concentration between warm and cold periods were mirrored about a trend-line that decreases from 380 µL L^{-1} at the surface to 330−340 µL L^{-1} at 30 cm depth, demonstrating that cycles of CO_2 uptake (cold periods) and release (warm periods) occur. The amount of soil CO_2 taken up and released was greater at Site A than at Site B.

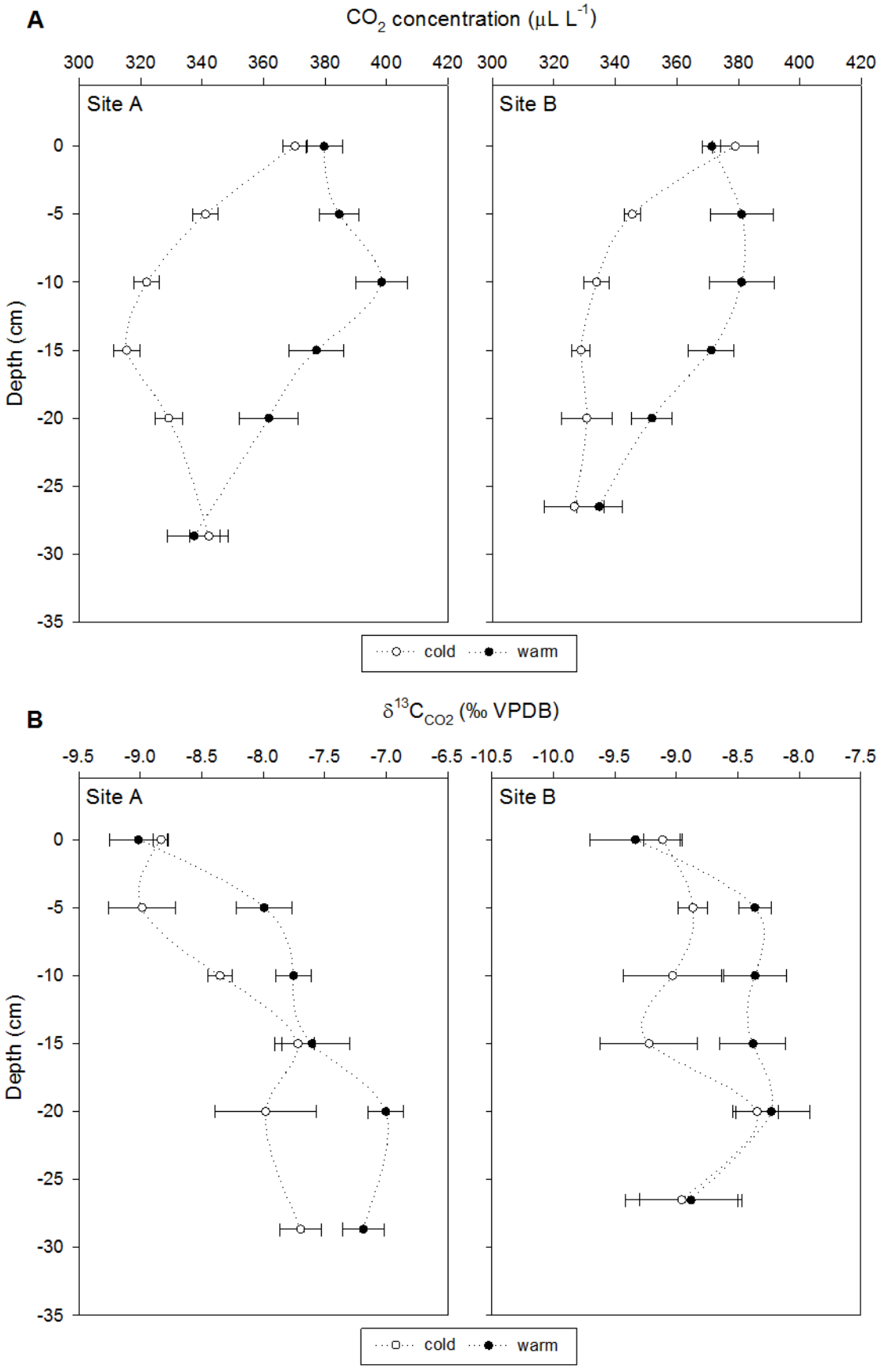

Figure 3.10 Soil profile CO_2 concentration **(A)** and $\delta^{13}C_{CO2}$ **(B)** at Sites A and B, Taylor Valley. Data shown represent averages for warm and cold sampling periods (n = 6 for 0 cm samples and n = 12 at all other depths, except for the cold sampling period at Site B, where n = 3 for 0 cm samples and n = 6 at all other depths). Error bars represent the SEM.

Soil profile $\delta^{13}C_{CO2}$ was relatively enriched during warm periods when compared to cold periods at both sites (Figure 3.10B). At Site A, $\delta^{13}C_{CO2}$ became more enriched with increasing depth in the profile during both warm and cold periods, although at 15 cm depth there were slight inflexions in the trends. Values ranged from −7.0 to −9.0‰, with a maximum difference between warm and cold periods of 1‰. At Site B, $\delta^{13}C_{CO2}$ remained relatively constant with depth during both warm and cold periods, ranging from −8.2 to −9.2‰, with differences of ≤ 0.9‰ between warm and cold periods. Soil profile $\delta^{13}C_{CO2}$ was similar to that of atmospheric CO_2 (−8.22‰ at the South Pole in December 2008; Keeling et al., 2001) during warm periods at Site B. At both sites, $\delta^{13}C_{CO2}$ was highly enriched relative to soil organic matter (Figure 3.8C).

Surface CO_2 fluxes

Surface CO_2 flux rates ranged from −0.050 to 0.048 µmol m^{-2} s^{-1} (Table 3.1). Periods of efflux (positive flux) and influx (negative flux) corresponded to warm and cold sampling periods, respectively. During warm periods (efflux), headspace CO_2 became progressively enriched (by up to 1.8‰), whereas during cold periods (influx), headspace CO_2 became depleted (by up to −2.0‰). The $\delta^{13}C_{CO2}$ values ranged from −6.5 to −10.6‰ during warm periods, and −7.4 to −11.2‰ during cold periods.

Table 3.1 Surface soil CO_2 fluxes and rate of change in $\delta^{13}C_{CO2}$ during surface CO_2 flux sampling at Sites A and B, Taylor Valley.

Site	Chamber	Sampling time [a]	CO_2 flux (µmol m^{-2} s^{-1})	$\frac{\Delta\delta^{13}C_{CO2}}{\Delta t}$ [b]	Site	Chamber	Sampling time [a]	CO_2 flux (µmol m^{-2} s^{-1})	$\frac{\Delta\delta^{13}C_{CO2}}{\Delta t}$ [b]
A	a	W_1	0.010	0.010	B	a	W_1	0.025	0.015
		W_2	0.000	0.013*			W_2	0.034**	0.010
		C_1	-0.041**	-0.006			C_1	-0.037	-0.018
		C_2	-0.003	-0.008					
A	b	W_1	0.034	0.022**	B	b	W_1	0.021	0.021
		W_2	0.026	0.014			W_2	0.018**	0.011
		C_1	-0.024	0.001			C_1	-0.028*	-0.025
		C_2	-0.044	-0.002					
A	c	W_1	0.048	0.000	B	c	W_1	0.045	-0.002
		W_2	0.019	0.003*			W_2	no data	no data
		C_1	-0.039**	-0.008			C_1	-0.050**	0.023
		C_2	-0.038**	0.004					
A	d	W_1	0.043**	0.024**	B	d	W_1	0.040*	0.012
		W_2	0.005	0.016			W_2	0.010	0.020*
		C_1	0.004	-0.022**			C_1	-0.013	-0.013
		C_2	-0.016	-0.016*					
A	e	W_1	0.034*	0.003	B	e	W_1	0.018	-0.011
		W_2	0.024*	0.007			W_2	0.018**	0.009
		C_1	0.001	-0.051			C_1	-0.029*	-0.008*
		C_2	-0.039**	-0.026**					
A	f	W_1	0.036	0.008	B	f	W_1	0.024*	0.004
		W_2	0.016**	0.029			W_2	0.013	0.011
		C_1	-0.023**	-0.011**			C_1	0.001	-0.004
		C_2	-0.024*	-0.021*					

[a] W and C denote warm and cold sampling periods, respectively. [b] Units are per mil min^{-1}. * represents P <0.1; ** represents P <0.05.

3.5 Discussion

3.5.1 Soil CO_2 uptake and release

The low soil CO_2 flux rates measured in this study are in close agreement with *in situ* surface flux rates in Taylor Valley reported by Burkins et al. (2001) and Parsons et al. (2004), but an order of magnitude lower than those reported by Ball et al. (2009), despite all studies having used soils with similar pH, EC, organic and inorganic C values. Higher flux rates such as those reported by Gregorich et al. (2006) were from soils with organic C contents of up to 35 mg g^{-1}. Such high organic C contents are unusual in Antarctic Dry Valley soils; this study focuses on CO_2 dynamics in typical Dry Valley soils characterised by high pH (~10) and low organic C contents (<1 mg g^{-1}).

It is well established that soil respiration increases with rising soil temperature (e.g. Lloyd and Taylor, 1994; Fang and Moncrieff, 2001). If CO_2 release during warm periods at the study sites were due to biological respiration, $\delta^{13}C_{CO2}$ values should reflect the $\delta^{13}C$ of the source organic material (Dörr and Münnich, 1980). Soil $\delta^{13}C_{CO2}$ values (Figure 3.10B) showed no relationship with soil organic matter $\delta^{13}C$ values (Figure 3.8C). Furthermore, if CO_2 uptake during cold periods were a result of algal photosynthesis, soil $\delta^{13}C_{CO2}$ should be enriched due to preferential uptake of $^{12}CO_2$ by photosynthetic organisms, thus concentrating the heavier $^{13}CO_2$ in the soil atmosphere (Park and Epstein, 1960). No biological mechanism can be invoked to account for the results. Instead, $\delta^{13}C_{CO2}$ values associated with the uptake (depleted $\delta^{13}C_{CO2}$) and release (enriched $\delta^{13}C_{CO2}$) of soil CO_2 indicate that CO_2 dynamics in Dry Valley soils are controlled by other mechanisms.

In studies of surface CO_2 fluxes in Taylor Valley, Ball et al. (2009) found that soil temperature fluctuations (at 5 cm depth) accounted for almost half of the variation observed in diel CO_2 fluxes. As similar diel cycles of CO_2 flux were also observed in heat-treated (120°C) soils, presumed to be free of biological activity, Ball et al. (2009) suggested that dissolution of CO_2 in soil water, consistent with Henry's Law, was a likely explanation for the diel variations observed. This hypothesis was tested by: 1) comparing soil profile CO_2 concentrations measured at warm and cold periods with values simulated by a model that incorporates Henry's Law dissolution of CO_2, and 2) comparing the measured changes in $\delta^{13}C_{CO2}$ with those expected from fractionation due to dissolution and exsolution of CO_2, biological respiration, and photosynthetic CO_2 fixation. The data were also used to quantify the relative contributions of biotic and abiotic processes to soil CO_2 uptake and release.

A model of abiotic CO_2 dynamics

At steady state, the closed-system partitioning of CO_2 between gaseous and dissolved CO_2 is determined by Henry's Law and solution pH. The temperature dependent Henry coefficient (K_H) (Stumm and Morgan, 1996) expresses the relationship between pCO_2 of the atmosphere and

dissolved gaseous CO_2 ($[CO_{2(aq)}] = [H_2CO_3]$), as $pCO_2 = K_H[CO_{2(aq)}]$. Total dissolved CO_2 (C_T), which includes the species H_2CO_3, HCO_3^- and CO_3^{2-}, is related to $[CO_{2(aq)}]$ and pH by:

$$C_T = \left[CO_{2_{(aq)}}\right]\left(1 + \frac{K_{a_1}}{[H^+]} + \frac{K_{a_1}K_{a_2}}{[H^+]^2}\right) \tag{3.2}$$

where K_{a1} and K_{a2} are the equilibrium constants for $[H^+]\,[HCO_3^-]/[H_2CO_3]$ and $[H^+]\,[CO_3^{2-}]/[HCO_3^-]$, respectively (Stumm and Morgan, 1996). The temperature dependence of K_H is such that as temperature increases, $[CO_{2(aq)}]$ decreases. Thus, as a result of changes in K_H, decreasing temperature causes CO_2 absorption, and increasing temperature causes CO_2 desorption. In a soil, the capacity of soil solution to absorb and desorb CO_2 depends on soil solution volume, soil pH, and the magnitude of soil temperature variation. From (3.2), it is evident that increasing soil solution pH (decreasing $[H^+]$) causes an increase in C_T. A high soil solution pH interacts with the volume of soil solution, amplifying the effect of CO_2 adsorption or desorption with changing temperature by providing for a larger source or sink of dissolved CO_2 involved in the exchanges.

Using the principles described above, and closed-system, steady-state assumptions, abiotic CO_2 dynamics in the soils at the study sites were modelled. The low flux rates measured (Table 3.1) suggest the closed-system assumption is not unreasonable, but this is explored further below. The model predicts the ratio of soil CO_2 concentrations ($[CO_2]_{warm}$: $[CO_2]_{cold}$) when temperature (T) drops from warm (T_{warm}) to cold (T_{cold}) in terms of the soil moisture content and pH of the system.

The ratio of subsurface soil CO_2 concentrations attributable to abiotic processes as a result of a change in temperature from T_{warm} to T_{cold} is given by:

$$\frac{[CO_2]_{warm}}{[CO_2]_{cold}} = \frac{\left(\frac{(\varphi - \theta)}{RT_{cold}} + \frac{\theta}{K_{H_{cold}}}\right)}{\left(\frac{(\varphi - \theta)}{RT_{warm}} + \frac{\theta}{K_{H_{warm}}}\right)} \times \frac{T_{cold}}{T_{warm}} \tag{3.3}$$

where φ is soil porosity (L voids L soil^{-1}), θ is soil volumetric moisture content (L water L soil^{-1}), R is the ideal gas constant (8.314 J K^{-1} mol^{-1}), T is soil temperature (K), K_H is Henry's coefficient (L atm mol^{-1}) and $[CO_2]$ is soil CO_2 concentration (µL L^{-1}). A full derivation of the model is given in Appendix A.

The dependence of $[CO_2]_{warm}$: $[CO_2]_{cold}$ on soil pH and moisture content for temperature changes (between warm and cold sampling periods) typical of those measured at 5 cm (Figure 3.11A) and 15 cm (Figure 3.11B) depth in the study area is shown in Figure 3.11. At low pH (≤ 6), C_T is low (3.2), and consequently a large soil solution volume (high moisture content) is required to provide the pool of dissolved inorganic C necessary for temperature-driven absorption/desorption processes to shift $[CO_2]_{warm}$: $[CO_2]_{cold}$ significantly. Between pH 7 and 9, C_T rises rapidly and the volume of soil solution

required to produce a given $[CO_2]_{warm}$: $[CO_2]_{cold}$ declines rapidly. For example, at pH 6, soil moisture content must be 0.32 (at or above field capacity in many soils) for $[CO_2]_{warm}$: $[CO_2]_{cold}$ to be 1.4 (T_{warm} = 286 K and T_{cold} = 274 K; Figure 3.11A). By contrast, for the same change in T at pH 9, the same ratio can be accommodated by a soil with a moisture content < 0.01 (< 1%). The magnitudes of $[CO_2]_{warm}$: $[CO_2]_{cold}$ simulated for 15 cm depth (Figure 3.11B) are much lower because of the smaller temperature fluctuation at this depth, but the relative sensitivity to soil pH and moisture content remains the same.

The model suggests that changes in soil profile CO_2 concentrations in the study area should be greatest at shallow soil depths, where temperature changes are greatest, pH is high (~10), and moisture content is adequate. Conversely, greater depths should have smaller changes in soil CO_2 concentrations due to smaller changes in soil temperature. However, the measured CO_2 concentration depth profiles (Figure 3.10A) show relatively low variation in CO_2 concentrations at shallow depths, with maximum differences at 10−15 cm. As predicted by the model, little variation occurs at the base of the profile.

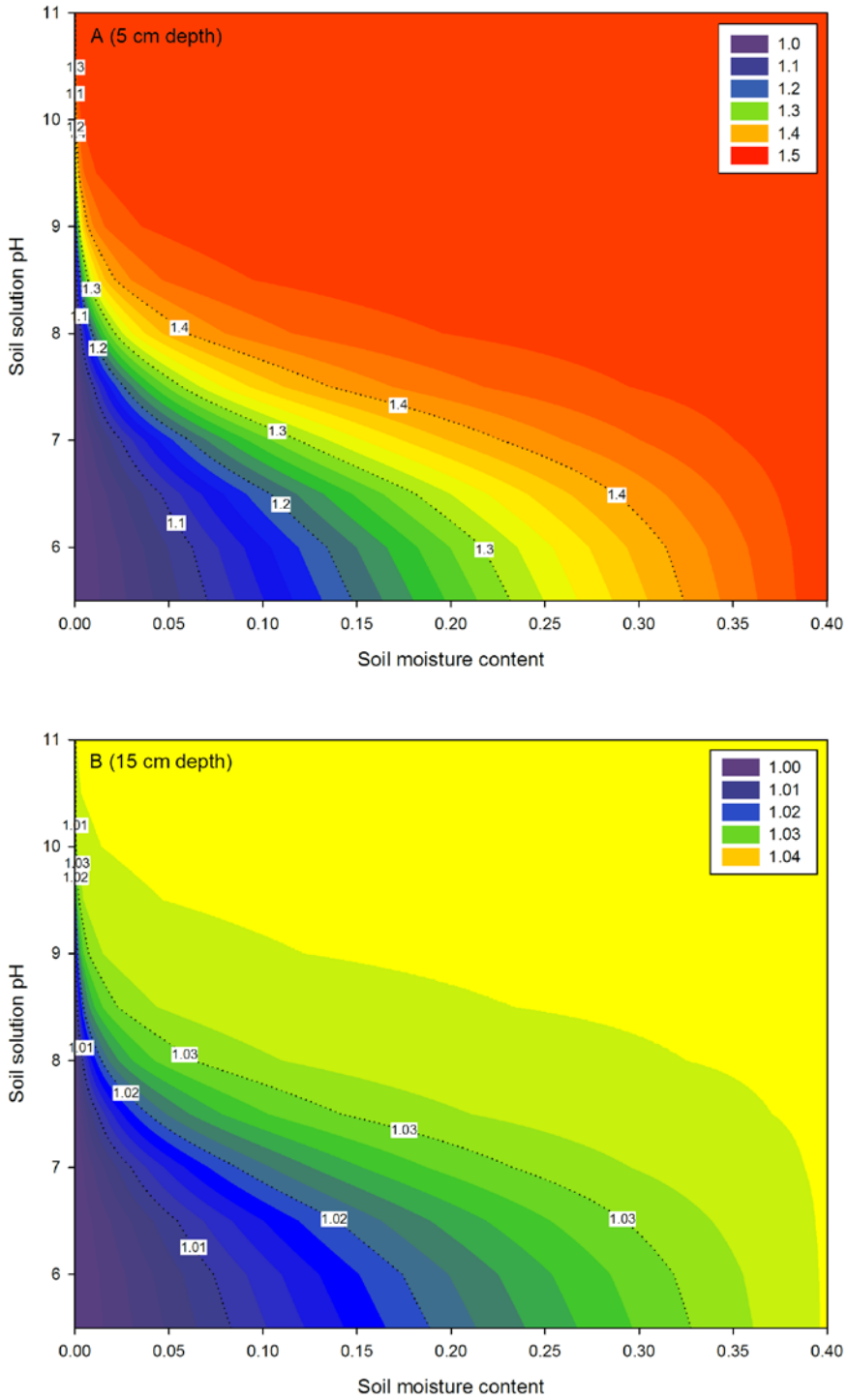

Figure 3.11 Ratios of simulated $[CO_2]_{warm}$: $[CO_2]_{cold}$ as influenced by soil moisture content and soil solution pH. Ratios are calculated using equation 3.3. In (**A**) T_{warm} = 286 K and T_{cold} = 274 K which are similar to soil temperatures measured at 5 cm depth, and in (**B**) T_{warm} = 278.3 K and T_{cold} = 277.3 K, similar to soil temperatures measured at warm and cold periods, respectively, at 15 cm depth in the study area. When the ratio of $[CO_2]_{warm}$: $[CO_2]_{cold}$ is 1, there is zero potential for CO_2 to be absorbed. This occurs when soil moisture is so low that no CO_2 can be dissolved. Higher ratios represent greater changes in soil CO_2 concentrations between warm and cold periods, and thus greater uptake and release of CO_2 by soils.

Measured and simulated ratios of $[CO_2]_{warm}$: $[CO_2]_{cold}$ were compared for 5, 15 and 25 cm depths using measured values of soil pH, temperature and moisture content (Figure 3.12). The 25 cm depth increment behaves as the model predicts. Ratios of $[CO_2]_{warm}$: $[CO_2]_{cold}$ are very close to 1 due to minimal changes in soil temperature between warm and cold periods. At this depth, the soil closely approximates a closed system because ice-cemented soil beneath provides a gas-impermeable lower barrier, and CO_2 concentration gradients are low (Figure 3.10A). At 15 cm depth, measured ratios are 15% and 9% greater than simulated ratios (their theoretical abiotic maximum) at Sites A and B, respectively, suggesting a possible biological respiration component. At 5 cm depth, measured $[CO_2]_{warm}$: $[CO_2]_{cold}$ ratios are considerably lower than simulated ratios. As the 5 cm depth increment is most likely to suffer from violation of the closed-system assumption of the model, this discrepancy is attributed to exchange between the soil and surface atmospheres. Leakage of CO_2 from the soil during warm periods when CO_2 is released via exsolution, and influx of atmospheric CO_2 during cold periods when soil CO_2 concentrations are depleted (CO_2 dissolution) would act to damp variation in measured CO_2 concentrations. These inferred fluxes are supported by the soil CO_2 concentration gradients at this depth (Figure 3.10A).

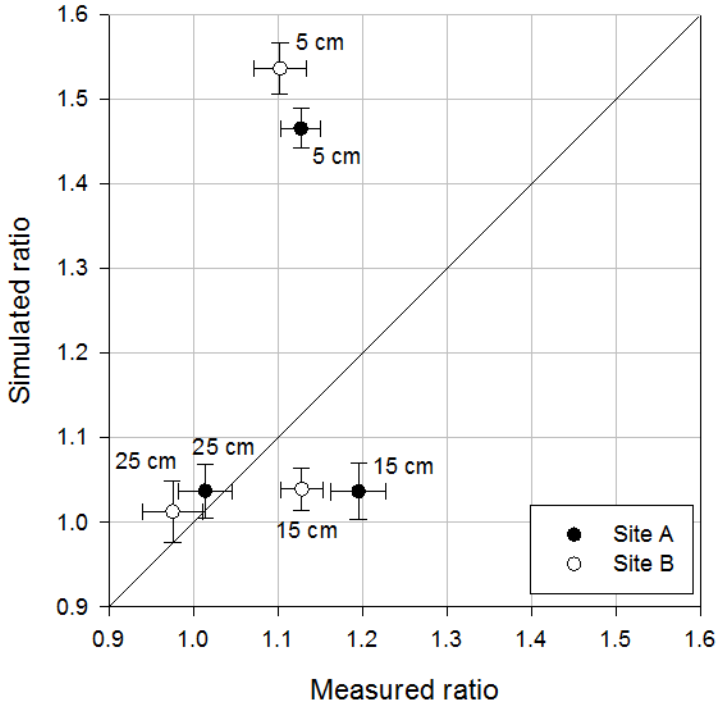

Figure 3.12 Comparison between measured and simulated $[CO_2]_{warm}$: $[CO_2]_{cold}$ ratios between warm and cold sampling periods for Sites A and B, Taylor Valley.

Discriminating between biotic and abiotic processes using stable C isotopes

Biotic production and consumption of CO_2 and the abiotic dissolution/exsolution processes outlined above produce distinctive soil $\delta^{13}C_{CO2}$ values. Biological respiration of highly depleted organic C would produce respired CO_2 of a very similar (highly depleted) C isotopic composition (Dörr and Münnich, 1980), as respiration does not (or only to a minor extent) discriminate against ^{13}C. Based on measured soil organic $\delta^{13}C$ values at both sites (Figure 3.8C), respired $\delta^{13}C_{CO2}$ values of ~ −30 to −21‰ in the upper 15 cm of the profiles, and ~ −20 to −16‰ below 15 cm depth would be expected. Thus, if biological respiration were responsible for the increase in soil CO_2 concentration during warm periods, $\delta^{13}C_{CO2}$ values would become relatively depleted. Conversely, discrimination against $^{13}CO_2$ in C_3 photosynthetic pathways would produce a $\delta^{13}C_{CO2}$-enriched atmosphere above actively photosynthesising organisms. Therefore, if soil CO_2 uptake during cold periods were due to photosynthetic CO_2 consumption, $\delta^{13}C_{CO2}$ values would become relatively enriched. The results are contrary to these patterns: soil profile $\delta^{13}C_{CO2}$ values were relatively enriched during warm periods (CO_2 release) and depleted during cold periods (CO_2 uptake; Figure 3.10B). Surface CO_2 flux data also showed progressive enrichment and depletion of $\delta^{13}C_{CO2}$ during warm and cold sampling periods, respectively (Table 3.1). The observed patterns are consistent with isotopic fractionation during CO_2 dissolution and its speciation to $HCO_3^{-}{}_{(aq)}$ and $CO_3^{2-}{}_{(aq)}$ (Table 3.2). At pH values >9, dissolved CO_2 species are dominated by the HCO_3^- and CO_3^{2-} forms (Stumm and Morgan, 1996). Equilibrium fractionation of CO_2 gas to HCO_3^- and CO_3^{2-} results in a ~−10‰ depletion of CO_2 gas relative to HCO_3^- or CO_3^{2-} (Thode et al., 1965; Mook et al., 1974; Table 2). Thus, dissolution of CO_2 to form HCO_3^- and CO_3^{2-} (at the high pH values measured) would result in depletion of $\delta^{13}C_{CO2}$ in the soil atmosphere, whereas exsolution would lead to enrichment of $\delta^{13}C_{CO2}$ in the soil atmosphere. The magnitudes of the isotopic shifts observed (~ −1‰) are less than ~−10‰ because only a proportion of the CO_2 in the soil atmosphere exchanges with soil solution (~ 10%).

Table 3.2 Carbon isotope fractionation in the CO_2–HCO_3–CO_3–$CaCO_3$ system under equilibrium conditions. $^{13}\varepsilon_{y/x}$ represents the fractionation of compound y relative to compound x. Soil temperatures (T) shown are similar to those measured during the sampling period. g = gaseous CO_2, a = dissolved CO_2, b = dissolved HCO_3^-, c = dissolved CO_3^{2-} ions, s = solid calcium carbonate. T_K = T (°C) + 273.15 K.

T (°C)	$^{13}\varepsilon_{g/a}$ [a] (‰)	$^{13}\varepsilon_{g/b}$ [b] (‰)	$^{13}\varepsilon_{g/c}$ [c] (‰)	$^{13}\varepsilon_{g/s}$ [d] (‰)
1	1.17	−10.70	−10.06	−10.47
5	1.15	−10.20	−9.61	−10.19

[a] $^{13}\varepsilon_{g/a} = -0.19‰ + 373/T_K$ (Vogel et al., 1970).
[b] $^{13}\varepsilon_{g/b} = 23.89‰ - 9483/T_K$ (Mook et al., 1974).
[c] $^{13}\varepsilon_{g/c} = {}^{13}\varepsilon_{g/b} + {}^{13}\varepsilon_{b/c}$ (= −2.52‰ + 867/T_K; Thode et al., 1965).
[d] $^{13}\varepsilon_{g/s} = 9.15‰ - 5380/T_K$ (Mook, 2000).

Although the $\delta^{13}C_{CO2}$ data confirm abiotic processes dominate CO_2 dynamics in soils of Taylor Valley, as postulated by Ball et al. (2009), the comparison of measured and simulated $[CO_2]_{warm}$: $[CO_2]_{cold}$ ratios suggests there is a component of CO_2 flux around 15 cm depth that cannot be accounted for by abiotic processes alone. Soil organic $\delta^{13}C$ values in conjunction with soil profile $\delta^{13}C_{CO2}$ values are used to further constrain the potential biotic contribution to soil CO_2 fluxes.

Quantifying the biotic contribution to soil CO_2 fluxes

The bulge in soil CO_2 concentration from 5−15 cm depth at Site A is likely to have a biological respiration component, as organic C content at this depth is relatively high (~ 0.6 mg C g soil^{-1}; Figure 3.8B) and the soil is relatively warm (Figure 3.6A). Assuming respired soil CO_2 at this depth would have an average $\delta^{13}C_{CO2}$ value of −28.2‰ (Figure 3.8C), a mixing model (Fry, 2006) can be used to calculate the biotic contribution (f_{biotic}) to soil CO_2 fluxes:

$$f_{biotic} = \frac{\delta^{13}C_{CO2-produced} - \delta^{13}C_{CO2-abiotic}}{\delta^{13}C_{biotic} - \delta^{13}C_{CO2-abiotic}} \quad (3.4)$$

where $\delta^{13}C_{CO2\text{-}produced}$ is the $\delta^{13}C_{CO2}$ (‰) produced from cold to warm periods (Appendix B), $\delta^{13}C_{CO2\text{-}abiotic}$ is the $\delta^{13}C_{CO2}$ (‰) of CO_2 produced due to abiotic processes, and $\delta^{13}C_{biotic}$ is the $\delta^{13}C$ (‰) of the organic source material (Figure 3.8C).

This calculation requires the isotopic composition of abiotically produced CO_2 ($\delta^{13}C_{CO2\text{-}abiotic}$) to be known. However, as it has not been empirically determined, f_{biotic} is calculated using a range of $\delta^{13}C_{CO2\text{-}abiotic}$ values (Table 3.3) appropriate to different assumptions about isotopic fractionation during dissolution and exsolution of CO_2. The proportion of biotic CO_2 production increases with increasing values of $\delta^{13}C_{CO2\text{-}abiotic}$. The most depleted value of $\delta^{13}C_{CO2\text{-}abiotic}$ (−8.22‰) assumes exsolved CO_2 has the same $\delta^{13}C_{CO2}$ as atmospheric CO_2 at the time of sampling. This is clearly unrealistic, because firstly, it produces a negative f_{biotic} value, and secondly, exsolved CO_2 this depleted would not allow a shift of soil $\delta^{13}C_{CO2}$ to > −8.22‰ as is measured at Site A (Figure 3.10B). A $\delta^{13}C_{CO2\text{-}abiotic}$ value of −4.1‰ suggests a biotic contribution of 5%. This value of $\delta^{13}C_{CO2\text{-}abiotic}$ is determined using a mass balance calculation of the C isotopic composition necessary to produce the shift in soil $\delta^{13}C_{CO2}$ from cold to warm sampling periods at Site B (see Appendix B for details of the calculation). Data from Site B are used because the low organic C status of the soil is likely to limit respiration to the extent that CO_2 uptake and release throughout the whole profile is dominated by abiotic processes. However, the model of abiotic soil CO_2 uptake and release suggests there may be as much as a 9% biological component to soil CO_2 production at 15 cm depth at Site B. Therefore, conservatively assuming a 10% biological contribution from respiration of soil organic C to soil CO_2 production over the whole profile at Site B, the value of $\delta^{13}C_{CO2\text{-}abiotic}$ is −1.42‰ (Appendix B), which results in a biological respiration component of 14%. The highest value of $\delta^{13}C_{CO2\text{-}abiotic}$ assumes no fractionation of CO_2

released by exsolution from a 50:50 mix of HCO_3^- and CO_3^{2-} in isotopic equilibrium with atmospheric CO_2. This is an unlikely scenario, but it establishes the most enriched possible value of $\delta^{13}C_{CO2\text{-}abiotic}$. The resultant biotic contribution to soil CO_2 fluxes is 24%.

Table 3.3 Proportion of the change in CO_2 concentration and isotopic composition attributable to biotic processes (f_{biotic}) at Site A, 5−15 cm depth. This depth has the greatest shift in CO_2 concentration between cold and warm periods (Figure 3.10A) and is the most likely place in which biological respiration may occur. The effects of changes in assumed $\delta^{13}C_{CO2\text{-}abiotic}$ values on f_{biotic} are shown.

f_{biotic}	$\delta^{13}C_{CO2\text{-}abiotic}$ (‰)	Source of $\delta^{13}C_{CO2\text{-}abiotic}$ value
−0.15	−8.22	Atmospheric $\delta^{13}C_{CO2}$ at the South Pole in December 2008 (Keeling et al., 2001).
0.05	−4.10	Average $\delta^{13}C_{CO2}$ emitted from the whole profile at Site B, assuming no biological contribution.
0.14	−1.42	Assumes Site B has a 10% biological contribution, as suggested by the comparison between measured and simulated $[CO_2]_{warm}$: $[CO_2]_{cold}$ ratios (Figure 3.12). The 10% biological contribution is conservatively applied to the whole profile.
0.24	2.16	Assumes no fractionation of CO_2 as it is exsolved from a 50:50 mix of HCO_3^-:CO_3^{2-} in isotopic equilibrium with atmospheric CO_2 (Table 3.2).

Implications for soil respiration measurements and C turnover times

Long-term records of soil respiration in the McMurdo Dry Valleys have been suggested as being one of the most sensitive indicators of ecosystem response to climate variability (Barrett et al., 2006c). However, it is essential that both biotic and abiotic contributions to soil CO_2 fluxes are identified and measured accurately, as both components are highly spatially and temporally variable. The techniques utilised here represent a first attempt.

The data presented in this chapter demonstrate that previously measured *in situ* soil CO_2 fluxes attributed to biological respiration may be significant overestimates (e.g. Burkins et al., 2001; Barrett et al., 2006b; Elberling et al., 2006; Gregorich et al., 2006), and C turnover times calculated on the basis of such fluxes may be significant underestimates (e.g. Burkins et al., 2001; Elberling et al., 2006). Based on their calculation of a mean organic C turnover time of 23 years, Burkins et al. (2001) inferred that C cycling in Taylor Valley is non-steady-state, and suggested that at least two organic C pools contribute to C cycling: a labile organic C pool replenished by *in situ* photosynthesis, and a more recalcitrant organic C pool derived from ancient glacial and lake sediments. Such a short C turnover time implies relatively low ecosystem resilience to fluctuations in C supply. The results from this study, which show that biological respiration accounts for a (conservative) maximum of 25% of measured soil CO_2 fluxes in the Dry Valleys environment, mean that present estimates of C turnover

times could be at least four times greater, in the order of 100–500 years. The increased turnover times resulting from lower rates of C utilisation imply that Dry Valley ecosystems are likely to be more resilient to environmental change than what present estimates of C turnover time suggest.

3.6 Conclusions

Soil CO_2 dynamics at the two sites studied in Taylor Valley are dominated by abiotic processes, with small changes in soil temperature capable of driving significant changes in soil CO_2 concentration. The isotopic data imply that biological respiration makes only a minor contribution to soil CO_2 fluxes in the Dry Valleys environment.

These results have significant implications for understanding C cycling in polar desert environments. The abiotic influence on soil CO_2 dynamics must be accounted for and monitored, as CO_2 effluxes cannot be assumed to be solely biologically driven.

3.7 Supplementary information

3.7.1 Model of abiotic CO_2 uptake and release

Model calculations were based on the following equations. Assuming a soil at steady state, at temperature T (K) for an increment of depth D (m), the partial pressure of CO_2, according to Henry's Law, is

$$pCO_2 = K_{H_T}\left[CO_{2(aq)}\right], \tag{3.5}$$

where K_H is the Henry coefficient (L atm mol^{-1}) and $[CO_{2(aq)}]$ is dissolved gaseous CO_2 (H_2CO_3).

Total dissolved CO_2 (C_T) is determined by the equilibrium constants for $[H^+]\,[HCO_3^-]/[H_2CO_3]$ and $[H^+]\,[CO_3^{2-}]/[HCO_3^-]$, K_{a1} and K_{a2}, respectively.

$$C_T = \left[CO_{2(aq)}\right]\left(1 + \frac{K_{a1}}{[H^+]} + \frac{K_{a_1}K_{a_2}}{[H^+]^2}\right) = \frac{pCO_2}{K_{H_T}{}'} = \frac{P[CO_2]}{K_{H_T}{}'}, \tag{3.6}$$

where $K_{H_T}{}' = K_{H_T}/\left(1 + \frac{K_{a1}}{[H^+]} + \frac{K_{a_1}K_{a_2}}{[H^+]^2}\right)$, $[CO_2]$ is the concentration of soil CO_2 (µL L^{-1}) and P is the pressure of the soil atmosphere (atm).

Per unit area of soil surface, the number of moles of dissolved CO_2 (µmol) is given by

$$nCO_{2\,dissolved} = \frac{P[CO_2]}{K_{H_T}{}'}\,D\theta, \tag{3.7}$$

where θ is the soil volumetric moisture content (L water L $soil^{-1}$). The number of moles of CO_2 in the soil atmosphere (µmol)

$$nCO_{2\,soil\,atmos} = \frac{[CO_2]\,PV_{soil\,atmos}}{RT} = \frac{P[CO_2]\,D(\varphi - \theta)}{RT}, \tag{3.8}$$

where $V_{soil\,atmos}$ is the volume of the soil atmosphere (L), and φ is soil porosity (L voids L $soil^{-1}$).

At temperature T_1, total moles of CO_2 in volume D

$$= \frac{P_1[CO_2]_{T1}D(\varphi - \theta)}{RT_1} + \frac{P_1[CO_2]_{T1}}{K_{H_{T1}}{}'}\,D\theta = P_1[CO_2]_{T1}D\left(\frac{(\varphi - \theta)}{RT_1} + \frac{\theta}{K_{H_{T1}}{}'}\right). \tag{3.9}$$

Under the closed-system assumption, conservation of mass dictates that between T_1 and T_2,

$$P_2[CO_2]_{T2}D\left(\frac{(\varphi-\theta)}{RT_2}+\frac{\theta}{K_{H_{T_2}}'}\right)= P_1[CO_2]_{T1}D\left(\frac{(\varphi-\theta)}{RT_1}+\frac{\theta}{K_{H_{T_1}}'}\right), \tag{3.10}$$

and therefore

$$\frac{P_1[CO_2]_{T1}}{P_2[CO_2]_{T2}}=\frac{\left(\frac{(\varphi-\theta)}{RT_2}+\frac{\theta}{K_{H_{T_2}}'}\right)}{\left(\frac{(\varphi-\theta)}{RT_1}+\frac{\theta}{K_{H_{T_1}}'}\right)}. \tag{3.11}$$

Given the exchanges of CO_2 between atmosphere and solution phases are small in relation to the total mass of the soil atmosphere, from the ideal gas law, the ratio of the pressures of the soil atmosphere between T_1 and T_2 is equal to the ratio of the temperatures, and therefore

$$\frac{[CO_2]_{T1}}{[CO_2]_{T2}}=\frac{\left(\frac{(\varphi-\theta)}{RT_2}+\frac{\theta}{K_{H_{T_2}}'}\right)}{\left(\frac{(\varphi-\theta)}{RT_1}+\frac{\theta}{K_{H_{T_1}}'}\right)}\times\frac{T_2}{T_1}. \tag{3.12}$$

3.7.2 Calculating the isotopic composition of abiotically-produced CO_2 ($\delta^{13}C_{CO2\text{-}abiotic}$)

Using a mass balance approach, the average $\delta^{13}C_{CO2}$ of the CO_2 produced between cold and warm sampling periods must satisfy the following

$$\int_0^D \delta^{13}C_{CO2_{cold}}[CO_2]_{cold}dz+\overline{\delta^{13}C_{CO2-produced}}[CO_2]_{produced} = \int_0^D \delta^{13}C_{CO2_{warm}}[CO_2]_{warm}dz, \tag{3.13}$$

where z is soil depth (m), D is the depth to ice cement (m), $[CO_2]$ is soil CO_2 concentration (µL L^{-1}) and $\overline{\delta^{13}C_{CO2-produced}}$ is the concentration-weighted mean $\delta^{13}C_{CO2}$ of the produced CO_2 (‰).

The term $[CO_2]_{produced}$ was calculated as

$$\int_0^D [CO_2]_{warm}\,dz-\int_0^D [CO_2]_{cold}\,dz. \tag{3.14}$$

Assuming there is no biological contribution to the CO_2 produced at Site B,

$$\overline{\delta^{13}C_{CO2-abiotic}}=\overline{\delta^{13}C_{CO2-produced}}. \tag{3.15}$$

If, however, there is a 10% biological contribution to the CO_2 produced at Site B, and assuming that $\delta^{13}C_{CO2}$ reflects the $\delta^{13}C$ of the organic source material ($\delta^{13}C_{biotic}$), then $\overline{\delta^{13}C_{CO2-abiotic}}$ (the mean $\delta^{13}C_{CO2}$ (‰) of CO_2 produced due to abiotic processes) can be derived as

$$\overline{\delta^{13}C_{CO2-abiotic}} = \frac{\overline{\delta^{13}C_{CO2-produced}} - 0.1\ (\delta^{13}C_{biotic})}{0.9}. \quad (3.16)$$

Values used to calculate $\delta^{13}C_{CO2\text{-}abiotic}$ are $[CO_2]_{produced}$ = 29 µL L^{-1}, $\delta^{13}C_{CO2\text{-}produced}$ = −4.1‰ and $\delta^{13}C_{biotic}$ = −28.2‰. The integrals were approximated from the point data shown in Figure 3.10.

3.7.3 Results of principal components analysis

Table 3.4 Eigenvector coefficients and component correlations for the first three principal components. Highlighted cells represent values higher than Mardia's criterion (0.7 times the highest coefficient for the component) for the eigenvector coefficients. Highlighted cells in the component correlations columns show variables that are well described by the components.

	Eigenvector coefficients			Component correlations		
Variable	Comp.1	Comp.2	Comp.3	Comp.1	Comp.2	Comp.3
pH	0.172	-0.369	0.128	0.418	-0.84	0.234
EC	-0.193	-0.325	-0.249	-0.469	-0.742	-0.456
Total C	-0.369	0.092	0.144	-0.898	0.209	0.263
Organic C	-0.252	-0.075	0.374	-0.613	-0.171	0.685
$\delta^{13}C$ organic	-0.031	0.376	-0.089	-0.076	0.857	-0.163
Inorganic C	-0.365	0.117	0.09	-0.888	0.266	0.166
$\delta^{13}C$ inorganic	-0.203	-0.253	0.124	-0.493	-0.578	0.227
Total N	-0.207	-0.104	0.401	-0.504	-0.236	0.733
$\delta^{15}N$	0.086	0.219	-0.198	0.209	0.499	-0.362
CN ratio	0.231	0.124	-0.345	0.561	0.283	-0.631
Ca^{2+}	-0.29	0.229	-0.228	-0.705	0.522	-0.418
K^{+}	-0.136	-0.245	-0.347	-0.33	-0.558	-0.634
Mg^{2+}	-0.342	0.144	-0.195	-0.831	0.328	-0.357
Na^{+}	-0.079	-0.401	-0.157	-0.191	-0.914	-0.287
Cl^{-}	-0.185	-0.274	-0.301	-0.449	-0.625	-0.551
NO_3^{-}	-0.322	0.06	0.037	-0.782	0.138	0.068
PO_4^{2-}	0.152	-0.278	0.007	0.369	-0.634	0.013
SO_4^{2-}	-0.261	-0.044	-0.289	-0.634	-0.1	-0.529

Chapter 4

Quantifying diel variations in biotic and abiotic soil CO_2 fluxes, Taylor Valley, Antarctica (I): Background rates in the absence of a contemporary organic carbon source

4.1 Introduction

In Chapter 3, assumptions of a closed system (no atmospheric exchange) and steady-state partitioning between gaseous and dissolved inorganic C according to Henry's Law were used to model abiotic subsoil CO_2 dynamics. Comparisons with data measured at the warmest and coldest parts of the day suggested this mechanism could account for subsoil CO_2 dynamics. Under the closed system assumption, changes in the C isotopic composition of soil CO_2 between the cold and warm time of the day in a relatively high organic C soil (Site A) limited a biological contribution to soil CO_2 fluxes to less than 25%, depending on the assumptions made about the isotopic composition of CO_2 exsolved from soil solution.

This chapter aims to further advance the understanding of Dry Valley soil CO_2 dynamics through the analysis of samples taken during a more intensive field sampling regime, in which samples were taken at four-hourly intervals over a 48-h period. Sampling was conducted at Site B in Taylor Valley, which is the same "Site B" as that studied in Chapter 3. The higher temporal resolution of the data, combined with the coupling of soil CO_2 concentration and $\delta^{13}C_{CO2}$ profiles with surface CO_2 fluxes, provides the first comprehensive study of CO_2 dynamics in Antarctic soils.

The objectives of the chapter are to:

1. Corroborate existing information on diel variation in surface CO_2 fluxes;
2. Quantify surface and subsurface (storage) fluxes in order to test the closed system assumption used in Chapter 3;
3. Partition biotic and abiotic contributions to surface soil CO_2 fluxes by exploiting differences in their C isotopic composition.

The field work which generated the data considered in this chapter was undertaken during the 2009/10 austral summer, a full year after the field work which yielded results for the previous chapter. The materials and methods utilised were essentially the same as those employed during the 2008/09 summer, although specific differences are noted below.

4.2 Materials and methods

4.2.1 Study area

At the time of gas sampling, soils at Site B were ice-cemented below 30 cm depth, as opposed to being ice-cemented below 26 cm during the sampling period in the 2008/09 austral summer.

4.2.2 Environmental variables

During the intensive 48-h gas sampling period, all data were recorded and logged every 2 minutes by a CR850 data logger (Campbell Scientific Inc., Logan, Utah, USA).

Soil temperature and moisture content measurements

Soil temperature and volumetric moisture content at 5, 15 and 25 cm depth were measured using Hydra Probes (Hydra Probe II, Stevens Water Monitoring Systems Inc., Portland, Oregon, USA).

The rate of change in soil temperature *($\Delta T/\Delta t_t$)* was calculated as the difference in temperatures (*T*) measured ten minutes apart, as follows:

$$\frac{\Delta T}{\Delta t_t} = \frac{T_{t+5\ min} - T_{t-5\ min}}{10\ min}. \quad (4.1)$$

Air temperature

Surface air temperature was measured 2 mm above the soil surface (CS215-L, Campbell Scientific Inc., Logan, Utah, USA).

Wind speed

Wind speed (#40C Anemometer, NRG Systems, Hinesburg, Vermont, USA) and direction (W200P Potentiometer Windvane, Vector Instruments, North Wales, UK) were measured 1.2 m and 1.3 m above the soil surface, respectively. These measurements were made at Site A, located 2.8 km east of Site B. As Site B was on a moraine crest, it is almost certain that wind speeds at Site B would have been the same as or greater than those measured at Site A.

4.2.3 Soil CO_2 sampling and analysis

The experimental set-up and sampling for surface soil CO_2 fluxes proceeded as in 2008/09 (Chapter 3), except that only three chambers were installed in each of two adjacent polygons at Site B. The reduced number of chambers enabled four 20 ml gas samples to be taken from each chamber at 15 min intervals over a 45 min period. The polygons in which gas samples were taken were located ~ 80 m west of the sampling site utilised in 2008/09, on the same geomorphic surface.

Soil profile CO_2 sampling also proceeded as per the previous summer, with subsurface sampling tubes installed adjacent to each of the three chambers in each polygon at depths of 5, 10, 15, 20 and 30 cm. Additionally, one sampling tube was installed horizontally, 1 cm above the desert pavement, in each polygon. Samples were taken from these tubes in the same manner as the subsurface sampling tubes, and provided an atmospheric CO_2 sample from just above the soil surface.

Soil CO_2 sampling began > 48 h after installation of equipment. Gas samples were taken every four hours over a 48-h period, starting at 14:30 h on December 29th, 2009. A selection of samples were analysed for CO_2 concentration and $\delta^{13}C_{CO2}$ using a Gas-bench II connected to a Delta^{Plus} Advantage isotope ratio mass spectrometer (both Thermo Finnigan, Bremen, Germany) at the Macaulay Land Use Research Institute in Aberdeen, Scotland, within 5 months of being collected. Budget constraints meant that it was not possible to analyse all of the samples collected. Standard reference gas samples collected in the field and standard reference gases prepared in New Zealand were included with samples sent to Scotland, and showed no sign of storage or transport effects. The analytical precision for CO_2 concentration and $\delta^{13}C_{CO2}$ values was ≤ 5 µL L^{-1} and ≤ 0.05‰, respectively.

4.2.4 Soil sampling, physical and chemical analyses

The gas samples at Site B were taken within 75 m of the soil pit sampled at Site B in 2008/09. Additional soil samples were taken from a soil pit located adjacent to the 2009/10 gas sampling site, although budget constraints meant that these samples were not analysed. However, based on the proximity of the 2009/10 gas sampling site to the previously sampled and analysed soil pit, the uniformity of the geomorphic surface on which samples were taken, and the similar physical appearance of soil pits dug and described in polygons adjacent to the 2009/10 gas sampling site (Figure 4.1), it was considered that the soil physical and chemical characteristics at Site B are accurately represented by the data presented in Chapter 3.

Figure 4.1 Morphological comparison between soil pits adjacent to gas sampling sites at Site B in the 2008/09 and 2009/10 austral summers. At the time of sampling, the soils (Typic Haploturbels) were ice-cemented below 26 and 30 cm depth in 2008/09 and 2009/10, respectively. Both profiles have been deepened with a concrete breaker and are moistened from melting of ice-cemented permafrost.

4.2.5 Statistical analyses and calculations

Surface CO_2 fluxes

Surface CO_2 fluxes were determined from changes in headspace CO_2 concentrations during the 45 min sampling period using the following equation:

$$n_{CO2} = [CO_2] \frac{PV}{RTA} \quad (4.2)$$

where n_{CO2} is the number of moles of CO_2 emitted per m^2 (µmol m^{-2}), [CO_2] is headspace CO_2 concentration (µL L^{-1}), P is atmospheric pressure (101325 Pa), V is the chamber volume (m^3), R is the ideal gas constant (8.314 J K^{-1} mol^{-1}), T is air temperature (K), and A is the area covered by the chamber (0.0177 m^2).

Surface CO_2 flux rates (µmol m^{-2} s^{-1}) were calculated by linear regression (Microsoft Excel® 2010) of surface CO_2 fluxes (µmol m^{-2}) against time over which samples were collected (s). Surface flux rates that were significantly different to zero ($p < 0.1$) were subsequently used to calculate the net CO_2 gained or lost from the surface chambers ($\Delta[CO_2]$), and the average $\delta^{13}C$ of the net CO_2 gained or lost ($\delta^{13}C_{\Delta CO2}$). Each significant surface CO_2 flux, which may be positive or negative, was considered individually, and calculations were as follows:

$$\Delta[CO_2] = [CO_2]_{final} - [CO_2]_{initial} \quad (4.3)$$

where $[CO_2]_{final}$ and $[CO_2]_{initial}$ are the final and initial CO_2 concentrations (µL L^{-1}) measured from the final and initial CO_2 samples taken from the chamber, respectively.

Using a mass balance approach,

$$\Delta[CO_2] \cdot \delta^{13}C_{\Delta CO2} = [CO_2]_{final} \cdot \delta^{13}C_{[CO2]final} - [CO_2]_{initial} \cdot \delta^{13}C_{[CO2]initial}, \quad (4.4)$$

where $\delta^{13}C_{\Delta CO2}$ (‰) is the $\delta^{13}C$ of the net CO_2 gained or lost between the final and initial measurements, and $\delta^{13}C_{[CO2]final}$ and $\delta^{13}C_{[CO2]initial}$ are the $\delta^{13}C_{CO2}$ values (‰) measured from the final and initial CO_2 samples taken from the chamber, respectively.

Therefore,

$$\delta^{13}C_{\Delta CO2} = \frac{[CO_2]_{final} \cdot \delta^{13}C_{[CO2]final} - [CO_2]_{initial} \cdot \delta^{13}C_{[CO2]initial}}{\Delta[CO_2]} . \quad (4.5)$$

Subsurface CO_2 fluxes

Subsurface CO_2 fluxes were estimated by calculating differences in the average soil profile CO_2 concentration between consecutive sampling times. The average soil profile CO_2 concentration was determined by using an analogue integration technique whereby the area under a paper plot of CO_2 concentration versus depth at each sampling time was weighed to determine the integral

$$\overline{[CO_2]} = \frac{\int_0^{30}[CO_2]\,dz}{30} \quad (4.6)$$

where z is depth in cm and $\overline{[CO_2]}$ is the profile average CO_2 concentration between 0 and 30 cm depth. The difference in $\overline{[CO_2]}$ between consecutive sampling times was used to determine the number of moles of CO_2 (n_{CO2}; µmol m^{-2}) gained or lost over the period between sampling times using the ideal gas law:

$$n_{CO2} = \Delta[CO_2]\,\frac{PV}{RT} \quad (4.7)$$

where $\Delta[CO_2]$ is the difference in the profile average CO_2 concentration between sampling times (µL L^{-1}), P is atmospheric pressure (101325 Pa), V is the soil gas volume (m^3 m^{-2}; calculated by multiplying soil depth (0.3 m) by the air-filled porosity (ε = 0.4)), R is the ideal gas constant (8.314 J K^{-1} mol^{-1}) and T is soil temperature (K). This was converted to a flux rate (µmol m^{-2} s^{-1}) by dividing by the time (s) over which n_{CO2} was gained or lost.

Calculated surface CO_2 fluxes and their C isotopic composition

To test that gas fluxes were dominantly diffusion-driven, surface CO_2 flux rates were plotted against near-surface CO_2 concentration gradients. Linear regression of this relationship yields a value for the effective diffusivity of CO_2 (D_e; $cm^2\ s^{-1}$) within the soil.

In a diffusion-driven system, the $\delta^{13}C_{\Delta CO2}$ of surface CO_2 fluxes is determined by subsurface CO_2 concentration and $\delta^{13}C_{CO2}$ gradients. Using data from subsurface profiles, the $\delta^{13}C_{\Delta CO2}$ of surface CO_2 fluxes can therefore be determined as follows:

$$R_{13} of\ flux = \frac{F_{13}}{F_{12}} \tag{4.8}$$

where R_{13} of flux is the ratio of ^{13}C to ^{12}C in the CO_2 flux, and F_{13} and F_{12} refer to the flux of $^{13}CO_2$ and $^{12}CO_2$, respectively. Each individual flux of $^{13}CO_2$ and $^{12}CO_2$ is derived separately, using Fick's Law, so:

$$F_{13} = {}^{13}D_s \frac{d^{13}CO_2}{dz}, and\ F_{12} = {}^{12}D_s \frac{d^{12}CO_2}{dz} \tag{4.9}$$

where $^{13}D_s$ and $^{12}D_s$ are the diffusivities of $^{13}CO_2$ and $^{12}CO_2$ in soil, respectively, and $d^{13}CO_2/dz$ and $d^{12}CO_2/dz$ are concentration gradients of ^{13}C and ^{12}C, respectively, where depth (z) increases downwards in the soil. As such, the negative sign normally seen in Fick's Law is not appropriate.

The ratio of ^{13}C to ^{12}C in the flux can therefore be derived as follows:

$$\frac{F_{13}}{F_{12}} = \frac{{}^{13}D_s}{{}^{12}D_s} \frac{\frac{d^{13}CO_2}{dz}}{\frac{d^{12}CO_2}{dz}}. \tag{4.10}$$

Any value presented in delta notation (e.g. $\delta^{13}C_{CO2}$, in units of per mil) is related to a standard reference material as follows:

$$\delta_{sample} = \left(\frac{R_{sample} - R_{standard}}{R_{standard}}\right) 1000\,, \tag{4.11}$$

where R_{sample} and $R_{standard}$ are the ratios of heavy to light isotopes in the sample and standard, respectively. Therefore, a $\delta^{13}C_{CO2}$ value can be presented as:

$$\delta^{13}C_{CO2} = \left(\frac{J}{R_{VPDB}} - 1\right) 1000\,, \tag{4.12}$$

where J is the ratio of ^{13}C to ^{12}C in the sample.

Therefore,

$$J = \left(\frac{\delta^{13}C_{CO2}}{1000} + 1\right) R_{VPDB}\,. \tag{4.13}$$

The concentration of $^{13}CO_2$ ($[^{13}CO_2]$) can be determined by

$$\left[^{13}CO_2\right] = \frac{J}{1+J}[CO_2]\,, \tag{4.14}$$

and the concentration of $^{12}CO_2$ is

$$\left[^{12}CO_2\right] = \frac{[CO_2]}{1+J}\,. \tag{4.15}$$

Therefore, the flux of $^{13}CO_2$ is

$$^{13}D_s\,\frac{d\left[^{13}CO_2\right]}{dz} = {}^{13}D_s\,\frac{d\left(\frac{J}{1+J}[CO_2]\right)}{dz}, \tag{4.16}$$

and the flux of $^{12}CO_2$ is

$$^{12}D_s\,\frac{d\left[^{12}CO_2\right]}{dz} = {}^{12}D_s\,\frac{d\left(\frac{[CO_2]}{1+J}\right)}{dz}. \tag{4.17}$$

Using the derivative of a product rule,

$$\frac{d\left[^{13}CO_2\right]}{dz} = [CO_2]\,\frac{d\left(\frac{J}{1+J}\right)}{dz} + \frac{J}{1+J}\frac{d[CO_2]}{dz}. \tag{4.18}$$

Using the rule for differentiation of a quotient for the first term on the right hand side of equation (4.18) (above),

$$\frac{d\left[^{13}CO_2\right]}{dz} = \frac{[CO_2]}{(1+J)^2}\frac{dJ}{dz} + \frac{J}{1+J}\frac{d[CO_2]}{dz}. \tag{4.19}$$

Again, using the quotient rule for differentiation of equation (4.17),

$$\frac{d\left[^{12}CO_2\right]}{dz} = \frac{(1+J)\frac{d[CO_2]}{dz} - [CO_2]\frac{dJ}{dz}}{(1+J)^2}, \tag{4.20}$$

hence

$$
\begin{aligned}
&{}^{13}D_s \frac{d\left[{}^{13}CO_2\right]}{dz} \Big/ {}^{12}D_s \frac{d\left[{}^{12}CO_2\right]}{dz} \qquad (4.21)\\
&= \frac{{}^{13}D_s}{{}^{12}D_s}\left(\frac{[CO_2]}{(1+J)^2}\frac{dJ}{dz} + \frac{J}{1+J}\frac{d[CO_2]}{dz}\right) \Big/ \left(\frac{(1+J)\frac{d[CO_2]}{dz} - [CO_2]\frac{dJ}{dz}}{(1+J)^2}\right)
\end{aligned}
$$

$$
= \frac{{}^{13}D_s}{{}^{12}D_s}\left(\frac{dJ}{dz}[CO_2] + J(1+J)\frac{d[CO_2]}{dz}\right) \Big/ \left((1+J)\frac{d[CO_2]}{dz} - [CO_2]\frac{dJ}{dz}\right) \qquad (4.22)
$$

$$
= \frac{{}^{13}D_s}{{}^{12}D_s}\left(\frac{d[CO_2]}{dz}J(1+J) + \frac{dJ}{dz}[CO_2]\right) \Big/ \left(\frac{d[CO_2]}{dz}(1+J) - \frac{dJ}{dz}[CO_2]\right). \qquad (4.23)
$$

Therefore,

$$
R_{13} = \frac{{}^{13}D_s}{{}^{12}D_s} \frac{\frac{d[CO_2]}{dz}J(1+J) + \frac{dJ}{dz}[CO_2]}{\frac{d[CO_2]}{dz}(1+J) - \frac{dJ}{dz}[CO_2]}. \qquad (4.24)
$$

Assuming $\frac{{}^{13}D_s}{{}^{12}D_s}$ scales as $\frac{{}^{13}D}{{}^{12}D}$, the ratio is given by

$$
\frac{D({}^{13}CO_2)}{D({}^{12}CO_2)} = \left(\frac{M({}^{12}CO_2)\,M_{air}}{M({}^{12}CO_2) + M_{air}} \frac{M({}^{13}CO_2) + M_{air}}{M({}^{13}CO_2)\,M_{air}}\right)^{\frac{1}{2}} = 0.9956. \qquad \text{(Craig, 1953)} \qquad (4.25)
$$

Therefore,

$$
R_{13} = 0.9956\left(\frac{\frac{d[CO_2]}{dz}J(1+J) + \frac{R_{VPDB}}{1000}\frac{d(\delta^{13}C)}{dz}[CO_2]}{\frac{d[CO_2]}{dz}(1+J) - \frac{R_{VPDB}}{1000}\frac{d(\delta^{13}C)}{dz}[CO_2]}\right). \qquad (4.26)
$$

R_{13} can be converted to standard delta notation using equation 4.11. R_{13} is substituted for R_{sample}, and R_{VPDB} is $R_{standard}$.

4.3 Results

4.3.1 Environmental variables

At the time of sampling (late December 2009), soils at Site B were ice-cemented below 30 cm. Air and soil temperatures varied diurnally, with the latter exhibiting progressively greater lags and damping in soil temperature response to surface heating and cooling with increasing depth in the profile (Figure 4.2A). Air temperature ranged from −4.4 to 6.1°C, and soil temperatures at 5 cm, 15 cm and 25 cm ranged from −1.5 to 11.7°C, 0.0 to 3.8°C and −0.4 to 0.8°C, respectively.

Soil moisture content was very low (Figure 4.2B), averaging 0.6, 0.4 and 1.3% at 5, 15 and 25 cm depth, respectively. Qualitative observations of limited melting of snow patches and lake ice in late December 2009 suggested that the summer was cooler than the previous summer of 2008/09. This was corroborated by the lack of ponded surface water evident at sites where it had been observed the previous summer, and the low soil moisture contents measured at Site B.

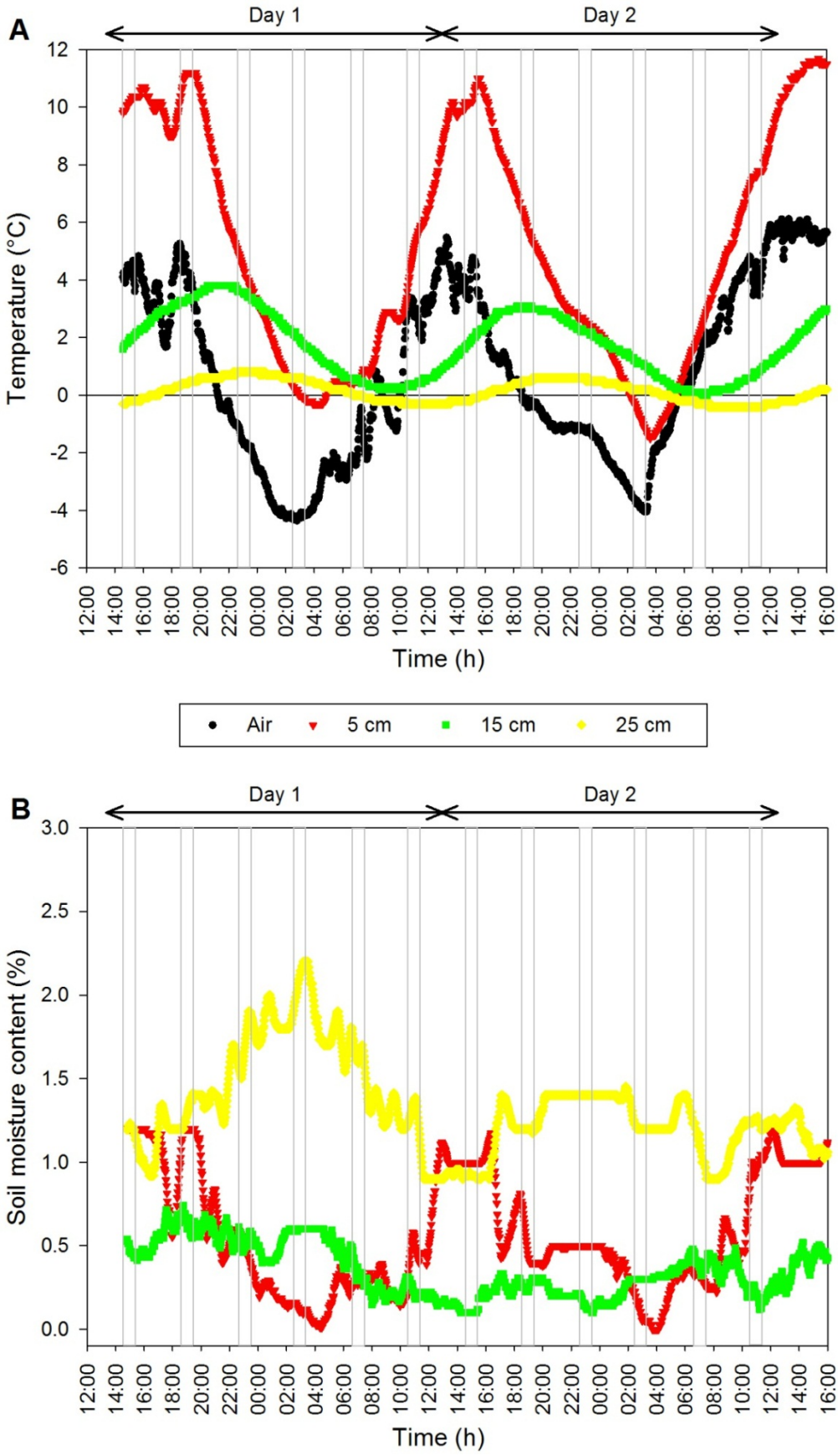

Figure 4.2 Soil temperature (A) and volumetric moisture content (B) during the 48-hour period over which gas samples were taken, Site B, Taylor Valley. Data plotted for moisture content are 30 min. moving averages. The narrow vertical grey boxes denote the periods during which gas samples were taken.

4.3.2 CO_2 dynamics

Surface CO_2 fluxes

Surface CO_2 flux rates at Site B were relatively low, with statistically significant fluxes (which comprised 81% of all surface CO_2 fluxes calculated) ranging from −0.053 to 0.074 µmol m^{-2} s^{-1} (Table 4.1). The average significant flux at each sampling time ranged between −0.041 and 0.058 µmol m^{-2} s^{-1} (Figure 4.3A). The highest and lowest (most negative) surface CO_2 flux rates occurred at 14:30 and 02:30 h, respectively. Temporal patterns of variation in surface CO_2 flux rates were similar to diel trends in wind speed (measured at Site A) and soil temperature at 5 cm depth, although changes in surface CO_2 flux rate led variations in soil temperature at 15 cm depth by around 4 h (Figure 4.3C). However, changes in surface CO_2 flux rates were in phase with variations in the rate of change of soil temperature at 15 cm depth (Figure 4.3D). The diel variation in significant surface CO_2 flux rates was asymmetrical about 0 µmol m^{-2} s^{-1}, with maximum positive fluxes, measured at the warmest time of day, being greater than minimum (negative) fluxes measured at the coolest time of day (Figure 4.3A).

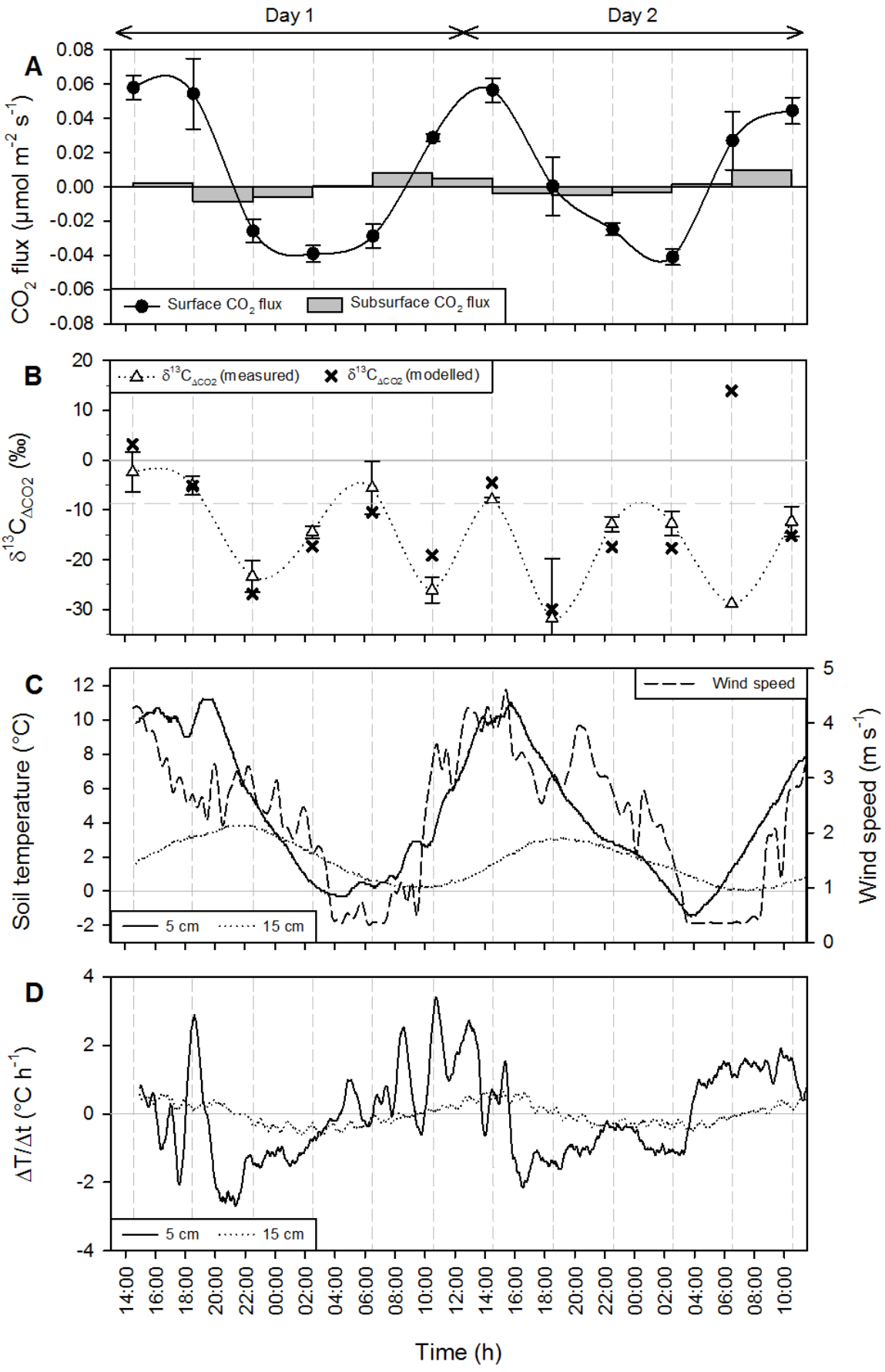

Figure 4.3 **(A)** Average significant surface and subsurface soil CO_2 flux rates at Site B, Taylor Valley. Error bars represent the standard error of the mean. Subsurface soil CO_2 storage fluxes are shown as grey bars which represent the net CO_2 flux over the 4-h period between

sampling. **(B)** Isotopic composition ($\delta^{13}C_{\Delta CO2}$) of measured and predicted surface CO_2 fluxes at Site B, Taylor Valley. Predicted values are calculated based on subsurface CO_2 concentration and $\delta^{13}C_{CO2}$ gradients at the time of sampling, according to equation 4.26. Error bars represent the standard error of the mean. The dashed horizontal line represents the average $\delta^{13}C_{CO2}$ of soil CO_2 (−8.8‰). **(C)** Soil temperature at 5 and 15 cm depth (left hand axis) during the gas sampling period, Site B, Taylor Valley. Wind speed data (right hand axis) are from Site A, Taylor Valley. **(D)** Rate of change in soil temperature at 5 and 15 cm depth during the gas sampling period, Site B, Taylor Valley. Data plotted are 30 min moving averages.
The dashed vertical lines correspond to the four-hourly intervals at which gas sampling began.

Table 4.1 Surface soil CO_2 fluxes at Site B, Taylor Valley.

Day 1					Day 2			
Date	Sampling time (h)	Replicate	CO_2 flux (μmol m^{-2} s^{-1})		Date	Sampling time (h)	Replicate	CO_2 flux (μmol m^{-2} s^{-1})
29/12/10	14:30	a	0.063**		30/12/10	14:30	a	0.046**
		b	0.028				b	0.043**
		c	0.006				c	0.067**
		d	0.053**				d	0.070**
29/12/10	18:30	a	0.056**		30/12/10	18:30	a	−0.008
		b	0.033**				b	−0.010**
		c	0.074**				c	−0.009*
		d	0.056				d	0.020**
29/12/10	22:30	a	−0.017*		30/12/10	22:30	a	−0.015**
		b	−0.045**				b	−0.028**
		c	−0.015**				c	−0.024**
		d	−0.026**				d	−0.032**
30/12/10	02:30	a	−0.037**		31/12/10	02:30	a	−0.051**
		b	−0.032**				b	−0.039*
		c	−0.053**				c	−0.029*
		d	−0.034**				d	−0.045**
30/12/10	06:30	a	−0.010		31/12/10	06:30	a	−0.010
		b	−0.037*				b	0.015**
		c	−0.025*				c	0.039**
		d	−0.024**				d	0.002
30/12/10	10:30	a	0.023*		31/12/10	10:30	a	0.039**
		b	0.028**				b	0.038
		c	0.034**				c	0.019
		d	0.030**				d	0.050**

* represents $P < 0.1$; ** represents $P < 0.05$.

The average $\delta^{13}C_{CO2}$ of the four gas samples taken from surface chambers during the 45-min sampling periods varied little from that of ambient atmospheric CO_2 (−8.8‰), ranging between −9.4 and −8.3‰. Where surface fluxes were statistically significant, changes in $\delta^{13}C_{CO2}$ between samples taken at times 0 and 45 min were used to calculate the $\delta^{13}C_{\Delta CO2}$ of the surface flux (4.5). The $\delta^{13}C_{\Delta CO2}$ of significant positive and negative surface CO_2 fluxes was highly variable, ranging from −2.4 to −31.8‰ (Figure 4.3B). The $\delta^{13}C_{\Delta CO2}$ of the highest effluxes ranged between −2.4 and −8.0‰, whereas the highest influxes had $\delta^{13}C_{\Delta CO2}$ values of −14.4 and −12.7‰. The most negative $\delta^{13}C_{\Delta CO2}$ values of −23.4 to −31.8‰ were measured following the four-hourly intervals during which a transition from positive to negative (or vice versa) fluxes occurred. The measured and predicted $\delta^{13}C_{\Delta CO2}$ values were generally in good agreement (Figure 4.3B).

Subsurface CO_2 profiles and fluxes

Values for CO_2 concentration and $\delta^{13}C_{CO2}$ at 0 cm depth were relatively consistent throughout the 48-h sampling period (Figure 4.4). Despite these samples being taken 1 cm above the ground surface, they are assumed to provide the soil–atmosphere boundary CO_2 concentration and $\delta^{13}C_{CO2}$ over the sampling period, averaging 400 ± 4 μL L^{-1}, and −8.8 ± 0.2‰, respectively. These values differ slightly from atmospheric CO_2 concentration (385 μL L^{-1}) and $\delta^{13}C_{CO2}$ (−8.2‰) measured at the South Pole in December 2009 (Keeling et al., 2001).

Temporal changes in CO_2 concentration and $\delta^{13}C_{CO2}$ profiles throughout the two 24-h sampling periods at Site B were generally symmetrical (Figure 4.4). The CO_2 concentration profiles were quasi-symmetrical about a vertical line corresponding to the local atmospheric CO_2 concentration (400 μL L^{-1}), with maximum variation in concentration ranging from 372 to 426 μL L^{-1} between 10 and 15 cm depth. Subsurface soil CO_2 concentrations were generally greater than atmospheric CO_2 concentration at 10:30, 14:30 and 18:30 h, and less than atmospheric CO_2 concentration at 22:30, 02:30 and 06:30 h.

Depth profiles of $\delta^{13}C_{CO2}$ were quasi-symmetrical about a line sloping from −8.8‰ at the surface to −8.3‰ at 30 cm depth for both 24-h periods (Figure 4.4). Changes in $\delta^{13}C_{CO2}$ values tended to correspond to changes in CO_2 concentration, with $\delta^{13}C_{CO2}$ generally becoming more depleted as CO_2 concentration decreased, and more enriched as CO_2 concentration increased. The maximum variation in $\delta^{13}C_{CO2}$ occurred at 5 cm depth, with $\delta^{13}C_{CO2}$ ranging between −9.1 and −8.3‰, whereas the minimum variation was at 15 cm depth.

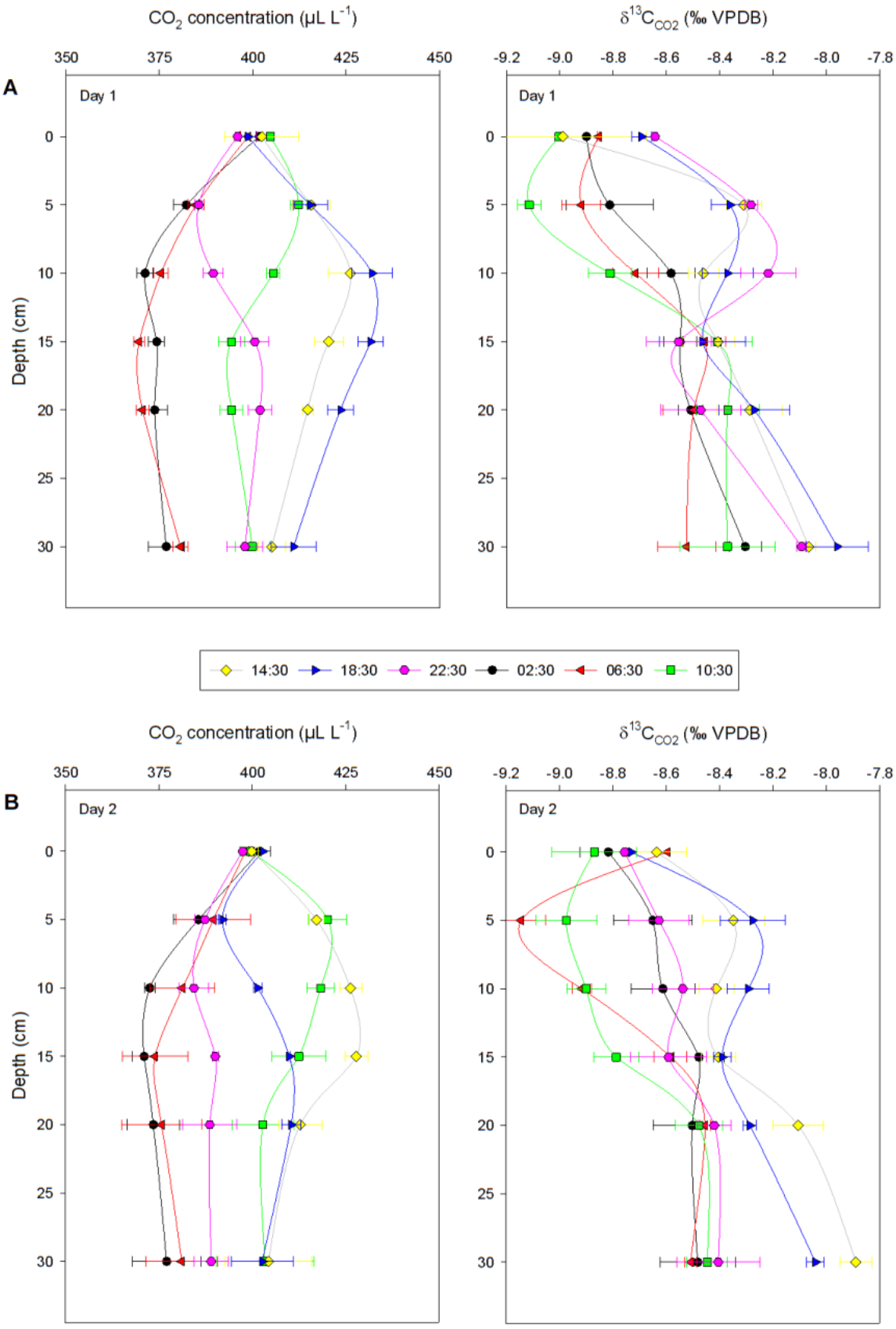

Figure 4.4 Soil profile CO_2 concentrations and $\delta^{13}C_{CO2}$ values at Site B, Taylor Valley. **(A)** and **(B)** represent data from Day 1 and Day 2, respectively. Data points are averages from each sampling time (n = 1 or 2 for 0 cm samples. At all other depths, n = 4). Error bars represent the standard error of the mean.

Subsurface storage CO_2 fluxes, calculated based on the change in the profile average CO_2 concentration between sampling times (equation 4.7), varied diurnally between positive and negative values, with the same periodicity as surface CO_2 fluxes. However, they were an order of magnitude lower, ranging from −0.01 to 0.01 μmol m^{-2} s^{-1} (Figure 4.3A). Changes in the direction of subsurface storage CO_2 fluxes preceded changes in the direction of surface fluxes by 4−6 h.

4.3.3 Linking surface and subsurface CO_2 dynamics

Day 1 (Figure 4.3 and Figure 4.4A)

14:30 – 18:30 h

Between 14:30 and 18:30 h, the soil was in a steady-state phase of net CO_2 efflux. Subsoil CO_2 concentrations were above ambient, and increased only slightly below 5 cm depth during this interval. The positive concentration gradients (increasing CO_2 concentration with depth) drove positive surface CO_2 fluxes, which remained close to the maximum rate of 0.058 μmol m^{-2} s^{-1} over this interval. Subsurface $\delta^{13}C_{CO2}$ values did not change significantly, and were close to their most enriched (−8.0 to −8.5‰).

Subsurface $\delta^{13}C_{CO2}$ gradients were also positive (increasing $\delta^{13}C_{CO2}$ with depth), which, together with the positive CO_2 concentration gradients, drove surface fluxes enriched in ^{13}C relative to the ambient soil atmosphere (~ −8.8‰). The $\delta^{13}C_{\Delta CO2}$ of the measured flux into surface chambers was −2.4 and −5.1‰ at 14:30 and 18:30 h, respectively; the $\delta^{13}C_{\Delta CO2}$ of fluxes calculated from CO_2 and $\delta^{13}C_{CO2}$ gradients at those times were 3.2 and −5.2‰, respectively. Over this period, soil temperature at 5 cm depth remained relatively constant and close to its daily maximum, and soil temperature at 15 cm depth increased linearly at close to its maximum rate of change.

18:30 – 22:30 h

Between 18:30 and 22:30 h, the soil entered a transient phase of CO_2 loss. Subsurface CO_2 concentrations decreased throughout the profile, most markedly between 5 and 15 cm depth, and by 22:30 h, the positive concentration gradient that existed between 0 and 10 cm depth at 18:30 h had shifted to a negative concentration gradient (decreasing with increasing depth) between 0 and 5 cm depth, with CO_2 concentrations above 15 cm depth all lower than that of atmospheric CO_2. Despite the efflux of CO_2 at 18:30 h being enriched in ^{13}C relative to ambient soil CO_2, the depth profile of $\delta^{13}C_{CO2}$ changed very little over the 4-h period, and the positive $\delta^{13}C_{CO2}$ gradient was maintained. Surface CO_2 fluxes shifted from positive to negative (0.054 to −0.026 μmol m^{-2} s^{-1}) in response to changes in the CO_2 concentration gradient. The switch to a negative CO_2 concentration gradient, combined with the persistent positive $\delta^{13}C_{CO2}$ gradient, drove a CO_2 influx depleted in ^{13}C. The $\delta^{13}C_{\Delta CO2}$ of CO_2 influxes calculated from surface chambers averaged −23.4‰ at 22:30 h, which was consistent with the $\delta^{13}C_{\Delta CO2}$ predicted from CO_2 and $\delta^{13}C_{CO2}$ gradients of −26.9‰.

The marked decrease in CO_2 concentration throughout the profile coincided with rapidly decreasing soil temperature at 5 cm depth, which shifted from increasing at close to its maximum positive rate to reach its daily maximum early in the interval, to decreasing at its maximum negative rate. Soil temperature at 15 cm depth increased over this period (albeit at a slower rate than during the previous 4-h period), reaching its daily maximum at the end of the interval.

22:30 – 02:30 h

Over the period from 22:30 to 02:30 h, the soil remained in a transient phase of CO_2 loss, although the rate of CO_2 absorption was lower than during the previous 4-h period. Subsurface CO_2 concentration decreased below 5 cm depth, and the negative concentration gradient between 0 and 5 cm depth at 22:30 h extended to 10 cm depth by 02:30 h, with soil CO_2 concentration being less than ambient atmospheric CO_2 concentration throughout the profile. Subsurface $\delta^{13}C_{CO2}$ values became significantly more depleted (by up to −0.5‰) in the upper 15 cm of the profile, consistent with the highly depleted surface influx established at 22:30 h, and resulting in a weak positive $\delta^{13}C_{CO2}$ gradient. Surface CO_2 fluxes became increasingly negative, consistent with the steeper negative concentration gradient in the subsoil, and reached a daily maximum (negative) rate of −0.039 µmol m^{-2} s^{-1} at the end of the interval. The average $\delta^{13}C_{\Delta CO2}$ of the CO_2 influx shifted from −23.4‰ at 22:30 h to −14.4‰ at 02:30 h, which was again consistent with predicted $\delta^{13}C_{\Delta CO2}$ values of the net surface CO_2 influx (−26.9 and −17.3‰ at 22:30 and 02:30 h, respectively). The rates of change in soil temperature at 5 and 15 cm depth were both negative, with the latter at its maximum negative rate by the end of the interval.

02:30 – 06:30 h

During this period, the soil was in a steady-state phase of net CO_2 influx. Subsurface soil CO_2 concentration and $\delta^{13}C_{CO2}$ depth profiles did not change significantly, despite there being CO_2 fluxes into the soil of −0.039 µmol m^{-2} s^{-1} at 02:30 h and −0.029 µmol m^{-2} s^{-1} at 06:30 h. This set of circumstances requires that the combination of biotic production (if any), abiotic consumption, and diffusion associated with the subsoil CO_2 concentration gradients have balanced effects with respect to the total mass of CO_2 and abundances of $^{12}CO_2$ and $^{13}CO_2$.

However, subtle changes in $\delta^{13}C_{CO2}$ values at 5 cm depth, owing to the $\delta^{13}C_{\Delta CO2}$ of the CO_2 influx at 02:30 h being isotopically lighter than ambient soil CO_2, acted to change the $\delta^{13}C_{CO2}$ gradient from a weak positive gradient at 02:30 h to a weak negative gradient at 06:30 h. This, combined with the negative CO_2 concentration gradient throughout the interval, drove a heavier influx of CO_2 at 06:30 h. The $\delta^{13}C_{\Delta CO2}$ of the surface CO_2 influx shifted from −14.4‰ at 02:30 h to −5.6‰ at 06:30 h; these values were similar to the predicted $\delta^{13}C_{\Delta CO2}$ values of −17.3 and −10.5‰ at 02:30 and 06:30 h, respectively. Soil temperature at 5 cm depth remained close to its daily minimum throughout the

interval, while soil temperature at 15 cm depth continued to decrease at close to its maximum negative rate. These temperature changes mirrored the soil temperature conditions that prevailed during the period of steady-state efflux (14:30 – 18:30 h).

06:30 – 10:30 h

Between 06:30 and 10:30 h, the soil entered a transient phase of CO_2 gain. Subsurface CO_2 concentrations increased significantly at all depths, at a rate which was close to the maximum subsurface accumulation rate. The negative CO_2 concentration gradient between 0 and 15 cm depth at 06:30 h switched to a slight positive gradient between 0 and 5 cm depth at 10:30 h; this was reflected in surface CO_2 fluxes which shifted from negative to positive over this period. Subsurface $\delta^{13}C_{CO2}$ values became slightly more depleted in the upper 10 cm of the profile and slightly more enriched in the lower 10 cm, thus increasing the negative $\delta^{13}C_{CO2}$ gradient. The change in CO_2 concentration gradient from negative to positive, combined with the persistent negative $\delta^{13}C_{CO2}$ gradient drove a highly depleted (−26.1‰) surface CO_2 efflux at 10:30 h. This value, although being very close to the $\delta^{13}C$ value of organic matter measured in the top 5 cm of the soil profile at Site B (Chapter 3, Figure 3.8C), is relatively close to that predicted by CO_2 concentration and $\delta^{13}C_{CO2}$ gradients (−19.1‰). Soil temperature at 5 cm depth increased from close to its daily minimum, and soil temperature at 15 cm depth decreased at a low rate, reaching its daily minimum by the end of the interval.

10:30 – 14:30 h

This interval completes a full 24-h cycle, thus data from the subsurface profile measured at 14:30 h are shown on the "Day 2" profile (Figure 4.4B). As for the Day 1 22:30 to 02:30 h period of subsoil consumption of CO_2 and negative surface fluxes, this interval also marks significant change in both CO_2 concentration and $\delta^{13}C_{CO2}$ profiles. Accumulation of CO_2 in the subsoil continued from the previous 4-h interval, and by 14:30 h, subsurface CO_2 concentrations were greater than atmospheric CO_2 concentration throughout the profile, with the positive CO_2 concentration gradient extending to 15 cm depth. The average surface CO_2 flux rate increased from 0.029 μmol m^{-2} s^{-1} at 10:30 h to the daily maximum rate of 0.057 μmol m^{-2} s^{-1} at 14:30 h, which is very similar to the maximum surface flux rate at 14:30 h on Day 1. Soil $\delta^{13}C_{CO2}$ became more enriched throughout the profile, consistent with the isotopically light efflux of CO_2 at 10:30 h acting to increase the abundance of the heavier ^{13}C isotope in the soil atmosphere, with a maximum shift from −9.1 to −8.3‰ at 5 cm depth. The enrichment in soil $\delta^{13}C_{CO2}$ acted to change the $\delta^{13}C_{CO2}$ gradient from negative to positive, and combined with the positive concentration gradient, drove a relatively heavy (−8.0‰) efflux of CO_2 at 14:30 h. This is close to the $\delta^{13}C_{\Delta CO2}$ of the CO_2 efflux (−4.5‰) predicted from the CO_2 concentration and $\delta^{13}C_{CO2}$ gradients at 14:30 h. Over this interval, soil temperature at both 5 and 15 cm depth

increased; temperature at 5 cm depth increased at its maximum rate, and soil temperature at 15 cm depth increased from its daily minimum.

Day 2 (Figure 4.3 and Figure 4.4B)

14:30 – 18:30 h

Unlike the steady-state condition that prevailed between 14:30 and 18:30 h on Day 1, during this interval, the subsoil CO_2 concentration decreased throughout the upper 20 cm of the profile, although the $\delta^{13}C_{CO2}$ changed very little. By 18:30 h, the positive concentration gradient that existed between 0 and 15 cm depth at 14:30 h had shifted to a negative concentration gradient between 0 and 5 cm depth, and the profile average CO_2 concentration was close to that of atmospheric CO_2. The $\delta^{13}C_{CO2}$ profiles did not change significantly in the upper 15 cm of the soil, as the efflux of CO_2 at 14:30 h was of similar isotopic composition to that of soil CO_2; below this depth, $\delta^{13}C_{CO2}$ became slightly more depleted. The average surface CO_2 flux rate decreased from its daily maximum positive rate to near zero in response to changes in the CO_2 concentration gradient. The switch to a negative concentration gradient, combined with the persistent positive $\delta^{13}C_{CO2}$ gradient acted to drive a relatively depleted flux at 18:30 h, with the average $\delta^{13}C_{\Delta CO2}$ of the net flux shifting from −8.0‰ at 14:30 h to −31.8‰ at 18:30 h. The $\delta^{13}C_{\Delta CO2}$ values of the net fluxes were consistent with predicted $\delta^{13}C_{\Delta CO2}$ values of −4.5 and −30.0‰ at 14:30 and 18:30 h, respectively. Soil temperatures at 5 and 15 cm depth reached their daily maxima during this interval. However, soil temperature at 5 cm depth predominantly decreased, at times at a rate close to its maximum negative rate of change, whilst soil temperature at 15 cm depth increased to its daily maximum at its maximum rate of change. These temperature changes, along with the subsurface absorption of CO_2, decrease in surface CO_2 flux rate, and decrease in subsurface CO_2 concentration with little change in subsurface $\delta^{13}C_{CO2}$ over this interval were very similar to those which occurred during the 18:30 to 22:30 h interval on Day 1.

18:30 – 22:30 h

Between 18:30 and 22:30 h, the soil continued to absorb CO_2, at a rate slightly higher than during the previous interval. Subsurface CO_2 concentrations decreased at all depths, and the negative concentration gradient between 0 and 5 cm depth at 18:30 h extended to 10 cm depth by 22:30 h, with CO_2 concentrations throughout the profile being less than that of atmospheric CO_2. Subsurface $\delta^{13}C_{CO2}$ values became significantly more depleted (by up to −0.4‰) throughout the profile. This change was consistent with a highly depleted CO_2 influx established by the CO_2 and $\delta^{13}C_{CO2}$ gradients at 18:30 h, and resulted in a weak positive $\delta^{13}C_{CO2}$ gradient. The average surface CO_2 flux rate became negative, and at 22:30 h, the $\delta^{13}C_{\Delta CO2}$ of the CO_2 influx was −12.9‰, which was consistent with the predicted $\delta^{13}C_{\Delta CO2}$ of −17.5‰. Soil temperatures decreased at both 5 and 15 cm depth. The soil temperature trends and changes in CO_2 dynamics observed during this period were similar to those occurring between 22:30 and 02:30 h on Day 1.

22:30 – 02:30 h

This period represents the closest approximation to a steady-state period of CO_2 influx on Day 2. During this period, the soil continued to absorb CO_2. Subsurface CO_2 concentrations continued to decrease below 5 cm depth, and the negative concentration gradient extended to 15 cm depth, although the subsurface $\delta^{13}C_{CO2}$ profile did not significantly change. The average surface CO_2 flux rate continued to become increasingly negative, reaching its maximum negative rate of −0.041 μmol m^{-2} s^{-1} by 02:30 h. The average $\delta^{13}C_{\Delta CO2}$ of the CO_2 influx remained very similar at −12.7‰, which was again consistent with the $\delta^{13}C_{\Delta CO2}$ of the CO_2 influx (−17.7‰) predicted from CO_2 concentration and $\delta^{13}C_{CO2}$ gradients at 02:30 h. As the $\delta^{13}C_{CO2}$ profiles did not change significantly, this implies that the CO_2 being absorbed during this period had a $\delta^{13}C_{CO2}$ value close to that of the CO_2 influx over this period (−12.9‰). Soil temperatures at 5 and 15 cm depth continued to decrease; the rate of change in soil temperature at 15 cm depth was close to its maximum negative rate. The decrease in subsurface CO_2 concentrations and surface flux rates was similar to the trends occurring during the 22:30 to 02:30 h interval on Day 1, with the main difference during this interval on Day 2 being that subsurface $\delta^{13}C_{CO2}$ values did not significantly change.

02:30 – 06:30 h

Over this interval, the subsoil returned to a transient CO_2 accumulation phase. However, the net accumulation was small; CO_2 concentrations remained below that of atmospheric throughout the profile, and the negative concentration gradient between 0 and 15 cm depth was maintained. Subsurface $\delta^{13}C_{CO2}$ values became significantly more depleted (by up to −0.5‰) in the upper 15 cm, with the maximum depletion in $\delta^{13}C_{CO2}$ occurring at 5 cm depth. The depletion in $\delta^{13}C_{CO2}$ is consistent with an influx of CO_2 isotopically lighter than that of the soil atmosphere at 02:30 h, and resulted in a negative $\delta^{13}C_{CO2}$ gradient at 06:30 h. The average surface CO_2 flux rate increased from the maximum negative rate at 02:30 h to a moderate positive rate by 06:30 h. The positive CO_2 flux at 06:30 h is inconsistent with the negative CO_2 concentration gradient that persisted throughout this interval. Additionally, the average $\delta^{13}C_{\Delta CO2}$ of the net CO_2 efflux at 06:30 h of −28.9‰ is inconsistent with the combination of CO_2 concentration and $\delta^{13}C_{CO2}$ gradients at that time, which predict a CO_2 influx at 13.9‰. The surface flux and its isotopic composition at 06:30 h are the only anomalous data points recorded throughout the 48-h sampling period.

Soil temperature at 5 cm depth reached its daily minimum during this interval, and soil temperature at 15 cm depth decreased at close to its maximum negative rate, reaching its daily minimum at the end of the interval. The subsurface CO_2 concentration profiles were similar to those observed during the 02:30 to 06:30 h interval on Day 1. However, during the Day 2 interval, subsurface $\delta^{13}C_{CO2}$ values became significantly more depleted in the upper 15 cm of the profile, which did not occur during the 02:30 to 06:30 h interval on Day 1. The increase in surface CO_2 flux rate from a negative to a positive

rate, and the changes in $\delta^{13}C_{\Delta CO2}$ of the net CO_2 exchanged within surface chambers from enriched to highly depleted values, along with changes in soil temperature, were more similar to those observed during the 06:30 to 10:30 h interval on Day 1.

06:30 – 10:30 h

From 06:30 h to the final sampling at 10:30 h, the soil continued its transient accumulation of CO_2 at its maximum rate. Subsurface CO_2 concentration increased throughout the profile, and by 10:30 h, the negative concentration gradient between 0 and 15 cm depth had shifted to a positive concentration gradient between 0 and 5 cm depth, with CO_2 concentrations throughout the profile being greater than that of atmospheric CO_2. Despite the significant increase in subsurface CO_2 concentrations, $\delta^{13}C_{CO2}$ values did not significantly change, and the $\delta^{13}C_{CO2}$ gradient remained negative. The average surface CO_2 flux rate continued to increase, and at 10:30 h, the average $\delta^{13}C_{\Delta CO2}$ of the net CO_2 efflux was −12.3‰, which was close to the predicted $\delta^{13}C_{\Delta CO2}$ value of −15.2‰. Soil temperature at 5 cm depth increased, and soil temperature at 15 cm depth increased from its daily minimum. The increases in surface CO_2 flux rate and increases in soil temperature observed over this period were similar to those that occurred during the 10:30 to 14:30 h interval on Day 1.

Summary

The symmetrical patterns in CO_2 concentration and $\delta^{13}C_{CO2}$ profiles exemplified by data from Day 1 highlight important periods of steady-state and transient CO_2 dynamics. At the warmest time of the day (14:30–18:30 h), the system was in steady-state. Subsurface CO_2 concentrations were high, positive concentration gradients drove surface effluxes, and the $\delta^{13}C_{CO2}$ of soil CO_2 was relatively enriched, with subsurface $\delta^{13}C_{CO2}$ values greater than that of atmospheric CO_2. As the soil began to cool, it entered a transient phase during which soil CO_2 concentrations decreased, such that by 22:30 h, the CO_2 concentration gradient was negative, whilst the $\delta^{13}C_{CO2}$ profile remained unchanged. This resulted in a surface influx of relatively depleted CO_2. By 02:30 h, soil CO_2 concentrations had reached a minimum. The depleted surface CO_2 influxes shifted the subsurface $\delta^{13}C_{CO2}$ to more negative values. The relatively depleted $\delta^{13}C_{CO2}$ profile, together with the low CO_2 concentrations, persisted in a phase of steady-state influx until 06:30 h. As the soil began to warm, another transient phase ensued. This was characterised by increased soil CO_2 concentrations and a shift back to a positive concentration gradient and surface efflux by 10:30 h, whilst the $\delta^{13}C_{CO2}$ profile remained unchanged. The switch in CO_2 concentration gradient from negative to positive, combined with an unchanged $\delta^{13}C_{CO2}$ profile drove a highly depleted surface efflux which acted to shift the soil $\delta^{13}C_{CO2}$ to more enriched values. By 14:30 h (the beginning of sampling on Day 2), the soil once again had relatively high CO_2 concentration and $\delta^{13}C_{CO2}$ values. Similar behaviour occurred over Day 2, but

subtle differences in soil temperature variability meant that the sampling periods captured different stages of the transient CO_2 dynamics.

4.4 Discussion

4.4.1 Diel variability in surface and subsurface storage CO_2 flux rates

The relatively small surface CO_2 fluxes measured throughout the 48-h sampling period are consistent with *in situ* surface flux rates measured in Taylor Valley by Burkins et al. (2001) and Parsons et al. (2004), as well as results presented in Chapter 3. However, they are an order of magnitude lower than *in situ* surface CO_2 flux rates measured by Ball et al. (2009). All studies utilised sites with similar soil pH, EC, organic and inorganic C values; soil moisture content and the magnitude of diel temperature variability were also comparable. Despite the relatively high flux rates measured by Ball et al. (2009), the variability in surface CO_2 fluxes seen in their study and by Parsons et al. (2004) showed similar diel patterns to those observed in this study, with positive and negative surface fluxes corresponding to periods when soil temperatures were increasing, and decreasing, respectively.

Surface CO_2 fluxes were most strongly correlated with air temperature, measured 2 cm above the soil surface (R^2 = 0.96; p = <0.001), and less so with soil temperature at 5 cm depth (R^2 = 0.78; p = <0.001; Figure 4.5). Aside from the correlation with air temperature, the best explanatory variable for the magnitude of surface flux rates was the rate of change in soil temperature at 15 cm depth (R^2 = 0.85; p = <0.001; Figure 4.6). The rate of change in soil temperature at 5 cm depth only explained 43% of flux variability (p = 0.02).

The strong correlation between surface CO_2 flux rate and air temperature is difficult to interpret, and there may in fact be no direct causative link. However, the strong correlation between surface CO_2 flux rate and $\Delta T/\Delta t$ at 15 cm depth is consistent with surface CO_2 fluxes being driven by temperature-controlled solubility of CO_2 in soil solution, according to Henry's Law, as posited by Parsons et al. (2004) and Ball et al. (2009). The greater influence of soil temperature changes at 15 cm depth relative to 5 cm is surprising, as the amplitude of temperature variability is greater at 5 cm depth, and soil moisture content is similar at both depths. The correlation between surface CO_2 flux rate and the rate of change in soil temperature at 15 cm depth in this study contrasts with the strong correlation between surface CO_2 flux rates and the rate of change in soil temperature at 5 cm depth shown by Parsons et al. (2004), although their study did not include soil temperature measurements at any other depths.

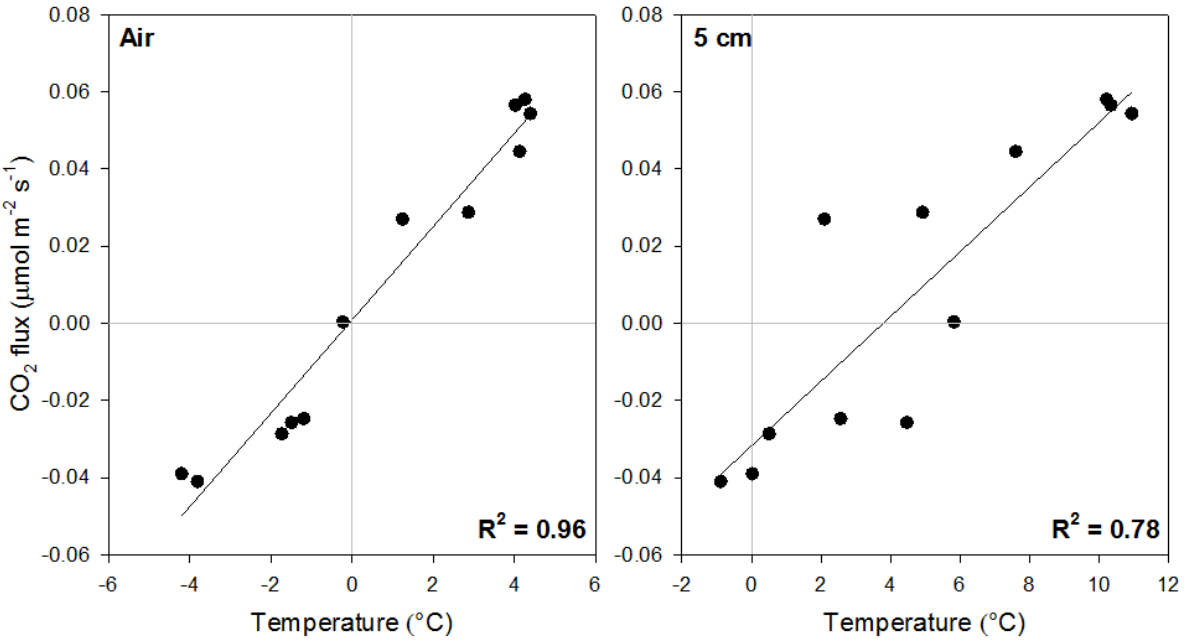

Figure 4.5 Relationship between average temperature over the surface flux sampling period and surface CO_2 flux rates at Site B, Taylor Valley.

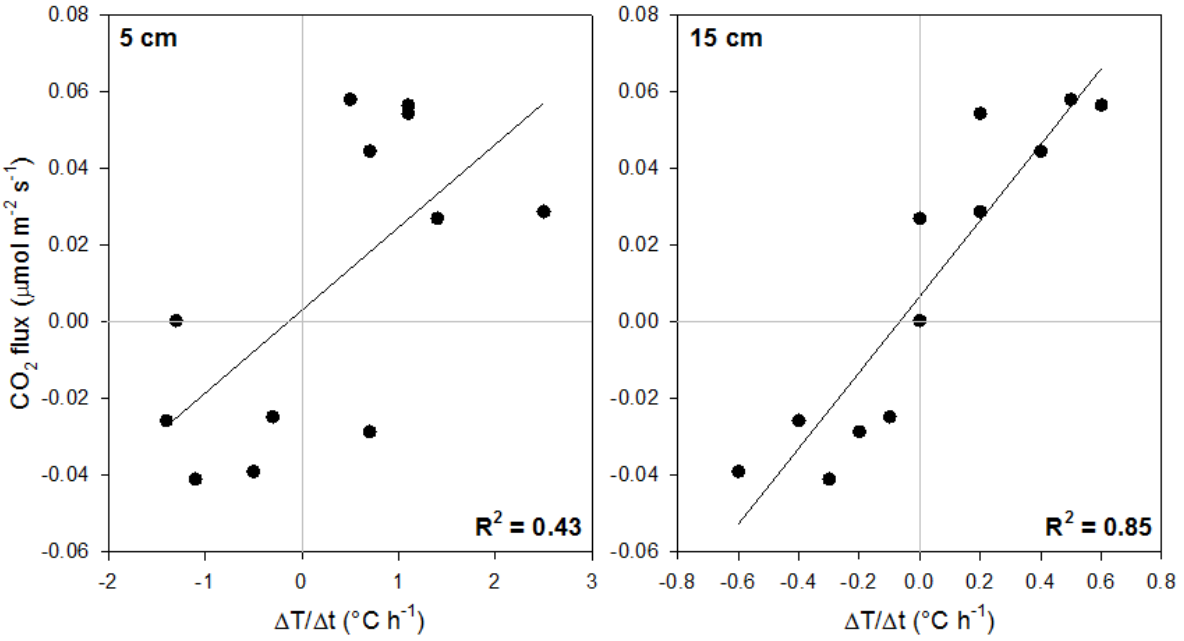

Figure 4.6 Relationship between the average rate of change in soil temperature over the surface flux sampling period at 5 cm and 15 cm depth with surface CO_2 flux rates at Site B, Taylor Valley.

Whereas Ball et al. (2009) inferred from their heat sterilised *in situ* microcosm study that a biological CO_2 flux was superimposed on the abiotic temperature-related fluxes, cumulative 24-hr CO_2 fluxes in

this study detect no statistically significant net flux over six successive 24-hr periods (Figure 4.7), and hence suggest a purely abiotically-driven system, where influxes and effluxes balance. Nonetheless, the presence of a biotic component to the flux must be considered. This is explored further below in relation to the $\delta^{13}C_{CO2}$ of the soil atmosphere and surface CO_2 fluxes. Regardless of the significance of a biological component to the total CO_2 flux, abiotic processes must be invoked – at least to explain CO_2 consumption beneath the opaque surface chambers used in this study, which precluded photosynthetic uptake of CO_2.

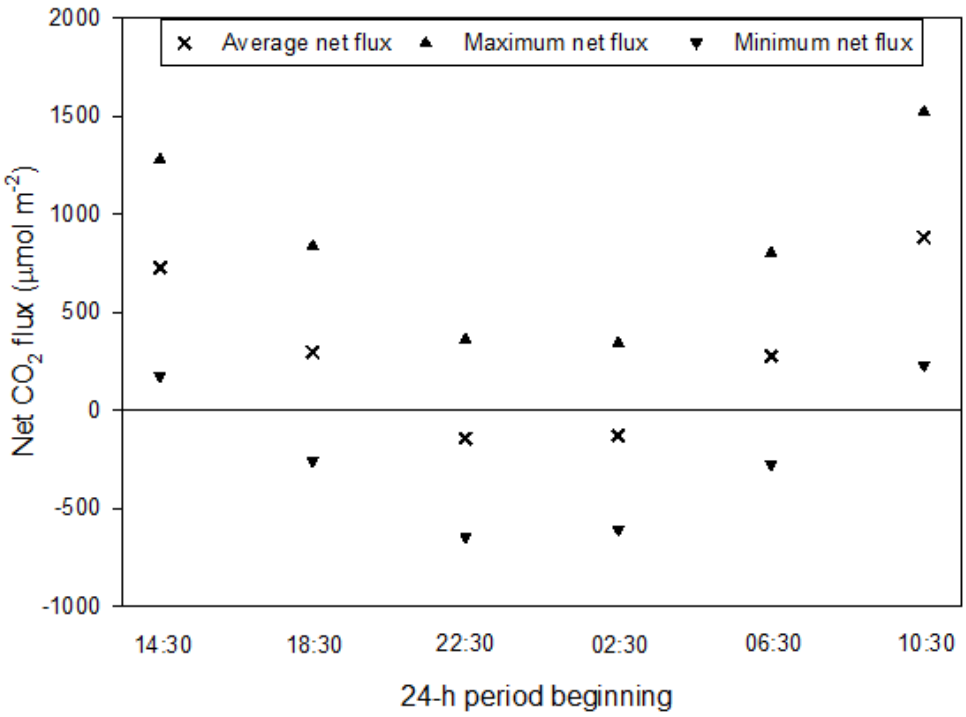

Figure 4.7 Net cumulative surface CO_2 fluxes at Site B, Taylor Valley, over consecutive 24-h periods beginning at 14:30 h on Day 1. Maximum and minimum net fluxes represent uncertainties calculated from the standard error of the mean.

In Chapter 3, temperature-controlled exsolution and dissolution of CO_2, according to Henry's Law, were modelled analytically and compared to measured changes in subsurface soil CO_2 concentrations, as a test of the hypothesis that this phenomenon was the main driver of CO_2 dynamics. However, this approach was predicated on a closed-system approximation. In this study, the relatively high frequency at which subsurface CO_2 concentration measurements were made enables subsurface storage fluxes (fluxes that result in changes in CO_2 storage in the soil) to be estimated over four-hourly intervals. Results show the amplitude of surface fluxes is more than five times larger than storage fluxes, and hence a closed system assumption is not appropriate, at least

for near-surface samples. However, the storage fluxes themselves provide another test of the hypothesis, as they reflect the production and consumption of CO_2 in the soil, and can be considered alongside soil temperature changes.

Like surface fluxes, storage fluxes also showed diel variation (Figure 4.3A), switching from positive to negative as CO_2 concentration within the profile increased and decreased, respectively. This variability led surface flux variations by 4–6 hours. Storage fluxes were explained by the rate of change in soil temperature at 5 cm depth (R^2 = 0.84; p = <0.001; Figure 4.8), but showed no relationship to the rate of change in soil temperature at 15 cm depth. This is consistent with the suggestion that Henry's Law-driven dissolution and exsolution of CO_2 drives changes in subsurface CO_2 concentrations, and indicates that, as expected, the shallower depths of the soil (where diel temperature changes are greatest) are the most important for determining the subsurface CO_2 concentration changes that ultimately drive surface fluxes. The better correlation between surface CO_2 flux rates and the rate of change in soil temperature at 15 cm depth compared to 5 cm depth discussed above is most likely an artefact. Lags in warming and cooling of the subsoil relative to shallower depths, and the lag between subsurface CO_2 production or consumption and changes in surface CO_2 flux may bring about coincidence of their behaviours and promote the strong correlation.

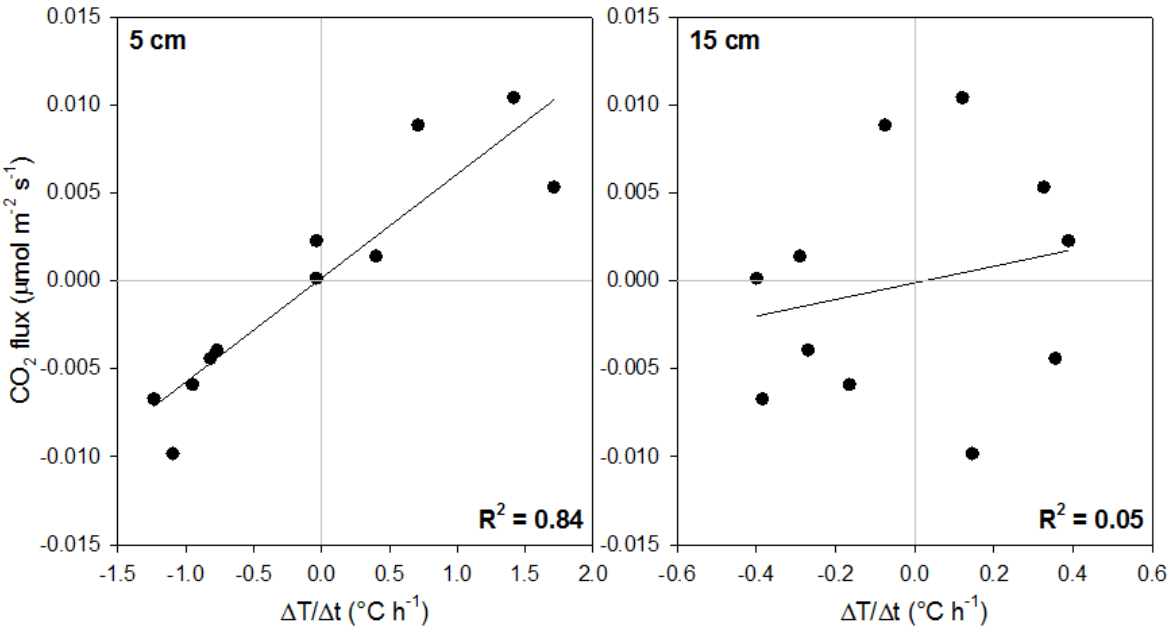

Figure 4.8 Relationship between the rate of change in soil temperature at 5 cm and 15 cm depth with subsurface storage CO_2 flux rates at Site B, Taylor Valley. The solid black lines represent linear relationships with equations as follows. At 5 cm depth, $y = 0.0059x + 0.0002$. At 15 cm depth, $y = 0.0047x - 0.0001$.

4.4.2 Soil gas transport

The significant linear relationship between subsurface CO_2 concentration gradient and surface CO_2 flux rate (R^2 = 0.91, p <0.001; Figure 4.9) is strong evidence that molecular diffusion processes, as described by Fick's Law, dominate CO_2 fluxes. The slope of the line approximates the effective diffusivity, D_e. However, advection caused by wind-induced pressure fluctuations (termed "wind pumping" or "pressure pumping"; Fukuda, 1955; Massman et al., 1997), which can be further modified by interactions with surface topography (Colbeck, 1989; Clarke and Waddington, 1991), must be considered. Wind pumping acts to enhance the rate of diffusive gas transport along a given concentration gradient, thereby producing flux rates greater than those expected from molecular diffusion alone (Bowling and Massman, 2011). This enhancement may be represented mathematically as an additive component to the effective diffusivity in a Fick's Law representation of gas transport:

$$Q = (D_e + K)\frac{dC}{dz}, \tag{4.27}$$

where Q is the gas flux, D_e is the effective molecular diffusivity, K is a wind-dependent enhanced diffusivity parameter (Bowling and Massman, 2011), and dC/dz is the gas concentration gradient.

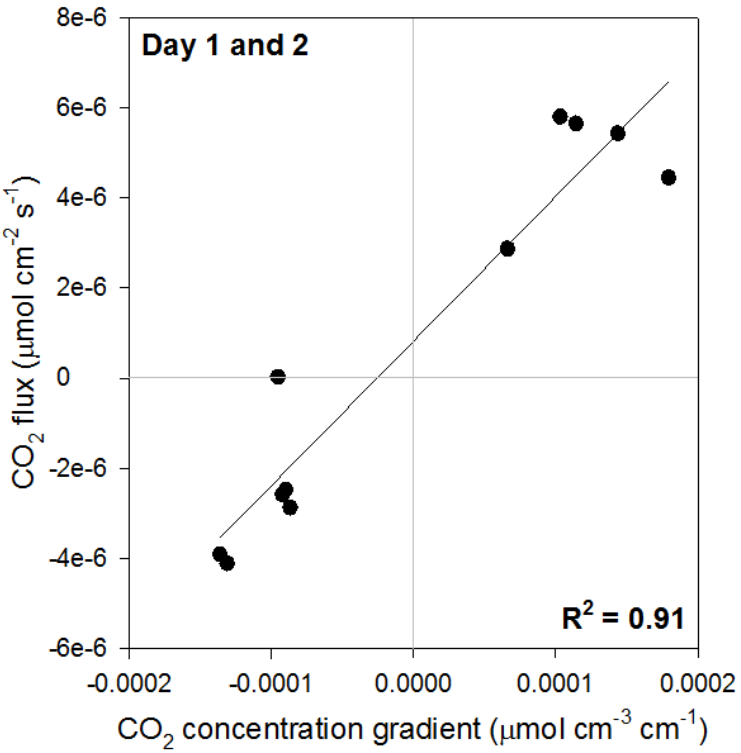

Figure 4.9 Relationship between subsurface CO_2 concentration gradient and surface CO_2 flux on combined data from Days 1 and 2, Site B, Taylor Valley. The solid black line represents a linear relationship: y = 0.032x + 8E-07; the slope of the line represents the effective diffusivity of CO_2 in the soil. Anomalous data from 06:30 h on Day 2 were excluded.

Therefore, the slope of the line in Figure 4.9 may be an overestimate of the true effective molecular diffusivity if it incorporates a wind pumping enhancement. Takle et al. (2004) found that under conditions conducive to wind pumping, surface soil CO_2 flux rates were up to ten times greater than those expected from molecular diffusion alone. Similarly, in a study of CO_2 transport in a mountain forest snowpack, Bowling and Massman (2011) found that wind pumping enhanced transport of CO_2 by up to 40% in the short term (hours). In this study, wind speed was measured 1.2 m above the soil surface at Site A, located 2.8 km east of Site B. The strong diel pattern in wind strength is consistent with an anabatic easterly wind blowing up-valley during the warmest parts of the day. It is almost certain that the same wind blew at Site B; at the very least, the exposed nature of the site means that wind speeds at Site B were unlikely to have been lower than those measured at Site A.

If wind pumping significantly enhanced the surface CO_2 flux rate for a given concentration gradient, then positive fluxes during the warmest parts of the day, when the wind was strongest (~ 4 m s^{-1}), would be greater than negative fluxes, which occurred during colder parts of the day when wind speeds were lower. This would manifest in a plot of concentration gradient versus surface CO_2 flux rate (Figure 4.9) as distinct linear relationships within the positive (steeper gradient) and negative (shallower gradient) flux domains. If such data were fitted with a single line, that line would have a significant, greater-than-zero, intercept. The intercept in Figure 4.9 is not significantly different from zero ($p = 0.067$). Further evidence of the relative unimportance of a wind pumping effect at this site is seen in a plot of wind speed versus surface CO_2 flux rate (Figure 4.10), which, despite the significant relationship ($p = 0.027$), accounts for only 40% of the variation in flux rate.

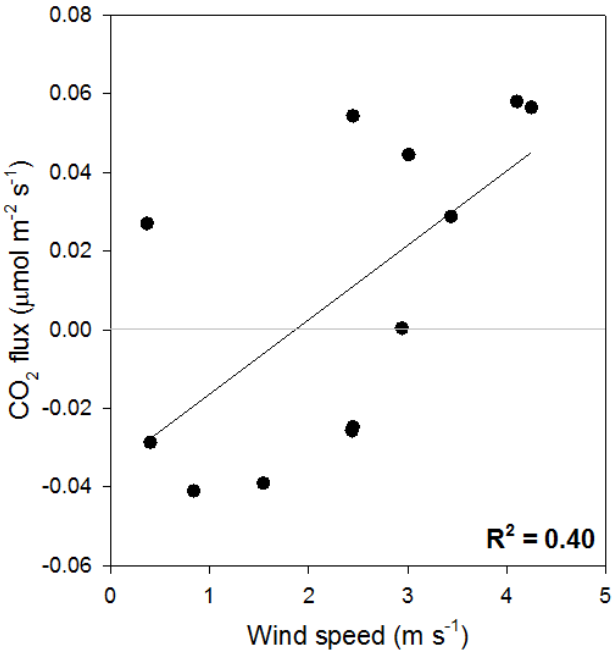

Figure 4.10 Relationship between wind speed and surface CO_2 flux rates at Site B, Taylor Valley. The solid black line represents a linear relationship: $y = 0.0189x - 0.0353$.

The apparent insignificance of wind pumping in this study is in contrast to Risk et al.'s (2013) study of CO_2 fluxes in the Dry Valleys, which found that measured CO_2 fluxes were best related to average wind speeds in the 16 days prior to flux measurements. However, given that CO_2 fluxes in Risk et al.'s (2013) year-long study were only sampled every 4 days during winter, and that Antarctic dry valley soils are characteristically dry and porous (McCraw, 1967; Campbell et al., 1997), it seems unlikely that any wind pumping due to strong winds over the previous 16 days would influence surface CO_2 fluxes. Any enhancement of surface CO_2 fluxes by wind pumping would likely be related to wind speed and associated changes in pressure at the time of sampling (e.g. Takle et al., 2004). However, differences in the frequency of sampling and the period over which data were obtained between this study and Risk et al.'s (2013) study means that there is not a good basis for comparing the datasets. The time-series of flux measurements presented in this study is too short to investigate long lag-time effects.

Therefore, assuming the slope of the line in Figure 4.9 is a reliable estimate of the effective (molecular) diffusivity D_e, and that the low soil moisture contents had a negligible influence on CO_2 diffusivity in the liquid phase (Fang and Moncrieff, 1999), particularly in this very dry soil, the relationship

$$D_e = D \cdot \varepsilon \cdot \tau \,, \qquad \text{(Massman, 2006)} \qquad (4.28)$$

where D is the free air diffusivity, and ε is the air-filled soil porosity, can be used to estimate the tortuosity factor, τ. Using a free air diffusivity for CO_2 (at 1°C and atmospheric pressure) of 0.140 cm^2 s^{-1} (Marrero and Mason, 1972), a soil porosity of 0.4 (from empirical data), a soil moisture content of 0.01, and a D_e of 0.032 ± 0.003 cm^2 s^{-1} yields a tortuosity value of 1.8 ± 0.2. This value is in good agreement with the range of tortuosity values (1.5 – 2.0) calculated by McKay et al. (1998) in their gas diffusion experiments on Dry Valley soils, and lends further support to the inference that wind pumping was not a significant modulator of CO_2 fluxes in this study. A wind pumping effect contributing to an overestimate of D_e would result in an unexpectedly large tortuosity factor.

In addition, the effective diffusivity determined from Figure 4.9 is in reasonable agreement with that estimated from the Millington−Quirk equation which is regarded as the best-performing soil type-independent model of gas diffusivity (Moldrup et al., 2004). A more advanced soil type-dependent prediction of gas diffusivity was not determined, owing to the unavailability of soil water characteristic data. Furthermore, the extremely low soil moisture content at this site meant that McCarthy and Johnson's (1995) modified version of the Millington−Quirk equation, which includes the effects of aqueous-phase diffusion, was not required.

4.4.3 Sources of CO_2

This study, for the first time in Antarctica, used stable C isotope ratios measured from subsurface soil CO_2 and surface CO_2 fluxes in an attempt to trace the sources of CO_2 in Dry Valley soils. Carbon stable isotope studies have been commonly used in temperate environments to distinguish between soil- and root-respired CO_2 in partitioning experiments that rely on the different isotopic composition of metabolised C sources (e.g. Rochette et al., 1999; Ekblad and Högberg, 2000), or in pulse labelling experiments where the soil is flooded with exotic CO_2 of distinctive (extreme) $\delta^{13}C$ value. As the potential sources of C in Dry Valley soils are limited to highly isotopically depleted organic C (Burkins et al., 2000; Hopkins et al., 2009) and relatively enriched inorganic C (Foley, 2005), it would appear that the two sources could be readily discriminated by using an isotopic approach.

However, characterising the isotopic composition of soil-produced CO_2 requires that the system is in steady state (Amundson et al., 1998). Under this condition, and only then, does the isotopic composition of a surface CO_2 flux match that of the CO_2 being produced in the soil. Under non-steady conditions, measured surface CO_2 flux rates do not represent CO_2 production at that time, and the $\delta^{13}C_{CO2}$ of the surface flux does not represent the true value of the $\delta^{13}C_{CO2}$ being produced (Nickerson and Risk, 2009c). Instead, even if the $\delta^{13}C$ of the CO_2 produced is constant, transient changes in the CO_2 production *rate*, driven by transient changes in environmental variables, combine with differences in the diffusivities of $^{12}CO_2$ and $^{13}CO_2$ to produce different concentration gradients for the two isotopologues. This induces a kinetic fractionation effect, and consequently, the isotopic composition of the surface CO_2 flux is different to that of the CO_2 being produced in the soil. The term 'dynamic fractionation' was coined by Nickerson and Risk (2009c) to describe this phenomenon.

Consequently, under conditions of dynamic fractionation, simple isotope mixing models cannot be used to partition contributions from different sources to a surface flux. The influence of dynamic fractionation on the $\delta^{13}C$ of surface CO_2 fluxes was highlighted by Moyes et al. (2010) in their study of variability in heterotrophic and rhizosphere sources of soil respiration under deciduous trees. During periods of low flux, they observed large diel variability in the $\delta^{13}C$ of surface CO_2 fluxes (up to 12‰). However, by modelling diffusive transport of $^{12}CO_2$ and $^{13}CO_2$ in the soil, under conditions of a constant $\delta^{13}C$ of respiratory production, they found that diel variability in the $\delta^{13}C$ of surface fluxes could be explained by dynamic fractionation, rather than requiring any change in the source substrate.

In this study, dynamic fractionation effects combined with switches from positive to negative CO_2 fluxes lead to extreme changes in the $\delta^{13}C_{CO2}$ of surface CO_2 fluxes. The isotopic composition of measured surface CO_2 fluxes ranged between −2.4 and −31.8‰ (Figure 4.3B), the greatest variability yet reported globally, while the isotopic composition of subsurface soil CO_2 varied minimally,

between −7.9 and −9.1‰ (Figure 4.4). The greatest shifts in the $\delta^{13}C_{CO2}$ of the surface flux occurred when fluxes were either rapidly increasing or decreasing, resulting from shifts in behaviour from CO_2 consumption to production, or vice versa, respectively. At these times, subsurface CO_2 concentration gradients typically changed quickly, while $\delta^{13}C_{CO2}$ gradients remained relatively unchanged. Consequently, subsurface CO_2 concentration and $\delta^{13}C_{CO2}$ gradients typically switched from having the same sign (positive or negative; Figure 4.11A and D), to being of opposite sign (Figure 4.11B and C). As gradients of $\delta^{13}C_{CO2}$ act in conjunction with CO_2 concentration gradients to influence the isotopic composition of the net efflux or influx of CO_2, any change in the sign of either gradient has a corresponding influence on the isotopic composition of the surface CO_2 flux, which subsequently influences the isotopic composition of the subsurface soil CO_2, as illustrated in the schematics below (Figure 4.11).

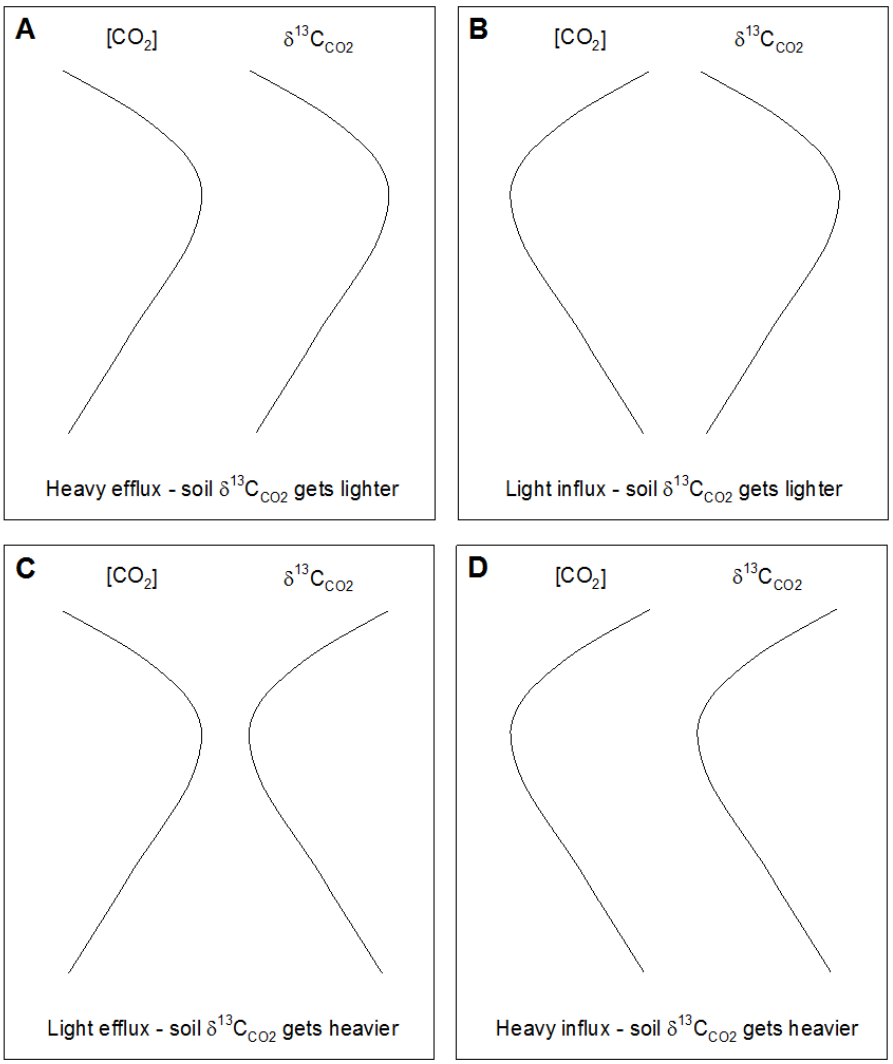

Figure 4.11 Schematics showing the influence of CO_2 concentration and $\delta^{13}C_{CO2}$ gradients on the $\delta^{13}C_{\Delta CO2}$ of surface CO_2 fluxes and on the $\delta^{13}C_{CO2}$ of soil CO_2. The letters **A**, **B**, **C**, and **D** refer to various scenarios described in the text.

A positive $\delta^{13}C_{CO2}$ gradient (increasing $\delta^{13}C_{CO2}$ with increasing depth) will act to preferentially drive $^{13}CO_2$ out of the profile when the CO_2 concentration gradient is positive (Figure 4.11A), whereas when the CO_2 concentration gradient is negative, the same positive $\delta^{13}C_{CO2}$ gradient will act to drive a preferential influx of $^{12}CO_2$ (Figure 4.11B). The transition from a positive to a negative concentration gradient, without a corresponding change in the $\delta^{13}C_{CO2}$ gradient, commonly occurred following a switch from a period of soil warming to soil cooling, and resulted in a relatively light CO_2 influx (Figure 4.11B). Similarly, a negative $\delta^{13}C_{CO2}$ gradient (decreasing $\delta^{13}C_{CO2}$ with increasing depth) will act to preferentially drive $^{12}CO_2$ out of the profile when the CO_2 concentration gradient is positive (Figure 4.11C), and the same negative $\delta^{13}C_{CO2}$ gradient will drive a preferential influx of $^{13}CO_2$ when the CO_2 concentration gradient is negative (Figure 4.11D). Following a switch from a period of soil cooling to soil warming, the subsurface CO_2 concentration gradient typically switched from negative to positive, whilst the $\delta^{13}C_{CO2}$ gradient remained relatively unchanged. This resulted in a relatively light CO_2 efflux (Figure 4.11C).

In addition, the $\delta^{13}C_{\Delta CO2}$ of surface CO_2 fluxes has a feedback effect on subsurface $\delta^{13}C_{CO2}$ values. At times when CO_2 concentration and $\delta^{13}C_{CO2}$ gradients drive a heavy efflux (Figure 4.11A) or light influx of CO_2 (Figure 4.11B), the isotopic composition of the soil CO_2 will become lighter. Conversely, at times when there is a light efflux (Figure 4.11C) or heavy influx of CO_2 (Figure 4.11D), the soil CO_2 will become isotopically heavier. Changes in subsurface $\delta^{13}C_{CO2}$ values were consistent with the direction and isotopic composition of the surface flux. As such, it is likely that changes in subsurface $\delta^{13}C_{CO2}$ values resulted from the large shifts in the $\delta^{13}C_{\Delta CO2}$ of surface CO_2 fluxes, rather than any major change in the $\delta^{13}C_{CO2}$ of CO_2 being produced or consumed.

The high diel variability in surface CO_2 flux rates in Dry Valley soils highlights their characteristically non-steady nature, and, as variability in the rate of CO_2 production has the potential to perpetuate non-steady conditions, dynamic fractionation is an important factor to consider in understanding the $\delta^{13}C_{\Delta CO2}$ of surface fluxes. The strong correlation ($R^2 = 0.80$; $p = <0.001$) between measured $\delta^{13}C_{\Delta CO2}$ values and those predicted based on CO_2 concentration and $\delta^{13}C_{CO2}$ gradients (Figure 4.12) suggests that the relatively coarse resolution (5 cm) at which CO_2 concentration and $\delta^{13}C_{CO2}$ profiles were sampled was sufficient to capture the zones of CO_2 production and consumption.

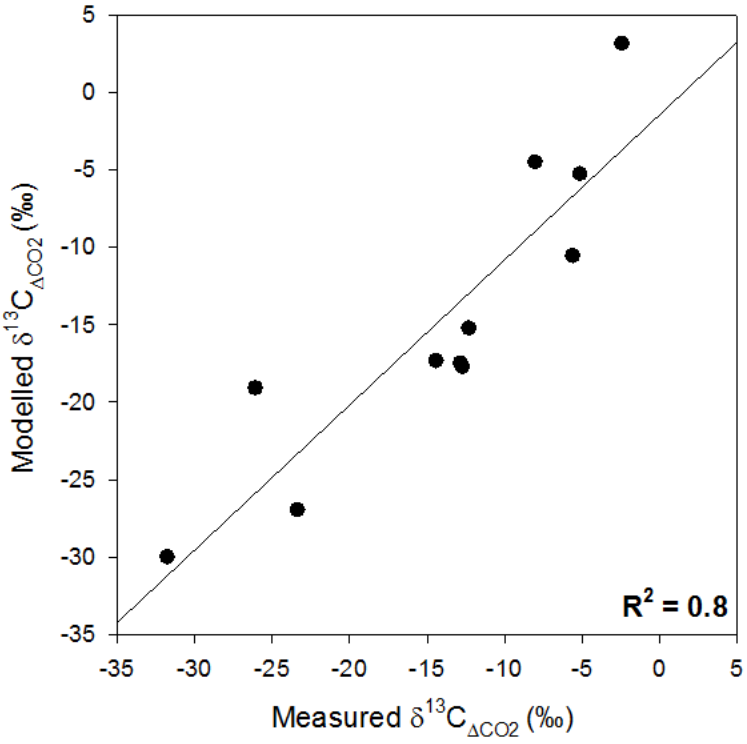

Figure 4.12 Relationship between the $\delta^{13}C_{\Delta CO2}$ of measured and modelled surface CO_2 fluxes from Days 1 and 2, Site B, Taylor Valley. The anomalous data point from 06:30 h on Day 2 was excluded from this plot and from the linear regression. The solid black line is a linear relationship relating *x* (measured) and *y* (modelled) values as follows: $y = 0.94x - 1.42$.

The only occasions when the $\delta^{13}C_{\Delta CO2}$ of surface CO_2 fluxes could be related to the isotopic composition of CO_2 produced or consumed within the soil was during three phases that approximated steady-state with respect to CO_2 concentration and $\delta^{13}C_{CO2}$ profiles. A phase approximating steady-state production of CO_2 (efflux) occurred between 14:30 and 18:30 h on Day 1, and phases approximating steady-state consumption of CO_2 (influx) occurred between 02:30 and 06:30 h on Day 1, and from 22:30 to 02:30 h on Day 2. During each of these steady-state phases, changes in both CO_2 concentration and $\delta^{13}C_{CO2}$ profiles were minimal (Figure 4.4). Consequently, during these periods, the rate of CO_2 efflux or influx must equal the rate of CO_2 production or consumption, respectively. Furthermore, the $\delta^{13}C_{\Delta CO2}$ of the net CO_2 flux must reflect the $\delta^{13}C_{CO2}$ of the net CO_2 being produced or consumed.

The phase of steady-state CO_2 efflux (14:30 – 18:30 h on Day 1) corresponded to a period when soil temperature at 5 cm depth remained relatively constant around its daily maximum, and soil temperature at 15 cm depth increased at its maximum rate (Figure 4.3C and D). Similarly, the phase of steady-state CO_2 influx on Day 1 (between 02:30 and 06:30 h) corresponded to a period when soil temperature at 5 cm depth remained relatively constant around its daily minimum, whilst soil temperature at 15 cm depth decreased at its maximum rate. The approximate steady-state influx

period between 22:30 and 02:30 h on Day 2 had similar changes in soil temperature at 15 cm depth, although soil temperature at 5 cm depth decreased during this period, rather than remaining relatively constant.

During the period of steady-state efflux of CO_2, the $\delta^{13}C_{\Delta CO2}$ of the efflux, and hence the $\delta^{13}C_{CO2}$ of CO_2 being produced in the soil, averaged −3.8‰. During the two phases of steady-state influx, the $\delta^{13}C_{CO2}$ of the CO_2 consumed within the soil averaged −11.4‰. An additional value for the $\delta^{13}C_{CO2}$ of CO_2 produced can be obtained from the 14:30 h sampling on Day 2. The $\delta^{13}C_{\Delta CO2}$ of the CO_2 efflux at this time is considered to reflect steady-state production of CO_2, as despite not spanning a four-hour period of steady-state due to day-to-day variation in soil temperature changes, the sampling at 14:30 h on Day 2 coincided with a period over which soil temperature at 5 cm depth remained relatively constant around its daily maximum, whilst soil temperature at 15 cm depth increased at its maximum rate (Figure 4.3C and D). These were the same conditions that prevailed during the period of steady-state efflux on Day 1. The $\delta^{13}C_{\Delta CO2}$ of the efflux at 14:30 h on Day 2 was −8.0‰.

Together with data from the steady-state efflux period on Day 1, these results suggest that during phases of CO_2 production, the $\delta^{13}C_{CO2}$ of the net CO_2 produced was approximately −5.2‰. In contrast, the average $\delta^{13}C_{CO2}$ of the net CO_2 consumed during steady-state consumption phases was more depleted (−11.4‰). These values are slightly lighter and heavier, respectively, than the average $\delta^{13}C_{\Delta CO2}$ values predicted from CO_2 concentration and $\delta^{13}C_{CO2}$ gradients during the steady-state periods of CO_2 efflux (−2.2‰) and influx (−15.8‰). Regardless, it appears that the net CO_2 produced during warm periods was isotopically heavier than the net CO_2 consumed at cold times of the day. This pattern cannot be accounted for by an isotopically light biological component.

If, during steady-state efflux (at times of warming), exsolution of relatively isotopically heavy CO_2 was accompanied by biological production of isotopically light CO_2, the resulting flux would have an isotopic composition intermediate between the two, i.e. lighter than that of the exsolved CO_2, but heavier than that of biologically-respired CO_2. At times of cooling, if dissolution of CO_2 and biological respiration occurred simultaneously, the soil atmosphere would experience a loss of relatively heavy CO_2 and a gain of relatively light CO_2. If this occurred during a period of steady-state influx, the net $\delta^{13}C_{CO2}$ of CO_2 being absorbed would be highly enriched, and would have to be balanced by a highly enriched surface influx. Therefore, the simultaneous occurrence of biological respiration with abiotically-controlled CO_2 exsolution or dissolution would, at steady-state, be evident as effluxes that were isotopically lighter than influxes. This is the opposite of what was observed.

Instead of a biological explanation, the pattern of relatively heavy CO_2 production (effluxes) and relatively light CO_2 consumption (influxes) can be explained by the kinetic fractionation that occurs as a result of preferential exsolution of $^{13}CO_2$ and preferential dissolution of $^{12}CO_2$ in the $CO_{2\,(g)} – CO_2$

$_{(dissolved)}$ system. Under conditions of equilibrium fractionation, exsolution of CO_2 concentrates $^{12}CO_2$ in the dissolved phase, making the $\delta^{13}C_{CO2}$ of gaseous CO_2 1.17‰ heavier than dissolved CO_2 (H_2CO_3) at 1°C (Vogel et al., 1970). Therefore, during phases of exsolution, kinetically fractionated CO_2 effluxes would be isotopically heavier than the CO_2 influxes during periods of dissolution, as was observed.

This phenomenon of exsolution of heavier CO_2 and dissolution of lighter CO_2 requires a long-term shift in the isotopic composition of the dissolved inorganic C pool, as $^{12}CO_2$ is being preferentially stored in soil solution, whereas $^{13}CO_2$ is being preferentially removed. As this fractionation effect is induced by increases and decreases in soil temperature, driving exsolution and dissolution of CO_2, it may be the cause of the trend in $\delta^{13}C_{CO2}$ profiles of increasing $\delta^{13}C_{CO2}$ with depth (Figure 4.4). This trend essentially favours $^{13}CO_2$ diffusing out of the soil, and $^{12}CO_2$ diffusing into the soil. That this isotopic disequilibrium persists well into mid-summer is evidence of the 'isotopic inertia' associated with the very large dissolved inorganic C pool at high soil pH (Gamnitzer et al., 2011), relative to the size of the fluxes.

4.4.4 Data reliability

The surface CO_2 flux rates measured in this study appear to be reliable measurements, as in addition to their linear relationship with subsurface CO_2 concentration gradients, artefacts associated with closed chamber sampling of surface fluxes in comparatively higher-flux environments are not apparent. The maximum change in headspace chamber CO_2 concentration over the sampling period was 46 µL L^{-1}, and changes in $\delta^{13}C_{CO2}$ were also low (up to 1.4‰). As such, any pressure changes caused by CO_2 concentration increases or decreases within chambers are likely to be negligible. Furthermore, the small changes in CO_2 concentration and $\delta^{13}C_{CO2}$ during surface flux sampling mean that chamber-to-soil feedbacks (caused by changes in headspace CO_2 concentration and $\delta^{13}C_{CO2}$ values), and associated errors caused by lateral diffusion (Nickerson and Risk, 2009a, 2009b), are unlikely to have introduced errors in calculated surface CO_2 flux rates and the $\delta^{13}C_{CO2}$ of the net flux. This is supported by the fact that calculated values of the $\delta^{13}C_{CO2}$ of net CO_2 fluxes closely matched $\delta^{13}C_{\Delta CO2}$ values calculated from CO_2 concentration and $\delta^{13}C_{CO2}$ gradients (Figure 4.3B). These gradients were determined from subsurface sampling tubes located adjacent to but not beneath the chambers.

4.4.5 Implications

The diel variability in surface CO_2 flux rates has profound implications for interpretation of soil biological activity and quantification of soil C turnover times. Aside from other studies investigating diel soil CO_2 fluxes (Parsons et al., 2004; Ball et al., 2009), previous measurements of soil CO_2 fluxes were often made around mid-day (Barrett et al., 2006c; Barrett et al., 2006b; Barrett et al., 2008a),

coinciding with the warmest part of the day, and were therefore assumed to represent the maximum rate of soil respiration. Other studies either did not specify the time(s) of sampling (Burkins et al., 2001; Gregorich et al., 2006; Ball et al., 2011) or specifically made measurements on days with contrasting air temperatures in order to investigate the relationship between soil CO_2 flux and temperature (Elberling et al., 2006), but did not investigate this effect through a diel cycle. Many of these studies found relationships between the rate of CO_2 efflux and soil temperature. However, given the data presented in this study, any CO_2-temperature relationship cannot be used to solely explain differences in rates of heterotrophic respiration. Whilst there may have been a biotic component to the flux, CO_2 effluxes in these studies will also have been influenced by abiotic processes.

The potential for misinterpretation of surface CO_2 fluxes is exemplified by the data from 10:30 h on Day 1 (Figure 4.3). At this time, the soil was warming, the CO_2 flux was positive, and had a $\delta^{13}C_{\Delta CO2}$ of −26.1‰. Without the insight into diel variability and dynamic fractionation effects demonstrated in this study, these values would be incorrectly interpreted as a flux of biological origin.

The dynamic nature of CO_2 production and consumption in dry, low C soils such as those at Site B, and associated changes in $\delta^{13}C_{\Delta CO2}$, mean that periods approximating steady-state, and therefore periods during which the surface CO_2 flux and its isotopic composition are a true representation of the soil CO_2 being produced, are short-lived. Consequently, studies using stable C isotopes to quantify heterotrophic respiration would require at least semi-continuous monitoring to identify periods of steady-state. This approach requires that both the isotopic composition of the source organic material and the abiotically-produced CO_2 are known. The latter is as yet unknown, and must be the focus of further research. However, as the isotopic composition of CO_2 that is dissolved into and exsolved from soil solution will be influenced by kinetic fractionation, it is likely to be dependent on the rate of soil warming and cooling, thus adding a further requirement of detailed soil temperature measurements during sampling periods.

Alternatively, semi-continuous monitoring of sufficient frequency and precision could be used to calculate net CO_2 fluxes over diel cycles, and any net positive flux could be attributed to heterotrophic respiration. However, this assumption relies on any additional sources of CO_2 such as a flux of geological origin (Risk et al., 2013), or an enhanced flux due to wind pumping being excluded. It also requires that there is no net change in soil inorganic C storage as a result of changing soil conditions (primarily temperature, moisture content and pH).

4.5 Summary and conclusions

Surface CO_2 fluxes from the dry, low C, high pH, low EC soils at Site B were low, and varied diurnally between −0.04 and 0.06 μmol m^{-2} s^{-1}. The diel pattern of positive and negative surface CO_2 fluxes was such that the net flux over six overlapping 24-h periods was not significantly different from zero. Diel variation in soil temperatures was the primary driver of surface CO_2 fluxes, which were predominantly diffusion-driven in response to CO_2 concentration gradients generated by dissolution and exsolution of CO_2 in accordance with Henry's Law.

The isotopic composition of surface CO_2 fluxes was extremely variable, ranging between −2.4 and −31.8‰. This was due to dynamic fractionation effects arising as a result of the interaction between different diffusion coefficients for $^{12}CO_2$ and $^{13}CO_2$ and transient CO_2 concentration gradients. As such, dynamic fractionation, rather than heterotrophic respiration, accounted for the highly depleted positive surface CO_2 fluxes which occurred during warm parts of the day. At these times, transient CO_2 concentration and $\delta^{13}C_{CO2}$ gradients meant that neither the flux rate nor the isotopic composition of the surface CO_2 flux was representative of soil CO_2 production at that time.

Steady-state phases of CO_2 production and consumption, during which the isotopic composition of the surface CO_2 flux reflected that of the CO_2 being produced or consumed within the soil, were short-lived. These phases were limited to periods of efflux and influx during which soil temperature at 15 cm depth increased or decreased at its maximum rate, respectively. Phases of steady-state showed that soil CO_2 effluxes were isotopically heavier than CO_2 influxes. This pattern of behaviour is consistent with kinetic fractionation associated with Henry's Law-controlled exsolution and dissolution of CO_2 into soil solution, but inconsistent with simultaneous production of an isotopically light biological component to the flux.

All lines of evidence (no net flux over diel periods, dynamically fractionated depleted surface fluxes, and the relatively heavy isotopic composition of CO_2 produced) suggest that surface CO_2 fluxes were driven by abiotic mechanisms, and there was no readily distinguishable biological component to the surface CO_2 flux at this site. Consequently, previous measurements of surface CO_2 fluxes from Dry Valley soils with similar characteristics are likely to have interpreted the abiotic surface CO_2 flux as a biological flux, thus overestimating the rate of heterotrophic respiration.

In addition, the relative magnitude of surface fluxes and subsurface storage fluxes shown in this chapter indicate that the closed-system assumption invoked in Chapter 3 is too strict a simplification. This violation probably accounts for the discrepancies between measured and modelled subsurface CO_2 concentrations in Chapter 3, particularly at shallower depths (Chapter 3, Figure 3.12). Furthermore, estimates of biotic and abiotic contributions to subsurface CO_2 at the moist, relatively

high organic C site (Site A) were based on a simple isotope mixing model incorporating two internal sources: a biotic component derived from metabolisation of soil organic C, and an abiotic source with a range of isotopic compositions under various scenarios (Chapter 3, Table 3.3). This chapter has shown that the direction of surface CO_2 fluxes makes an important contribution to changes in subsurface soil CO_2 concentrations, and dynamic fractionation of these CO_2 fluxes is the major determinant of the changes in the isotopic composition of soil CO_2. As such, estimates of the biological contribution to subsurface soil CO_2 production at Site A made in Chapter 3 are likely to be in error.

The generality of these conclusions, along with further discussion of diel variability in surface CO_2 fluxes and implications for soil respiration measurements in the McMurdo Dry Valleys is considered in Chapter 6. This chapter follows an additional results chapter which presents new data from an equally intensive sampling regime for Site A, a site with higher levels of organic C and soil moisture but with similar soil chemistry to that at Site B.

Chapter 5

Quantifying diel variations in biotic and abiotic soil CO_2 fluxes, Taylor Valley, Antarctica (II): The influence of a contemporary organic carbon source

5.1 Introduction

Chapter 4 showed that diel variability in surface CO_2 fluxes at a site in Taylor Valley with no contemporary lacustrine organic C source was predominantly driven by abiotic processes. Surface CO_2 fluxes were primarily diffusion-driven in response to CO_2 gradients generated by dissolution and exsolution of CO_2 in accordance with Henry's Law. As such, diel variation in soil temperatures was the primary driver of variation in surface CO_2 flux rates. Variation in subsurface CO_2 concentration and $\delta^{13}C_{CO2}$ values were influenced by surface CO_2 fluxes, and vice versa. Dynamic fractionation, which determined the isotopic composition of the surface CO_2 flux, occurred during subsurface diffusion of CO_2, with feedback from the direction and isotopic composition of the surface flux acting to change the isotopic composition of soil CO_2. Despite several occurrences of highly depleted surface CO_2 fluxes (as low as −31.8‰), no distinguishable biological component to surface CO_2 fluxes was detected. The highly depleted surface fluxes, rather than being driven by steady state production of highly depleted biologically-produced CO_2, were a result of dynamic fractionation of a relatively enriched CO_2 source, and occurred when CO_2 concentration and $\delta^{13}C_{CO2}$ gradients were of opposite sign. Further support for an abiotic driver of CO_2 fluxes was seen in the $\delta^{13}C_{\Delta CO2}$ of surface fluxes during periods of steady state CO_2 production. The relatively enriched $\delta^{13}C_{\Delta CO2}$ (−5.2‰) of surface fluxes at these times is consistent with the kinetic fractionation that occurs as a result of preferential exsolution of $^{13}CO_2$ in the $CO_{2\,(g)} - CO_{2\,(dissolved)}$ system.

This chapter aims to further advance the understanding of Dry Valley soil CO_2 dynamics by applying knowledge gained from Site B, a site with no contemporary lacustrine organic C source, to Site A, located adjacent to a small lake in Taylor Valley. Algae formed in the lake during the austral summer are driven to the shore by wind and wave action, and subsequently blown onto nearby soils. This contemporary organic C source provides an opportunity to investigate CO_2 fluxes in soils with above average organic C, and thereby identify the relative contributions of biotic and abiotic processes to surface CO_2 fluxes at such sites. As in Chapter 4 (Site B), four-hourly measurements of surface CO_2 flux rates and subsurface CO_2 concentration and $\delta^{13}C_{CO2}$ profiles were made over a 48-h period. This chapter is focused on Site A, the same "Site A" in Taylor Valley as that studied in Chapter 3.

The field work which generated the data considered in this chapter was undertaken concurrently (during the 2009/10 austral summer) with the field work providing the data considered in the previous chapter. This work was conducted a full year after the field work which yielded results for Chapter 3. The materials and methods utilised were the same as those carried out at Site B during the 2009/10 summer (Chapter 4), although differences pertinent to Site A are noted below.

5.2 Materials and methods

5.2.1 Study area

At the time of gas sampling, soils at Site A were ice-cemented below 35 cm depth, which was the same as the depth of ice cement measured during the sampling period in 2008/09.

5.2.2 Environmental variables

During the intensive 48-h gas sampling period, all data were recorded and logged every 2 minutes by a CR1000 data logger (Campbell Scientific Inc., Logan, Utah, USA).

Soil temperature and moisture content measurements

Soil temperature and volumetric moisture content at 5, 15 and 25 cm depth were measured using Hydra Probes (Hydra Probe II, Stevens Water Monitoring Systems Inc., Portland, Oregon, USA). As in the 2008/09 sampling period at Site A, an intermittent fault occurred in the probe installed at 5 cm depth. Consequently, the soil temperature and moisture content data shown for 5 cm depth are from an additional data logger installed in an adjacent polygon. The additional logger included the same equipment, with Hydra Probes installed at the same soil depths, and was located ~ 10 m SSW of the primary logger at Site A. The soil and environmental conditions in the two polygons were very similar. Consequently, data from the probe at 5 cm depth in the secondary polygon are considered to be an appropriate surrogate for the missing data.

The rate of change in soil temperature $(\Delta T/\Delta t_t)$ was calculated as the difference in temperatures (T) measured ten minutes apart, as follows:

$$\frac{\Delta T}{\Delta t_t} = \frac{T_{t+5\ min} - T_{t-5\ min}}{10\ min}. \quad (5.1)$$

Air temperature

Surface air temperature was measured 2 mm above the soil surface (CS215-L, Campbell Scientific Inc., Logan, Utah, USA).

Wind speed

Wind speed (#40C Anemometer, NRG Systems, Hinesburg, Vermont, USA) and direction (W200P Potentiometer Windvane, Vector Instruments, North Wales, UK) were measured 1.2 m and 1.3 m above the soil surface, respectively.

5.2.3 Soil CO_2 sampling and analysis

The experimental set-up and sampling for surface soil CO_2 fluxes proceeded as at Site B in 2009/10 (Chapter 4). Three chambers were installed in each of two adjacent polygons at Site A; four 20 ml gas samples were taken from each chamber at 15 min intervals over a 45 min period. The polygons in which gas samples were taken were located ~ 45 m south-west of the sampling site utilised at Site A in 2008/09, on the same geomorphic surface.

Soil profile CO_2 sampling also proceeded as at Site B, with subsurface sampling tubes installed adjacent to each of the three chambers in each polygon at depths of 5, 10, 15, 20 and 30 cm. Additionally, one sampling tube was installed horizontally, 1 cm above the desert pavement, in each polygon. Gas samples from these tubes provided an atmospheric CO_2 sample from just above the soil surface.

Soil CO_2 sampling began > 70 h after installation of equipment. Gas samples were taken every four hours over a 48-h period, starting at 14:30 h on December 29th, 2009. Gas sampling at Site A proceeded concurrently with gas sampling at Site B, thus data from each sampling time are directly comparable between the two sites. However, localised effects of topographic shading dictate that the timing of maxima and minima in air and soil temperatures were slightly offset. A selection of samples were analysed for CO_2 concentration and $\delta^{13}C_{CO2}$ using a Gas-bench II connected to a Delta^{Plus} Advantage isotope ratio mass spectrometer (both Thermo Finnigan, Bremen, Germany) at the Macaulay Land Use Research Institute in Aberdeen, Scotland, within 5 months of being collected. Budget constraints meant that it was not possible to analyse all of the samples collected. Standard reference gas samples collected in the field and standard reference gases prepared in New Zealand and included with samples sent to Scotland showed no sign of storage or transport effects. The analytical precision for CO_2 concentration and $\delta^{13}C_{CO2}$ values was ≤5 µL L^{-1} and ≤0.05‰, respectively.

5.2.4 Soil sampling, physical and chemical analyses

The gas samples at Site A were taken within 30 m of the soil pit sampled at Site A in 2008/09. Based on the proximity of the 2009/10 gas sampling site to the previously sampled and analysed soil pit, the uniformity of the geomorphic surface on which samples were taken, and the similar physical appearance of soil pits dug and described in polygons adjacent to the 2009/10 gas sampling site

(Figure 5.1), the soil physical and chemical characteristics at Site A were considered to be accurately represented by the data presented in Chapter 3.

Figure 5.1 Morphological comparison between soil pits adjacent to gas sampling sites at Site A in the 2008/09 and 2009/10 austral summers. At the time of sampling, both soils (Typic Haploturbels) were ice-cemented below 35 cm depth. The moistening of the upper ~ 2 cm of the 2009/10 profile is from melting of recent snowfall.

5.2.5 Statistical analyses and calculations

Surface CO_2 fluxes

As for Site B (Chapter 4), surface CO_2 fluxes were determined from changes in headspace CO_2 concentrations during the 45 min sampling period as follows:

$$n_{CO_2} = [CO_2] \frac{PV}{RTA} \quad (5.2)$$

where n_{CO2} is the number of moles of CO_2 emitted per m^2 (µmol m^{-2}), [CO_2] is headspace CO_2 concentration (µL L^{-1}), P is atmospheric pressure (101325 Pa), V is the chamber volume (m^3), R is the ideal gas constant (8.314 J K^{-1} mol^{-1}), T is air temperature (K), and A is the area covered by the chamber (0.0177 m^2).

Surface CO_2 flux rates (µmol m^{-2} s^{-1}) were calculated by linear regression (Microsoft Excel® 2010) of surface CO_2 fluxes (µmol m^{-2}) against time over which samples were collected (s). Surface flux rates

that were significantly different to zero ($p < 0.1$) were subsequently used to calculate the net CO_2 gained or lost from the surface chambers ($\Delta[CO_2]$), and the average $\delta^{13}C$ of the net CO_2 gained or lost ($\delta^{13}C_{\Delta CO2}$). Each significant surface CO_2 flux, which may be positive or negative, was considered individually, and calculations were as follows:

$$\Delta[CO_2] = [CO_2]_{final} - [CO_2]_{initial} \tag{5.3}$$

where $[CO_2]_{final}$ and $[CO_2]_{initial}$ are the final and initial CO_2 concentrations (µL L^{-1}) measured from the final and initial CO_2 samples taken from the chamber, respectively.

Using a mass balance approach,

$$\Delta[CO_2] \cdot \delta^{13}C_{\Delta CO2} = [CO_2]_{final} \cdot \delta^{13}C_{[CO2]final} - [CO_2]_{initial} \cdot \delta^{13}C_{[CO2]initial}, \tag{5.4}$$

where $\delta^{13}C_{\Delta CO2}$ (‰) is the $\delta^{13}C$ of the net CO_2 gained or lost between the final and initial measurements, and $\delta^{13}C_{[CO2]final}$ and $\delta^{13}C_{[CO2]initial}$ are the $\delta^{13}C_{CO2}$ values (‰) measured from the final and initial CO_2 samples taken from the chamber, respectively.

Therefore,

$$\delta^{13}C_{\Delta CO2} = \frac{[CO_2]_{final} \cdot \delta^{13}C_{[CO2]final} - [CO_2]_{initial} \cdot \delta^{13}C_{[CO2]initial}}{\Delta[CO_2]} \cdot \tag{5.5}$$

Subsurface storage CO_2 fluxes

Subsurface storage CO_2 fluxes were estimated by calculating differences in the average soil profile CO_2 concentration between consecutive sampling times. The average soil profile CO_2 concentration was determined by using an analogue integration technique whereby the area under a paper plot of CO_2 concentration versus depth at each sampling time was weighed to determine the integral

$$\overline{[CO_2]} = \frac{\int_0^{30}[CO_2]\,dz}{30} \tag{5.6}$$

where z is depth in cm and $\overline{[CO_2]}$ is the profile average CO_2 concentration between 0 and 30 cm depth. The difference in $\overline{[CO_2]}$ between consecutive sampling times was used to determine the number of moles of CO_2 (n_{CO2}; µmol m^{-2}) gained or lost over the period between sampling times using the ideal gas law:

$$n_{CO_2} = \Delta[CO_2]\,\frac{PV}{RT} \tag{5.7}$$

where Δ[CO_2] is the difference in the profile average CO_2 concentration between sampling times (μL L^{-1}), P is atmospheric pressure (101325 Pa), V is the soil gas volume (m^3 m^{-2}; calculated by multiplying soil depth (0.3 m) by the air-filled porosity (ε = 0.4)), R is the ideal gas constant (8.314 J K^{-1} mol^{-1}) and T is soil temperature (K). This was converted to a flux rate (μmol m^{-2} s^{-1}) by dividing by the time (s) over which n_{CO2} was gained or lost.

Calculated surface CO_2 fluxes and their C isotopic composition

As a test of surface CO_2 flux rates calculated from surface chamber CO_2 measurements, surface CO_2 flux rates (F) were also estimated using near-surface CO_2 concentration gradients to solve Fick's Law

$$F = -D_e \frac{dC}{dz}, \tag{5.8}$$

where D_e is the effective diffusivity of CO_2 (cm^2 s^{-1}), and dC/dz is the CO_2 concentration gradient. The value of D_e used (0.032 cm^2 s^{-1}) was derived from the relationship between surface CO_2 flux rates and near-surface CO_2 concentration gradients at Site B, and it is considered that this value can be reliably extrapolated to Site A as the soils were similarly coarse textured, with low levels of moisture.

In a diffusion-driven system, the $\delta^{13}C_{\Delta CO2}$ of surface CO_2 fluxes is determined by subsurface CO_2 concentration and $\delta^{13}C_{CO2}$ gradients. Using data from subsurface profiles, the $\delta^{13}C_{\Delta CO2}$ of surface CO_2 fluxes can therefore be determined as follows:

$$R_{13} = \frac{F_{13}}{F_{12}} \tag{5.9}$$

where R_{13} is the ratio of ^{13}C to ^{12}C in the CO_2 flux, and F_{13} and F_{12} refer to the flux of $^{13}CO_2$ and $^{12}CO_2$, respectively. The full derivation of this calculation is given in Chapter 4 (equations 4.8 – 4.26), which shows that:

$$R_{13} = 0.9956 \left(\frac{\frac{d[CO_2]}{dz} J(1+J) + \frac{R_{VPDB}}{1000} \frac{d(\delta^{13}C)}{dz} [CO_2]}{\frac{d[CO_2]}{dz}(1+J) - \frac{R_{VPDB}}{1000} \frac{d(\delta^{13}C)}{dz} [CO_2]} \right), \tag{5.10}$$

where $J = (\delta^{13}C_{CO2}/1000 + 1)\ R_{VPDB}$.

Mixing model

As in Chapter 3, a mixing model (Fry, 2006) was used to constrain the biological contribution (f_{biotic}) to surface CO_2 fluxes as follows:

$$f_{biotic} = \frac{\delta^{13}C_{\Delta CO2} - \delta^{13}C_{CO2-abiotic}}{\delta^{13}C_{biotic} - \delta^{13}C_{CO2-abiotic}} \quad (5.11)$$

where $\delta^{13}C_{\Delta CO2}$ is the isotopic composition of the net surface CO_2 flux (‰), $\delta^{13}C_{biotic}$ is the concentration-weighted $\delta^{13}C$ of soil organic C (between 0 and 30 cm depth) at Site A (−22.8‰; Chapter 3, Figure 3.8), and $\delta^{13}C_{CO2\text{-}abiotic}$ is the average $\delta^{13}C_{\Delta CO2}$ of the surface CO_2 efflux during periods of steady state at Site B (−5.2‰; Chapter 4, section 4.4.3). As soil CO_2 dynamics at Site B appear to be abiotically-driven, this value is considered to represent abiotic production of CO_2 within the soil.

5.3 Results

5.3.1 Environmental variables

At the time of sampling (late December 2009), soils at Site A were ice-cemented below 35 cm. Air and soil temperatures varied diurnally, with the latter exhibiting progressively greater lags and damping in soil temperature response to surface heating and cooling with increasing depth in the profile (Figure 5.2A). Air and soil temperatures were slightly warmer at Site A than Site B, with air temperature at Site A ranging from −3.6 to 8.7°C, and soil temperatures at 5 cm, 15 cm and 25 cm ranging from −0.8 to 11.0°C, 1.0 to 5.3°C and 0.8 to 2.9°C, respectively.

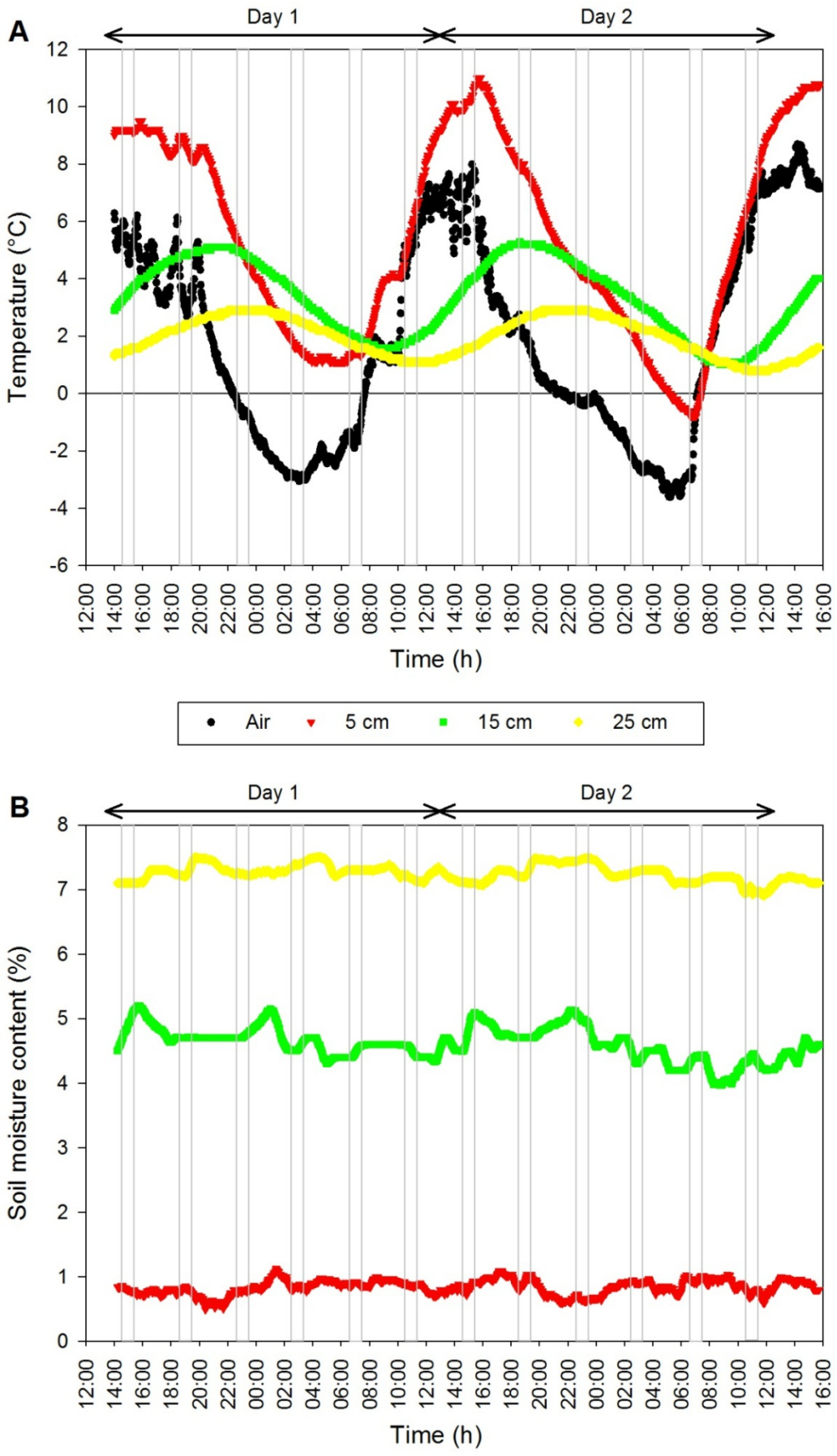

Figure 5.2 Soil temperature **(A)** and volumetric moisture content **(B)** during the 48-h period over which gas samples were taken, Site A, Taylor Valley. Data plotted for moisture content are 30 min. moving averages. The narrow vertical grey boxes denote the periods during which gas samples were taken.

Soil moisture content remained relatively constant throughout the sampling period (Figure 5.2B), and increased with depth in the profile, averaging 0.8, 4.6 and 7.3% at 5, 15 and 25 cm, respectively. This was significantly higher than soil moisture content at Site B, which averaged 0.8% over the three depths at which measurements were made. Qualitative observations of limited melting of snow patches and lake ice in late December 2009 suggested that the summer was cooler than the previous summer of 2008/09. This was corroborated by the lack of ponded surface water evident at sites close to Site A where it had been observed the previous summer, and low soil moisture contents measured at Site B. However, soil moisture contents at Site A were similar to those measured during the 2008/09 sampling period.

5.3.2 CO_2 dynamics

Surface CO_2 fluxes

Surface CO_2 flux rates at Site A were highly spatially and temporally variable, ranging from −0.44 to 0.17 µmol m^{-2} s^{-1} (Table 5.1). However, only 25% of the surface CO_2 fluxes calculated were statistically significant, and, of these, 83% occurred at either the 06:30 or 10:30 h sampling periods. At 14:30, 18:30, 22:30 and 02:30 h, surface chamber CO_2 concentrations generally varied non-systematically throughout the 45-min sampling period (Figure 5.3), hence surface flux rates were unable to be calculated. Consequently, it is difficult to determine the timing of maximum and minimum surface CO_2 fluxes and their relationship with wind speed, soil temperature, and the rate of change in soil temperature (Figure 5.4).

In the absence of a large proportion of significant linear relationships between chamber headspace CO_2 concentration and time, surface CO_2 fluxes were predicted according to Fick's Law (5.8). At times of low flux (06:30 and 10:30 h), the measured and predicted fluxes were in good agreement (Figure 5.4A). As such, it appears that the relationship between subsurface CO_2 concentration gradient and surface CO_2 flux rate (and hence D_e) derived from Site B is transferable to Site A. However, the statistically significant high-flux measurements at 18:30 and 22:30 h on Day 1 were lower than the predicted fluxes at those times, with the discrepancy at 22:30 h being such that the measured and predicted fluxes were of opposite sign. Furthermore, these two occurrences of statistically significant high-flux measurements originated from a single chamber. As the chamber that produced the significant results differed at each of the two sampling times, it suggests that the apparently significant fluxes may result from a coincidental artefact, rather than representing a statistically significant, repeatable result.

Table 5.1 Surface soil CO_2 fluxes at Site A, Taylor Valley.

Day 1					Day 2			
Date	Sampling time (h)	Replicate	CO_2 flux (μmol m^{-2} s^{-1})		Date	Sampling time (h)	Replicate	CO_2 flux (μmol m^{-2} s^{-1})
29/12/10	14:30	a	0.034		30/12/10	14:30	a	−0.018
		b	0.042				b	−0.168
		c	0.005				c	0.013
		d	0.047				d	−0.080
29/12/10	18:30	a	0.133**		30/12/10	18:30	a	−0.017
		b	0.033				b	0.033
		c	−0.026				c	−0.001
		d	−0.001				d	−0.001
29/12/10	22:30	a	0.031		30/12/10	22:30	a	−0.012
		b	−0.008				b	−0.018
		c	−0.020				c	0.017
		d	−0.197**				d	−0.077
30/12/10	02:30	a	−0.071		31/12/10	02:30	a	−0.012
		b	0.102				b	−0.439
		c	0.010				c	−0.114
		d	0.173				d	−0.227
30/12/10	06:30	a	−0.017		31/12/10	06:30	a	−0.018
		b	−0.031**				b	0.065*
		c	−0.057*				c	−0.020
		d	−0.026				d	−0.030*
30/12/10	10:30	a	0.027		31/12/10	10:30	a	0.032**
		b	0.040**				b	0.031*
		c	0.022				c	0.033**
		d	0.040**				d	0.060**

* represents $P < 0.1$; ** represents $P < 0.05$.

The average $\delta^{13}C_{CO2}$ of the four gas samples taken from surface chambers during the 45-min sampling periods ranged from −8.6‰ to −11.4‰. Where surface fluxes were statistically significant, changes in $\delta^{13}C_{CO2}$ between samples taken at times 0 and 45 min were used to calculate the $\delta^{13}C_{\Delta CO2}$ of the surface flux (5.5). The $\delta^{13}C_{\Delta CO2}$ of significant surface CO_2 fluxes ranged from −9.3 to −29.8‰ (Figure 5.4B). The predicted $\delta^{13}C_{\Delta CO2}$ of surface fluxes, based on CO_2 concentration and $\delta^{13}C_{CO2}$ gradients (5.10), ranged from −8.1 to −25.3‰. However, the lack of significant surface CO_2 fluxes limited comparisons between measured and predicted $\delta^{13}C_{\Delta CO2}$ values. On several occasions, the measured and predicted $\delta^{13}C_{\Delta CO2}$ values were in good agreement, whereas at other times, they were considerably different.

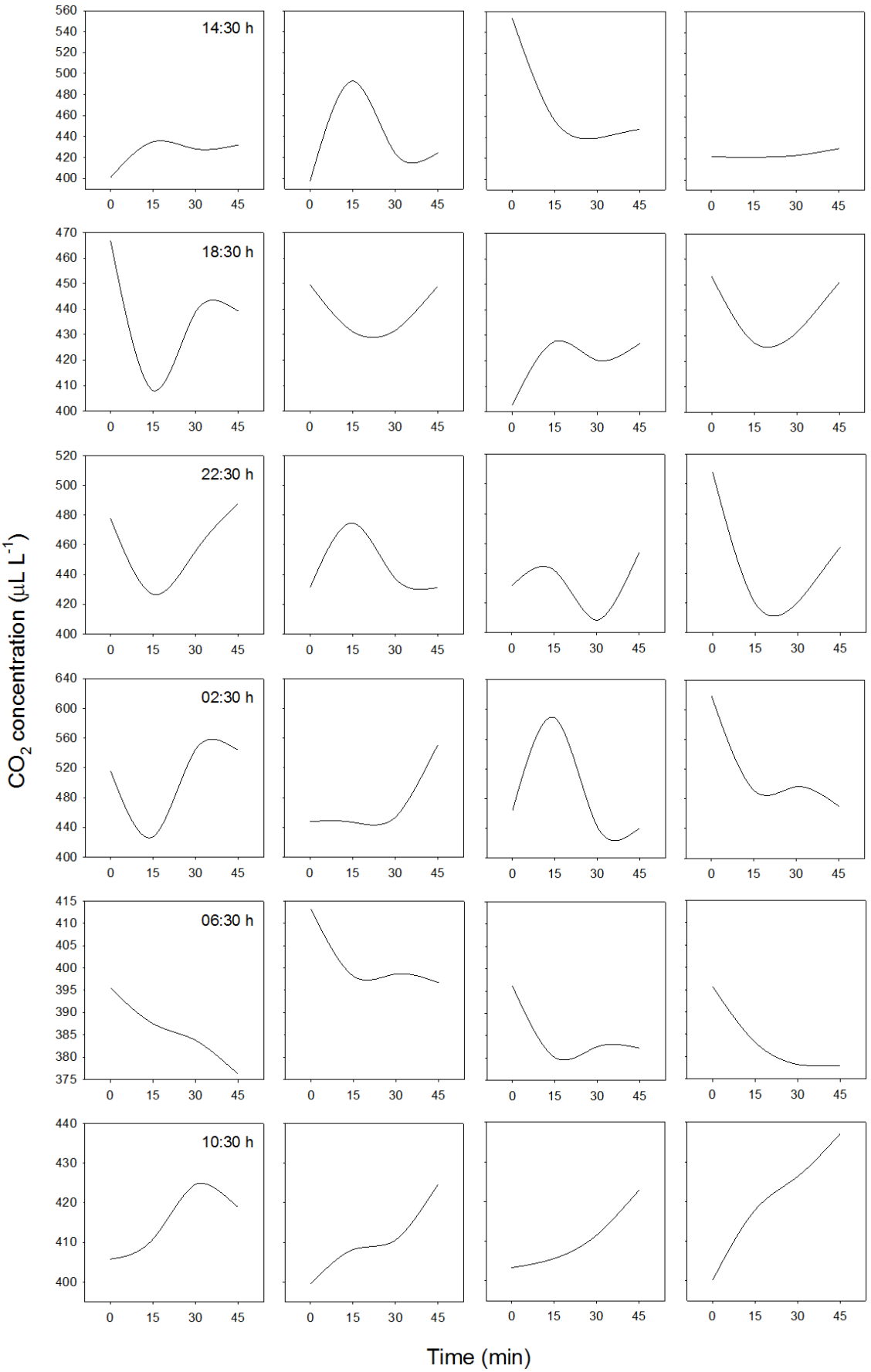

Figure 5.3 Selection of CO_2 time-series data from surface headspace chambers, Site A, Taylor Valley, showing variation in CO_2 concentration over the 45-min sampling period. Note that data from each sampling period are plotted on different CO_2 concentration scales.

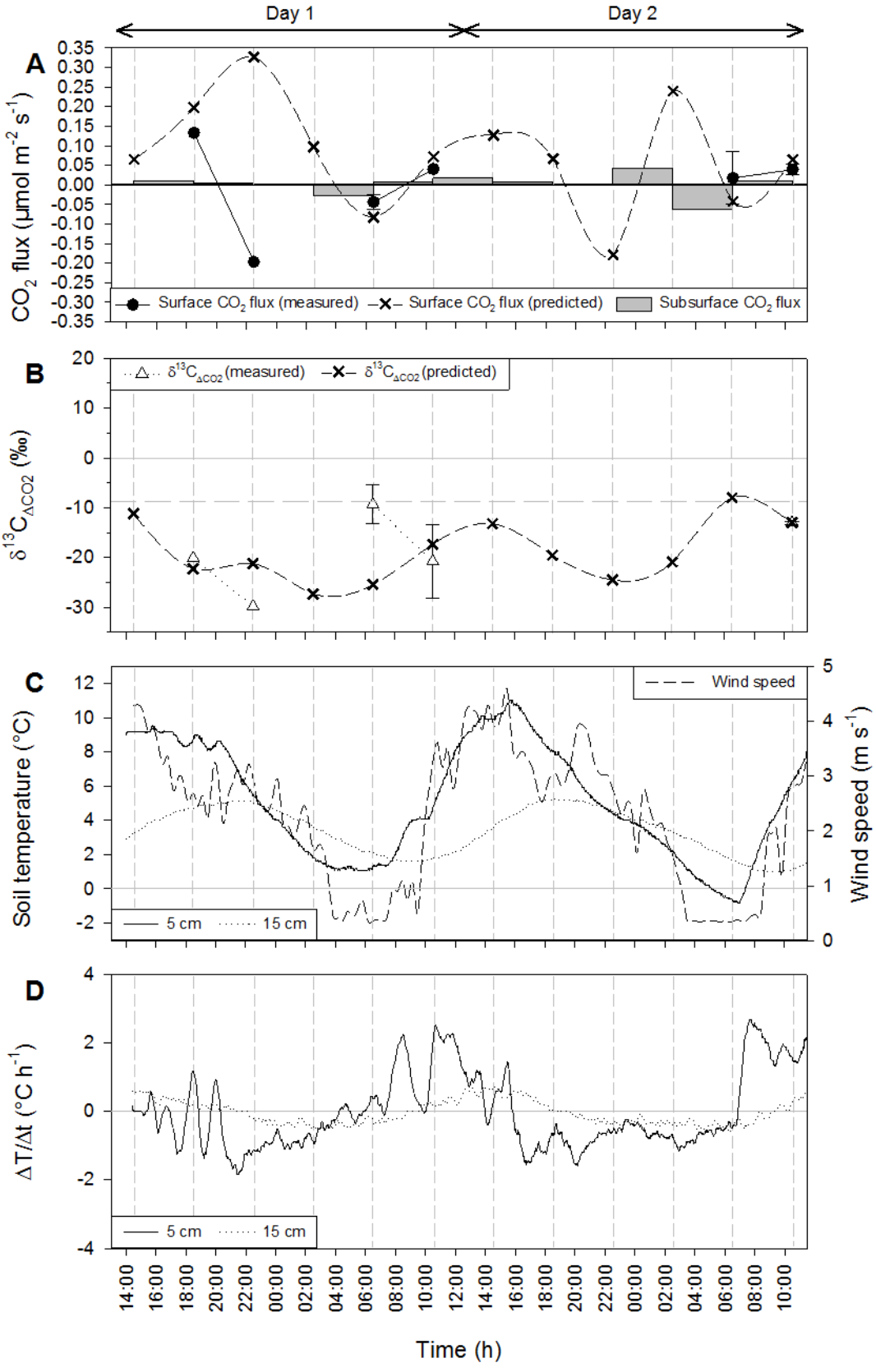

Figure 5.4 **(A)** Average significant measured surface CO_2 flux rates, predicted surface CO_2 flux rates, and subsurface soil CO_2 storage flux rates at Site A, Taylor Valley. Error bars represent the standard error of the mean. Subsurface soil CO_2 storage fluxes are shown as grey bars, which represent the net CO_2 flux over the 4-h period between sampling. **(B)** Isotopic composition ($\delta^{13}C_{\Delta CO2}$) of measured and predicted surface CO_2 fluxes at Site A, Taylor Valley. Predicted values are calculated based on subsurface CO_2 concentration

and $\delta^{13}C_{CO2}$ gradients at the time of sampling. Error bars represent the standard error of the mean. The dashed horizontal line represents the average $\delta^{13}C_{CO2}$ of ambient atmospheric CO_2 (−8.8‰). **(C)** Soil temperature at 5 and 15 cm depth (left hand axis) and wind speed (right hand axis) during the gas sampling period, Site A, Taylor Valley. **(D)** Rate of change in soil temperature at 5 and 15 cm depth during the gas sampling period, Site A, Taylor Valley. Data plotted are 30 min moving averages.
The dashed vertical lines correspond to the four-hourly intervals at which gas sampling began.

Subsurface CO_2 profiles and fluxes

Values for CO_2 concentration and $\delta^{13}C_{CO2}$ at 0 cm depth varied throughout the 48-h sampling period (Figure 5.5), suggesting that the 0 cm sampling tube (1 cm above the soil surface) was located within a partially mixed surface boundary layer. The highest CO_2 concentrations and most depleted $\delta^{13}C_{CO2}$ values occurred at 22:30 and 02:30 h on both days.

Temporal changes in CO_2 concentration and $\delta^{13}C_{CO2}$ profiles throughout the two 24-h sampling periods at Site A were highly variable (Figure 5.5). Between 06:30 and 14:30 h, CO_2 concentration profiles were generally symmetrical about a vertical line corresponding to the local ambient atmospheric CO_2 concentration (400 ± 4 µL L^{-1}, as revealed by data from 0 cm sampling tubes at Site B). CO_2 concentrations were below that of atmospheric CO_2 concentration throughout the profile at 06:30 h, and in the lower part of the profile at 10:30 h, after which they increased to be above that of atmospheric CO_2 concentration throughout the profile by 14:30 h. Between 14:30 and 02:30 h, soil CO_2 concentrations throughout the profile remained greater than that of ambient atmospheric CO_2 concentration. The highest subsurface CO_2 concentrations were measured at 02:30 h on Day 2, reaching a maximum of 700 µL L^{-1} at 15 cm depth. The greatest change in subsurface CO_2 concentrations occurred between 02:30 and 06:30 h, when concentrations decreased from maximum to minimum values (below atmospheric CO_2 concentration).

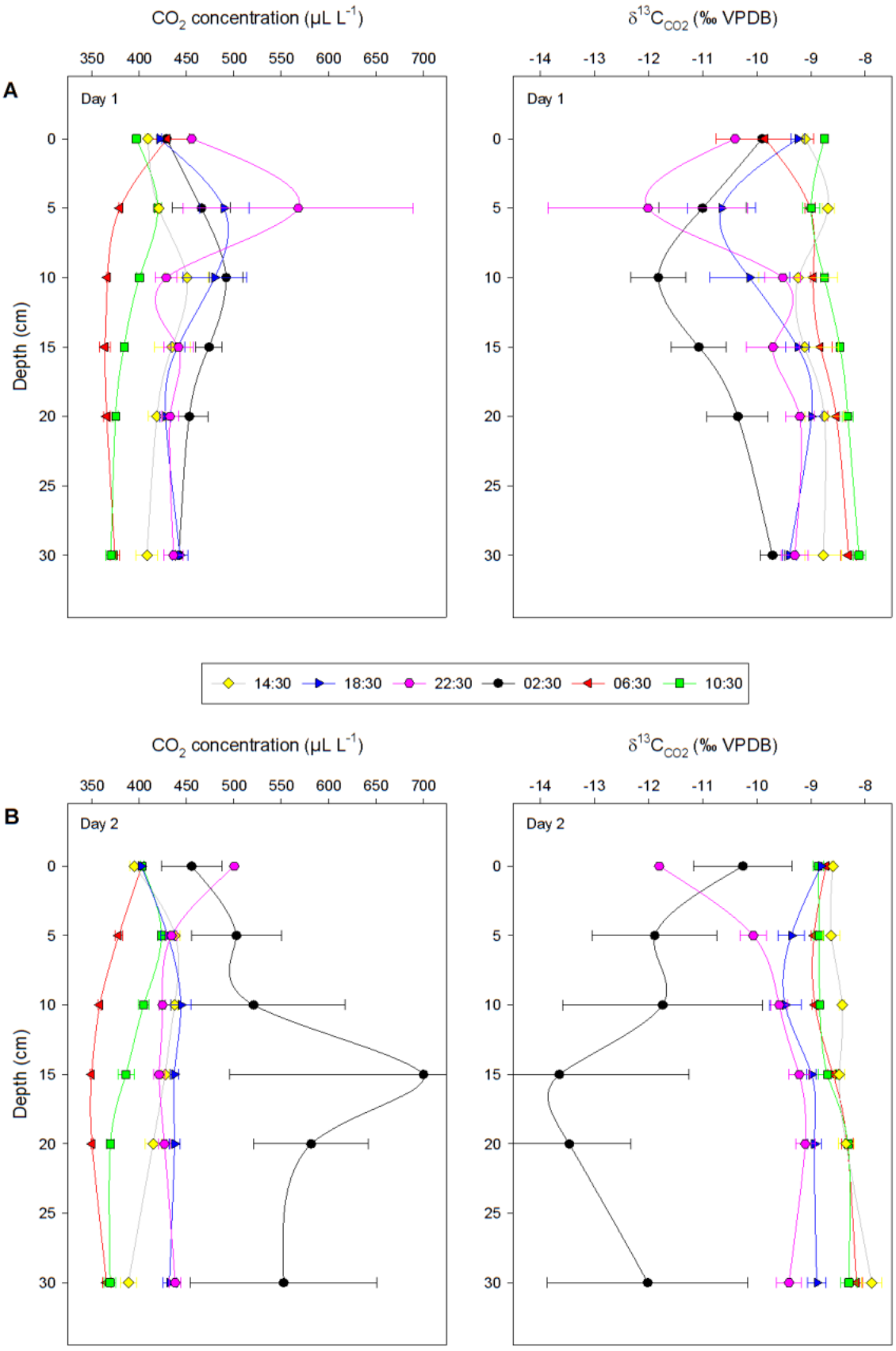

Figure 5.5 Soil profile CO_2 concentration and $\delta^{13}C_{CO2}$ at Site A, Taylor Valley. **(A)** and **(B)** represent data from Day 1 and Day 2, respectively. Data shown represent averages from each sampling time (n = 1 or 2 for 0 cm samples. At all other depths, n = 4). Error bars represent the standard error of the mean.

Depth profiles of $\delta^{13}C_{CO2}$ were also highly variable (Figure 5.5). Between 06:30 and 14:30 h, $\delta^{13}C_{CO2}$ values remained close to that of ambient atmospheric CO_2 (−8.8 ± 0.2‰) throughout the profile, although $\delta^{13}C_{CO2}$ values tended to increase with depth. Between 14:30 and 02:30 h, $\delta^{13}C_{CO2}$ became significantly more depleted than that measured between 06:30 and 14:30 h. The most depleted $\delta^{13}C_{CO2}$ values (as low as −13.7‰) were measured at 02:30 h, although the uncertainty associated with $\delta^{13}C_{CO2}$ values on Day 2 indicates that there was high spatial variability in $\delta^{13}C_{CO2}$ values at this time. As with subsurface CO_2 concentrations, the greatest change in subsurface $\delta^{13}C_{CO2}$ values occurred between 02:30 and 06:30 h, when $\delta^{13}C_{CO2}$ shifted from its most depleted to close to that of ambient atmospheric CO_2. Changes in $\delta^{13}C_{CO2}$ values coincided with changes in CO_2 concentrations, with $\delta^{13}C_{CO2}$ generally becoming more depleted in ^{13}C as CO_2 concentrations increased, and more enriched in ^{13}C as CO_2 concentrations decreased. This is the opposite of what was observed at Site B.

Subsurface storage CO_2 fluxes were calculated based on the change in the profile average CO_2 concentration between sampling times (5.7), and ranged between −0.07 and 0.05 µmol m^{-2} s^{-1} (Figure 5.4A). The only negative subsurface storage fluxes occurred during the period between 02:30 and 06:30 h each day.

5.3.3 Linking surface and subsurface CO_2 dynamics

Day 1 (Figure 5.4 and Figure 5.5A)

14:30 – 18:30 h

Between 14:30 and 18:30 h, the subsoil gained CO_2. At the start of the interval, subsurface CO_2 concentrations were above ambient atmospheric CO_2 concentration; concentration increased over the interval at all depths, with the most significant increases in the upper 10 cm of the profile. The greatest increase was at 5 cm depth, with CO_2 concentration increasing from 420 to 490 µL L^{-1}. Subsurface $\delta^{13}C_{CO2}$ values became more depleted, with the largest shifts corresponding to the concentration increases in the upper 10 cm of the profile. The maximum depletion in $\delta^{13}C_{CO2}$ occurred at 5 cm depth, shifting from −8.7 to −10.7‰.

No significant surface CO_2 fluxes were measured at 14:30 h, but at 18:30 h, there was one significant surface flux at a rate of 0.13 µmol m^{-2} s^{-1}. Surface CO_2 fluxes calculated from subsurface CO_2 concentration gradients increased from 0.07 µmol m^{-2} s^{-1} at 14:30 h to 0.20 µmol m^{-2} s^{-1} at 18:30 h, meaning that the predicted flux at 18:30 h was around 30% higher than the single significant measured flux.

The shift in soil profile $\delta^{13}C_{CO2}$ to more depleted values meant that the subsurface $\delta^{13}C_{CO2}$ gradient switched from being positive at 14:30 h to negative at 18:30 h. Combined with the persistent positive CO_2 concentration gradient, the switch in $\delta^{13}C_{CO2}$ gradient acted to drive a relatively depleted flux at

18:30 h, with the $\delta^{13}C_{\Delta CO2}$ of the flux calculated from CO_2 and $\delta^{13}C_{CO2}$ gradients shifting from −11.2‰ at 14:30 h to −22.3‰ at 18:30 h. The $\delta^{13}C_{\Delta CO2}$ of the predicted flux at 18:30 h was very similar to the $\delta^{13}C_{\Delta CO2}$ of the single measured significant flux (−20.1‰). Over this period, soil temperature at 5 cm depth remained relatively constant (around 9°C), and soil temperature at 15 cm depth increased to close to its daily maximum by the end of the interval.

18:30 – 22:30 h

Over this interval, the soil gained a small amount of CO_2. Subsurface CO_2 concentration increased at 5 cm depth to a daily maximum of 570 µL L^{-1} at 22:30 h, although this mean value has a high standard error due to high spatial variability amongst samples. CO_2 concentration decreased at 10 cm depth, and did not change between 15 and 30 cm depth, thus CO_2 concentrations throughout the profile remained greater than that of atmospheric CO_2. Changes in subsurface $\delta^{13}C_{CO2}$ values corresponded to changes in CO_2 concentration; $\delta^{13}C_{CO2}$ at 5 cm depth reached the daily minimum value of −12.0‰ at 22:30 h. However, as with CO_2 concentrations, the $\delta^{13}C_{CO2}$ at this depth was highly spatially variable. $\delta^{13}C_{CO2}$ became less depleted at 10 cm depth, and remained similar between 15 and 30 cm depth.

The sign of the single measured significant surface CO_2 flux shifted from positive at 18:30 h to negative at 22:30 h (0.13 to −0.20 µmol m^{-2} s^{-1}). This was in contrast to the predicted surface CO_2 flux rates, which were positive throughout this 4-h period, and reached a daily maximum at 22:30 h. However, the high flux predicted at 22:30 h should be interpreted with caution, as there was large uncertainty in the CO_2 concentration value at 5 cm depth, from which the CO_2 concentration gradient used in the flux calculation was derived.

The $\delta^{13}C_{\Delta CO2}$ of the significant measured surface fluxes (n = 1 at each sampling time) shifted from −20.1‰ at 18:30 h to −29.8‰ at 22:30 h. The highly depleted flux measured at 22:30 h was consistent with the relatively light efflux expected from the persistent combination of a positive CO_2 concentration gradient and a negative $\delta^{13}C_{CO2}$ gradient, although it was considerably more depleted than that calculated from CO_2 concentration and $\delta^{13}C_{CO2}$ gradients at that time (−21.3‰). The increase in surface CO_2 flux rates over this period was coincident with rapidly decreasing soil temperature at 5 cm depth, at times at close to its maximum negative rate of change. Soil temperature at 15 cm depth remained close to its daily maximum throughout the interval.

22:30 – 02:30 h

Between 22:30 and 02:30 h, there was no net change in subsurface CO_2 concentrations. Subsurface CO_2 concentration decreased at 5 cm depth, and increased between 10 and 30 cm depth, giving a profile average CO_2 concentration of 460 µL L^{-1}, the same as that at 22:30 h. Subsurface $\delta^{13}C_{CO2}$

became more enriched at 5 cm depth, but was significantly more depleted throughout the rest of the profile. The maximum depletion occurred at 10 cm depth, with $\delta^{13}C_{CO2}$ shifting from −9.5 to −11.8‰.

No significant surface CO_2 fluxes were measured at 02:30 h, hence the $\delta^{13}C_{\Delta CO2}$ of the net flux could not be calculated from surface chamber data. Predicted surface CO_2 flux rates decreased from 0.33 µmol m^{-2} s^{-1} at 22:30 h to 0.10 µmol m^{-2} s^{-1} at 02:30 h in response to the reduced concentration gradient. The positive CO_2 concentration and negative $\delta^{13}C_{CO2}$ gradients persisted throughout the interval, and the $\delta^{13}C_{\Delta CO2}$ of the predicted surface flux at 02:30 h was highly depleted (−27.3‰). The rate of change in soil temperatures at 5 and 15 cm depth were both negative, with the latter at its maximum negative rate by the end of the interval.

02:30 – 06:30 h

During this period, the subsoil lost CO_2 at a rate of −0.03 µmol m^{-2} s^{-1}; the associated changes in subsurface CO_2 concentrations and $\delta^{13}C_{CO2}$ were the most significant observed on Day 1. Subsurface CO_2 concentrations decreased at all depths, declining from a profile average of 460 µL L^{-1} at 02:30 h to a profile average of 375 µL L^{-1} (below atmospheric CO_2 concentration) at 06:30 h. $\delta^{13}C_{CO2}$ became more enriched at all depths, with the greatest shift (from −11.8 to −9.0‰) coinciding with the greatest decrease in CO_2 concentration at 10 cm depth. At 06:30 h, two significant surface CO_2 fluxes were measured, averaging –0.04 µmol m^{-2} s^{-1}, whereas the surface flux rate predicted at this time was −0.08 µmol m^{-2} s^{-1}. The significant decrease in CO_2 concentration between 02:30 h and 06:30 h changed the concentration gradient from positive to negative, and the associated enrichment in $\delta^{13}C_{CO2}$ changed the $\delta^{13}C_{CO2}$ gradient from negative to positive, thus driving a relatively depleted predicted influx of CO_2 (−25.4‰). This was in contrast to the relatively enriched average $\delta^{13}C_{\Delta CO2}$ of the measured surface influxes at 06:30 h (−9.3‰). Soil temperature at 5 cm depth remained close to its daily minimum (1.1°C) throughout the interval, while soil temperature at 15 cm depth continued to decrease at its maximum (negative) rate.

06:30 – 10:30 h

Between 06:30 and 10:30 h, the soil gained CO_2, with subsurface CO_2 concentrations increasing between 0 and 20 cm depth. However, subsurface CO_2 concentrations remained below that of atmospheric CO_2 beneath 10 cm depth. Subsurface $\delta^{13}C_{CO2}$ values became slightly more enriched between 5 and 30 cm depth. The profile average $\delta^{13}C_{CO2}$ of −8.4‰ at 10:30 h was the most enriched measured on Day 1.

Surface CO_2 fluxes shifted from negative to positive over this period, with significant fluxes of 0.04 µmol m^{-2} s^{-1} measured from two chambers at 10:30 h. This was consistent with predicted surface fluxes, which also shifted from negative (−0.08 µmol m^{-2} s^{-1}) to positive (0.07 µmol m^{-2} s^{-1}). The

change in surface flux rate was also accompanied by a significant shift in the $\delta^{13}C_{\Delta CO2}$ of the surface flux. At 06:30 h, the average $\delta^{13}C_{\Delta CO2}$ of the measured CO_2 influx was −9.3‰, which was substantially more enriched than that predicted from CO_2 concentration and $\delta^{13}C_{CO2}$ gradients at that time (−25.4‰). By 10:30 h, surface CO_2 fluxes were positive, and the average $\delta^{13}C_{\Delta CO2}$ of the measured CO_2 efflux was −20.8‰, similar to the predicted $\delta^{13}C_{\Delta CO2}$ value of −17.4‰. Soil temperature at 5 cm depth increased from close to its daily minimum, and soil temperature at 15 cm depth decreased at a low rate, reaching its daily minimum in the second half of the interval.

10:30 – 14:30 h

This interval completes a full 24-h cycle, thus data from the subsurface profile measured at 14:30 h are shown on the "Day 2" profile (Figure 4.4B). Accumulation of CO_2 in the subsoil continued at a greater rate than during the previous 4-h interval, and by 14:30 h, subsurface CO_2 concentrations were greater than atmospheric CO_2 concentration in the upper 20 cm of the profile. $\delta^{13}C_{CO2}$ became slightly heavier in the upper 10 cm of the profile, with a maximum shift from −9.0 to −8.6‰ at 5 cm depth. As at 14:30 h on Day 1, no significant surface CO_2 fluxes were measured, thus the $\delta^{13}C_{\Delta CO2}$ of the surface flux could not be calculated from surface chamber data. Predicted surface flux rates increased from 0.07 to 0.13 µmol m^{-2} s^{-1}, with the predicted $\delta^{13}C_{\Delta CO2}$ of the flux shifting from −17.4 to −13.2‰. Soil temperature at 5 cm depth increased at close to its maximum rate, and soil temperature at 15 cm depth increased from its daily minimum, reaching its maximum rate of change by the end of the interval.

Day 2 (Figure 5.4 and Figure 5.5B)

Day 2 showed the same general patterns of behaviour in surface and subsurface CO_2 dynamics, with some differences in detail as described below. A step-by-step description of the surface and subsurface CO_2 dynamics is given in section 5.6.

Surface CO_2 flux rates

On Day 1, predicted surface flux rates increased from low positive values at 14:30 h to a maximum at 22:30 h. Flux rates then decreased to negative values by 06:30 h before rising again to positive rates by 10:30 h. The pattern of fluxes on Day 2 was similar, except for an anomalous negative predicted flux at 22:30 h. On close examination, this negative flux is predicted as a consequence of a CO_2 concentration at 0 cm depth which was greater than both the ambient soil and surface atmospheres. The high CO_2 concentration in the boundary layer must have been supported by CO_2 production at some shallow depth, which was not resolved by the relatively coarse (5 cm) sampling increments employed. A concentration peak between 0 and 5 cm depth would have driven positive surface fluxes.

Subsurface CO_2 concentration and $\delta^{13}C_{CO2}$ profiles

Between 14:30 and 18:30, while the soil was warming at 15 cm depth, the CO_2 concentration profiles remained similar, but $\delta^{13}C_{CO2}$ values became more depleted at all depths. In the following 4-h period to 22:30 h, CO_2 concentration and $\delta^{13}C_{CO2}$ profiles remained similar, other than an increase in concentration (from 400−500 µL L^{-1}) and associated depletion in $\delta^{13}C_{CO2}$ (from −8.8 to −11.8‰) at 0 cm depth. This is similar to the increase in concentration and depletion in $\delta^{13}C_{CO2}$ at 5 cm depth between 18:30 and 22:30 h on Day 1.

The period from 22:30 to 02:30 h marked the greatest increase in CO_2 concentration and decrease in $\delta^{13}C_{CO2}$ (up to 700 µL L^{-1} and −13.7‰, respectively, at 15 cm depth) while temperature was decreasing throughout the profile. Between 02:30 and 06:30 h, subsurface CO_2 concentrations decreased from their maximum to below atmospheric CO_2, and $\delta^{13}C_{CO2}$ became more enriched, with values close to that of atmospheric CO_2. As for Day 1, the final 4-h period, from 06:30 to 10:30 h, was marked by an increase in concentration throughout the profile to above atmospheric CO_2 concentration in the upper 10 cm, but with no change in subsurface $\delta^{13}C_{CO2}$ profile. As for Day 1, significant surface CO_2 flux rates were measured at the beginning and end of this 4-h period.

5.4 Discussion

Statistically significant surface CO_2 flux rates at Site A were limited to 25% of the fluxes calculated from surface chamber data. This limits the discussion of diel variation in surface CO_2 flux rates to those predicted from CO_2 concentration gradients.

Predicted surface CO_2 flux rates were highly variable, ranging from −0.18 to 0.33 µmol m^{-2} s^{-1} (Figure 5.4A). The duration and magnitude of positive surface CO_2 flux rates exceeded that of negative flux rates, and the $\delta^{13}C_{\Delta CO2}$ of the fluxes (also predicted) was predominantly around −22‰, which is very similar to the concentration-weighted $\delta^{13}C$ of soil organic C in the upper 30 cm of the profile at Site A (−22.8‰; Chapter 3, Figure 3.8). This pattern contrasts with that at Site B, where positive and negative CO_2 fluxes balanced, and the $\delta^{13}C_{\Delta CO2}$ of the measured fluxes was highly variable, ranging between −2.4 and −31.8‰ (Chapter 4, Figure 4.3). Furthermore, whereas at Site B, surface CO_2 flux rates varied in a sinusoidal manner with the same period, although not the same phase, as soil temperature variation, the variability in predicted surface CO_2 flux rates at Site A was not coupled to soil temperature or the rate of change in soil temperature (Figure 5.6 and Figure 5.7).

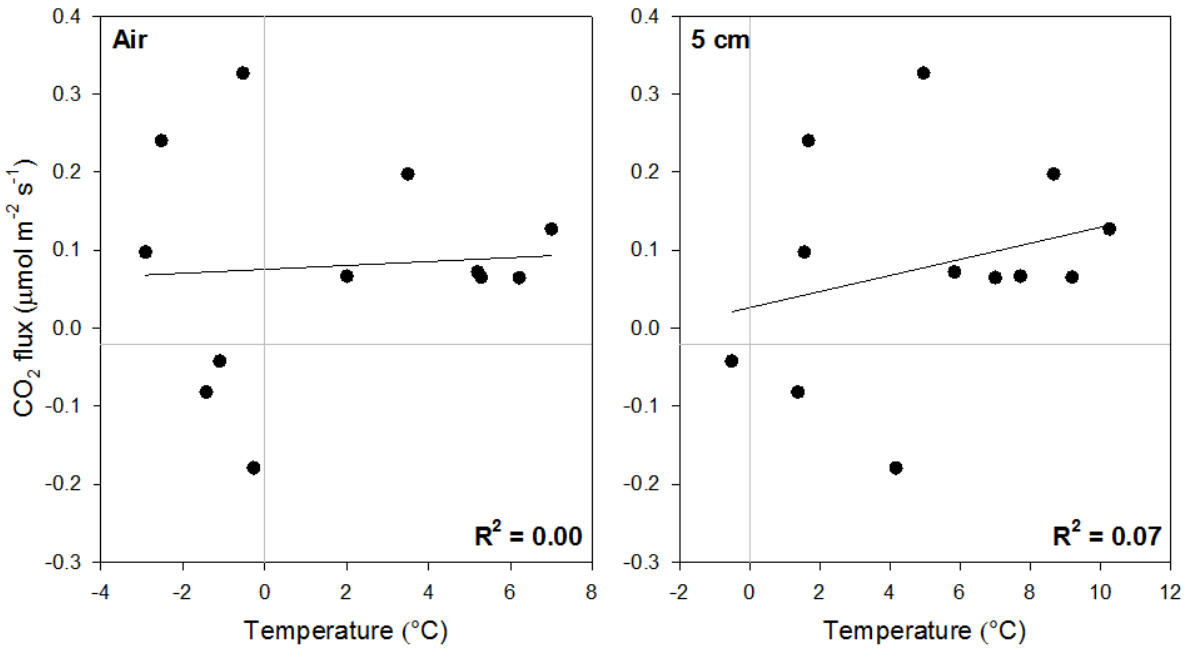

Figure 5.6 Relationship between average temperature over the surface flux sampling period and predicted surface CO_2 flux rates at Site A, Taylor Valley. Regressions are not significant ($p > 0.1$).

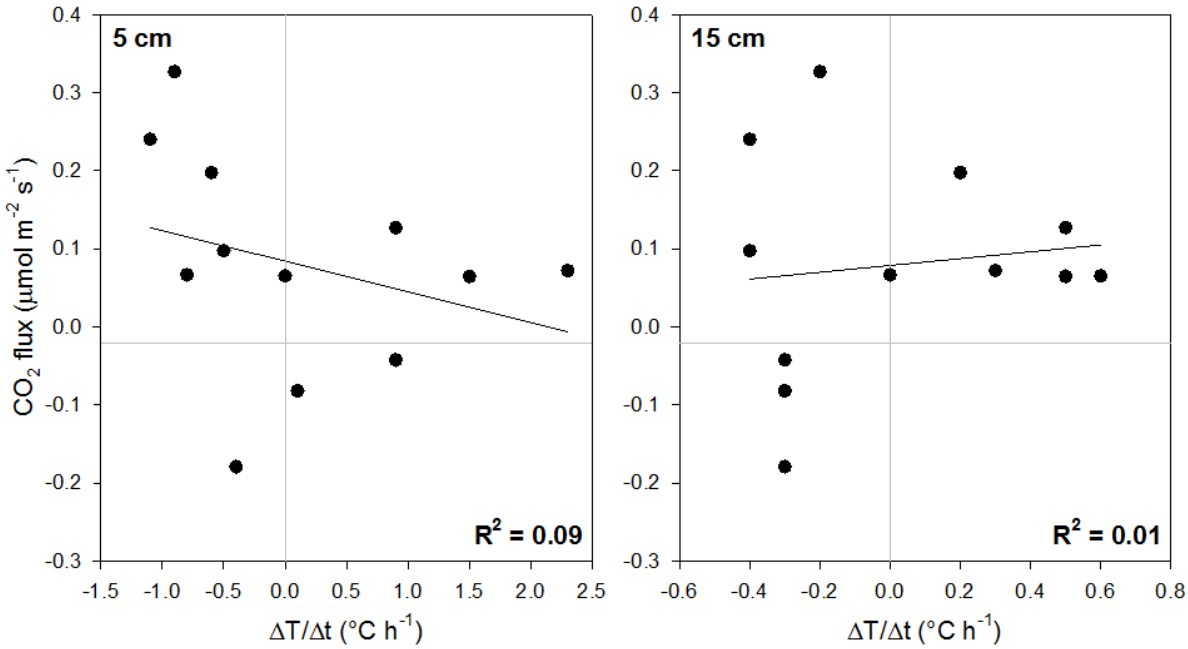

Figure 5.7 Relationship between the average rate of change in soil temperature over the surface flux sampling period at 5 cm and 15 cm depth with predicted surface CO_2 flux rates at Site A, Taylor Valley. Regressions are not significant ($p > 0.1$).

At Site A, the highest surface CO_2 flux rates and greatest increases in subsurface CO_2 concentration (and depletion in $\delta^{13}C_{CO2}$) occurred at times when soil temperatures were cooling (22:30 and 02:30 h;

Figure 5.4 and Figure 5.5), thus eliminating exsolution of CO_2 according to Henry's Law as a possible driver. Instead, the relatively high CO_2 concentrations and associated depletion in $\delta^{13}C_{CO2}$ values must be due to biological processes. The highest predicted flux rate of 0.33 µmol m^{-2} s^{-1} is similar to rates measured by Ball et al. (2009) at a site with slightly lower soil organic C content, but lower than rates measured by Gregorich et al. (2006) in lakeshore soils with higher C and moisture levels. The finding that the maximum rate of biological CO_2 production occurred during periods when soil temperatures were cooling runs counter to research which demonstrates an increase in biological activity with increasing temperature (e.g. Lloyd and Taylor, 1994; Fang and Moncrieff, 2001). Nonetheless, this evidence strongly suggests that diel CO_2 dynamics at Site A were substantially influenced by heterotrophic respiration, most likely fostered by the higher soil organic C and moisture levels at this site. However, abiotic processes must still contribute, as shown by the negative CO_2 flux rates that occurred at 06:30 h, when soil temperatures were cooling and subsurface CO_2 concentrations were lower than that of atmospheric CO_2.

The four-hourly sampling intervals, combined with the dynamic nature of subsurface CO_2 concentration and $\delta^{13}C_{CO2}$ profiles, precluded the identification of any steady-state phases. Consequently, a mixing model approach could not be routinely applied to quantify the relative contributions of biotic and abiotic processes to surface CO_2 fluxes. In addition, the absence of steady-state phases means that the $\delta^{13}C_{\Delta CO2}$ of predicted surface fluxes will have been affected by dynamic fractionation effects (Amundson et al., 1998; Nickerson and Risk, 2009c), and thus cannot be directly attributed to microbial utilisation of soil organic C, despite the $\delta^{13}C_{\Delta CO2}$ values being close to that of soil organic matter.

Nonetheless, there were two phases from which subsurface CO_2 concentration and $\delta^{13}C_{CO2}$ profiles could be utilised, together with predicted surface flux $\delta^{13}C_{\Delta CO2}$ values, to provide data suitable for incorporation into a mixing model to constrain the contribution of biological production of CO_2 within the soil. The first occurred between 10:30 h on Day 1, and the first sampling on Day 2, at 14:30 h. During this period, the soil produced CO_2, and subsurface $\delta^{13}C_{CO2}$ values became heavier (Figure 5.5). The surface CO_2 flux was positive over this period, and the $\delta^{13}C_{\Delta CO2}$ of the predicted surface CO_2 flux shifted from −17.4 to −13.2‰ (Figure 5.4A and B). Assuming an intermediate isotopic composition of −15.3‰ over this period, and combined with the fact that subsurface $\delta^{13}C_{CO2}$ values became heavier whilst CO_2 concentration increased, the soil must have been producing CO_2 with an isotopic composition heavier than −15.3‰. For this condition to be satisfied, the mixing model calculation (5.11) limits the biotic contribution to the flux to a maximum of 57%. This is based on the assumption that 1) the $\delta^{13}C_{CO2}$ of biologically-produced CO_2 was −22.8‰, reflecting that of the source organic material (Dörr and Münnich, 1980), and 2) the $\delta^{13}C_{CO2}$ of abiotically-produced CO_2 was −5.2‰, as determined from steady-state periods of CO_2 production at Site B.

The second phase that yielded data suitable for constraining biological contributions to surface CO_2 fluxes occurred between 14:30 and 18:30 h on Day 2. During this period, subsurface CO_2 concentration profiles remained steady whilst subsurface $\delta^{13}C_{CO2}$ values became more depleted (Figure 5.5B), and the $\delta^{13}C_{\Delta CO2}$ of the predicted surface CO_2 flux shifted from −13.2 to −19.6‰ (Figure 5.4B). The fact that there was no change in subsurface CO_2 concentration whilst subsurface $\delta^{13}C_{CO2}$ values became more depleted implies that the CO_2 being produced in the soil must be isotopically lighter than the surface flux over this period. Assuming the surface flux had an intermediate isotopic composition of −16.4‰ throughout this interval, and the same assumptions as to the $\delta^{13}C_{CO2}$ of biologically- and abiotically-produced CO_2 described above, the mixing model calculation (5.11) requires that the proportion of biological CO_2 production over this period is at least 64%. This period represents steady-state with respect to CO_2 production, and hence the predicted surface CO_2 flux rate equals the rate of soil CO_2 production. Therefore, the biotic component of the flux is at least 64% of the predicted flux. Assuming an average CO_2 flux of 0.1 µmol m^{-2} s^{-1} over this 4-h period (Figure 5.4A), the biotic component to the total CO_2 flux would be at least 0.06 µmol m^{-2} s^{-1}.

The high spatial variability in subsurface CO_2 concentrations and $\delta^{13}C_{CO2}$ values during the cooler periods of the day, when CO_2 production was greatest, suggests that biological activity occurs in discrete zones, perhaps controlled by highly localised organic C concentrations associated with micro-scale landscape features (Moorhead et al., 2003). Alternatively, this variability may arise as a result of pulses of CO_2 from organisms responding to subtle and highly localised changes in soil moisture conditions. An increase in the relative humidity within the soil as soil temperatures decreased could be sufficient to provide additional moisture that may have activated biota (Büdel et al., 2008), although any evidence of increased soil moisture content during these periods was not detected by the Hydra Probes installed throughout the soil profile.

It is important to note that the periods of high production had a consistent pattern with respect to soil temperature changes: peak CO_2 production corresponded to the mid-point in soil temperature decline at the depth at which CO_2 was being produced. For example, the maximum CO_2 concentration at 22:30 h on Day 1 was at 5 cm depth (Figure 5.5A); at this time, soil temperature at 5 cm depth was at the mid-point in its decline (Figure 5.4C). Similarly, the peak in soil CO_2 concentration at 02:30 h on Day 1 was at 10 cm depth (Figure 5.5A), where soil temperature was inferred to have been at the mid-point of its decline (Figure 5.4C). The CO_2 peaks at 0 and 15 cm depth at 22:30 and 02:30 h on Day 2, respectively, also corresponded to the mid-point in soil temperature decline at those depths. This suggests that the soil biological community may be responding to the combination of a decrease in temperature (to between ~3−5°C) and corresponding increase in relative humidity. However, at temperatures below ~3−5°C, activity appears to be inhibited.

5.4.1 Data reliability

The significant surface CO_2 fluxes measured during low flux periods (06:30 and 10:30 h) were in good agreement with those predicted using subsurface CO_2 concentration gradients (Figure 5.4A). This suggests that lateral diffusion and chamber-to-soil feedback effects during low flux periods were negligible. However, the fact that not all of the surface CO_2 fluxes calculated from these periods were significant suggests that such data should be treated with caution. The limited number of statistically significant measured surface fluxes also highlights the value of subsurface CO_2 concentration profiles: without them there is no means of validating surface CO_2 flux rates.

At times when subsurface CO_2 concentrations were above the ambient atmospheric CO_2 concentration (400 µL L^{-1}; at 14:30, 18:30, 22:30 and 02:30 h), surface CO_2 flux rates were unable to be derived from static chamber measurements because concentration changes were not systematic over the 45 min sampling period (Figure 5.3). At Site A, where soils are characteristically dry and porous, and biological activity is highly spatially and temporally variable, any non-linearities in accumulation of CO_2 in headspace chambers may be due to short-lived pulses of CO_2 being produced during the sampling period. The high spatial and temporal variability in biological activity is highlighted in Figure 5.5, with relatively short-lived periods of biological CO_2 production occurring heterogeneously throughout the study area, often at times during which biological activity was unexpected.

In addition, non-linearity in headspace chamber CO_2 concentrations can be caused by chamber-to-soil feedbacks. Increases (or decreases) in CO_2 concentration within the chamber distorts the subsurface CO_2 concentration gradient (Healy et al., 1996; Conen and Smith, 2000), inducing lateral diffusion of CO_2 (Creelman et al., 2013) as well as gas storage within the profile (Conen and Smith, 2000), thus causing underestimation of the surface CO_2 flux rate. Despite the dry, porous nature of the soil at Site A, lateral diffusion effects were minimised by installing the lowermost edges of the chambers to 6 cm below the soil surface, and maximising their height above the soil surface as much as was practicable given the expected flux rate (Healy et al., 1996; Conen and Smith, 2000). However, as the expected surface CO_2 flux rate, based on data obtained in the 2008/09 field season (Chapter 3, Table 3.1), was low, the 45 min chamber deployment would likely have exacerbated lateral diffusion effects during periods of comparatively high (> 0.05 µmol m^{-2} s^{-1}) CO_2 fluxes. A shorter deployment period during times of high flux may have reduced lateral diffusion effects, and therefore increased the likelihood of measuring statistically significant surface CO_2 flux rates.

Chamber-to-soil feedback effects commonly manifest as quadratic or exponential growth curves of CO_2 concentration (Creelman et al., 2013). However, no such monotonic increases in CO_2 concentration were observed. Despite the variability in initial CO_2 concentrations within the

chambers, the non-linearities were not systematic (Figure 5.3), which suggests that the changes in CO_2 concentration may have been a result of highly temporally (and spatially) variable CO_2 production, rather than a chamber-induced feedback effect. Furthermore, the inflections in the time-series data (Figure 5.3) would require CO_2 to be diffusing out of the chambers at times. Diffusion into the soil is unlikely given the pervasive positive concentration gradients that existed during all sampling periods other than that at 06:30 h. Wind pumping effects are possible, but they were not observed during simultaneous sampling periods at Site B, where wind speeds would have been equal to or greater than those measured at Site A. Such effects cannot be evaluated for Site A, as surface CO_2 flux rates were predicted from subsurface CO_2 concentration gradients. The observed non-linearities could also have arisen from analytical error, although this is considered unlikely. Samples from Sites A and B were analysed in the same runs, on multiple days, and there was no evidence of analytical error. The cause of the inflections remains unknown.

5.4.2 Implications

Despite the lack of significant surface CO_2 fluxes throughout most of the 48-h sampling period, diel variation in subsurface CO_2 concentrations and $\delta^{13}C_{CO2}$ at Site A clearly demonstrates that production of CO_2 does not occur at a constant rate throughout the 24-h cycle, nor does the maximum rate of CO_2 production correspond to maximum soil temperatures. Instead, the maximum rate of CO_2 production at Site A (inferred from subsurface CO_2 concentration and $\delta^{13}C_{CO2}$ profiles) occurred during periods when soil temperatures were low and decreasing. This implies that soil biological activity at this site is influenced by interactions between temperature and moisture availability. Although not a surprising result in itself, the inference that subtle changes in relative humidity, driven by *decreases* in soil temperature, suggests that other abiotic factors known to influence biological activity (e.g. soil geochemistry; Barrett et al., 2004; Poage et al., 2008) are of lesser importance at this site. The assumption that some microorganisms may be able to directly absorb water vapour (Cary et al., 2010; Stomeo et al., 2012) supports the idea that the biological community at this site may comprise organisms that are able to respond to subtle changes in relative humidity.

The finding that CO_2 production is non-steady, with peak production during cooler parts of the day, reinforces the significance of the results presented in this study and highlights problems that were not identified during previous studies of Dry Valley soil CO_2 fluxes. It can no longer be assumed that: 1) surface CO_2 fluxes are solely biological in origin, 2) the maximum rate of CO_2 production occurs during the warmest parts of the day, and 3) surface CO_2 flux rates are representative of soil CO_2 production (i.e. the system is in steady-state). An understanding of both surface and subsurface CO_2 dynamics is vital for identifying periods of steady-state, during which time surface CO_2 fluxes and

their isotopic composition are representative of CO_2 production within the soil (Amundson et al., 1998; Nickerson and Risk, 2009c). It is only during such periods that a valid assessment of the relative contributions of biotic and abiotic processes to surface CO_2 fluxes can be made.

Previous studies of soil CO_2 flux rates in the McMurdo Dry Valleys have not differentiated between biotic and abiotic components of the flux. Furthermore, it has been assumed that maximum surface CO_2 flux rates, measured at the warmest times of the day, represent maximum rates of biological respiration (Burkins et al., 2001; Ball et al., 2009). Having demonstrated that biological activity appears to be greatest during periods of low and decreasing soil temperatures at Site A, and that soil CO_2 production is non-steady, any inferences about soil respiration rates that are based solely on surface flux data should be re-evaluated. Further discussion of the implications of these results on interpretation of surface soil CO_2 fluxes measured in Dry Valley soils will be presented in the following chapter.

The limited number of significant surface CO_2 flux rates measured at Site A highlights the importance of tailoring sampling protocols to suit expected flux rates at each site. The higher organic C and soil moisture content at Site A is likely to support a more active biological community than that at Site B, away from any localised sources of C or moisture. In retrospect, the sampling period at Site A should have been shortened in anticipation of greater biological activity, although data from the 2008/09 field season (Chapter 3) were wrongly assumed to have captured the maximum variability in surface CO_2 flux rates. The fact that they did not means that assumptions made in Chapter 3 are inappropriate with respect to the inferred maximum biological contribution to surface CO_2 fluxes.

The surprising result that maximum CO_2 production occurred during periods when soil temperatures were low and decreasing meant that the 45-min sampling periods were probably too long to produce reliable surface chamber data. However, despite the fact that data from the 45-min sampling periods at Site A largely failed to show a consistent increase (or decrease) in CO_2 concentration with time, the non-systematic variability in CO_2 concentrations suggested that temporal variability in CO_2 production, rather than lateral diffusion of CO_2 in response to distorted subsurface concentration gradients, limited the calculation of surface CO_2 flux rates. Predictions of surface CO_2 flux rates based on consistent subsurface CO_2 concentration profiles appeared reliable during low flux periods, but high spatial variability in subsurface CO_2 concentration profiles during cooler parts of the day limited their reliability for predicting surface CO_2 flux rates at times of high flux (> 0.10 µmol m^{-2} s^{-1}). Nonetheless, the spatial variability in subsurface CO_2 concentrations suggests that any biological component of soil CO_2 fluxes is unlikely to be homogenous, even throughout a relatively small sampling area. Observed variability in surface CO_2 flux rates may be in response to the distribution of organic C or to localised sources of moisture, or a combination of both factors. As such, any study

attempting to differentiate between biotic and abiotic components of surface CO_2 fluxes cannot discount the possibility that within a sampling area, some fluxes may have a negligible biological component. Studies combining subsurface CO_2 concentration and $\delta^{13}C_{CO2}$ profiles with surface flux measurements are vital in order to identify periods of steady-state, during which surface CO_2 fluxes and their isotopic composition are representative of CO_2 production within the soil. In addition, subsurface CO_2 concentration and $\delta^{13}C_{CO2}$ profiles enable identification of the depth at which biological CO_2 production is occurring.

5.5 Summary and conclusions

The diel changes in subsurface CO_2 concentration and $\delta^{13}C_{CO2}$ profiles described in this chapter are likely to be representative of subsurface CO_2 dynamics in Dry Valley soils with relatively high pH, low EC, and above-average organic C and moisture content. In these soils, subsurface (and surface) CO_2 dynamics are driven by a combination of biotic and abiotic processes, with the relative proportions of each determined by trends in soil temperature. The above-average organic C and moisture content in soils at Site A sustained biotic contributions that were undetectable at Site B, where pH and EC were similar, but organic C and moisture content were considerably lower.

Despite the inability to calculate surface CO_2 fluxes from chamber measurements and the lack of periods of steady state at Site A, and therefore a means by which to quantify the relative proportions of biotic and abiotic components of surface CO_2 fluxes, the subsurface CO_2 dynamics provided a basis for semi-quantitative interpretation of the timing and relative contribution of biological CO_2 production. Subsurface CO_2 concentration and $\delta^{13}C_{CO2}$ profiles in this *relatively* moist and high C environment were highly spatially and temporally variable, and, most significantly, it appears that biological production of CO_2 was greatest between 5 and 20 cm depth, at times when soil temperatures were low and decreasing. At these times (22:30−02:30 h), soil CO_2 production and surface CO_2 fluxes were most likely entirely of biological origin. Previous interpretations of surface CO_2 flux rates in the Dry Valleys, which assumed that maximum surface flux rates occurred during the warmest part of the day and represented the maximum rate of biological activity, should be re-evaluated for two main reasons. Firstly, surface CO_2 flux rates are highly variable, comprising both biotic and abiotic components, and the maximum rate of CO_2 production, at least at this site, occurred during cooler parts of the day. Secondly, as CO_2 production is non-steady, surface CO_2 flux rates are not representative of the rate of CO_2 production within the soil.

The generality of these conclusions and their relationship to data from Site B, along with further discussion of diel variability in surface CO_2 fluxes and implications for soil respiration measurements in the McMurdo Dry Valleys is considered in the following chapter.

5.6 Supplementary information

5.6.1 Detailed description of surface and subsurface CO_2 dynamics on Day 2

The following descriptive summaries of surface and subsurface CO_2 dynamics on Day 2 relate to data presented in Figure 5.4 and Figure 5.5B.

14:30 – 18:30 h

Over this interval, the subsoil continued to accumulate a small amount of CO_2. Increases in CO_2 concentration occurred beneath 10 cm depth, and by 18:30 h, CO_2 concentrations were greater than that of atmospheric CO_2 throughout the profile. Despite the relatively small increases in CO_2 concentration, $\delta^{13}C_{CO2}$ became significantly more depleted throughout the profile, with a maximum shift from −8.4 to −9.5‰ at 10 cm depth. No significant surface CO_2 fluxes were measured at 14:30 or 18:30 h, thus the $\delta^{13}C_{\Delta CO2}$ of the flux could not be calculated from surface chamber data. Predicted surface flux rates decreased from 0.13 to 0.07 µmol m^{-2} s^{-1}, and the $\delta^{13}C_{\Delta CO2}$ of the flux became more depleted, shifting from −13.2 to −19.6‰.

Soil temperatures at 5 and 15 cm depth reached their daily maxima during this interval. However, soil temperature at 5 cm depth reached its maximum early in the interval and then decreased, at times at a rate close to its maximum negative rate of change, whereas soil temperature at 15 cm depth increased throughout the interval, initially at its maximum rate, reaching its daily maximum at the end of the interval. The increase in subsurface CO_2 concentrations and the depletion in soil $\delta^{13}C_{CO2}$ and predicted surface flux $\delta^{13}C_{\Delta CO2}$ values over this interval is similar to that which occurred during the 14:30 to 18:30 h interval on Day 1. Soil temperatures at 5 and 15 cm depth during the 14:30 to 18:30 h interval on Day 1 were also similar to those measured during this interval.

18:30 – 22:30 h

Between 18:30 and 22:30 h, subsurface CO_2 concentrations increased in the upper 5 cm of the profile, and decreased slightly between 5 and 20 cm depth, although concentrations remained greater than that of atmospheric CO_2 concentration throughout the profile. However, there was no net change in subsurface CO_2 concentration. Subsurface $\delta^{13}C_{CO2}$ values became significantly more depleted in the upper 5 cm of the profile, and slightly more depleted throughout the remainder of the profile. Surface CO_2 fluxes remained non-significant, perpetuating the inability to determine the $\delta^{13}C_{\Delta CO2}$ of the net CO_2 flux from surface chamber data. Predicted surface CO_2 fluxes decreased from 0.07 to −0.18 µmol m^{-2} s^{-1}. However, the negative predicted flux at 22:30 h is spurious, as the high CO_2 concentration in the boundary layer, as measured by the 0 cm sampling tube (Figure 4.4B), means that the concentration gradient into the soil is negative, yet there is a positive CO_2 concentration gradient between the boundary layer and the turbulent atmosphere above. This

situation probably arises from CO_2 production at a shallow soil depth, which is unable to be resolved by the sampling strategy employed. The change in CO_2 concentration and $\delta^{13}C_{CO2}$ gradients acted to switch surface fluxes from a relatively depleted predicted efflux (−19.6‰) at 18:30 h to a more depleted predicted influx (−24.5‰) at 22:30 h, although the high CO_2 concentration at 0 cm depth at 22:30 h means that this value is unreliable. Soil temperature at 5 cm depth decreased, at times at close to its maximum negative rate, whereas soil temperature at 15 cm depth gradually decreased from its daily maximum. The soil temperature trends observed during this period were similar to those that occurred between 18:30 and 22:30 h on Day 1. Subsurface CO_2 concentration and $\delta^{13}C_{CO2}$ profiles were also similar, although predicted surface CO_2 flux rates were substantially greater on Day 1 than Day 2.

22:30 – 02:30 h

During this period, the soil gained CO_2 at its maximum rate of 0.05 µmol m^{-2} s^{-1}. Subsurface CO_2 concentrations increased significantly throughout the profile, with a maximum increase from 420 to 700 µL L^{-1} at 15 cm depth. Significant depletions in subsurface $\delta^{13}C_{CO2}$ values accompanied the increases in CO_2 concentration; the maximum depletion in $\delta^{13}C_{CO2}$ was at 15 cm depth, shifting from −9.2 to −13.7‰. The profile average CO_2 concentration (560 µL L^{-1}) and $\delta^{13}C_{CO2}$ (−12.6‰) at 02:30 h were the highest and most depleted, respectively, recorded throughout the 48-h sampling period. However, surface CO_2 fluxes were again not significant, thus the $\delta^{13}C_{\Delta CO2}$ of the net CO_2 flux could not be calculated from surface chamber data. The predicted surface flux was 0.24 µmol m^{-2} s^{-1} at 02:30 h, and changes in the CO_2 concentration and $\delta^{13}C_{CO2}$ gradients drove a relatively depleted predicted efflux (−20.9‰) at this time. Soil temperatures at 5 and 15 cm depth continued to decrease; the rate of change in soil temperature at 15 cm depth was close to its maximum negative rate. The significant increase in subsurface CO_2 concentrations and depletion in $\delta^{13}C_{CO2}$ was considerably greater than that which occurred during the 22:30 to 02:30 h interval on Day 1, despite soil temperatures at 5 and 15 cm depth being similar on both days.

02:30 – 06:30 h

Over this interval, the subsoil lost CO_2 at its maximum rate of −0.07 µmol m^{-2} s^{-1} as CO_2 concentrations decreased from their maximum to their minimum. By 06:30 h, subsurface CO_2 concentrations were less than that of atmospheric CO_2 concentration throughout the profile, with the greatest decrease from 700 to 350 µL L^{-1} at 15 cm depth. Subsurface $\delta^{13}C_{CO2}$ values became significantly more enriched throughout the profile, with the maximum enrichment in $\delta^{13}C_{CO2}$ (up to 5.1‰) occurring between 15 and 20 cm depth. At 06:30 h, one significant positive flux and one significant negative flux were measured, suggesting that surface CO_2 fluxes were spatially variable at this time (note that Figure 5.4 shows the average significant flux), although the surface flux predicted from the CO_2 concentration gradient at 06:30 h was −0.04 µmol m^{-2} s^{-1}. The $\delta^{13}C_{\Delta CO2}$ of the net CO_2

gained in the surface chamber with the significant positive flux (0.07 µmol m^{-2} s^{-1}) was −6.6‰, whereas the $\delta^{13}C_{\Delta CO2}$ of the net CO_2 lost in the surface chamber with the significant negative flux (−0.03 µmol m^{-2} s^{-1}) was 5.2‰. The significant changes in CO_2 concentration and $\delta^{13}C_{CO2}$ throughout the profile resulted in a relatively heavy predicted influx of CO_2 (−8.0‰). Soil temperatures at both 5 and 15 cm depth decreased during this interval, with the latter decreasing at its maximum negative rate. The dramatic changes in subsurface CO_2 concentration and $\delta^{13}C_{CO2}$ profiles were similar to those observed during the 02:30 to 06:30 h interval on Day 1, although the changes during this interval were considerably greater. Changes in soil temperature during the 02:30 to 06:30 h intervals on both Days 1 and 2 were almost identical at 15 cm depth, but soil temperature at 5 cm depth decreased from 2.2 to −0.6°C on Day 2, as opposed to remaining relatively constant around 1.5°C on Day 1.

06:30 – 10:30 h

From 06:30 h to the final sampling at 10:30 h, the soil returned to net accumulation of CO_2. Subsurface CO_2 concentration increased throughout the profile, and by 10:30 h, CO_2 concentrations were greater than that of atmospheric CO_2 concentration in the upper 10 cm of the profile. Despite the increase in subsurface CO_2 concentrations, $\delta^{13}C_{CO2}$ values did not change significantly. Significant surface CO_2 fluxes were recorded in all four surface chambers, averaging 0.04 µmol m^{-2} s^{-1}. This was similar to the predicted surface CO_2 flux rate at 10:30 h (0.06 µmol m^{-2} s^{-1}). The average $\delta^{13}C_{\Delta CO2}$ of the net CO_2 flux in the surface chambers was −13.0‰; this was identical to that predicted based on CO_2 concentration and $\delta^{13}C_{CO2}$ gradients at 10:30 h. Soil temperature at 5 cm depth decreased to its daily minimum early in the interval, before increasing at its maximum rate. Soil temperature at 15 cm depth decreased, reaching its daily minimum in the second half of the interval. The increase in subsurface CO_2 concentrations, significant positive surface CO_2 flux rates and relatively enriched $\delta^{13}C_{\Delta CO2}$ of the surface flux, along with changes in soil temperature observed over this period were similar to those that occurred during the 06:30 to 10:30 h interval on Day 1.

Chapter 6

Synthesis and Summary

6.1 Introduction

The Dry Valleys of Antarctica are home to life at the limit, where the terrestrial environment is characterised by short summers, long dark winters, and extremes in temperature and wind. Precipitation is extremely limited, and moisture availability is controlled by temperature, which dictates availability of meltwater from glaciers and snow patches, as well as melting of ice-cemented permafrost, during short periods in the austral summer when temperatures are above freezing. Despite the generally high salinity and low levels of C, N and moisture in Dry Valley soils, biological communities are widely distributed throughout the landscape. However, biological activity tends to be concentrated in "hotspots" where nutrients are adequate, salinities are relatively low, and temperatures during the austral summer are sufficiently warm to sustain liquid water.

There remains considerable interest in understanding the structure and function of the communities that survive within the harsh Dry Valleys environment. As well as allowing fundamental questions of life at the limit to be addressed, which is of great interest for astrobiology, the resilient communities inhabiting Dry Valley terrestrial ecosystems, where there are no vascular plants, allow for trophic interactions to be examined in a low-complexity system (Hogg et al., 2006). Whilst early research concluded that biological diversity was low, modern sequencing techniques have shown that the distribution and diversity of organisms inhabiting the Dry Valleys is considerable, with abiotic factors exerting the dominant control on community structure and function (Lee et al., 2012; Stomeo et al., 2012; Van Horn et al., 2013).

One major focus of Dry Valley terrestrial ecosystem research has been identifying the sources of C that sustain these communities. Two models, which are not necessarily mutually exclusive, have been proposed. The first to be suggested was a "legacy" model, whereby ecosystems are primarily sustained by lacustrine-derived organic C inherited from primary production within large paleolakes (Burkins et al., 2000). An alternate explanation, the "spatial subsidy" hypothesis, proposes that contemporary, wind dispersed lacustrine-derived organic C is sufficient to sustain modern ecosystem activity (Elberling et al., 2006). However, this model may be of limited applicability to the broader Dry Valleys region, as it requires a relatively high source (primary production zone – i.e. lakes) to sink (area which is devoid of primary productivity zones) ratio, which is uncommon.

Support for both hypotheses has come from studies investigating soil respiration rates and C turnover times (Burkins et al., 2001; Barrett et al., 2005, 2006a; Elberling et al., 2006), as well as studies using C and N isotopes to define the provenance of the source organic materials (Burkins et al., 2000; Hopkins et al., 2009). Previous studies of *in situ* soil respiration rates have implicitly assumed that surface CO_2 fluxes are representative of CO_2 production within soils. This requires steady-state conditions, which, until now, have not been tested, despite several studies showing that surface CO_2 flux rates are highly variable (Parsons et al., 2004; Ball et al., 2009). The diel variability in surface CO_2 flux rates, documented by Parsons et al. (2004) and Ball et al. (2009), extended to negative CO_2 fluxes during parts of the day. As no biological explanation can be invoked to explain the CO_2 influxes, Parsons et al. (2004) and Ball et al. (2009) suggested that there was an abiotic component to the fluxes that could be explained by dissolution and exsolution of CO_2 in accordance with Henry's Law.

This current study aimed to test the hypothesis of abiotic CO_2 dissolution and exsolution using stable C isotope signatures to determine what contribution abiotic processes can make to surface CO_2 fluxes in Dry Valley soils.

6.2 Key findings

This study focused on two sites with contrasting soil organic C contents in eastern Taylor Valley. Soils at both sites were coarse textured, formed in glacial drift, and classified as Typic Haploturbels. Site A was located near a small lake, and can be considered a "biological hotspot", with the lake providing a contemporary organic C source via algal growth during summer months. Subsequent wind dispersal of algae accumulated on the lake shore is inferred to provide a local source of organic C to nearby soils. Interestingly, as well as the $\delta^{13}C$ values of soil organic C at Site A being typical of a lacustrine-derived source, C isotopic signatures characteristic of endolithically-derived organic matter (Burkins et al., 2000; Hopkins et al., 2009) were evident between 5 and 15 cm depth (Chapter 3, Figure 3.8). In contrast, Site B was distal from any contemporary lacustrine inputs, thus limiting the source of organic C to local inputs via spalling of rock containing endolithic communities (Mergelov et al., 2012), and "legacy" C from large paleolakes that existed during the Last Glacial Maximum. Alternatively, it could be argued that Site B receives inputs of organic C via spatial subsidies, although this is unlikely considering the small source-to-sink ratio in Taylor Valley. The only substantial contemporary sources of organic C in Taylor Valley are from moats around Lakes Bonney, Hoare, and Fryxell, as well as smaller lakes such as at Site A, and other ephemeral ponds and streams (Moorhead, 2007); these zones of productivity represent only a small proportion of the total landscape. Furthermore, variation in the isotopic signature of soil organic C with elevation in Taylor

Valley suggests limited transport of organic C in the landscape (Burkins et al., 2000). The $\delta^{13}C$ profile of soil organic C at Site B implies that endolithically-derived C overlies low levels of lacustrine-derived organic matter (Chapter 3, Figure 3.8).

Chapter 3 aimed to verify the observations of Parsons et al. (2004) and Ball et al. (2009) by examining subsurface CO_2 concentration and $\delta^{13}C_{CO2}$ profiles measured during the 2008/09 austral summer. Concentration profiles measured at the warmest and coolest times of the day were consistent with positive and negative surface CO_2 fluxes, respectively. A physical model, capturing the temperature-driven dissolution and exsolution of CO_2, which utilised empirical data (soil moisture content, pH, and temperature changes measured in the field), provided an adequate explanation of the observed subsoil CO_2 dynamics. The model assumed equilibrium partitioning of dissolved inorganic C species and a closed system with respect to CO_2 fluxes, and this study, like previous studies of soil respiration, was predicated on the assumption that the maximum rate of CO_2 production occurred during the warmest part of the day. A two-component mixing model, based on the assumption that the $\delta^{13}C_{CO2}$ of biologically-produced CO_2 was the same as the $\delta^{13}C$ of the source organic C, and a range of assumptions as to the $\delta^{13}C_{CO2}$ of abiotically-produced CO_2, constrained the biological contribution to subsurface CO_2 production (between 5 and 15 cm depth) at Site A to < 25%.

The results from the first study (Chapter 3), based on a twice-daily sampling regime, did not resolve diel changes or rates of change in surface CO_2 fluxes and subsurface CO_2 concentration and $\delta^{13}C_{CO2}$ profiles. Furthermore, it was not known if steady-state phases occurred, from which the rate of soil CO_2 production could be estimated from surface CO_2 flux rates. These questions formed the basis for the sampling strategy implemented during the second (2009/10 austral summer) field season.

During the 2009/10 austral summer, a 48-h time-series of surface CO_2 fluxes and subsurface CO_2 concentration and $\delta^{13}C_{CO2}$ profiles was measured at 4-hourly intervals at Site B (Chapter 4). The surface CO_2 flux rates and subsurface CO_2 concentration and $\delta^{13}C_{CO2}$ profiles measured at the warmest and coolest times of the day were consistent with measurements made in the previous season. However, the increased sampling frequency revealed the dynamic behaviour of subsurface CO_2 concentration and $\delta^{13}C_{CO2}$ as soil temperatures varied throughout the diel cycle. The subsurface CO_2 concentration gradients were consistent with the direction of the surface CO_2 flux, with positive and negative concentration gradients driving positive and negative surface CO_2 fluxes, respectively. Changes in surface CO_2 flux rates and subsurface CO_2 storage flux rates were statistically significantly related to the rate of change in subsurface soil temperature. These results support Henry's Law-controlled CO_2 exsolution and dissolution driving production and consumption of CO_2, respectively. In addition, the ^{13}C isotopic composition of the net surface CO_2 fluxes ($\delta^{13}C_{\Delta CO2}$) could be reliably predicted from subsurface CO_2 concentration and $\delta^{13}C_{CO2}$ gradients, confirming that the approach

used for calculating the $\delta^{13}C_{\Delta CO2}$ of measured surface fluxes was appropriate. Keeling plots could not be used because of the small changes in CO_2 concentration in the chambers over the 45 min sampling interval. The relationship between surface CO_2 flux rate and near-surface CO_2 concentration gradients also allowed an effective diffusivity to be calculated.

The variability in subsurface CO_2 concentration and $\delta^{13}C_{CO2}$ profiles demonstrated that CO_2 production was characteristically non-steady. Over the 48-h sampling period, CO_2 concentration and $\delta^{13}C_{CO2}$ profiles varied symmetrically about ambient atmospheric CO_2 concentration and $\delta^{13}C_{CO2}$ (Chapter 4, Figure 4.4). The non-steady conditions induced dynamic fractionation, which resulted in highly depleted surface CO_2 fluxes (as low as ~ −30‰) that could not be attributed to heterotrophic respiration from organisms utilising a highly depleted organic C source. Where short periods (4 h) of steady-state efflux were identified, they showed CO_2 production (exsolution) of relatively enriched CO_2 (−5.2‰); periods of steady-state influx showed consumption (dissolution) of lighter CO_2 (−11.4‰). This pattern is consistent with the kinetic fractionation expected as a result of preferential exsolution of $^{13}CO_2$ and preferential dissolution of $^{12}CO_2$ in the $CO_{2\ (g)} – CO_{2\ (dissolved)}$ system. Despite the relatively low surface CO_2 flux rates measured at Site B, the magnitude of surface fluxes was large relative to subsurface storage CO_2 fluxes. This finding confirmed that the closed system assumption used in Chapter 3 was an over-simplification, which most significantly affected comparisons between measured and simulated ratios of subsurface CO_2 concentration in the near-surface zone (0–5 cm), as speculated in Chapter 3. Together, the results of Chapter 4 confirm that at Site B, with low levels of soil organic C and no significant contemporary source of organic C, there was no detectable biological contribution to CO_2 production.

Chapter 5 presents the same suite of data as at Site B, measured concurrently and at the same frequency so as to provide insights into CO_2 dynamics at a contrasting biological “hotspot” (Site A). The aim of this chapter was to test the generality of the findings at Site B at a site with a contemporary organic C supply, which can be considered a “biological hotspot” (Site A). As at Site B, the CO_2 concentration and $\delta^{13}C_{CO2}$ profiles measured at the warmest and coolest times of the day were similar to those measured during the previous season. However, the increased temporal resolution of subsurface CO_2 concentration and $\delta^{13}C_{CO2}$ profiles revealed contrasting behaviour to that at Site B. At 06:30, 10:30 and 14:30 h, the CO_2 concentration and $\delta^{13}C_{CO2}$ profiles resembled those at Site B. However, at 18:30, 22:30 and 02:30 h, CO_2 concentrations were well above those measured at Site B, reaching a maximum at 02:30 h; the most depleted $\delta^{13}C_{CO2}$ values were also measured at this time. The high CO_2 concentrations and relatively depleted $\delta^{13}C_{CO2}$ values imply biological production of CO_2, despite occurring at a time when the soil was cooling, although soil temperatures remained above freezing. Consequently, it is suggested that the high CO_2 concentration and associated depletion in $\delta^{13}C_{CO2}$ was a result of cooling-induced condensation,

providing soil biota with liquid water, or at least high humidity, sufficient to stimulate their activity. This inference suggests that the assumption that the maximum rate of CO_2 production occurs during the warmest part of the day, as used in Chapter 3 and in previous studies of Dry Valley soil respiration, is not appropriate for all sites.

Surface CO_2 flux rates at Site A could not be reliably calculated, as CO_2 concentrations varied non-systematically throughout the 45-min chamber sampling periods. Consequently, subsurface CO_2 concentration gradients, together with a value for effective diffusivity of CO_2 derived from Site B, were used to estimate surface CO_2 flux rates. The $\delta^{13}C_{\Delta CO2}$ of surface CO_2 fluxes was predicted from CO_2 concentration and $\delta^{13}C_{CO2}$ gradients, but despite often being similar to the $\delta^{13}C$ of the soil organic C, the non-steady CO_2 dynamics (and resulting dynamic fractionation) limit the interpretations that can be made as to the biological contribution to the flux to semi-quantitative estimates. Nonetheless, the changes in subsurface CO_2 concentration and $\delta^{13}C_{CO2}$ profiles are consistent with the inference that heterotrophic respiration is an important, and at times, dominant component of subsurface CO_2 production and surface CO_2 fluxes at Site A. The CO_2 dynamics at this site are likely to be representative of "biological hotspots" in the Dry Valleys, where organic C and liquid water are less limiting than in other parts of the landscape.

6.3 Implications of research findings

The diel variability in surface CO_2 flux rates and subsurface CO_2 concentration and $\delta^{13}C_{CO2}$ profiles has important implications for the interpretation of Dry Valley soil CO_2 flux measurements. The results presented in this study are particularly relevant to studies investigating ecosystem activity and response to environmental change, and C turnover times in the Dry Valleys, as well as CO_2 flux studies in other deserts (e.g. Ma et al., 2013; Brummell et al., 2014).

Previous studies of Dry Valley soil CO_2 fluxes have not considered surface and subsurface CO_2 dynamics in such detail, and have based their interpretations of surface CO_2 flux rates on the following two assumptions: 1) that maximum surface CO_2 flux rates occur at the warmest times of the day and represent the maximum rate of soil CO_2 production, and 2) that surface CO_2 fluxes are representative of CO_2 production within the soil (i.e. the system is in steady-state). This study has demonstrated that these two assumptions do not hold for all sites, hence new approaches to characterisation of Dry Valley soil CO_2 fluxes are necessary.

6.3.1 Comparisons of Dry Valley ecosystem activity

The misinterpretation of surface CO_2 flux rates as representing the rate of CO_2 production within the soil is problematic for studies comparing the timing and magnitude of ecosystem activity between sites. Firstly, the results presented in this study have demonstrated that Dry Valley CO_2 dynamics are characteristically non-steady. Therefore, the surface CO_2 flux is not representative of soil CO_2 production at the time of measurement. Characteristic response times (t) for diffusive systems are related to length scales (L) and diffusivity (D) by $t = L^2/D$ (Anderson and Anderson, 2010). For the effective diffusivity of the coarse-textured soils studied (0.03 $cm^2\ s^{-1}$), perturbations in CO_2 production at 15 cm depth would take ~2 h to affect surface fluxes. Therefore, periods of steady-state production that persist for up to 2 h are probably necessary to yield steady surface CO_2 flux rates. This appears to occur in soils where biological CO_2 production is low (Site B), but CO_2 dynamics in soils where biological CO_2 production is relatively high (Site A) are characterised by high spatial and temporal variability in subsurface CO_2 production, hence steady-state is rarely observed. Secondly, site-specific differences in the timing of maximum CO_2 production are likely to be regulated by local soil temperature and moisture availability, as well as the functionality of the biological community present. This means that local site conditions must be carefully monitored to ensure comparability between datasets. Finally, this study shows that surface CO_2 flux rates alone do not provide an indication as to the relative proportions of biotic and abiotic contributions to the flux. Consequently, comparisons between ecosystem activity based on surface CO_2 flux rates may be misleading.

6.3.2 Carbon turnover times

Estimates of C turnover times are contingent on reliable measures of heterotrophic soil respiration. The caveats discussed above suggest that existing estimates of C turnover times may be erroneous. At sites where there is a substantial abiotic component to the flux, turnover times calculated on the basis that soil CO_2 fluxes represent biological CO_2 production will be underestimates. Any abiotic component to the flux means that C utilisation rates will be less than previously assumed, hence C pools will have a longer turnover time. Alternatively, at sites with high biological activity, turnover times could be underestimates if the surface CO_2 flux rates on which they are based did not capture flux rates at the time of maximum CO_2 production. This has implications for the legacy and spatial subsidy models of C supply. Current estimates of C turnover time, based on *in situ* CO_2 flux rates, range from 23 to 130 years (Burkins et al., 2001; Elberling et al., 2006), which is incompatible with the legacy model. However, it has been suggested that there may be at least 2 pools of organic C involved in Dry Valley C cycling: a small, labile organic C pool which is sustained via *in situ* autotrophic productivity, and a larger, more recalcitrant organic C pool derived from ancient glacial and lake sediments (Burkins et al., 2001; Barrett et al., 2005). Regardless of the organic C pools involved, if soil

CO_2 flux rates used in calculations of C turnover times are overestimates, then current ecosystem activity may in fact be able to be sustained by legacy C.

6.3.3 Field and laboratory manipulations

The results presented in this study can also be used to inform laboratory studies that utilise Dry Valley soils. As with temperate soils, laboratory studies of Dry Valley soil microbial activity also show a greater respiratory response to increased soil temperatures (Elberling et al., 2006; Hopkins et al., 2006). However, most of these studies also increased moisture content and provided additions of C and N (Hopkins et al., 2006; Hopkins et al., 2008; Sparrow et al., 2011), thereby providing favourable conditions for biological activity. No studies have attempted to simulate the diel temperature variability that characterises field conditions, instead maintaining a relatively high but stable temperature equivalent to the maximum summertime soil temperature (Hopkins et al., 2006; Hopkins et al., 2008; Sparrow et al., 2011). Without temperature variability, there is no mechanism for abiotic CO_2 production, and thus on the basis of increased respiration rates under consistently warm temperatures (and following substrate addition), these studies have concluded that soil CO_2 production is of biological origin. However, without a genuine simulation of field conditions, results from subsidy experiments do not provide sufficient evidence to preclude abiotic CO_2 production under field conditions. Similarly, laboratory decomposition studies that show $\delta^{13}C$ values of emitted CO_2 are similar to the $\delta^{13}C$ values of source organic materials (Hopkins et al., 2009) simply confirm the inference of a biological response to increased temperature and substrate addition. Again, this would be expected in a laboratory environment, but it cannot be used to infer that biological processes dominate CO_2 production in the field. As steady-state (with respect to temperature) laboratory experiments cannot simulate the range of processes occurring in the field, such studies will generally eliminate abiotic processes. Consequently, conclusions from studies conducted at a constant temperature must be re-evaluated before being assumed to fully describe CO_2 dynamics in the field.

Field manipulations such as those incorporating substrate additions, and artificially increasing soil temperature and moisture content, will also benefit from insight gained through this study. In particular, the timing and frequency of soil CO_2 flux measurements is critical, and may significantly influence the interpretations made. Further insight could be readily gained from studies such as Barrett et al.'s (2008a) tracer study, which used a ^{13}C-labelled sugar to track heterotrophic CO_2 production from nematodes. If the measured surface CO_2 fluxes (from which the nematode contribution to surface fluxes was calculated) included an abiotic component, then the contribution to biological respiration by nematodes could be significantly more than the ~7% calculated.

6.4 Future research

This study is the first study that has attempted to characterise subsurface soil CO_2 dynamics in the Dry Valleys. The data presented in this thesis therefore represent a first attempt at quantifying the biotic and abiotic contributions to surface CO_2 fluxes at two sites that represent two of the major soil ecosystems in the Dry Valleys region. As a result of its exploratory nature, this study has led to various questions that must yet be addressed in order to develop a better understanding of Dry Valley soil C cycling, which will subsequently contribute to knowledge used in predicting the implications of changing environmental conditions on soil C dynamics throughout the Dry Valleys.

6.4.1 Laboratory studies

Firstly, and arguably most importantly, the $\delta^{13}C_{CO2}$ of abiotically-produced CO_2 must be empirically derived. This will remove the need for imprecisely-constrained or assumed values of $\delta^{13}C_{CO2\text{-}abiotic}$ in mixing model calculations. This value can be obtained by sampling soil CO_2 from cores within "Dry Valley simulators", which, as the name suggests, can simulate the diel temperature variability experienced in Dry Valley soils. As fractionation during exsolution of CO_2 is kinetically-driven, experiments that replicate rates of soil temperature change at different soil depths or at different times of the year would be informative.

Metagenomic studies of the biological communities at different depths at Sites A and B will also enable questions about community structure and function to be addressed; subsequent studies in a controlled environment in which abiotic factors are varied will facilitate a better understanding of the controls on the biological community function at each site. As most studies of Dry Valley soil biological communities focus on samples from the top 10 cm of the profile, characterisation of the communities present between 10 and 20 cm depth may reveal unexpected differences in community structure. This is of particular relevance at Site A, as biological CO_2 production appears to be greatest between 10 and 20 cm depth at cooler times of the day.

6.4.2 Numerical modelling studies

Modelling studies have not been incorporated into this study as several key parameters (the $\delta^{13}C_{CO2}$ of abiotically-produced CO_2, and the rates of biotic and abiotic CO_2 production) needed to inform realistic simulations have not yet been quantified. However, once these parameters are obtained, much insight into soil CO_2 dynamics under differing soil physical and chemical conditions could be gained from modelling studies.

Physical models (based on field data), such as those developed by Nickerson and Risk (2009c) to test lag responses and dynamic fractionation effects resulting from changes in the rate and isotopic

composition of soil CO_2 production throughout diel cycles, would aid the interpretation of field-derived surface CO_2 flux measurements. Coupling Nickerson and Risk's (2009c) and Risk and Kellman's (2008) models that incorporate the diffusivity of the individual $^{12}CO_2$ and $^{13}CO_2$ isotopologues with physicochemical models such as those used in Chapter 3 (and also by Ma et al. (2013)) to describe the effects of temperature change on CO_2 dissolution and exsolution would provide a powerful means for predicting the rate and isotopic composition of abiotic CO_2 production in desert ecosystems. Temperature variation could easily be driven by mechanistic models simulating heat transport within the soil profile; the models could be parameterised by data from this study.

6.4.3 Field soil CO_2 flux experimental design

The data presented in this study highlight the need for high-resolution measurements of both surface CO_2 fluxes and subsurface CO_2 concentration gradients. However, this study has demonstrated that static chambers are not a reliable method for determining surface CO_2 flux rates at biological hotspots. Automated infra-red gas analysers, which have been used in previous studies of Dry Valley soil CO_2 flux rates (and can be adapted so as to provide greater sensitivity to the low flux rates typical of Dry Valley soils (e.g. Parsons et al., 2004; Ball et al., 2009)), can determine surface CO_2 flux rates over considerably shorter measurement periods (up to 200 s; Parsons et al., 2004; Elberling et al., 2006). A shorter measurement period would likely remove some of the high-frequency temporal variability measured in static chambers at Site A, and the automated sampling mechanism would enable a greater number of measurements to be made, thus providing a better opportunity to assess fine-to-medium scale spatial variability.

However, measurements of surface CO_2 flux rates alone, regardless of whether they coincide with a period of steady-state subsurface CO_2 concentrations, cannot provide any estimate as to the relative contributions from biotic and abiotic sources. In the absence of C isotopic data, a surface CO_2 flux rate measured during a period of steady-state only represents the net rate of soil CO_2 production, which may comprise biotic and abiotic components. It is only when the $\delta^{13}C_{\Delta CO2}$ of the net flux and the $\delta^{13}C_{CO2}$ of the biotic and abiotic components of that flux are known that the contributions of each component can be quantified.

Soil CO_2 fluxes as a biometric of change

Soil CO_2 fluxes have considerable potential as a biometric that can be used to identify changes in Dry Valley ecosystems. However, in order to provide a valuable, quantitative metric of change, surface CO_2 fluxes must be able to be partitioned into their biotic and abiotic components. At the very least, this requires detailed measurements of subsurface CO_2 concentration and $\delta^{13}C_{CO2}$ which are currently not easily obtained. However, development of promising new technology such as the Iso-FD (Nickerson et al., 2013) should enable this to be achieved, with carefully managed automated

sensors able to provide considerable insight into soil CO_2 flux dynamics beyond the short austral summer field season. In particular, records over well-defined timescales (24-h, weekly, monthly, seasonal and annual) will enable integration of the cyclical abiotic effects, thus, in the absence of any long-term low-level continuous abiotic flux (e.g. geological; Risk et al., 2013), revealing any net biological effect. It is only once the biotic and abiotic contributions are constrained that soil CO_2 fluxes will provide a valuable long-term record of, and tool for predicting ecosystem response to, future environmental change.

References

Adams, B.J., Bardgett, R.D., Ayres, E., Wall, D.H., Aislabie, J., Bamforth, S., Bargagli, R., Cary, C., Cavacini, P., Connell, L., Convey, P., Fell, J.W., Frati, F., Hogg, I.D., Newsham, K.K., O'Donnell, A., Russell, N., Seppelt, R.D., Stevens, M.I., 2006. Diversity and distribution of Victoria Land biota. Soil Biology & Biochemistry, 38, 3003-3018.

Amundson, R., Stern, L., Baisden, T., Wang, Y., 1998. The isotopic composition of soil and soil-respired CO_2. Geoderma, 82, 83-114.

Anderson, R.S., Anderson, S.P., 2010. Geomorphology; the mechanics and chemistry of landscapes. Cambridge University Press, Cambridge, 637 pp.

Ball, B.A., Virginia, R.A., Barrett, J.E., Parsons, A.N., Wall, D.H., 2009. Interactions between physical and biotic factors influence CO_2 flux in Antarctic dry valley soils. Soil Biology & Biochemistry, 41, 1510-1517.

Ball, B.A., Barrett, J.E., Gooseff, M.N., Virginia, R.A., Wall, D.H., 2011. Implications of meltwater pulse events for soil biology and biogeochemical cycling in a polar desert. Polar Research, 30, 14555. doi:10.3402/polar.v30i0.14555

Bao, H., Marchant, D.R., 2006. Quantifying sulfate components and their variations in soils of the McMurdo Dry Valleys, Antarctica. Journal of Geophysical Research, 111, D16301.

Bao, H., Barnes, J.D., Sharp, Z.D., Marchant, D.R., 2008. Two chloride sources in soils of the McMurdo Dry Valleys, Antarctica. Journal of Geophysical Research-Atmospheres, 113. doi:10.1029/2007jd008703

Barrett, J.E., Virginia, R.A., Parsons, A.N., Wall, D.H., 2005. Potential soil organic matter turnover in Taylor Valley, Antarctica. Arctic, Antarctic, and Alpine Research, 37, 108-117.

Barrett, J.E., Virginia, R.A., Parsons, A.N., Wall, D.H., 2006a. Soil carbon turnover in the McMurdo Dry Valleys, Antarctica. Soil Biology & Biochemistry, 38, 3065-3082.

Barrett, J.E., Virginia, R.A., Wall, D.H., Adams, B.J., 2008a. Decline in a dominant invertebrate species contributes to altered carbon cycling in a low-diversity soil ecosystem. Global Change Biology, 14, 1734-1744.

Barrett, J.E., Virginia, R.A., Wall, D.H., Parsons, A.N., Powers, L.E., Burkins, M.B., 2004. Variation in biogeochemistry and soil biodiversity across spatial scales in a polar desert ecosystem. Ecology, 85, 3105-3118.

Barrett, J.E., Virginia, R.A., Wall, D.H., Cary, S.C., Adams, B.J., Hacker, A.L., Aislabie, J.M., 2006b. Co-variation in soil biodiversity and biogeochemistry in northern and southern Victoria Land, Antarctica. Antarctic Science, 18, 535-548. doi:10.1017/s0954102006000587

Barrett, J.E., Virginia, R.A., Wall, D.H., Doran, P.T., Fountain, A.G., Welch, K.A., Lyons, W.B., 2008b. Persistent effects of a discrete warming event on a polar desert ecosystem. Global Change Biology, 14, 1-13. doi:10.1111/j.1365-2486.2008.01641.x

Barrett, J.E., Virginia, R.A., Hopkins, D.W., Aislabie, J., Bargagli, R., Bockheim, J.G., Campbell, I.B., Lyons, W.B., Moorhead, D.L., Nkem, J.N., Sletten, R.S., Steltzer, H., Wall, D.H., Wallenstein, M.D., 2006c. Terrestrial ecosystem processes of Victoria Land, Antarctica. Soil Biology & Biochemistry, 38, 3019-3034.

Barrett, P.J., Froggatt, P.C., 1978. Densities, porosities, and seismic velocities of some rocks from Victoria Land, Antarctica. N.Z. Journal of Geology and Geophysics, 21, 175-187.

Bockheim, J.G., 1980. Properties and classification of some desert soils in coarse-textured glacial drift in the Arctic and Antarctic. Geoderma, 24, 45-69.

Bockheim, J.G., 1990. Soil development rates in the Transantarctic Mountains. Geoderma, 47, 59-77.

Bockheim, J.G., 1997. Properties and classification of cold desert soils from Antarctica. Soil Science Society of America Journal, 61, 224-231.

Bockheim, J.G., 2002. Landform and soil development in the McMurdo Dry Valleys, Antarctica: a regional synthesis. Arctic, Antarctic, and Alpine Research, 34, 308-317.

Bockheim, J.G., 2010. Evolution of desert pavements and the vesicular layer in soils of the Transantarctic Mountains. Geomorphology, 118, 433-443. doi:10.1016/j.geomorph.2010.02.012

Bockheim, J.G., McLeod, M., 2008. Soil distribution in the McMurdo Dry Valleys, Antarctica. Geoderma, 144, 43-49. doi:10.1016/j.geoderma.2007.10.015

Bockheim, J.G., Prentice, M.L., McLeod, M., 2008. Distribution of glacial deposits, soils, and permafrost in Taylor Valley, Antarctica. Arctic, Antarctic, and Alpine Research, 40, 279-286. doi:10.1657/1523-0430(06-057)[bockheim]2.0.co;2

Boström, B., Comstedt, D., Ekblad, A., 2007. Isotope fractionation and ^{13}C enrichment in soil profiles during the decomposition of soil organic matter. Oecologia, 153, 89-98.

Bowling, D.R., Massman, W.J., 2011. Persistent wind-induced enhancement of diffusive CO_2 transport in a mountain forest snowpack. Journal of Geophysical Research, 116, G04006.

Brummell, M.E., Farrell, R.E., Hardy, S.P., Siciliano, S.D., 2014. Greenhouse gas production and consumption in High Arctic deserts. Soil Biology and Biochemistry, 68, 158-165. doi:http://dx.doi.org/10.1016/j.soilbio.2013.09.034

Büdel, B., Bendix, J., Bicker, F.R., Green, T.G.A., 2008. Dewfall as a water source frequently activates the endolithic cyanobacterial communities in the granites of Taylor Valley, Antarctica. Journal of Phycology, 44, 1415-1424.

Burkins, M.B., Virginia, R.A., Wall, D.H., 2001. Organic carbon cycling in Taylor Valley, Antarctica: quantifying soil reservoirs and soil respiration. Global Change Biology, 7, 113-125.

Burkins, M.B., Virginia, R.A., Chamberlain, C.P., Wall, D.H., 2000. Origin and Distribution of Soil Organic Matter in Taylor Valley, Antarctica. Ecology, 81, 2377-2391.

Campbell, I.B., Claridge, G.G.C., 1975. Morphology and age relationships of Antarctic Soils. In: Suggate, R.P., Cresswell, M.M. (Eds.), Quaternary Studies. The Royal Society of New Zealand, Wellington, pp. 83-88.

Campbell, I.B., Claridge, G.G.C., 1982. The influence of moisture on the development of soils of the cold deserts of Antarctica. Geoderma, 28, 221-238.

Campbell, I.B., Claridge, G.G.C., 2006. Permafrost properties, patterns and processes in the Transantarctic Mountains region. Permafrost and Periglacial Processes, 17, 215-232. doi:10.1002/ppp.557

Campbell, I.B., Claridge, G.G.C., Balks, M.R., Campbell, D.I., 1997. Moisture content in soils of the McMurdo Sound and Dry Valley region of Antarctica. In: Lyons, W.B., Howard-Williams, C., Hawes, I. (Eds.), Ecosystem Processes in Antarctic Ice-Free Landscapes. A.A. Balkema, Rotterdam, pp. 61-76.

Campbell, I.B., Claridge, G.G.C., Campbell, D.A., Balks, M.R., 1998. Permafrost properties in the McMurdo Sound−Dry Valley region of Antarctica. In: Lewkowicz, A.G., Allard, M. (Eds.), Proceedings of the Seventh International Conference on Permafrost, 121-126.

Cary, S.C., McDonald, I.R., Barrett, J.E., Cowan, D.A., 2010. On the rocks: the microbiology of Antarctic Dry Valley Soils. Nature Reviews Microbiology, 8, 129-138.

Cerling, T.E., 1984. The stable isotopic composition of modern soil carbonate and its relationship to climate. Earth and Planetary Science Letters, 71, 229-240.

Cerling, T.E., Solomon, D.K., Quade, J., Bowman, J.R., 1991. On the isotopic composition of carbon in soil carbon dioxide. Geochimica et Cosmochimica Acta, 55, 3403-3405.

Claridge, G.G.C., 1965. The clay mineralogy and chemistry of some soils from the Ross Dependency, Antarctica. New Zealand Journal of Geology and Geophysics, 8, 186-220.

Claridge, G.G.C., Campbell, I.B., 1977. The salts in Antarctic soils, their distribution and relationship to soil processes. Soil Science, 123, 377-384.

Clarke, G.K.C., Waddington, E.D., 1991. A three-dimensional theory of wind pumping. Journal of Glaciology, 37, 89-96.

Clow, G.D., McKay, C.P., Simmons, G.M., (Jr.), Wharton, R.A., (Jr.), 1988. Climatological observations and predicted sublimation rates at Lake Hoare, Antarctica. Journal of Climate, 1, 715-728.

Colbeck, S.C., 1989. Air movement in snow due to windpumping. Journal of Glaciology, 35, 209-213.

Conen, F., Smith, K.A., 2000. An explanation of linear increases in gas concentration under closed chambers used to measure gas exchange between soil and the atmosphere. European Journal of Soil Science, 51, 111-117.

Conovitz, P.A., McKnight, D.M., MacDonald, L.H., Fountain, A.G., House, H.R., 1998. Hydrologic processes influencing streamflow variation in Fryxell Basin, Antarctica. In: Priscu, J.C. (Ed.), Ecosystem dynamics in a polar desert: The McMurdo Dry Valleys, Antarctica, vol. 72. American Geophysical Union, Washington, D.C., pp. 93-108.

Craig, H., 1953. The geochemistry of the stable carbon isotopes. Geochimica et Cosmochimica Acta, 3, 53-92.

Creelman, C., Nickerson, N., Risk, D., 2013. Quantifying lateral diffusion error in soil carbon dioxide respiration estimates using numerical modeling. Soil Science Society of America Journal, 77, 699-708. doi:10.2136/sssaj2012.0352

Dana, G.L., Wharton, R.A., (Jr.), Dubayah, R., 1998. Solar radiation in the McMurdo Dry Valleys, Antarctica. In: Priscu, J.C. (Ed.), Ecosystem dynamics in a polar desert: The McMurdo Dry Valleys, Antarctica. American Geophysical Union, Washington, D.C., pp. 39-64.

Davidson, E.A., Savage, K., Verchot, L.V., Navarro, R., 2002. Minimizing artifacts and biases in chamber-based measurements of soil respiration. Agricultural and Forest Meteorology, 113, 21-37.

Denton, G.H., Bockheim, J.G., Wilson, S.C., Stuiver, M., 1989. Late Wisconsin and early Holocene glacial history, inner Ross Embayment, Antarctica. Quaternary Research, 31, 151-182. doi:10.1016/0033-5894(89)90004-5

Doran, P.T., McKay, C.P., Clow, G.D., Dana, G.L., Fountain, A.G., Nylen, T., Lyons, W.B., 2002a. Valley floor climate observations from the McMurdo dry valleys, Antarctica, 1986-2000. Journal of Geophysical Research-Atmospheres, 107

Doran, P.T., McKay, C.P., Fountain, A.G., Nylen, T., McKnight, D.M., Jaros, C., Barrett, J.E., 2008. Hydrologic response to extreme warm and cold summers in the McMurdo Dry Valleys, East Antarctica. Antarctic Science, 20, 499-509. doi:10.1017/s0954102008001272

Doran, P.T., Priscu, J.C., Lyons, W.B., Walsh, J.E., Fountain, A.G., McKnight, D.M., Moorhead, D.L., Virginia, R.A., Wall, D.H., Clow, G.D., Fritsen, C.H., McKay, C.P., Parsons, A.N., 2002b. Antarctic climate cooling and terrestrial ecosystem response. Nature, 415, 517-520.

Dörr, H., Münnich, K.O., 1980. Carbon-14 and carbon-13 in soil CO_2. Radiocarbon, 22, 909-918.

Ekblad, A., Högberg, P., 2000. Analysis of $\delta^{13}C$ of CO_2 distinguishes between microbial respiration of added C_4-sucrose and other soil respiration in a C_3-ecosystem. Plant and Soil, 219, 197-209.

Elberling, B., Gregorich, E.G., Hopkins, D.W., Sparrow, A.D., Novis, P., Greenfield, L.G., 2006. Distribution and dynamics of soil organic matter in an Antarctic dry valley. Soil Biology & Biochemistry, 38, 3095-3106.

Elberling, B., Greenfield, L.G., Gregorich, E.G., Hopkins, D.W., Novis, P., Sparrow, A.D., 2013. Comments on "Abiotic processes dominate CO_2 flux in Antarctic soils" by Shanhun et al. Soil Biology & Biochemistry 53, 99-111 (2012). Soil Biology & Biochemistry, *In Press*. doi:http://dx.doi.org/10.1016/j.soilbio.2013.10.046

Fang, C., Moncrieff, J.B., 1999. A model for soil CO_2 production and transport 1: Model development. Agricultural and Forest Meteorology, 95, 225-236.

Fang, C., Moncrieff, J.B., 2001. The dependence of soil CO_2 efflux on temperature. Soil Biology & Biochemistry, 33, 155-165.

Foley, K.K., 2005. Pedogenic carbonate distribution within glacial till in Taylor Valley, southern Victoria Land, Antarctica, vol. Master of Science. The Ohio State University, pp. 100.

Foley, K.K., Lyons, W.B., Barrett, J.E., Virginia, R.A., 2006. Pedogenic carbonate distribution within glacial till in Taylor Valley, Southern Victoria Land, Antarctica. In: Alonso-Zarza, A.M., Tanner, L.H. (Eds.), Paleoenvironmental Record and Applications of Calcretes and Palustrine Carbonates: Geological Society of America Special Paper 416. Geological Society of America, pp. 89-103.

Fountain, A.G., Nylen, T.H., Monaghan, A., Basagic, H.J., Bromwich, D., 2010. Snow in the McMurdo Dry Valleys, Antarctica. International Journal of Climatology, 30, 633-642. doi:10.1002/joc.1933

Fountain, A.G., Lyons, W.B., Burkins, M.B., Dana, G.L., Doran, P.T., Lewis, K.J., McKnight, D.M., Moorhead, D.L., Parsons, A.N., Priscu, J.C., Wall, D.H., Wharton, R.A., (Jr.), Virginia, R.A., 1999. Physical controls on the Taylor Valley ecosystem, Antarctica. BioScience, 49, 961-971.

Freckman, D.W., Virginia, R.A., 1997. Low-diversity Antarctic soil nematode communities: Distribution and response to disturbance. Ecology, 78, 363-369.

Fry, B., 2006. Stable Isotope Ecology. Springer, New York

Fukuda, H., 1955. Air and vapor movement in soil due to wind gustiness. Soil Science, 79, 249-256.

Gamnitzer, U., Moyes, A.B., Bowling, D.R., Schnyder, H., 2011. Measuring and modelling the isotopic composition of soil respiration: insights from a grassland tracer experiment. Biogeosciences, 8, 1333-1350.

Gregorich, E.G., Hopkins, D.W., Elberling, B., Sparrow, A.D., Novis, P., Greenfield, L.G., Rochette, P., 2006. Emission of CO_2, CH_4 and N_2O from lakeshore soils in an Antarctic dry valley. Soil Biology & Biochemistry, 38, 3120-3129.

Hall, B.L., Denton, G.H., 2000. Radiocarbon Chronology of Ross Sea Drift, Eastern Taylor Valley, Antarctica: Evidence for a Grounded Ice Sheet in the Ross Sea at the Last Glacial Maximum. Geografiska Annaler: Series A, Physical Geography, 82, 305-336. doi:10.1111/j.0435-3676.2000.00127.x

Hall, B.L., Denton, G.H., Hendy, C.H., 2000. Evidence from Taylor Valley for a grounded ice sheet in the Ross Sea, Antarctica. Geografiska Annaler: Series A, Physical Geography, 82, 275-303. doi:10.1111/j.0435-3676.2000.00126.x

Harris, D., Horwath, W.R., van Kessel, C., 2001. Acid fumigation of soils to remove carbonates prior to total organic carbon or carbon-13 isotopic analysis. Soil Science Society of America Journal, 65, 1853-1856.

Healy, R.W., Striegl, R.G., Russell, T.F., Hutchinson, G.L., Livingston, G.P., 1996. Numerical evaluation of static-chamber measurements of soil–atmosphere gas exchange: identification of physical processes. Soil Science Society of America Journal, 60, 740-747.

Hendy, C.H., 2000. Late Quaternary lakes in the McMurdo Sound region of Antarctica. Geografiska Annaler: Series A, Physical Geography, 82, 411-432. doi:10.1111/j.0435-3676.2000.00131.x

Hendy, C.H., Healy, T.R., Rayner, E.M., Shaw, J., Wilson, A.T., 1979. Late Pleistocene glacial chronology of the Taylor Valley, Antarctica, and the global climate. Quaternary Research, 11, 172-184.

Higgins, S., Denton, G.H., Hendy, C.H., 2000a. Glacial Geomorphology of Bonney Drift, Taylor Valley, Antarctica. Geografiska Annaler: Series A, Physical Geography, 82, 365-389. doi:10.1111/j.0435-3676.2000.00129.x

Higgins, S.M., Hendy, C.H., Denton, G.H., 2000b. Geochronology of Bonney Drift, Taylor Valley, Antarctica: Evidence for Interglacial Expansions of Taylor Glacier. Geografiska Annaler: Series A, Physical Geography, 82, 391-409. doi:10.1111/j.0435-3676.2000.00130.x

Hoefs, J., 2009. Stable Isotope Geochemistry. Springer-Verlag, Berlin

Hogg, I.D., Cary, S.C., Convey, P., Newsham, K.K., O'Donnell, A.G., Adams, B.J., Aislabie, J., Frati, F., Stevens, M.I., Wall, D.H., 2006. Biotic interactions in Antarctic terrestrial ecosystems: Are they a factor? Soil Biology & Biochemistry, 38, 3035-3040.

Hopkins, D.W., Sparrow, A.D., Elberling, B., Gregorich, E.G., Novis, P.M., Greenfield, L.G., Tilston, E.L., 2006. Carbon, nitrogen and temperature controls on microbial activity in soils from an Antarctic dry valley. Soil Biology & Biochemistry, 38, 3130-3140.

Hopkins, D.W., Sparrow, A.D., Shillam, L.L., English, L.C., Dennis, P.G., Novis, P., Elberling, B., Gregorich, E.G., Greenfield, L.G., 2008. Enzymatic activities and microbial communities in an Antarctic dry valley soil: Responses to C and N supplementation. Soil Biology & Biochemistry, 40, 2130-2136.

Hopkins, D.W., Sparrow, A.D., Gregorich, E.G., Elberling, B., Novis, P., Fraser, F., Scrimgeour, C., Dennis, P.G., Meier-Augenstein, W., Greenfield, L.G., 2009. Isotopic evidence for the provenance and turnover of organic carbon by soil microorganisms in the Antarctic dry valleys. Environmental Microbiology, 11, 597-608. doi:10.1111/j.1462-2920.2008.01830.x

Keeling, C.D., Piper, S.C., Bacastow, R.B., Wahlen, M., Whorf, T.P., Heimann, M., Meijer, H.A., 2001. Exchanges of atmospheric CO_2 and $^{13}CO_2$ with the terrestrial biosphere and oceans from 1978 to 2000. I. Global aspects, SIO Reference Series, No. 01-06. Scripps Institution of Oceanography, San Diego, pp. 88. http://scrippsco82.ucsd.edu/data/atmospheric_co82.html.

Kendall, C., Caldwell, E.A., 1998. Fundamentals of Isotope Geochemistry. In: Kendall, C., McDonnell, J.J. (Eds.), Isotope Tracers in Catchment Hydrology. Elsevier Science B.V., Amsterdam, pp. 51-86.

Keys, J.R., 1980. Air temperature, wind, precipitation and atmospheric humidity in the McMurdo Region. Department of Geology Publication No. 17, Victoria University of Wellington, Wellington, NZ, 57 pp.

Keys, J.R., Williams, K., 1981. Origin of crystalline, cold desert salts in the McMurdo region, Antarctica. Geochimica Et Cosmochimica Acta, 45, 2299-2309.

Kirschbaum, M.U.F., 1995. The temperature dependence of soil organic matter decomposition, and the effect of global warming on soil organic C storage. Soil Biology & Biochemistry, 27, 753-760.

Knohl, A., Werner, R.A., Geilmann, H., Brand, W.A., 2004. Kel-F^{TM} discs improve storage time of canopy air samples in 10-mL vials for CO_2-$\delta^{13}C$ analysis. Rapid Communications in Mass Spectrometry, 18, 1663-1665.

Lee, C.K., Barbier, B.A., Bottos, E.M., McDonald, I.R., Cary, S.C., 2012. The inter-valley soil comparative survey: the ecology of Dry Valley edaphic microbial communities. The ISME Journal, 6, 1046-1057. doi:10.1038/ismej.2011.170

Levy, J., 2013. How big are the McMurdo Dry Valleys? Estimating ice-free area using Landsat image data. Antarctic Science, 25, 119-120. doi:10.1017/S0954102012000727

Levy, J.S., Fountain, A.G., Gooseff, M.N., Welch, K.A., Lyons, W.B., 2011. Water tracks and permafrost in Taylor Valley, Antarctica: Extensive and shallow groundwater connectivity in a cold desert ecosystem. GSA Bulletin, 123, 2295-2311.

Lloyd, J., Taylor, J.A., 1994. On the temperature dependence of soil respiration. Functional Ecology, 8, 315-323.

Lyons, W.B., Welch, K.A., Carey, A.E., Doran, P.T., Wall, D.H., Virginia, R.A., Fountain, A.G., Csathó, B.M., Tremper, C.M., 2005. Groundwater seeps in Taylor Valley Antarctica: an example of a subsurface melt event. Annals of Glaciology, 40, 200-206.

Ma, J., Wang, Z.Y., Stevenson, B.A., Zheng, X.J., Li, Y., 2013. An inorganic CO_2 diffusion and dissolution process explains negative CO_2 fluxes in saline/alkaline soils. Scientific Reports, 3, 7. doi:10.1038/srep02025

Magalhães, C., Stevens, M.I., Cary, S.C., Ball, B.A., Storey, B.C., Wall, D.H., Türk, R., Ruprecht, U., 2012. At limits of life: Multidisciplinary insights reveal environmental constraints on biotic diversity in continental Antarctica. Plos One, 7, e44578. doi:10.1371/journal.pone.0044578

Marrero, T.R., Mason, E.A., 1972. Gaseous Diffusion Coefficients. Journal of Physical and Chemical Reference Data, 1, 1-118.

Massman, W.J., 2006. Advective transport of CO_2 in permeable media induced by atmospheric pressure fluctuations: 1. An analytical model. Journal of Geophysical Research, 111, G03004.

Massman, W.J., Sommerfeld, R.A., Mosier, A.R., Zeller, K.F., Hehn, T.J., Rochelle, S.G., 1997. A model investigation of turbulence-driven pressure-pumping effects on the rate of diffusion of CO_2, N_2O, and CH_4 through layered snowpacks. Journal of Geophysical Research, 102, 18,851-818,863.

McCarthy, K.A., Johnson, R.L., 1995. Measurement of trichloroethylene diffusion as a function of moisture content in sections of gravity-drained soil columns. Journal of Environmental Quality, 24, 49-55.

McCraw, J.D., 1967. Soils of Taylor Dry Valley, Victoria Land, Antarctica, with notes on soils from other localities in Victoria Land. New Zealand Journal of Geology and Geophysics, 10, 498-539.

McKay, C.P., Mellon, M.T., Friedmann, E.I., 1998. Soil temperatures and stability of ice-cemented ground in the McMurdo Dry Valleys, Antarctica. Antarctic Science, 10, 31-38.

McKnight, D.M., Niyogi, D.K., Alger, A.S., Bomblies, A., Conovitz, P.A., Tate, C.M., 1999. Dry valley streams in Antarctica: Ecosystems waiting for water. Bioscience, 49, 985-995.

Mergelov, N.S., Goryachkin, S.V., Shorkunov, I.G., Zazovskaya, E.P., Cherkinsky, A.E., 2012. Endolithic pedogenesis and rock varnish on massive crystalline rocks in East Antarctica. Eurasian Soil Science, 45, 901-917.

Michalski, G., Bockheim, J.G., Kendall, C., Thiemens, M., 2005. Isotopic composition of Antarctic Dry Valley nitrate: Implications for NO_y sources and cycling in Antarctica. Geophysical Research Letters, 32, L13817.

Midwood, A.J., Millard, P., 2011. Challenges in measuring the $\delta^{13}C$ of the soil surface CO_2 efflux. Rapid Communications in Mass Spectrometry, 25, 232-242. doi:10.1002/rcm.4857

Moldrup, P., Olesen, T., Yoshikawa, S., Komatsu, T., Rolston, D.E., 2004. Three-porosity model for predicting the gas diffusion coefficient in undisturbed soil. Soil Science Society of America Journal, 68, 750-759.

Mook, W.G., Bommerson, J.C., Staverman, W.H., 1974. Carbon isotope fractionation between dissolved bicarbonate and gaseous carbon dioxide. Earth and Planetary Science Letters, 22, 169-176. doi:10.1016/0012-821x(74)90078-8

Mook, W.G. (Ed.). 2000. Environmental isotopes in the hydrological cycle: Principles and applications (Volume 1). Paris: UNESCO.

Moorhead, D.L., 2007. Mesoscale dynamics of ephemeral wetlands in the Antarctic Dry Valleys: Implications to production and distribution of organic matter. Ecosystems, 10, 86-94.

Moorhead, D.L., Barrett, J.E., Virginia, R.A., Wall, D.H., Porazinska, D., 2003. Organic matter and soil biota of upland wetlands in Taylor Valley, Antarctica. Polar Biology, 26, 567-576.

Moyes, A.B., Gaines, S.J., Siegwolf, R.T.W., Bowling, D.R., 2010. Diffusive fractionation complicates isotopic partitioning of autotrophic and heterotrophic sources of soil respiration. Plant, Cell and Environment, 33, 1804-1819.

Nickerson, N., Risk, D., 2009a. A numerical evaluation of chamber methodologies used in measuring the $\delta^{13}C$ of soil respiration. Rapid Communications in Mass Spectrometry, 23, 2802-2810. doi:10.1002/rcm.4189

Nickerson, N., Risk, D., 2009b. Keeling plots are non-linear in non-steady state diffusive environments. Geophysical Research Letters, 36, L08401. doi:10.1029/2008GL036945

Nickerson, N., Risk, D., 2009c. Physical controls on the isotopic composition of soil-respired CO_2. Journal of Geophysical Research, 114, G01013. doi:10.1029/2008JG000766

Nickerson, N., Egan, J., Risk, D., 2013. Iso-FD: A novel method for measuring the isotopic signature of surface flux. Soil Biology & Biochemistry, 62, 99-106.

Nielsen, U.N., Wall, D.H., Adams, B.J., Virginia, R.A., Ball, B.A., Gooseff, M.N., McKnight, D.M., 2012. The ecology of pulse events: insights from an extreme climatic event in a polar desert ecosystem. Ecosphere, 3, Article 17. doi:http://dx.doi.org/10.1890/ES11-00325.1

Nylen, T.H., Fountain, A.G., Doran, P.T., 2004. Climatology of katabatic winds in the McMurdo dry valleys, southern Victoria Land, Antarctica. Journal of Geophysical Research-Atmospheres, 109. doi:10.1029/2003jd003937

O'Leary, M.H., 1981. Carbon isotope fractionation in plants. Phytochemistry, 20, 553-567.

O'Leary, M.H., 1988. Carbon isotopes in photosynthesis. Bioscience, 38, 328-336.

Park, R., Epstein, S., 1960. Carbon isotope fractionation during photosynthesis. Geochimica et Cosmochimica Acta, 21, 110-126.

Parsons, A.N., Barrett, J.E., Wall, D.H., Virginia, R.A., 2004. Soil carbon dioxide flux in Antarctic Dry Valley ecosystems. Ecosystems, 7, 286-295.

Pastor, J., Bockheim, J.G., 1980. Soil development on moraines of Taylor Glacier, lower Taylor Valley, Antarctica. Soil Science Society of America Journal, 44, 341-348.

Poage, M.A., Barrett, J.E., Virginia, R.A., Wall, D.H., 2008. The influence of soil geochemistry on nematode distribution, McMurdo Dry Valleys, Antarctica. Arctic, Antarctic, and Alpine Research, 40, 119-128.

Pumpanen, J., Kolari, P., Ilvesniemi, H., Minkkinen, K., Vesala, T., Niinistö, S., Lohila, A., Larmola, T., Morero, M., Pihlatie, M., Janssens, I., Yuste, J.C., Grünzweig, J.M., Reth, S., Subke, J.-A., Savage, K., Kutsch, W., Østreng, G., Ziegler, W., Anthoni, P., Lindroth, A., Hari, P., 2004. Comparison of different chamber techniques for measuring soil CO_2 efflux. Agricultural and Forest Meteorology, 123, 159-176. doi:10.1016/j.agrformet.2003.12.001

Rayment, M.B., 2000. Closed chamber systems underestimate soil CO_2 efflux. European Journal of Soil Science, 51, 107-110.

Risk, D., Kellman, L., 2008. Isotopic fractionation in non-equilibrium diffusive environments. Geophysical Research Letters, 35, L02403. doi:10.1029/2007/GL032374

Risk, D., Lee, C.K., MacIntyre, C., Cary, S.C., 2013. First year-round record of Antarctic Dry Valley soil CO_2 flux. Soil Biology & Biochemistry, 66, 193-196.

Rochette, P., Bertrand, N., 2003. Soil air sample storage and handling using polypropylene syringes and glass vials. Canadian Journal of Soil Science, 631-637.

Rochette, P., Flanagan, L.B., Gregorich, E.G., 1999. Separating soil respiration into plant and soil components using analyses of the natural abundance of carbon-13. Soil Science Society of America Journal, 63, 1207-1213. doi:10.2136/sssaj1999.6351207x

Smith, J.L., Barrett, J.E., Tusnady, G., Rejto, L., Cary, S.C., 2010. Resolving environmental drivers of microbial community structure in Antarctic soils. Antarctic Science, 22, 673-680. doi:10.1017/s0954102010000763

Sparrow, A.D., Gregorich, E.G., Hopkins, D.W., Novis, P., Elberling, B., Greenfield, L.G., 2011. Resource limitations on soil microbial activity in an Antarctic dry valley. Soil Science Society of America Journal, 75, 2188-2197.

Staff, U.S.S.L., 1954. Diagnosis and Improvement of Saline and Alkali Soils. United States Department of Agriculture, Washington, D.C.

Stomeo, F., Makhalanyane, T.P., Valverde, A., Pointing, S.B., Stevens, M.I., Cary, S.C., Tuffin, M.I., Cowan, D.A., 2012. Abiotic factors influence microbial diversity in permanently cold soil horizons of a maritime-associated Antarctic Dry Valley. FEMS Microbiology Ecology, 82, 326-340.

Stumm, W., Morgan, J.J., 1996. Aquatic chemistry: chemical equilibria and rates in natural waters, 3rd ed. Wiley Interscience, New York

Subke, J.-A., Bahn, M., 2010. On the 'temperature sensitivity' of soil respiration: Can we use the immeasurable to predict the unknown? Soil Biology & Biochemistry, 42, 1653-1656.

Takle, E.S., Massman, W.J., Brandle, J.R., Schmidt, R.A., Zhou, X., Litvina, I.V., Garcia, R., Doyle, G., Rice, C.W., 2004. Influence of high-frequency ambient pressure pumping on carbon dioxide efflux from soil. Agricultural and Forest Meteorology, 124, 193-206.

Thode, H.G., Shima, M., Rees, C.F., Krishnamurty, K.V., 1965. Carbon-13 isotope effects in systems containing carbon dioxide, bicarbonate, carbonate and metal ions. Canadian Journal of Chemistry, 43, 582-595.

Thompson, D.C., Craig, R.M.F., Bromley, A.M., 1971. Climate and surface heat balance in an Antarctic Dry Valley. New Zealand Journal of Science, 14, 245-251.

Toner, J.D., Sletten, R.S., Prentice, M.L., 2013. Soluble salt accumulations in Taylor Valley, Antarctica: Implications for paleolakes and Ross Sea Ice Sheet dynamics. Journal of Geophysical Research: Earth Surface, 118, 198-215. doi:10.1029/2012JF002467

Treonis, A.M., Wall, D.H., 2005. Soil nematodes and desiccation survival in the extreme arid environment of the Antarctic Dry Valleys. Integrative and Comparative Biology, 45, 741-750.

Treonis, A.M., Wall, D.H., Virginia, R.A., 1999. Invertebrate biodiversity in Antarctic dry valley soils and sediments. Ecosystems, 2, 482-492.

Treonis, A.M., Wall, D.H., Virginia, R.A., 2000. The use of anhydrobiosis by soil nematodes in the Antarctic Dry Valleys. Functional Ecology, 14, 460-467. doi:10.1046/j.1365-2435.2000.00442.x

Treonis, A.M., Wall, D.H., Virginia, R.A., 2002. Field and microcosm studies of decomposition and soil biota in a cold desert soil. Ecosystems, 5, 159-170.

Van Horn, D.J., Van Horn, M.L., Barrett, J.E., Gooseff, M.N., Altrichter, A.E., Geyer, K.M., Zeglin, L.H., Takacs-Vesbach, C.D., 2013. Factors Controlling Soil Microbial Biomass and Bacterial Diversity and Community Composition in a Cold Desert Ecosystem: Role of Geographic Scale. Plos One, 8, e66103. doi:10.1371/journal.pone.0066103

Vogel, J.C., Grootes, P.M., Mook, W.G., 1970. Isotope fractionation between gaseous and dissolved carbon dioxide. Zeitschrift für Physik, 230, 225-238.

Wall, D.H., Virginia, R.A., 1999. Controls on soil biodiversity: insights from extreme environments. Applied Soil Ecology, 13, 137-150.

Werth, M., Kuzyakov, Y., 2010. ^{13}C fractionation at the root–microorganisms–soil interface: A review and outlook for partitioning studies. Soil Biology & Biochemistry, 42, 1372-1384.

Wilch, T.I., Denton, G.H., Lux, D.R., McIntosh, W.C., 1993. Limited Pliocene glacier extent and surface uplift in middle Taylor Valley, Antarctica. Geografiska Annaler, 75 A 331-351.

Zhu, B., Cheng, W., 2011. Constant and diurnally-varying temperature regimes lead to different temperature sentivities of soil organic carbon decomposition. Soil Biology & Biochemistry, 43, 866-869.

Appendix A

Publications resulting from this thesis

Soil Biology & Biochemistry 53 (2012) 99–111

Contents lists available at SciVerse ScienceDirect

Soil Biology & Biochemistry

journal homepage: www.elsevier.com/locate/soilbio

Abiotic processes dominate CO_2 fluxes in Antarctic soils

Fiona L. Shanhun*, Peter C. Almond, Tim J. Clough, Carol M.S. Smith

Department of Soil and Physical Sciences, PO Box 84, Lincoln University, Lincoln 7647, New Zealand

ARTICLE INFO

Article history:
Received 20 September 2011
Received in revised form
5 April 2012
Accepted 19 April 2012
Available online 18 May 2012

Keywords:
Soil respiration
$\delta^{13}C_{CO2}$
Organic C
Inorganic C
McMurdo Dry Valleys
Antarctic soils

ABSTRACT

Ecosystems within the McMurdo Dry Valleys of Antarctica are highly sensitive to environmental change. Increases in soil temperature and/or moisture content may dramatically change rates of soil respiration and soil carbon (C) turnover. Present estimates of soil respiration rates and C turnover times are based on surface carbon dioxide (CO_2) fluxes and soil organic C content. However, the assumption that surface CO_2 fluxes are purely biological in origin has not been rigorously tested. We use concentration and, for the first time, the stable C isotopic composition of surface soil CO_2 fluxes and subsurface CO_2 profiles to: 1) examine mechanisms of soil CO_2 uptake and release, 2) identify the location of potential CO_2 sources and sinks within the soil profile, and 3) discriminate between biotic and abiotic contributions to CO_2 fluxes in soils of Taylor Valley. Surface CO_2 fluxes and subsurface CO_2 profiles confirm that these soils take up and release CO_2 on a daily basis (during the austral summer), associated with small changes in soil temperature. Shifts in the C isotopic composition of soil CO_2 are inconsistent with biological mechanisms of CO_2 production and consumption. Instead, the isotopic shifts can be accounted for by Henry's Law dissolution and exsolution of CO_2 into a solution of high pH, driven by changes in soil temperature. Our results constrain the biological component of soil CO_2 fluxes in Taylor Valley to less than 25% (and likely to be significantly less). This finding implies that previous measurements of surface soil CO_2 fluxes are overestimates of soil respiration, thus C turnover times calculated from them are underestimates. Discriminating between biotic and abiotic contributions to CO_2 fluxes in Antarctic dry valley soils is essential if the effects of climate change on these sensitive ecosystems are to be accurately identified.

1. Introduction

Predicting the impact of changes in climate conditions on Antarctic ice-free areas necessitates a detailed understanding of the rates and dynamics of processes operating in these extreme environments. Previous studies of soil respiration in Antarctic ecosystems have been conducted in order to quantify the turnover time of the soil organic carbon (C) pool (Burkins et al., 2001; Barrett et al., 2006a; Elberling et al., 2006), and to provide a basis for comparing ecosystem functioning between sites (Barrett et al., 2006b). Investigations of Antarctic soil respiration rates have also provided insight into the physical controls on soil carbon dioxide (CO_2) flux (Parsons et al., 2004) and the effects of climate variation on C cycling (Ball et al., 2009) in dry valley ecosystems. Surface CO_2 fluxes in the McMurdo Dry Valleys generally range from −0.1 to 0.15 μmol CO_2 m^{-2} s^{-1} (e.g. Burkins et al., 2001; Parsons et al., 2004; Elberling et al., 2006; Ball et al., 2009), although at sites with higher C and moisture contents, rates can be as high as 0.78 μmol CO_2 m^{-2} s^{-1} (Gregorich et al., 2006). Previous studies have generally focused on relating soil respiration rates to environmental variables such as soil temperature and moisture content (Parsons et al., 2004; Elberling et al., 2006; Gregorich et al., 2006) and observing responses to *in situ* (Burkins et al., 2001; Ball et al., 2009) and laboratory manipulations (Burkins et al., 2001; Treonis et al., 2002; Parsons et al., 2004; Barrett et al., 2005, 2006a; Elberling et al., 2006; Hopkins et al., 2006, 2008, 2009).

Studies by Parsons et al. (2004) and Ball et al. (2009) found that soil CO_2 fluxes in the McMurdo Dry Valleys follow diel variations, with soil temperature accounting for almost half of the variation in CO_2 flux (Ball et al., 2009). Both authors conclude that soil CO_2 flux is strongly influenced by abiotic factors, and suggest that dissolution of CO_2 in soil water, consistent with Henry's Law, is the likely explanation for the diel variation observed. This is in contrast to many other ecosystems, where temperature predominantly influences biotic factors.

An abiotic contribution to soil CO_2 flux has potentially profound implications for interpretation of CO_2 fluxes in terms of soil respiration and C cycling in the McMurdo Dry Valleys. Present estimates of turnover times based on *in situ* soil respiration rates are between 23 and 130 years (Burkins et al., 2001; Elberling et al., 2006). Any

* Corresponding author. Tel.: +64 3 321 8246; fax: +64 3 325 3607.
E-mail addresses: fiona.shanhun@lincoln.ac.nz (F.L. Shanhun), peter.almond@lincoln.ac.nz (P.C. Almond), timothy.clough@lincoln.ac.nz (T.J. Clough), carol.smith@lincoln.ac.nz (C.M.S. Smith).

0038-0717/$ – see front matter © 2012 Elsevier Ltd. All rights reserved.
doi:10.1016/j.soilbio.2012.04.027

abiotic contributions to CO_2 fluxes would mean that soil respiration rates overestimate the biological contributions, and turnover times calculated from such fluxes would be underestimates.

In this paper, we present data from a study aimed to advance the mechanistic understanding of the processes governing CO_2 fluxes in Antarctic soils. We use surface soil CO_2 fluxes and subsurface soil CO_2 concentration profiles to characterise diel soil CO_2 dynamics, and identify potential CO_2 sources and sinks within the soil profile. We then test the hypothesis of Ball et al. (2009) and Parsons et al. (2004) by: 1) comparing measured subsurface soil CO_2 concentrations with values simulated by a model that incorporates Henry's Law dissolution of CO_2, and 2) quantifying the biotic and abiotic components of soil CO_2 by utilising the contrasting relationships between concentration and C isotopic composition of soil CO_2 ($\delta^{13}C_{CO_2}$) characteristic of biotic and abiotic processes.

2. Materials and methods

2.1. Study area

The study was conducted during the 2008/09 austral summer at two sites in Taylor Valley, in the McMurdo Dry Valleys, Antarctica. The McMurdo Dry Valleys are the largest ice-free region in Antarctica (~4800 km^2) and comprise a polar desert landscape dominated by coarse-textured soils formed in glacial drift, interspersed with alpine glaciers, ephemeral streams, and perennially ice-covered lakes. Vascular vegetation is absent, and biota consists of microorganisms and a limited number of invertebrate species (Adams et al., 2006; Cary et al., 2010). Mean annual air temperature in Taylor Valley ranges from −14.8 °C to −23.1 °C (Doran et al., 2002), and annual water-equivalent precipitation is <50 mm, with snow transported by katabatic winds supplying up to another 50 mm (water-equivalent) to the valley floor (Fountain et al., 2010).

Site A was on relatively young glacial drift (Ross Sea drift, ~9–28 ka; Hall and Denton, 2000), adjacent to a small lake (~0.05 km^2) situated 700 m east of Howard Glacier (77° 39.572′S, 163° 07.394′E). This site was selected to provide soils with relatively low salt concentrations and higher inputs of organic C. During summer, when a moat forms around the edge of the lake, algae are driven to the lake margins by winds and are eventually blown onshore, providing a local source of organic C. Soils at Site A are weakly developed, strongly cryoturbated, and contain ice-cemented permafrost within 70 cm of the soil surface (Typic Haploturbels; Bockheim et al., 2008). At the time of sampling (late December 2008), soils at Site A were ice-cemented below 35 cm depth. Site B was on an older moraine crest (Taylor III drift, 250–340 ka; Higgins et al., 2000), approximately 1.5 km west of Howard Glacier (77° 39.540′S, 163° 00.484′E). Soils at Site B were expected to have higher salt concentrations due to their age, and lower organic C levels as there was no lake nearby to provide a local source of organic material. Soils formed in Taylor III drift are mapped as Typic Anhyorthels (Bockheim et al., 2008), which by definition should not contain ice-cemented permafrost in the upper 70 cm of the profile. However, soils at Site B had a similar morphology to those at Site A (Typic Haploturbels), and were ice-cemented below 26 cm depth. Both sites were characterised by patterned ground comprised of flat-centred polygons measuring approximately 15 × 15 m.

2.2. Soil temperature and moisture content measurements

Soil temperature and volumetric moisture content at 5, 15 and 25 cm depth were measured using Hydra Probes (Hydra Probe II, Stevens Water Monitoring Systems Inc., Portland, Oregon, USA). An intermittent fault occurred in the probe installed at 5 cm depth at Site A; data from this probe are only available for one of the CO_2 sampling periods. Surface air temperature was measured 2 mm above the soil surface (CS215-L, Campbell Scientific Inc., Logan, Utah, USA). All data were recorded every 2 min, with 20 min averages calculated and logged by a CR 1000 data logger (Campbell Scientific Inc., Logan, Utah, USA).

2.3. Soil CO_2 sampling

Soil CO_2 sampling was replicated in two adjacent polygons at each site. Within each polygon, five opaque tubes (iPLex® Novadrain uPVC access tubes – 15 cm diameter by 16 cm high; iPLEX® DWV 136.150) were pressed into the soil surface to a depth of 6 cm. An opaque uPVC lid (iPLEX® DWV 136C.150) with an internal rubber O-ring, drilled to fit a pressure release bung and an injectable septum (Baxter Interlink Injection Site Ref #2N3399K), was screwed on to the tubes immediately before surface CO_2 flux sampling. This created a chamber with a mean effective headspace of 0.0018 m^3. In order to determine surface soil CO_2 fluxes, 20 ml gas samples were taken from the headspace chambers immediately after the chamber lids were fitted and vented, with three subsequent samples taken at 20 min intervals over a 1 h period. Surface CO_2 fluxes were calculated based on headspace CO_2 concentrations during the 1 h sampling period using the following equation:

$$nCO_2 = [CO_2]\frac{PV}{RTA} \quad (1)$$

where nCO_2 is the number of moles of CO_2 emitted per m^2 (μmol m^{-2}), $[CO_2]$ is headspace CO_2 concentration (μL L^{-1}), P is atmospheric pressure (101325 Pa), V is the chamber volume (m^3), R is the ideal gas constant (8.314 J K^{-1} mol^{-1}), T is air temperature (K), and A is the area covered by the chamber (0.0177 m^2). Surface CO_2 flux rates (μmol m^{-2} s^{-1}) were calculated by linear regression of surface CO_2 fluxes (μmol m^{-2}) against time over which samples were collected (s). Linear regression was also used to determine the rate of change of $\delta^{13}C_{CO_2}$ (‰ min^{-1}) in the headspace chamber samples.

Soil profile CO_2 samples were taken from polyethylene subsurface sampling tubes (Bev-A-Line® Tubing; 0.32 cm ID, 0.64 cm OD) installed adjacent to three of the five headspace chambers in each polygon at depths of 5, 10, 15, 20, and 30 cm (or to the depth of ice-cemented soil). The exposed tube above the soil surface was sealed with an injectable septum (Baxter Interlink Injection Site Ref #2N3399K); the buried base of the subsurface sampling tube was covered with fine polyester mesh to prevent soil particle ingress during CO_2 sampling. Gas samples from each of the subsurface sampling tubes were taken during the surface soil CO_2 flux-sampling period. Residual air within each sampling tube was extracted and discarded before a 20 ml sample was taken.

Soil CO_2 sampling began >96 h after installation of equipment. Gas samples were taken during the warmest and coolest periods of the day, based on surface air temperature measurements at each site, on two days in late December 2008. Site B was only sampled during one "cold" period due to an error in determining the timing of the coldest part of the day. All CO_2 samples were taken using gas-tight syringes (BD 30 ml syringe; Ref 309650) fitted with 3-way stopcocks (Baxter 2C6201) and 26G ½" needles (BD PrecisionGlide). Samples were injected into evacuated (0 atm) 12 ml vials (Exetainers®, Labco Inc., UK) fitted with additional polytetrafluoroethylene (PTFE) septa (Supelco Analytical, USA) to maintain sample integrity (Rochette and Bertrand, 2003; Knohl et al., 2004), and stored in insulated containers prior to transport back to New Zealand. All samples were analysed for CO_2 concentration and $\delta^{13}C_{CO_2}$ using a trace gas module (TGII, Sercon Ltd., Cheshire, UK) connected to a continuous flow isotope ratio mass spectrometer (Sercon Ltd., Cheshire, UK). The $\delta^{13}C$ values are expressed in parts per thousand (‰) enrichment or depletion of ^{13}C, relative to Vienna

Pee Dee Belemnite (VPDB). Soil profile CO_2 samples were analysed at Lincoln University, New Zealand (within 4 months of being collected), and surface CO_2 flux samples at the University of California Davis Stable Isotope Facility, California, USA (within 8 months of being collected). Standard reference gas samples were also collected in the field following surface CO_2 flux and subsurface CO_2 sampling, and were analysed with the samples. The standards showed no sign of storage effects. The analytical precision of CO_2 concentration and $\delta^{13}C$ values was $\leq$5 ppm and $\leq$0.1‰, respectively.

2.4. Soil sampling, physical and chemical analyses

In polygons adjacent to CO_2 sampling sites, soil pits were dug by hand to ice cement, and deepened to a minimum of 55 cm depth using a concrete breaker to penetrate ice-cemented material. Soils were described and classified using USDA nomenclature before being volumetrically sampled (500 cm^3) at 5 cm contiguous intervals to 50 cm depth. All samples were returned to New Zealand where they were air-dried, and weighed to determine bulk density (ρ_b) before being sieved (<2 mm). All chemical analyses were performed in duplicate on the <2 mm fraction.

Soil pH and electrical conductivity were determined on a 1:5 soil:deionised water suspension (United States Salinity Laboratory Staff, 1954). Samples were subsequently filtered through 0.45 μm syringe filters (Advantec MFS-25) to remove suspended sediment prior to analysing for cations and anions. Cations were determined by inductively coupled plasma optical emission spectroscopy (720-ES, Varian, Melbourne, Australia) and anions by ion exchange chromatography (DX-120, Dionex, Sunnyvale, California, USA). Total C and nitrogen (N) contents of solid samples were determined on a finely ground (<50 μm) subsample of the <2 mm fraction. Samples were combusted at 1000 °C using a Europa ANCA-GSL CN analyser connected to a continuous flow isotope ratio mass spectrometer which also determined $\delta^{13}C$ and $\delta^{15}N$ values (Sercon Ltd., Cheshire, UK). The $\delta^{13}C$ and $\delta^{15}N$ values are expressed relative to VPDB and atmospheric N_2, respectively. Two separate runs were performed in order to obtain total soil $\delta^{13}C$ and organic $\delta^{13}C$ values, and to enable calculation of soil inorganic C content. Samples analysed for total soil C, N, $\delta^{13}C$ and $\delta^{15}N$ were not subjected to any treatment. Samples analysed for organic $\delta^{13}C$ and total organic C content were fumigated with HCl to remove all inorganic C prior to analysis. Subsamples of the finely ground fraction were put into small glass vials, moistened with deionised water, and placed in a vacuum desiccator with a beaker containing 100 ml of concentrated (12 *M*) HCl for 12 h (Harris et al., 2001). Samples were then dried at 60 °C, cooled in a desiccator and capped tightly prior to being weighed into tin capsules for analysis. Soil inorganic C contents were calculated by subtracting the total C content of the HCl fumigated samples from the total C values obtained from the untreated samples.

2.5. Statistical analyses

Principal component analysis (PCA) was used to identify the main components influencing the variance in soil chemical properties with depth and between sites. PCA was completed using the function 'princomp' in R 2.11.1 (The R Foundation). Linear regression was used in Microsoft Excel® 2007 to determine surface CO_2 fluxes and the rate of change in $\delta^{13}C_{CO_2}$ in surface flux samples.

3. Results

3.1. Environmental variables

At the time of sampling (late December 2008), soils at Sites A and B were ice-cemented below 35 and 26 cm, respectively, although soil temperatures during the sampling periods were very similar at both sites (Figs. 1A and 2A). The strongest vertical soil temperature gradients occurred during "warm" sampling periods, with soil temperatures reaching 13–14 °C at 5 cm depth, and 1.3–2.6 °C at 25 cm depth. During "cold" sampling periods, soil temperature gradients were lower, with temperatures ranging from ~0.5 °C at 5 cm depth to ~1.6–3.6 °C at 25 cm depth. The progressively greater lag in soil temperature response to surface heating with increasing depth in the profile meant that soil temperatures at 25 cm depth during the "cold" sampling period were slightly warmer than those measured during the "warm" sampling period. The rate of change in soil temperature during warm and cold sampling periods was always greatest at 5 cm depth, and decreased with depth in the soil profile.

Soil moisture content remained relatively constant throughout the sampling period at Site A (Fig. 1B), with no moisture detected at 5 cm depth. Ponded water was observed on the soil surface in low-lying areas within 300 m of the sampling area, suggesting subsurface melt from ice-cemented soils on adjacent north-facing hill slopes was contributing to the relatively high moisture content (~5%) observed at 15 cm depth at this site. Soil moisture content at 25 cm depth was around 6%. At Site B, soil moisture content at 5 cm depth was higher during warm sampling periods, whereas at 15 cm depth it remained relatively constant (~1%) (Fig. 2B). Soil moisture content at 25 cm depth increased from 4 to 8% over the sampling period due to thawing ice cement at the base of the profile.

3.2. Soil physical and chemical properties

Soil bulk density ranged from 1.5 to 2.3 g cm^{-3}. These values correspond to soil porosities ranging from 18 to 45%, assuming a particle density of 2.8 g cm^{-3} (Barrett and Froggatt, 1978) which is appropriate for the dominantly mafic igneous rocks of the study area.

Principal component analysis of soil chemical data revealed three principal components which explained 80% of the variance in the original soil chemical data. Principal component (PC) 1 represents total C, inorganic C, calcium (Ca^{2+}), magnesium (Mg^{2+}), nitrate (NO_3^-) and sulphate (SO_4^{2-}) (Supplementary Table 1). PC 1 can be considered a C component as it is dominated by total C and inorganic C. PC 2 represents pH, EC and sodium (Na^+), and is effectively a measure of saltiness. PC 3 represents total N, organic C, potassium (K^+), chloride (Cl^-) and sulphate, although component correlations suggest that total N and organic C are the variables best described by PC 3. Depth profiles, contrasts and similarities between the soils at each site are discussed below in terms of the major variables contributing to the three principal components.

3.2.1. Inorganic C (PC 1)

Inorganic C was higher at Site A than at Site B (Fig. 3A). At Site A, inorganic C decreased from 2 mg g^{-1} to 1 mg g^{-1} in the upper 15 cm of the profile, and increased with depth below 15 cm. The maximum inorganic C content (4 mg g^{-1}) occurred in the 40–45 cm depth increment, coinciding with the approximate maximum thaw depth of the active layer. Despite inorganic C content in the upper 15 cm being the lowest in the profile at Site A, it was more than double the organic C content. Below 15 cm depth, inorganic C was always more than four times greater than organic C at the same depth. At Site B, inorganic C decreased from 2 mg g^{-1} in the top 5 cm to 0.3 mg g^{-1} between 10 and 25 cm depth. Below 25 cm depth, inorganic C increased, and was always more than five times greater than organic C at the same depth.

3.2.2. Organic C (PC 3)

Total organic C decreased with depth down the profile at Site A (Fig. 3B), except for a secondary peak of 0.6 mg g^{-1} at 40–45 cm

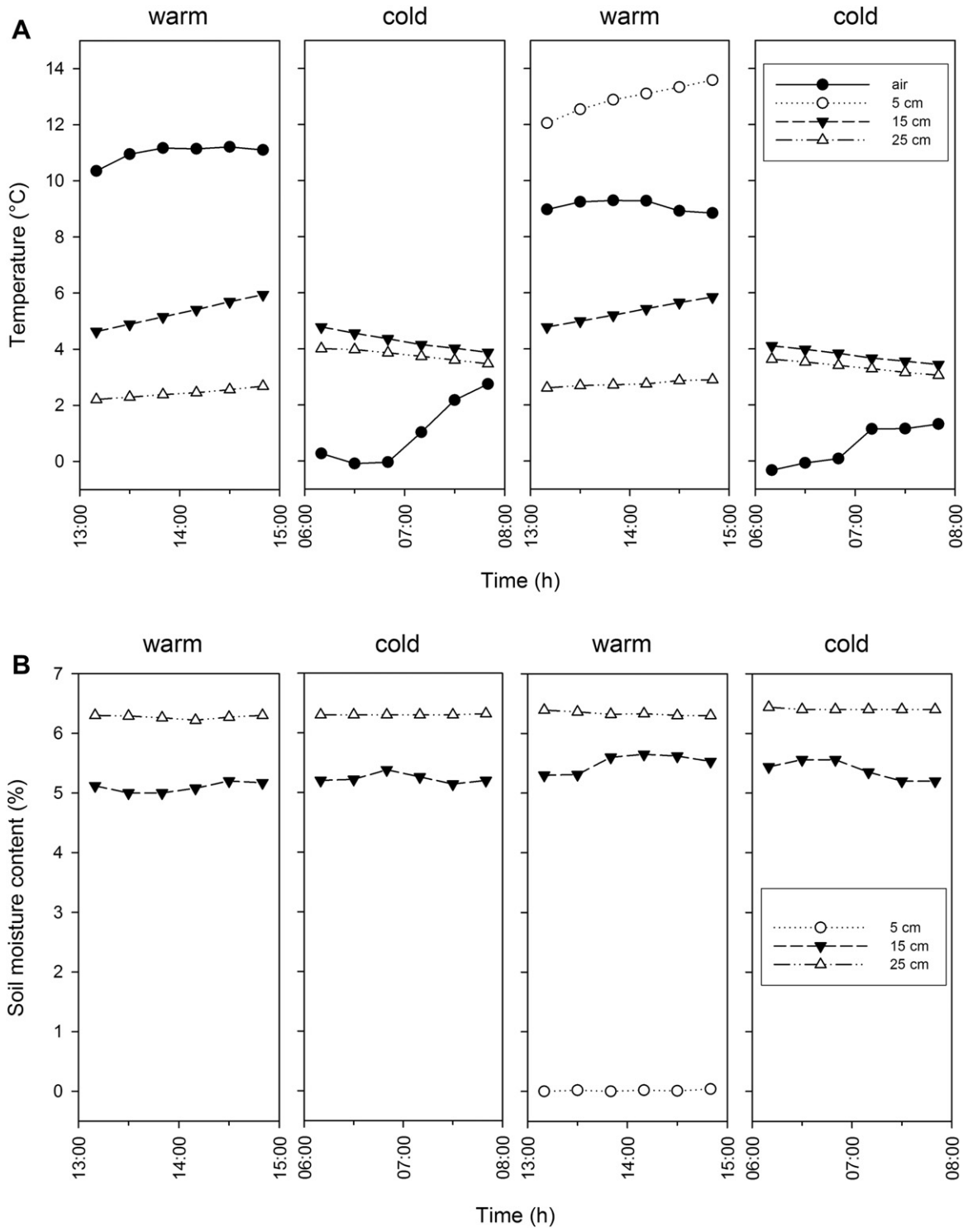

Fig. 1. Soil temperature (A) and volumetric moisture content (B) during gas sampling periods, Site A Taylor Valley. Note: data at 5 cm depth were only recorded during one sampling period due to a faulty probe.

depth, which was only slightly lower than values measured between 0 and 10 cm depth. The depth of the secondary peak corresponds to the estimated maximum thaw depth of the active layer. At Site B, total organic C values were very low (0.16–0.32 mg g^{-1}) and decreased slightly with depth.

From 5 to 15 cm depth at Site A, and in the upper 10 cm of the profile at Site B, $\delta^{13}C$ values were highly depleted relative to VPDB, ranging from −25.7 to −30.7‰ (Fig. 3C). The upper 5 cm at Site A had a comparatively enriched $\delta^{13}C$ value of −21.6‰; below 15 cm depth, values ranged from −15.8 to −19.6‰. At Site B, $\delta^{13}C$ values beneath 10 cm depth were more depleted relative to those at Site A, ranging from −18.6 to −20.6‰.

3.2.3. Soil pH and electrical conductivity (PC 2)

Soil pH ranged from ~10 in the upper part of the profile at both sites to between 8.8 and 9.4 at 45–50 cm depth (Fig. 4A). Electrical

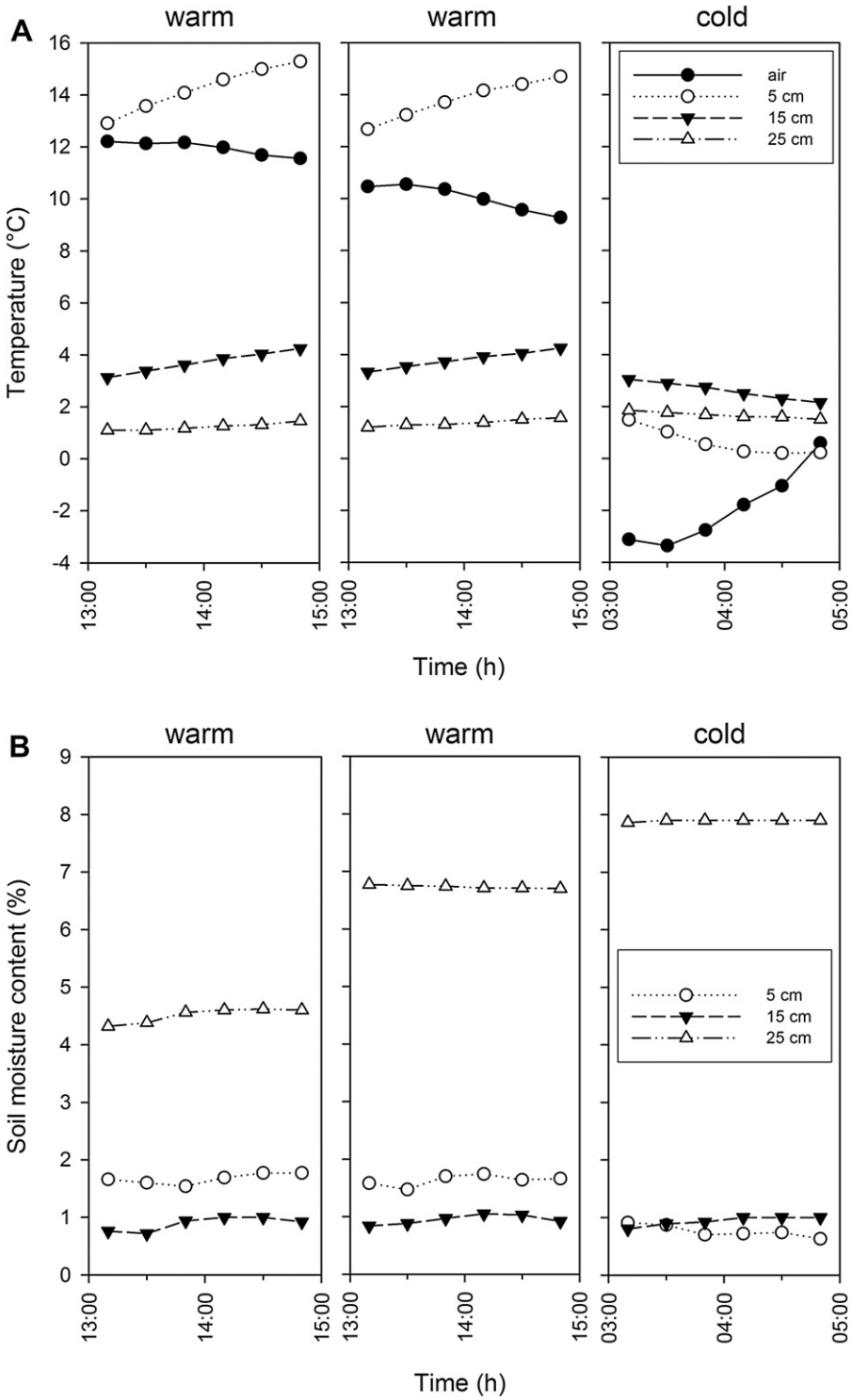

Fig. 2. Soil temperature (A) and volumetric moisture content (B) during gas sampling periods, Site B Taylor Valley. Note: this site was only sampled during one "cold" period due to an error in determining the timing of the coldest part of the day.

conductivity (EC), a proxy for soil salt concentration, was higher in the upper 10 cm of the soil at Site B than at Site A (Fig. 4B). At both sites, EC values were relatively low and constant between 10 and 40 cm depth. Between 40 and 50 cm depth, EC values at both sites increased to a level similar to that in the upper 5 cm at Site A (Fig. 4B).

3.3. CO_2 dynamics

3.3.1. Subsurface CO_2 profiles

Subsurface CO_2 concentrations were significantly different between warm and cold periods at both sites (Fig. 5A). During warm periods, soil CO_2 concentrations were greater than

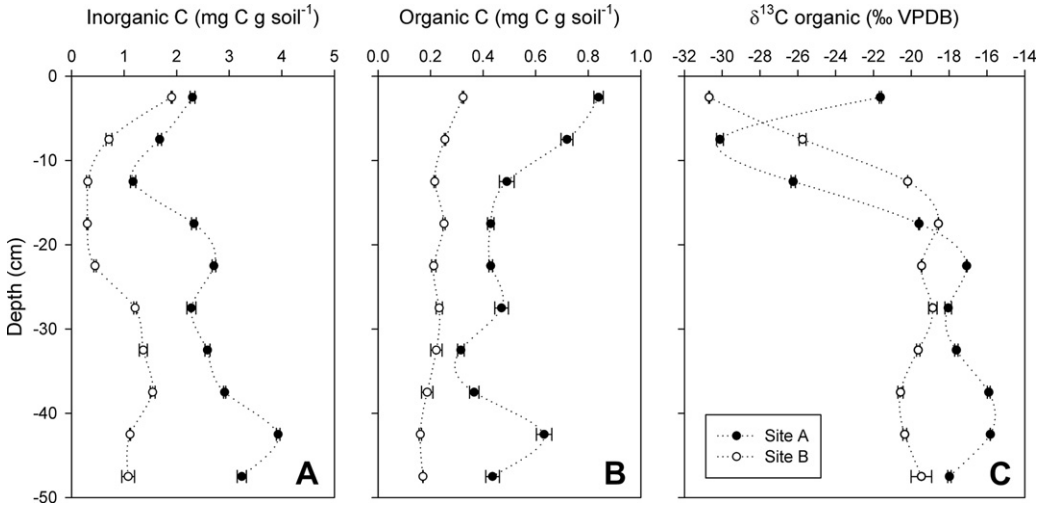

Fig. 3. Depth profiles of A) soil inorganic C, B) soil organic C, and C) C isotopic composition of soil organic C at Sites A and B, Taylor Valley (error bars are ±1 standard deviation; $n = 2$).

atmospheric CO_2 concentration (383.3 μL L^{-1} at the South Pole in December 2008; Keeling et al., 2001) in the upper 10 cm of the profile at Site A, reaching a maximum of 400 μL L^{-1} at 10 cm depth. Samples taken during cold sampling periods showed soil CO_2 concentrations were substantially below that of atmospheric CO_2, the lowest being 315 μL L^{-1} at 15 cm depth at Site A. At both sites, shifts in soil CO_2 concentration between warm and cold periods were mirrored about a trend-line that decreases from 380 μL L^{-1} at the surface to 330–340 μL L^{-1} at 30 cm depth, demonstrating that cycles of CO_2 uptake (cold periods) and release (warm periods) occur. The amount of soil CO_2 taken up and released was greater at Site A than at Site B.

Soil profile $\delta^{13}C_{CO_2}$ was relatively enriched during warm periods when compared to cold periods at both sites (Fig. 5B). At Site A, $\delta^{13}C_{CO_2}$ became more enriched with increasing depth in the profile during both warm and cold periods, although at 15 cm depth there were slight inflexions in the trends. Values ranged from −7.0 to −9.0‰, with a maximum difference between warm and cold periods of 1‰. At Site B, $\delta^{13}C_{CO_2}$ remained relatively constant with depth during both warm and cold periods, ranging from −8.2 to −9.2‰, with differences of ≤0.9‰ between warm and cold periods. Soil profile $\delta^{13}C_{CO_2}$ was similar to that of atmospheric CO_2 (−8.22‰ at the South Pole in December 2008; Keeling et al., 2001) during warm periods at Site B. At both sites, $\delta^{13}C_{CO_2}$ was highly enriched relative to soil organic matter (Fig. 3C).

3.3.2. Surface CO_2 fluxes

Surface CO_2 flux rates ranged from −0.050 to 0.048 μmol m^{-2} s^{-1} (Table 1). Periods of efflux (positive flux) and influx (negative flux) corresponded to warm and cold sampling periods, respectively. During warm periods (efflux), headspace CO_2 became progressively enriched (by up to 1.8‰), whereas during cold periods (influx), headspace CO_2 became depleted (by up to −2.0‰). The $\delta^{13}C_{CO_2}$ values ranged from −6.5 to −10.6‰ during warm periods, and −7.4 to −11.2‰ during cold periods.

4. Discussion

4.1. Soil CO_2 uptake and release

The low soil CO_2 flux rates measured in this study are in close agreement with *in situ* surface flux rates in Taylor Valley reported by Burkins et al. (2001) and Parsons et al. (2004), but an order of magnitude lower than those reported by Ball et al. (2009), despite

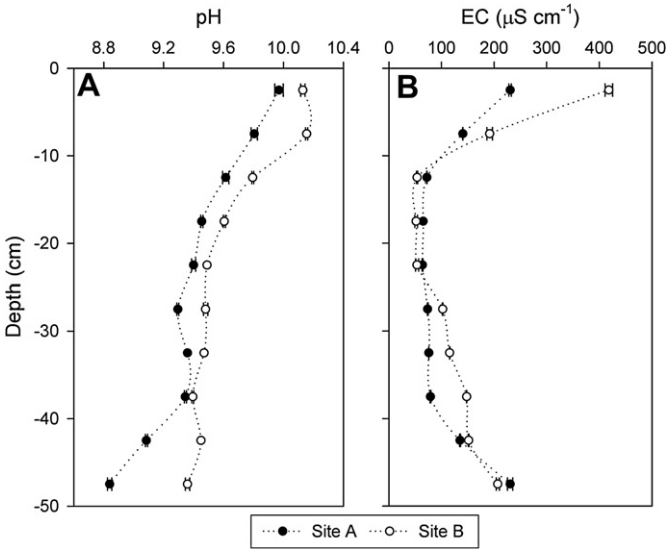

Fig. 4. Depth profiles of A) soil pH, and B) electrical conductivity at Sites A and B, Taylor Valley (error bars are ±1 standard deviation; $n = 2$).

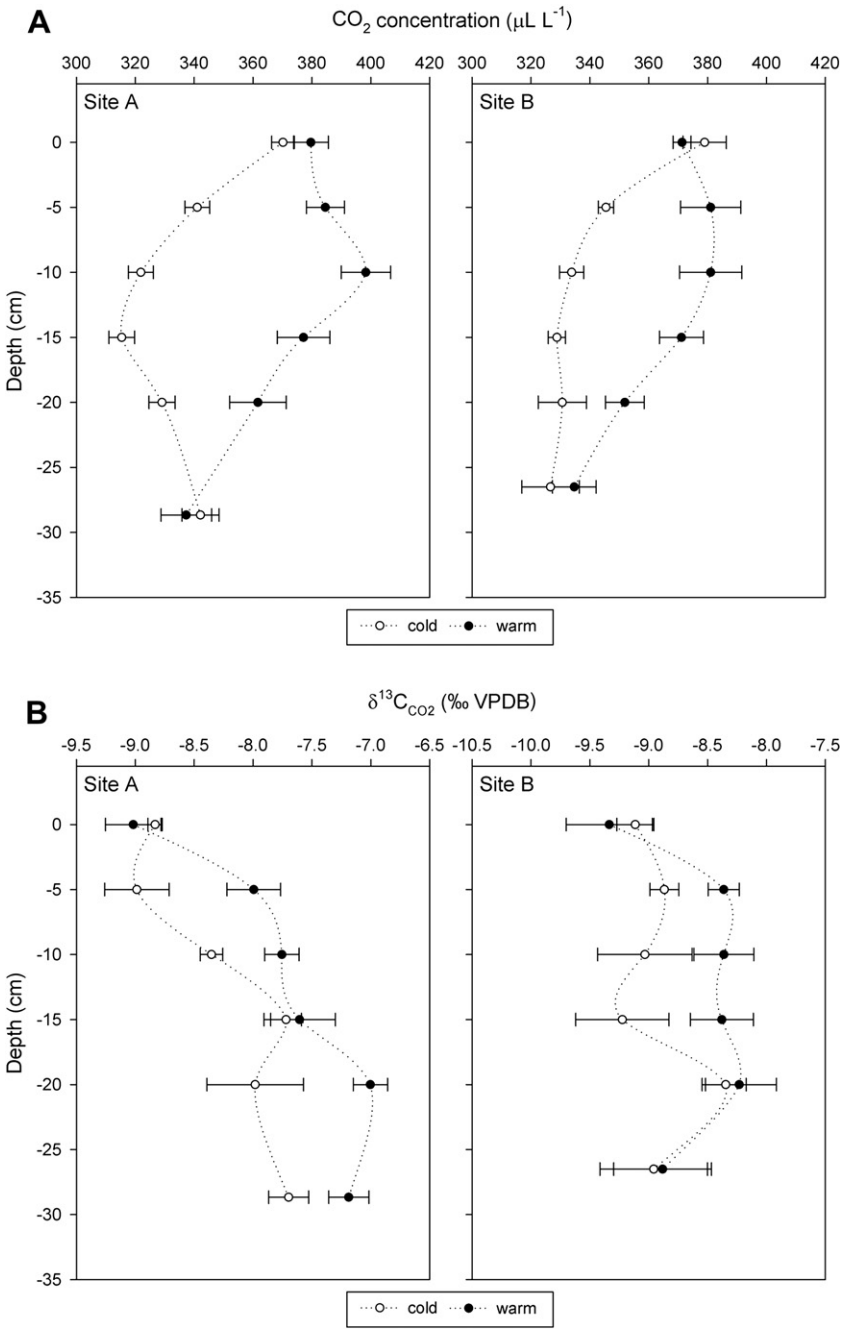

Fig. 5. Soil profile CO_2 concentration (A) and $\delta^{13}C_{CO_2}$ (B) at Sites A and B, Taylor Valley. Data shown represent averages for warm and cold sampling periods ($n = 6$ for 0 cm samples and $n = 12$ at all other depths, except for the cold sampling period at Site B, where $n = 3$ for 0 cm samples and $n = 6$ at all other depths). Error bars represent the SEM.

all studies having used soils with similar pH, EC, organic and inorganic C values. Higher flux rates such as those reported by Gregorich et al. (2006) were from soils with organic C contents of up to 35 mg g^{-1}. Such high organic C contents are unusual in Antarctic dry valley soils; this study focuses on CO_2 dynamics in typical dry valley soils characterised by high pH (~10) and low organic C contents (<1 mg g^{-1}).

It is well established that soil respiration increases with rising soil temperature (e.g. Lloyd and Taylor, 1994; Fang and Moncrieff, 2001). If CO_2 release during warm periods at our study sites were due to biological respiration, $\delta^{13}C_{CO_2}$ values should reflect the $\delta^{13}C$ of the source organic material (Dörr and Münnich, 1980). Soil $\delta^{13}C_{CO_2}$ values (Fig. 5B) showed no relationship with soil organic matter $\delta^{13}C$ values (Fig. 3C). Furthermore, if CO_2 uptake during cold periods were a result of algal photosynthesis, we would expect soil $\delta^{13}C_{CO_2}$ to be enriched due to preferential uptake of $^{12}CO_2$ by photosynthetic organisms, thus concentrating the heavier $^{13}CO_2$ in the soil atmosphere (Park and Epstein, 1960). No biological mechanism can be invoked to account for our results. Instead, $\delta^{13}C_{CO_2}$ values associated with the uptake (depleted $\delta^{13}C_{CO_2}$) and release (enriched $\delta^{13}C_{CO_2}$) of soil CO_2 indicate that CO_2 dynamics in Antarctic soils are controlled by other mechanisms.

In studies of surface CO_2 fluxes in Taylor Valley, Ball et al. (2009) found that soil temperature fluctuations (at 5 cm depth) accounted for almost half of the variation observed in diel CO_2 fluxes. As similar diel cycles of CO_2 flux were also observed in heat-treated (120 °C) soils, presumed to be free of biological activity, Ball et al.

Table 1
Surface soil CO_2 fluxes and rate of change in $\delta^{13}C_{CO_2}$ during surface CO_2 flux sampling at Sites A and B, Taylor Valley.

Site	Chamber	Sampling time[a]	CO_2 flux (μmol m^{-2} s^{-1})	$\frac{\Delta\delta^{13}C_{CO_2}}{\Delta t}$[b]
A	a	W_1	0.010	0.010
		W_2	0.000	0.013*
		C_1	−0.041**	−0.006
		C_2	−0.003	−0.008
A	b	W_1	0.034	0.022**
		W_2	0.026	0.014
		C_1	−0.024	0.001
		C_2	−0.044	−0.002
A	c	W_1	0.048	0.000
		W_2	0.019	0.003*
		C_1	−0.039**	−0.008
		C_2	−0.038**	0.004
A	d	W_1	0.043**	0.024**
		W_2	0.005	0.016
		C_1	0.004	−0.022**
		C_2	−0.016	−0.016*
A	e	W_1	0.034*	0.003
		W_2	0.024*	0.007
		C_1	0.001	−0.051
		C_2	−0.039**	−0.026**
A	f	W_1	0.036	0.008
		W_2	0.016**	0.029
		C_1	−0.023**	−0.011**
		C_2	−0.024*	−0.021*
B	a	W_1	0.025	0.015
		W_2	0.034**	0.010
		C_1	−0.037	−0.018
B	b	W_1	0.021	0.021
		W_2	0.018**	0.011
		C_1	−0.028*	−0.025
B	c	W_1	0.045	−0.002
		W_2	no data	no data
		C_1	−0.050**	0.023
B	d	W_1	0.040*	0.012
		W_2	0.010	0.020*
		C_1	−0.013	−0.013
B	e	W_1	0.018	−0.011
		W_2	0.018**	0.009
		C_1	−0.029*	−0.008*
B	f	W_1	0.024*	0.004
		W_2	0.013	0.011
		C_1	0.001	−0.004

* represents $P < 0.1$; ** represents $P < 0.05$.
[a] W and C denote warm and cold sampling periods, respectively.
[b] Units are per mil min^{-1}.

(2009) suggested that dissolution of CO_2 in soil water, consistent with Henry's Law, was a likely explanation for the diel variations observed. We test this hypothesis by: 1) comparing soil profile CO_2 concentrations measured at warm and cold periods with values simulated by a model that incorporates Henry's Law dissolution of CO_2, and 2) comparing the measured changes in $\delta^{13}C_{CO_2}$ with those expected from fractionation due to dissolution and exsolution of CO_2, biological respiration, and photosynthetic CO_2 fixation. We also use our data to quantify the relative contributions of biotic and abiotic processes to soil CO_2 uptake and release.

4.1.1. A model of abiotic CO_2 dynamics

At steady state, the closed-system partitioning of CO_2 between gaseous and dissolved CO_2 is determined by Henry's Law and solution pH. The temperature dependent Henry coefficient (K_H) (Stumm and Morgan, 1996) expresses the relationship between pCO_2 of the atmosphere and dissolved gaseous CO_2 ($[CO_{2(aq)}] = [H_2CO_3]$), as $pCO_2 = K_H[CO_{2(aq)}]$. Total dissolved CO_2 (C_T), which includes the species H_2CO_3, HCO_3^- and CO_3^{2-}, is related to $[CO_{2(aq)}]$ and pH by:

$$C_T = \left[CO_{2_{(aq)}}\right]\left(1 + \frac{K_{a_1}}{[H^+]} + \frac{K_{a_1}K_{a_2}}{[H^+]^2}\right) \quad (2)$$

where K_{a_1} and K_{a_2} are the equilibrium constants for $[H^+]$ $[HCO_3^-]/[H_2CO_3]$ and $[H^+]$ $[CO_3^{2-}]/[HCO_3^-]$, respectively (Stumm and Morgan, 1996). The temperature dependence of K_H is such that as temperature increases, $[CO_{2(aq)}]$ decreases. Thus, as a result of changes in K_H, decreasing temperature causes CO_2 absorption, and increasing temperature causes CO_2 desorption. In a soil, the capacity of soil solution to absorb and desorb CO_2 depends on soil solution volume, soil pH, and the magnitude of soil temperature variation. From Eq. (2), it is evident that increasing soil solution pH (decreasing $[H^+]$) causes an increase in C_T. A high soil solution pH interacts with the volume of soil solution, amplifying the effect of CO_2 adsorption or desorption with changing temperature by providing for a larger source or sink of dissolved CO_2 involved in the exchanges.

Using the principles described above, and closed-system, steady state assumptions, we model abiotic CO_2 dynamics in the soils at our study sites. The low flux rates measured (Table 1) suggest the closed-system assumption is not unreasonable, but we explore this further below. The model predicts the ratio of soil CO_2 concentrations ($[CO_2]_{warm}$:$[CO_2]_{cold}$) when temperature (T) drops from warm (T_{warm}) to cold (T_{cold}) in terms of the soil moisture content and pH of the system.

The ratio of subsurface soil CO_2 concentrations attributable to abiotic processes as a result of a change in temperature from T_{warm} to T_{cold} is given by:

$$\frac{[CO_2]_{warm}}{[CO_2]_{cold}} = \frac{\left(\frac{(\varphi-\theta)}{RT_{cold}} + \frac{\theta}{K_{H_{cold}}}\right)}{\left(\frac{(\varphi-\theta)}{RT_{warm}} + \frac{\theta}{K_{H_{warm}}}\right)} \times \frac{T_{cold}}{T_{warm}} \quad (3)$$

where φ is soil porosity (L voids L $soil^{-1}$), θ is soil volumetric moisture content (L water L $soil^{-1}$), R is the ideal gas constant (8.314 J K^{-1} mol^{-1}), T is soil temperature (K), K_H is Henry's coefficient (L atm mol^{-1}) and $[CO_2]$ is soil CO_2 concentration (μL L^{-1}). A full derivation of the model is given in Appendix A.

The dependence of $[CO_2]_{warm}$:$[CO_2]_{cold}$ on soil pH and moisture content for temperature changes (between warm and cold sampling periods) typical of those measured at 5 cm (Fig. 6A) and 15 cm (Fig. 6B) depth in the study area is shown in Fig. 6. At low pH ($\leq$6), C_T is low (Eq. (2)), and consequently a large soil solution volume (high moisture content) is required to provide the pool of dissolved inorganic C necessary for temperature-driven absorption/desorption processes to shift $[CO_2]_{warm}$:$[CO_2]_{cold}$ significantly. Between pH 7 and 9, C_T rises rapidly and the volume of soil solution required to produce a given $[CO_2]_{warm}$:$[CO_2]_{cold}$ declines rapidly. For example, at pH 6, soil moisture content must be 0.32 (at or above field capacity in many soils) for $[CO_2]_{warm}$:$[CO_2]_{cold}$ to be 1.4 (T_{warm} = 286 K and T_{cold} = 274 K; Fig. 6A). By contrast, for the same change in T at pH 9, the same ratio can be accommodated by a soil with a moisture content < 0.01 (<1%). The magnitudes of $[CO_2]_{warm}$:$[CO_2]_{cold}$ simulated for 15 cm depth (Fig. 6B) are much lower because of the smaller temperature fluctuation at this depth, but the relative sensitivity to soil pH and moisture content remains the same.

The model suggests that changes in soil profile CO_2 concentrations in the study area should be greatest at shallow soil depths, where temperature changes are greatest, pH is high (~10), and moisture content is adequate. Conversely, greater depths should have smaller changes in soil CO_2 concentrations due to smaller

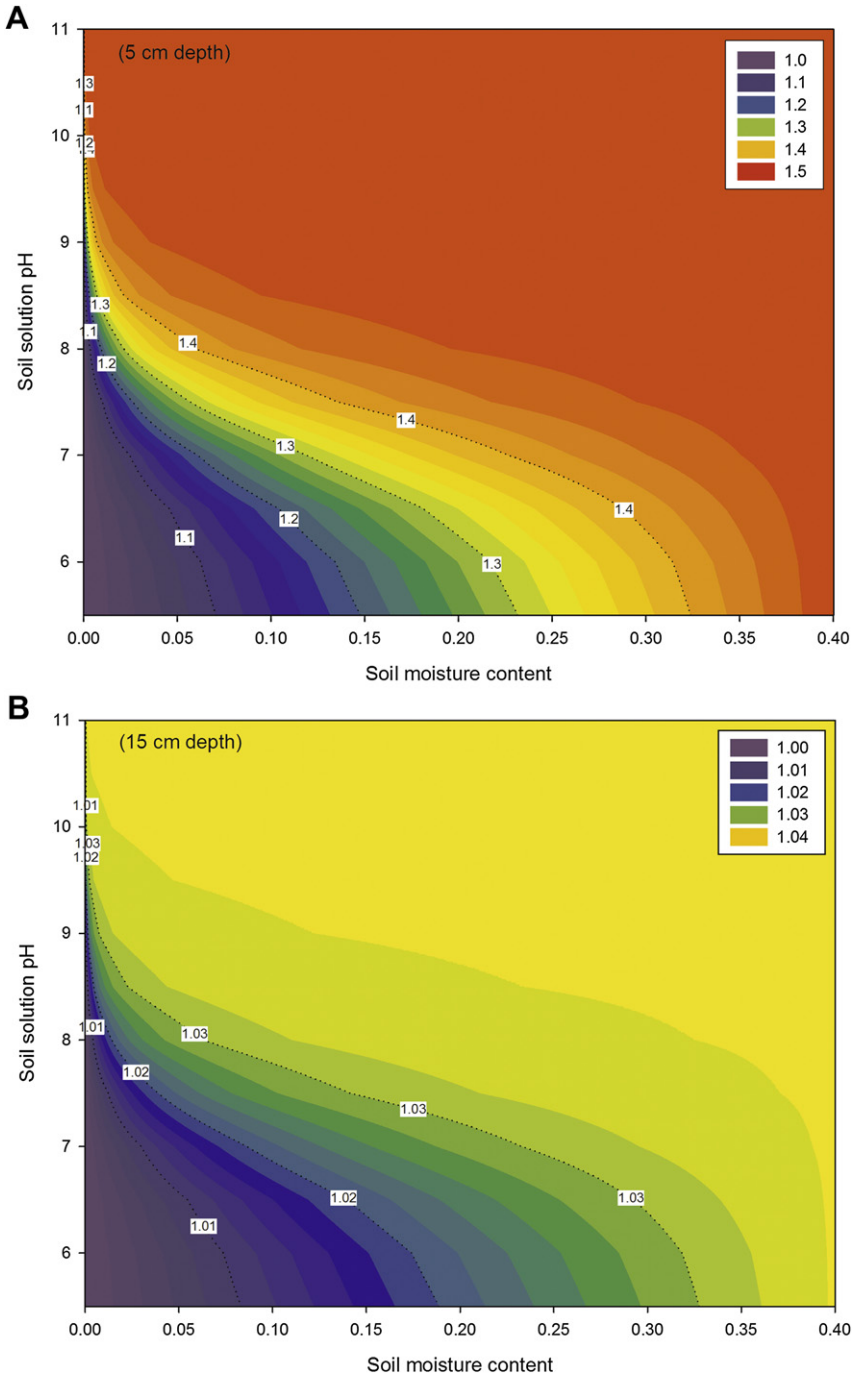

Fig. 6. Ratios of simulated $[CO_2]_{warm}$:$[CO_2]_{cold}$ as influenced by soil moisture content and soil solution pH. Ratios are calculated using Eq. (3). In (A) $T_{warm} = 286$ K and $T_{cold} = 274$ K which are similar to soil temperatures measured at 5 cm depth, and in (B) $T_{warm} = 278.3$ K and $T_{cold} = 277.3$ K, similar to soil temperatures measured at warm and cold periods, respectively, at 15 cm depth in the study area. When the ratio of $[CO_2]_{warm}$:$[CO_2]_{cold}$ is 1, there is zero potential for CO_2 to be absorbed. This occurs when soil moisture is so low that no CO_2 can be dissolved. Higher ratios represent greater changes in soil CO_2 concentrations between warm and cold periods, and thus greater uptake and release of CO_2 by soils.

changes in soil temperature. However, our measured CO_2 concentration depth profiles (Fig. 5A) show relatively low variation in CO_2 concentrations at shallow depths, with maximum differences at 10–15 cm. As predicted by the model, little variation occurs at the base of the profile.

Measured and simulated ratios of $[CO_2]_{warm}$:$[CO_2]_{cold}$ were compared for 5, 15 and 25 cm depths using measured values of soil pH, temperature and volumetric moisture content (Fig. 7). The 25 cm depth increment behaves as the model predicts. Ratios of $[CO_2]_{warm}$:$[CO_2]_{cold}$ are very close to 1 due to minimal changes in soil temperature between warm and cold periods. At this depth, the soil closely approximates a closed system because ice-cemented soil beneath provides a gas-impermeable lower barrier, and CO_2 concentration gradients are low (Fig. 5A). At 15 cm depth, measured ratios are 15% and 9% greater than simulated ratios (their theoretical abiotic maximum) at Sites A and B, respectively, suggesting a possible biological respiration component. At 5 cm depth, measured $[CO_2]_{warm}$:$[CO_2]_{cold}$ ratios are considerably lower than simulated ratios. As the 5 cm depth increment is most likely to suffer from violation of the closed-system assumption of the model,

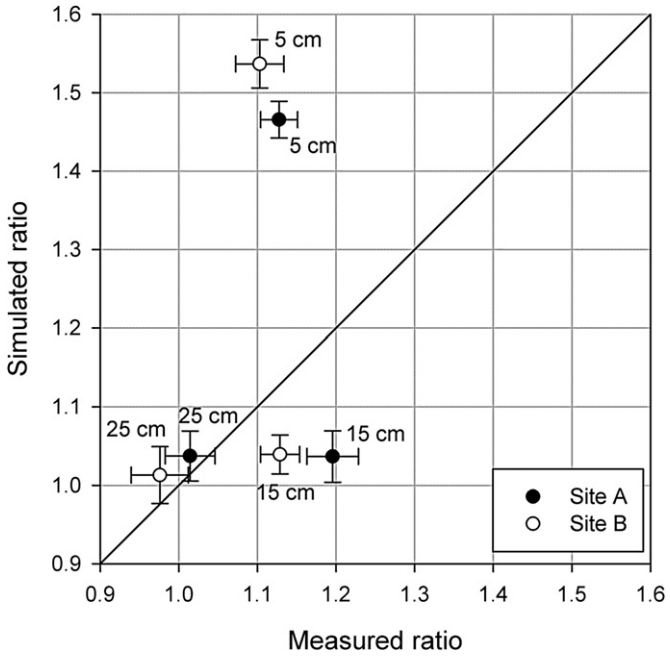

Fig. 7. Comparison between measured and simulated $[CO_2]_{warm}$:$[CO_2]_{cold}$ ratios between warm and cold sampling periods for Sites A and B, Taylor Valley.

we attribute this discrepancy to exchange between the soil and surface atmospheres. Leakage of CO_2 from the soil during warm periods when CO_2 is released via exsolution, and influx of atmospheric CO_2 during cold periods when soil CO_2 concentrations are depleted (CO_2 dissolution) would act to damp variation in measured CO_2 concentrations. These inferred fluxes are supported by the soil CO_2 concentration gradients at this depth (Fig. 5A).

4.1.2. Discriminating between biotic and abiotic processes using stable C isotopes

Biotic production and consumption of CO_2 and the abiotic dissolution/exsolution processes outlined above produce distinctive soil $\delta^{13}C_{CO_2}$ values. Biological respiration of highly depleted organic C would produce respired CO_2 of a very similar (highly depleted) C isotopic composition (Dörr and Münnich, 1980), as respiration does not (or only to a minor extent) discriminate against ^{13}C. Based on measured soil organic $\delta^{13}C$ values at both sites (Fig. 3C), we would expect respired $\delta^{13}C_{CO_2}$ values of ~ −30 to −21‰ in the upper 15 cm of the profiles, and ~ −20 to −16‰ below 15 cm depth. Thus, if biological respiration were responsible for the increase in soil CO_2 concentration during warm periods, $\delta^{13}C_{CO_2}$ values would become relatively depleted. Conversely, discrimination against $^{13}CO_2$ in C_3 photosynthetic pathways would produce a $\delta^{13}C_{CO_2}$-enriched atmosphere above actively photosynthesising organisms. Therefore, if soil CO_2 uptake during cold periods were due to photosynthetic CO_2 consumption, $\delta^{13}C_{CO_2}$ values would become relatively enriched. Our results are contrary to these patterns: soil profile $\delta^{13}C_{CO_2}$ values were relatively enriched during warm periods (CO_2 release) and depleted during cold periods (CO_2 uptake; Fig. 5B). Surface CO_2 flux data also showed progressive enrichment and depletion of $\delta^{13}C_{CO_2}$ during warm and cold sampling periods, respectively (Table 1). The observed patterns are consistent with isotopic fractionation during CO_2 dissolution and its speciation to $HCO_{3\,(aq)}^-$ and $CO_{3\,(aq)}^{2-}$ (Table 2). At pH values >9, dissolved CO_2 species are dominated by the HCO_3^- and CO_3^{2-} forms (Stumm and Morgan, 1996). Equilibrium fractionation of CO_2 gas to HCO_3^- and CO_3^{2-} results in a ~ −10‰ depletion of CO_2 gas relative to HCO_3^- or CO_3^{2-} (Thode et al., 1965; Mook et al., 1974; Table 2). Thus, dissolution of CO_2 to form HCO_3^- and CO_3^{2-} (at the high pH values measured) would result in depletion of $\delta^{13}C_{CO_2}$ in the soil atmosphere, whereas exsolution would lead to enrichment of $\delta^{13}C_{CO_2}$ in the soil atmosphere. The magnitudes of the isotopic shifts we observe (~ −1‰) are less than ~ −10‰ because only a proportion of the CO_2 in the soil atmosphere exchanges with soil solution (~10%).

Although the $\delta^{13}C_{CO_2}$ data confirm abiotic processes dominate CO_2 dynamics in soils of Taylor Valley, as postulated by Ball et al. (2009), our comparison of measured and simulated $[CO_2]_{warm}$:$[CO_2]_{cold}$ ratios suggests there is a component of CO_2 flux around 15 cm depth that cannot be accounted for by abiotic processes alone. We use soil organic $\delta^{13}C$ values in conjunction with soil profile $\delta^{13}C_{CO_2}$ values to further constrain the potential biotic contribution to soil CO_2 fluxes.

Table 2
Carbon isotope fractionation in the CO_2–HCO_3–CO_3–$CaCO_3$ system under equilibrium conditions. $^{13}\varepsilon_{y/x}$ represents the fractionation of compound y relative to compound x. Soil temperatures (T) shown are similar to those measured during the sampling period. g = gaseous CO_2, a = dissolved CO_2, b = dissolved HCO_3^-, c = dissolved CO_3^{2-} ions, s = solid calcium carbonate. $T_K = T$ (°C) + 273.15 K.

T (°C)	$^{13}\varepsilon_{g/a}$ [a] (‰)	$^{13}\varepsilon_{g/b}$ [b] (‰)	$^{13}\varepsilon_{g/c}$ [c] (‰)	$^{13}\varepsilon_{g/s}$ [d] (‰)
1	1.17	−10.70	−10.06	−10.47
5	1.15	−10.20	−9.61	−10.19

[a] $^{13}\varepsilon_{g/a} = -0.19‰ + 373/T_K$ (Vogel et al., 1970).
[b] $^{13}\varepsilon_{g/b} = 23.89‰ - 9483/T_K$ (Mook et al., 1974).
[c] $^{13}\varepsilon_{g/c} = {}^{13}\varepsilon_{g/b} + {}^{13}\varepsilon_{b/c}$ (= −2.52‰ + 867/T_K; Thode et al., 1965).
[d] $^{13}\varepsilon_{g/s} = 9.15‰ - 5380/T_K$ (Mook, 2000).

4.1.3. Quantifying the biotic contribution to soil CO_2 fluxes

The bulge in soil CO_2 concentration from 5 to 15 cm depth at Site A is likely to have a biological respiration component, as organic C content at this depth is relatively high (~0.6 mg C g soil^{-1}; Fig. 3B) and the soil is relatively warm (Fig. 1A). Assuming respired soil CO_2 at this depth would have an average $\delta^{13}C_{CO_2}$ value of −28.2‰ (Fig. 3C), we can use a mixing model (Fry, 2006) to calculate the biotic contribution (f_{biotic}) to soil CO_2 fluxes:

$$f_{biotic} = \frac{\delta^{13}C_{CO_2-produced} - \delta^{13}C_{CO_2-abiotic}}{\delta^{13}C_{biotic} - \delta^{13}C_{CO_2-abiotic}} \quad (4)$$

Table 3
Proportion of the change in CO_2 concentration and isotopic composition attributable to biotic processes (f_{biotic}) at Site 1, 5–15 cm depth. This depth has the greatest shift in CO_2 concentration between cold and warm periods (Fig. 5A) and is the most likely place in which biological respiration may occur. The effects of changes in assumed $\delta^{13}C_{CO_2-abiotic}$ values on f_{biotic} are shown.

f_{biotic}	$\delta^{13}C_{CO_2-abiotic}$ (‰)	Source of $\delta^{13}C_{CO_2-abiotic}$ value
−0.15	−8.22	Atmospheric $\delta^{13}C_{CO_2}$ at the South Pole in December 2008 (Keeling et al., 2001).
0.05	−4.10	Average $\delta^{13}C_{CO_2}$ emitted from the whole profile at Site 3, assuming no biological contribution.
0.14	−1.42	Assumes Site 3 has a 10% biological contribution, as suggested by the comparison between measured and simulated $[CO_2]_{warm}$:$[CO_2]_{cold}$ ratios (Fig. 7). The 10% biological contribution is conservatively applied to the whole profile.
0.24	2.16	Assumes no fractionation of CO_2 as it is exsolved from a 50:50 mix of HCO_3^-:CO_3^{2-} in isotopic equilibrium with atmospheric CO_2 at 1 °C (Table 2).

where $\delta^{13}C_{CO_2-produced}$ is the $\delta^{13}C_{CO_2}$ (‰) produced from cold to warm periods (Appendix B), $\delta^{13}C_{CO_2-abiotic}$ is the $\delta^{13}C_{CO_2}$ (‰) of CO_2 produced due to abiotic processes, and $\delta^{13}C_{biotic}$ is the $\delta^{13}C$ (‰) of the organic source material (Fig. 3C).

This calculation requires that we know the isotopic composition of abiotically produced CO_2 ($\delta^{13}C_{CO_2-abiotic}$). We calculate f_{biotic} using a range of $\delta^{13}C_{CO_2-abiotic}$ values (Table 3) appropriate to different assumptions about isotopic fractionation during dissolution and exsolution of CO_2. The proportion of biotic CO_2 production increases with increasing values of $\delta^{13}C_{CO_2-abiotic}$. The most depleted value of $\delta^{13}C_{CO_2-abiotic}$ (−8.22‰) assumes exsolved CO_2 has the same $\delta^{13}C_{CO_2}$ as atmospheric CO_2 at the time of sampling. This is clearly unrealistic, because firstly, it produces a negative f_{biotic} value, and secondly, exsolved CO_2 this depleted would not allow a shift of soil $\delta^{13}C_{CO_2}$ to > −8.22‰ as is measured at Site A (Fig. 5B). A $\delta^{13}C_{CO_2-abiotic}$ value of −4.1‰ suggests a biotic contribution of 5%. This value of $\delta^{13}C_{CO_2-abiotic}$ is determined using a mass balance calculation of the C isotopic composition necessary to produce the shift in soil $\delta^{13}C_{CO_2}$ from cold to warm sampling periods at Site B (see Appendix B for details of the calculation). Data from Site B are used because the low organic C status of the soil is likely to limit respiration to the extent that CO_2 uptake and release throughout the whole profile is dominated by abiotic processes. However, our model of abiotic soil CO_2 uptake and release suggests there may be as much as a 9% biological component to soil CO_2 production at 15 cm depth at Site B. Therefore, conservatively assuming a 10% biological contribution from respiration of soil organic C to soil CO_2 production over the whole profile at Site B, the value of $\delta^{13}C_{CO_2-abiotic}$ is −1.42‰ (Appendix B), which results in a biological respiration component of 14%. The highest value of $\delta^{13}C_{CO_2-abiotic}$ assumes no fractionation of CO_2 released by exsolution from a 50:50 mix of HCO_3^- and CO_3^{2-} in isotopic equilibrium with atmospheric CO_2. This is an unlikely scenario, but it establishes the most enriched possible value of $\delta^{13}C_{CO_2-abiotic}$. The resultant biotic contribution to soil CO_2 fluxes is 24%.

4.1.4. Implications for soil respiration measurements and C turnover times

Long-term records of soil respiration in the McMurdo Dry Valleys have been suggested as being one of the most sensitive indicators of ecosystem response to climate variability (Barrett et al., 2006c). However, it is essential that both biotic and abiotic contributions to soil CO_2 fluxes are identified and measured accurately, as both components are highly spatially and temporally variable. The techniques we have utilised represent a first attempt.

Our data demonstrate that previously measured *in situ* soil CO_2 fluxes attributed to biological respiration may be significant overestimates (e.g. Burkins et al., 2001; Barrett et al., 2006b; Elberling et al., 2006; Gregorich et al., 2006), and C turnover times calculated on the basis of such fluxes may be significant underestimates (e.g. Burkins et al., 2001; Elberling et al., 2006). Based on their calculation of a mean organic C turnover time of 23 years, Burkins et al. (2001) inferred that C cycling in Taylor Valley is non-steady state, and suggested that at least two organic C pools contribute to C cycling: a labile organic C pool replenished by *in situ* photosynthesis, and a more recalcitrant organic C pool derived from ancient glacial and lake sediments. Such a short C turnover time implies relatively low ecosystem resilience to fluctuations in C supply. Our results, which show that biological respiration accounts for a (conservative) maximum of 25% of measured soil CO_2 fluxes in the Dry Valleys environment, mean that present estimates of C turnover times could be at least four times greater, in the order of 100–500 years. The increased turnover times resulting from lower rates of C utilisation imply that Dry Valley ecosystems are likely to be more resilient to environmental change than what present estimates of C turnover time suggest.

5. Conclusions

Soil CO_2 dynamics at the two sites studied in Taylor Valley are dominated by abiotic processes, with small changes in soil temperature capable of driving significant changes in soil CO_2 concentration. The isotopic data imply that biological respiration makes only a minor contribution to soil CO_2 fluxes in the Dry Valleys environment.

Our results have significant implications for understanding C cycling in polar desert environments. The abiotic influence on soil CO_2 dynamics must be accounted for and monitored, as CO_2 effluxes cannot be assumed to be biologically driven.

Acknowledgements

We thank Prof. James Bockheim for his assistance and enthusiasm in the field, Neil Smith for his expert technical help with data logger and field equipment set-up, and Roger Cresswell for his invaluable assistance with sample analyses. We gratefully acknowledge the excellent logistical support provided by Antarctica New Zealand. Operational support was provided by the Lincoln University Research Fund. F.L.S thanks Helicopters New Zealand, the William Machin Trust, Freemasons New Zealand and the Kate Sheppard Memorial Trust for financial support. We also thank two anonymous reviewers for their constructive comments on the manuscript.

Appendices

Appendix A. Model of abiotic CO_2 uptake and release

Model calculations were based on the following equations. Assuming a soil at steady state, at temperature T (K) for an increment of depth D (m), the partial pressure of CO_2, according to Henry's Law, is

$$pCO_2 = K_{H_T}\left[CO_{2(aq)}\right], \quad (A.1)$$

where K_H is the Henry coefficient (L atm mol^{-1}) and $[CO_{2(aq)}]$ is dissolved gaseous CO_2 (H_2CO_3).

Total dissolved CO_2 (C_T) is determined by the equilibrium constants for $[H^+][HCO_3^-]/[H_2CO_3]$ and $[H^+][CO_3^{2-}]/[HCO_3^-]$, K_{a_1} and K_{a_2}, respectively.

$$C_T = \left[CO_{2_{(aq)}}\right]\left(1+\frac{K_{a_1}}{[H^+]}+\frac{K_{a_1}K_{a_2}}{[H^+]^2}\right) = \frac{pCO_2}{K'_{H_T}} = \frac{P[CO_2]}{K'_{H_T}}, \quad (A.2)$$

where $K'_{H_T} = K_{H_T}(1+(K_{a_1}/[H^+])+(K_{a_1}K_{a_2}/[H^+]^2))$, $[CO_2]$ is the concentration of soil CO_2 ($\mu L\ L^{-1}$) and P is the pressure of the soil atmosphere (atm).

Per unit area of soil surface, the number of moles of dissolved CO_2 (μmol) is given by

$$nCO_{2\text{dissolved}} = \frac{P[CO_2]}{K'_{H_T}}D\theta, \quad (A.3)$$

where θ is the soil volumetric moisture content (L water L soil^{-1}). The number of moles of CO_2 in the soil atmosphere (μmol)

$$nCO_{2_{\text{soil atmos}}} = \frac{[CO_2]PV_{\text{soil atmos}}}{RT} = \frac{P[CO_2]D(\varphi-\theta)}{RT}, \quad (A.4)$$

where $V_{\text{soil atmos}}$ is the volume of the soil atmosphere (L), and φ is soil porosity (L voids L soil^{-1}).

At temperature T_1, total moles of CO_2 in volume D

$$\begin{aligned} &= \frac{P_1[CO_2]_{T_1}D(\varphi-\theta)}{RT_1}+\frac{P_1[CO_2]_{T_1}}{K'_{H_{T_1}}}D\theta \\ &= P_1[CO_2]_{T_1}D\left(\frac{(\varphi-\theta)}{RT_1}+\frac{\theta}{K'_{H_{T_1}}}\right). \end{aligned} \quad (A.5)$$

Under the closed-system assumption, conservation of mass dictates that between T_1 and T_2,

$$P_2[CO_2]_{T_2}D\left(\frac{(\varphi-\theta)}{RT_2}+\frac{\theta}{K'_{H_{T_2}}}\right) = P_1[CO_2]_{T_1}D\left(\frac{(\varphi-\theta)}{RT_1}+\frac{\theta}{K'_{H_{T_1}}}\right), \quad (A.6)$$

and therefore

$$\frac{P_1[CO_2]_{T_1}}{P_2[CO_2]_{T_2}} = \frac{\left(\frac{(\varphi-\theta)}{RT_2}+\frac{\theta}{K'_{H_{T_2}}}\right)}{\left(\frac{(\varphi-\theta)}{RT_1}+\frac{\theta}{K'_{H_{T_1}}}\right)}. \quad (A.7)$$

Given the exchanges of CO_2 between atmosphere and solution phases are small in relation to the total mass of the soil atmosphere, from the ideal gas law, the ratio of the pressures of the soil atmosphere between T_1 and T_2 is equal to the ratio of the temperatures, and therefore

$$\frac{[CO_2]_{T_1}}{[CO_2]_{T_2}} = \frac{\left(\frac{(\varphi-\theta)}{RT_2}+\frac{\theta}{K'_{H_{T_2}}}\right)}{\left(\frac{(\varphi-\theta)}{RT_1}+\frac{\theta}{K'_{H_{T_1}}}\right)}\times\frac{T_2}{T_1}. \quad (A.8)$$

Appendix B. Calculating the isotopic composition of abiotically produced CO_2 ($\delta^{13}C_{CO_2-abiotic}$)

Using a mass balance approach, the average $\delta^{13}C_{CO_2}$ of the CO_2 produced between cold and warm sampling periods must satisfy the following

$$\begin{aligned} &\int_0^D \delta^{13}C_{CO_2\text{cold}}[CO_2]_{\text{cold}}dz + \overline{\delta^{13}C_{CO_2-\text{produced}}}[CO_2]_{\text{produced}} \\ &\quad = \int_0^D \delta^{13}C_{CO_2\text{warm}}[CO_2]_{\text{warm}}dz, \end{aligned} \quad (B.1)$$

where z is soil depth (m), D is the depth to ice cement (m), $[CO_2]$ is soil CO_2 concentration ($\mu L\ L^{-1}$) and $\overline{\delta^{13}C_{CO_2-\text{produced}}}$ is the concentration-weighted mean $\delta^{13}C_{CO_2}$ of the produced CO_2 (‰).

The term $[CO_2]_{\text{produced}}$ was calculated as

$$\int_0^D [CO_2]_{\text{warm}}dz - \int_0^D [CO_2]_{\text{cold}}dz. \quad (B.2)$$

Assuming there is no biological contribution to the CO_2 produced at Site B,

$$\delta^{13}C_{CO_2-\text{abiotic}} = \delta^{13}C_{CO_2-\text{produced}}. \quad (B.3)$$

If, however, there is a 10% biological contribution to the CO_2 produced at Site B, and assuming that $\delta^{13}C_{CO_2}$ reflects the $\delta^{13}C$ of the organic source material ($\delta^{13}C_{\text{biotic}}$), then $\overline{\delta^{13}C_{CO_2-\text{abiotic}}}$ (the mean $\delta^{13}C_{CO_2}$ (‰) of CO_2 produced due to abiotic processes) can be derived as

$$\overline{\delta^{13}C_{CO_2-\text{abiotic}}} = \frac{\overline{\delta^{13}C_{CO_2-\text{produced}}} - 0.1\left(\delta^{13}C_{\text{biotic}}\right)}{0.9}. \quad (B.4)$$

Values used to calculate $\delta^{13}C_{CO_2-\text{abiotic}}$ are $[CO_2]_{\text{produced}} = 29\ \mu L\ L^{-1}$, $\delta^{13}C_{CO_2-\text{produced}} = -4.1‰$ and $\delta^{13}C_{\text{biotic}} = -28.2‰$. The integrals were approximated from the point data shown in Fig. 5.

Appendix C. Supplementary material

Supplementary material associated with this article can be found, in the online version, at doi:10.1016/j.soilbio.2012.04.027.

References

Adams, B.J., Bardgett, R.D., Ayres, E., Wall, D.H., Aislabie, J., Bamforth, S., Bargagli, R., Cary, C., Cavacini, P., Connell, L., Convey, P., Fell, J.W., Frati, F., Hogg, I.D., Newsham, K.K., O'Donnell, A., Russell, N., Seppelt, R.D., Stevens, M.I., 2006. Diversity and distribution of Victoria Land biota. Soil Biology & Biochemistry 38, 3003–3018.

Ball, B.A., Virginia, R.A., Barrett, J.E., Parsons, A.N., Wall, D.H., 2009. Interactions between physical and biotic factors influence CO_2 flux in Antarctic dry valley soils. Soil Biology & Biochemistry 41, 1510–1517.

Barrett, P.J., Froggatt, P.C., 1978. Densities, porosities, and seismic velocities of some rocks from Victoria Land, Antarctica. N.Z. Journal of Geology and Geophysics 21, 175–187.

Barrett, J.E., Virginia, R.A., Parsons, A.N., Wall, D.H., 2005. Potential soil organic matter turnover in Taylor Valley, Antarctica. Arctic, Antarctic, and Alpine Research 37, 108–117.

Barrett, J.E., Virginia, R.A., Parsons, A.N., Wall, D.H., 2006a. Soil carbon turnover in the McMurdo Dry Valleys, Antarctica. Soil Biology & Biochemistry 38, 3065–3082.

Barrett, J.E., Virginia, R.A., Wall, D.H., Cary, S.C., Adams, B.J., Hacker, A.L., Aislabie, J.M., 2006b. Co-variation in soil biodiversity and biogeochemistry in northern and southern Victoria Land, Antarctica. Antarctic Science 18, 535–548. doi:10.1017/s0954102006000587.

Barrett, J.E., Virginia, R.A., Hopkins, D.W., Aislabie, J., Bargagli, R., Bockheim, J.G., Campbell, I.B., Lyons, W.B., Moorhead, D.L., Nkem, J.N., Sletten, R.S., Steltzer, H., Wall, D.H., Wallenstein, M.D., 2006c. Terrestrial ecosystem processes of Victoria Land, Antarctica. Soil Biology & Biochemistry 38, 3019–3034.

Bockheim, J.G., Prentice, M.L., McLeod, M., 2008. Distribution of glacial deposits, soils, and permafrost in Taylor Valley, Antarctica. Arctic, Antarctic, and Alpine Research 40, 279–286. doi:10.1657/1523-0430(06-057).

Burkins, M.B., Virginia, R.A., Wall, D.H., 2001. Organic carbon cycling in Taylor Valley, Antarctica: quantifying soil reservoirs and soil respiration. Global Change Biology 7, 113–125.

Cary, S.C., McDonald, I.R., Barrett, J.E., Cowan, D.A., 2010. On the rocks: the microbiology of Antarctic Dry Valley soils. Nature Reviews Microbiology 8, 129–138.

Doran, P.T., McKay, C.P., Clow, G.D., Dana, G.L., Fountain, A.G., Nylen, T., Lyons, W.B., 2002. Valley floor climate observations from the McMurdo dry valleys, Antarctica, 1986–2000. Journal of Geophysical Research-Atmospheres 107.

Dörr, H., Münnich, K.O., 1980. Carbon-14 and carbon-13 in soil CO_2. Radiocarbon 22, 909–918.

Elberling, B., Gregorich, E.G., Hopkins, D.W., Sparrow, A.D., Novis, P., Greenfield, L.G., 2006. Distribution and dynamics of soil organic matter in an Antarctic dry valley. Soil Biology & Biochemistry 38, 3095–3106.

Fang, C., Moncrieff, J.B., 2001. The dependence of soil CO_2 efflux on temperature. Soil Biology & Biochemistry 33, 155–165.

Fountain, A.G., Nylen, T.H., Monaghan, A., Basagic, H.J., Bromwich, D., 2010. Snow in the McMurdo Dry Valleys, Antarctica. International Journal of Climatology 30, 633–642. doi:10.1002/joc.1933.

Fry, B., 2006. Stable Isotope Ecology. Springer, New York.

Gregorich, E.G., Hopkins, D.W., Elberling, B., Sparrow, A.D., Novis, P., Greenfield, L.G., Rochette, P., 2006. Emission of CO_2, CH_4 and N_2O from lakeshore soils in an Antarctic dry valley. Soil Biology & Biochemistry 38, 3120–3129.

Hall, B.L., Denton, G.H., 2000. Radiocarbon Chronology of Ross Sea Drift, Eastern Taylor Valley, Antarctica: Evidence for a Grounded Ice Sheet in the Ross Sea at the Last Glacial Maximum. Geografiska Annaler: Series A, Physical Geography 82, 305–336. doi:10.1111/j.0435-3676.2000.00127.x.

Harris, D., Horwath, W.R., van Kessel, C., 2001. Acid fumigation of soils to remove carbonates prior to total organic carbon or carbon-13 isotopic analysis. Soil Science Society of America Journal 65, 1853–1856.

Higgins, S.M., Hendy, C.H., Denton, G.H., 2000. Geochronology of Bonney drift, Taylor Valley, Antarctica: evidence for Interglacial Expansions of Taylor Glacier. Geografiska Annaler: Series A, Physical Geography 82, 391–409. doi:10.1111/j.0435-3676.2000.00130.x.

Hopkins, D.W., Sparrow, A.D., Elberling, B., Gregorich, E.G., Novis, P.M., Greenfield, L.G., Tilston, E.L., 2006. Carbon, nitrogen and temperature controls on microbial activity in soils from an Antarctic dry valley. Soil Biology & Biochemistry 38, 3130–3140.

Hopkins, D.W., Sparrow, A.D., Shillam, L.L., English, L.C., Dennis, P.G., Novis, P., Elberling, B., Gregorich, E.G., Greenfield, L.G., 2008. Enzymatic activities and microbial communities in an Antarctic Dry Valley soil: responses to C and N supplementation. Soil Biology & Biochemistry 40, 2130–2136.

Hopkins, D.W., Sparrow, A.D., Gregorich, E.G., Elberling, B., Novis, P., Fraser, F., Scrimgeour, C., Dennis, P.G., Meier-Augenstein, W., Greenfield, L.G., 2009. Isotopic evidence for the provenance and turnover of organic carbon by soil microorganisms in the Antarctic Dry Valleys. Environmental Microbiology 11, 597–608. doi:10.1111/j.1462-2920.2008.01830.x.

Keeling, C.D., Piper, S.C., Bacastow, R.B., Wahlen, M., Whorf, T.P., Heimann, M., Meijer, H.A., 2001. Exchanges of Atmospheric CO_2 and $^{13}CO_2$ with the Terrestrial Biosphere and Oceans from 1978 to 2000. I. Global aspects, SIO Reference Series, No. 01-06. Scripps Institution of Oceanography, San Diego, 88 pp. http://scrippsco82.ucsd.edu/data/atmospheric_co82.html.

Knohl, A., Werner, R.A., Geilmann, H., Brand, W.A., 2004. Kel-F™ discs improve storage time of canopy air samples in 10-mL vials for CO_2-$\delta^{13}C$ analysis. Rapid Communications in Mass Spectrometry 18, 1663–1665.

Lloyd, J., Taylor, J.A., 1994. On the temperature dependence of soil respiration. Functional Ecology 8, 315–323.

Mook, W.G., Bommerson, J.C., Staverman, W.H., 1974. Carbon isotope fractionation between dissolved bicarbonate and gaseous carbon dioxide. Earth and Planetary Science Letters 22, 169–176. doi:10.1016/0012-821x(74)90078-8.

Mook, W.G. (Ed.), 2000. Environmental isotopes in the hydrological cycle: Principles and applications, vol. 1. UNESCO, Paris, p. 280.

Park, R., Epstein, S., 1960. Carbon isotope fractionation during photosynthesis. Geochimica et Cosmochimica Acta 21, 110–126.

Parsons, A.N., Barrett, J.E., Wall, D.H., Virginia, R.A., 2004. Soil carbon dioxide flux in Antarctic Dry Valley ecosystems. Ecosystems 7, 286–295.

Rochette, P., Bertrand, N., 2003. Soil air sample storage and handling using polypropylene syringes and glass vials. Canadian Journal of Soil Science, 631–637.

Stumm, W., Morgan, J.J., 1996. Aquatic Chemistry: Chemical Equilibria and Rates in Natural Waters, third ed. Wiley Interscience, New York.

Thode, H.G., Shima, M., Rees, C.F., Krishnamurty, K.V., 1965. Carbon-13 isotope effects in systems containing carbon dioxide, bicarbonate, carbonate and metal ions. Canadian Journal of Chemistry 43, 582–595.

Treonis, A.M., Wall, D.H., Virginia, R.A., 2002. Field and microcosm studies of decomposition and soil biota in a cold desert soil. Ecosystems 5, 159–170.

United States Salinity Laboratory Staff, 1954. Diagnosis and Improvement of Saline and Alkali Soils. United States Department of Agriculture, Washington, D.C.

Vogel, J.C., Grootes, P.M., Mook, W.G., 1970. Isotope fractionation between gaseous and dissolved carbon dioxide. Zeitschrift für Physik 230, 225–238.

Soil Biology & Biochemistry xxx (2013) 1–2

Contents lists available at ScienceDirect

Soil Biology & Biochemistry

journal homepage: www.elsevier.com/locate/soilbio

Comments on "Abiotic processes dominate CO_2 fluxes in Antarctic soils" by Shanhun et al. Soil Biology & Biochemistry 53, 99–111 (2012)

We appreciate the new insights into soil CO_2 efflux in an Antarctic Dry Valley provided by Shanhun et al. (2012) in their recent paper. Their observations that abiotic processes may contribute to CO_2 efflux and evidence for a dynamic equilibrium between CO_2 in the gaseous and dissolved phases which is influenced by temperature and moisture content provide a mechanistic explanation for the CO_2 dynamics observed by Parsons et al. (2004) at low temperatures. However, to extrapolate from their observations which were made during the warmest and coldest periods of two days at two sites in one of the Dry Valleys (the Taylor Valley) in Antarctica to all or any soil in Antarctica, as is implied by the title, and to use these data to conclude that abiotic processes dominate CO_2 efflux is unsound.

As Shanhun et al. (2012) state, the Antarctic Dry Valleys represent the largest contiguous, or near contiguous, ice-free region of Antarctica. However, the soils are far from typical of all soils in Antarctica. The Dry Valley soils typically contain only traces of organic matter, have very low water contents and remain frozen for long periods of the year. This is in marked contrast to the ornithogenic soils in coastal regions and the maritime Antarctic, the volcanic soils in Antarctica, the organic rich, peats at some sites on the Antarctic Peninsula and on some islands, or the lithomorphic soils in the mountains. Even within the Dry Valleys region, there is significant diversity in soils (Bockheim et al., 2008) and associated CO_2 fluxes (Elberling et al., 2006) which are overlooked by Shanhun et al. (2012). Put simply, failure to recognise the diversity of soils in Antarctica at different scales limits the relevance of the observations: one model of CO_2 cannot be applied to all Antarctic soils as implied by Shanhun et al. (2012). Their blanket references to "the Dry Valleys environment" mask the considerable pedological, geological, biological, hydrological, and climatic heterogeneity that must be accounted for in a large-scale model of soil CO_2 exchange.

Shanhun et al. (2012) refer to our work in the Dry Valleys region (Elberling et al., 2006; Hopkins et al., 2006a, 2006b, 2008, 2009; Gregorich et al., 2006) and claim that their work challenges our biological interpretations of soil CO_2 fluxes. However, very little of our work is directly relevant to the Taylor Valley and only one paper (Hopkins et al., 2009) contains any data for soils from the Taylor Valley. In fact, much of our work, including more recently published research (Sparrow et al., 2011; Dennis et al., 2013) has focused on biological hotspots, such as near streams and at lake margins, and on the effect of amendment of the soils with organic substrates on soil microbial activity. There is compelling evidence to suggest that the response observed in subsidy experiments is biological in origin. The response to added substrate applied in the field occurred relatively rapidly and with a wide range of substrates. As well, short-term incubation respiration rates measured under controlled laboratory conditions (Hopkins et al., 2006a, 2006b; Sparrow et al., 2011) are not influenced by these abiotic factors. Hence before revising our view that CO_2 efflux from Dry Valley soils is predominantly biological, a mechanism is needed to explain the increased CO_2 efflux in subsidy experiments according to the process suggested by Shanhun et al. (2012).

Shanhun et al. (2012) developed a model of abiotic CO_2 dynamics based on steady-state conditions at contrasting temperatures. However, under field conditions the processes of CO_2 dissolution and degassing are kinetically limited and this limitation increases at colder temperatures. Their measurements on warm and cold days were conducted over a period of less than 2 h, but it is well-established from pH measurements and groundwater monitoring studies that it often takes up to 24 h for equilibrium between atmospheric and soil CO_2 to be reached (Elberling and Jakobsen, 2000).

The effluxes measured by Elberling et al. (2006) ranged from 0.02 to 0.05 μmol CO_2–C m^{-2} s^{-1} for six landscape elements which cover the majority of the land area in a Dry Valley (the Garwood Valley), but rising as high as 0.80 μmol CO_2–C m^{-2} s^{-1} at biological hotspots. Shanhun et al.'s (2012) largest net efflux (0.048 μmol CO_2–C m^{-2} s^{-1}) is in the same range. If, as Shanhun et al. (2012) suggest, most of the CO_2 efflux is driven by abiotic process, it is difficult to explain the measurements made by Elberling et al. (2006) which showed a strong trend in soil CO_2 efflux across the landscape and correlated with soil organic carbon contents. Furthermore, the $\delta^{13}C$ values for CO_2 collected from dry valleys soils incubated under stable temperature and moisture conditions correspond closely to the $\delta^{13}C$ values for potential organic substrates for soil microorganisms, such as algal and cyanobacteria detritus and dead lichen and moss biomass (Hopkins et al., 2009), strongly supporting a biological mechanism for CO_2 production.

We do not dispute that there could be an abiotic contribution to CO_2 efflux under some conditions (this was reported in 2004 by Parsons et al.) and agree that determining these conditions and the magnitude of their impact over a variety of landscape elements is worthwhile. However, the evidence in Shanhun et al. (2012) is not strong enough to dismiss biological processes dominating CO_2 efflux. More importantly, they are not strong enough to undermine one of the main conclusions of our work, which is that contemporary sources of organic carbon are sufficient to sustain current soil biological activity (Elberling et al., 2006; Hopkins et al., 2009).

DOI of original article: http://dx.doi.org/10.1016/j.soilbio.2013.10.039.

0038-0717/$ – see front matter
http://dx.doi.org/10.1016/j.soilbio.2013.10.046

In summary, therefore, we urge caution in extrapolating from two sites in one of the Dry Valleys to all soils in Antarctica. The evidence of Shanhun et al. (2012) is not strong enough to support their conclusion that "biological respiration makes only a minor contribution to soil CO_2 fluxes in the Dry Valleys environment" based on measurements of "soil CO_2 dynamics at two sites studied in the Taylor Valley".

References

Bockheim, J.G., Prentice, M.L., McLeod, M., 2008. Distribution of glacial deposits, soils, and permafrost in Taylor Valley, Antarctica. Arctic Antarct. Alp. Res. 40, 279–286.

Dennis, P.G., Sparrow, A.D., Gregorich, E.G., Novis, P.M., Elberling, B., Greenfield, L.G., Hopkins, D.W., 2013. Microbial responses to carbon and nitrogen supplementation in an Antarctic Dry Valley soil. Antarct. Sci. 25, 55–61.

Elberling, B., Jakobsen, B.H., 2000. Soil solution pH measurements using in-line chambers with tension lysimeters. Can. J. Soil Sci. 80, 283–288.

Elberling, B., Gregorich, E.G., Hopkins, D.W., Sparrow, A.D., Novis, P., Greenfield, L.G., 2006. Distribution and dynamics of soil organic matter in an Antarctic Dry Valley. Soil Biol. Biochem. 38, 3095–3106.

Gregorich, E.G., Hopkins, D.W., Elberling, B., Novis, P., Greenfield, L.G., Sparrow, A.D., Rochette, P., 2006. Biogenic gas emission along a lake shore in an Antarctic Dry Valley. Soil Biol. Biochem. 38, 3120–3129.

Hopkins, D.W., Sparrow, A.D., Elberling, B., Gregorich, E.G., Novis, P., Greenfield, L.G., Tilston, E.L., 2006a. Carbon, nitrogen and temperature controls on microbial activity in soils from an Antarctic Dry Valley. Soil Biol. Biochem. 38, 3130–3140.

Hopkins, D.W., Sparrow, A.D., Novis, P.M., Gregorich, E.G., Elberling, B., Greenfield, L.G., 2006b. Controls on the distribution of productivity and organic resources in Antarctic Dry Valley soils. Proc. R. Soc. London B Biol. Sci. 273, 2687–2695.

Hopkins, D.W., Sparrow, A.D., Shillam, L.L., English, L.C., Dennis, P.G., Novis, P.M., Elberling, B., Gregorich, E.G., Greenfield, L.G., 2008. Enzymatic activities in Antarctic Dry Valley soil: responses to C and N supplementation. Soil Biol. Biochem. 40, 2130–2136.

Hopkins, D.W., Sparrow, A.D., Gregorich, E.G., Elberling, B., Novis, P., Fraser, F., Scrimgeour, C., Dennis, P.G., Meier-Augenstein, W., Greenfield, L.G., 2009. Isotopic evidence for the provenance and turnover of organic carbon by soil microorganisms in the Antarctic Dry Valleys. Environ. Microbiol. 11, 597–608.

Parsons, A.N., Barrett, J.E., Wall, D.H., Virginia, R.A., 2004. Soil carbon dioxide flux in Antarctic Dry Valley ecosystems. Ecosystems 7, 286–295.

Shanhun, F.L., Almond, P.C., Clough, T.J., Smith, M.S., 2012. Abiotic processes dominate CO_2 fluxes in Antarctic soils. Soil Biol. Biochem. 53, 99–111. http://dx.doi.org/10.1016/j.soilbio.2012.04.027.

Sparrow, A.D., Gregorich, E.G., Hopkins, D.W., Novis, P., Elberling, B., Greenfield, L.G., 2011. Resource limitations on the activity of a soil microbial community in the dry valleys of southern Victoria Land, Antarctica. Soil Sci. Soc. Am. J. 75, 2188–2197.

B. Elberling
University of Copenhagen, Denmark

L.G. Greenfield
University of Canterbury, Christchurch, New Zealand

E.G. Gregorich*
Agriculture & Agri-Food Canada, Ottawa, Canada

D.W. Hopkins
Heriot-Watt University, Edinburgh, UK

P. Novis
Landcare Research, Lincoln, New Zealand

A.D. Sparrow
CSIRO, Alice Springs, Australia

* Corresponding author.
E-mail address: Ed.Gregorich@agr.gc.ca (E.G. Gregorich).

8 July 2013
Available online xxx

Soil Biology & Biochemistry xxx (2013) 1–2

Contents lists available at ScienceDirect

Soil Biology & Biochemistry

journal homepage: www.elsevier.com/locate/soilbio

Letter to the Editor

Reply to Elberling et al.'s (2013) comments on "Abiotic processes dominate CO_2 fluxes in Antarctic soils" (Soil Biol. Biochem. 53, 99–111)

We are pleased that Elberling et al. (2013) recognise that our mechanistic model of abiotic CO_2 dynamics represents a new insight into understanding CO_2 fluxes in Antarctic dry valley soils. However, Elberling et al. (2013) disagree with our findings on two fronts: first, they argue that the soils we studied are not representative of all Antarctic soils, and second, they question whether or not the mechanism we have invoked is significant.

With regard to the first point, we acknowledge that our title, used for the sake of brevity, could be misconstrued by those unfamiliar with the Antarctic ice-free areas. We studied two soils on glacial drifts of different age in Taylor Valley, close to and distant from contemporary organic carbon sources. We freely acknowledge that these soils are not representative of ornithogenic soils, or soils formed in peat, or where there are vascular plants on the Antarctic Peninsula. The soils we studied are typical of the Typic Haploturbels, and soil maps of the Taylor (Bockheim et al., 2008) and Wright Valleys (McLeod et al., 2009), along with other areas within the McMurdo Dry Valleys region (Bockheim and McLeod, 2008), show that Typic Haploturbels are a significant component of the soil landscape. Elberling et al. (2013) emphasise biological hotspots as representing the important characteristics of soil CO_2 fluxes in Antarctica. By contrast, our emphasis is placed on understanding soil CO_2 fluxes over the most extensive terrestrial ecosystems in continental Antarctica. However, one of our sites, within 50 m of a lake, certainly satisfies "hotspot" criteria. As such, we maintain that the results of Shanhun et al. (2012) are relevant to a broader understanding of CO_2 dynamics in Antarctic terrestrial ecosystems, despite being located within part of one of the McMurdo Dry Valleys.

The significance of the abiotic CO_2 exsolution–dissolution mechanism we invoked to explain CO_2 dynamics is then downplayed by Elberling et al. (2013) on account of an inferred kinetic limitation to the process. An example of this limitation was cited from evidence of lags in pH changes in soil solution as a result of temperature changes (Elberling and Jakobsen, 2000). The soils we studied had <8% moisture, which, owing to their gravelly and sandy nature, would correspond to a matric potential of at most −1000 kPa and probably less than −1500 kPa. In this circumstance, water is held in very fine pores, or, given their likely absence, as thin films on clasts. These very high surface area to volume ratio water films would not suffer the same kinetic limitation as approximately 1 L of soil solution in a 2 L vessel with no soil matrix, as was the experimental setup of Elberling and Jakobsen (2000).

Additional support for an abiotic mechanism of CO_2 fluxes is demonstrated via negative CO_2 flux rates. The work of Parsons et al. (2004) and Ball et al. (2009) has shown negative CO_2 fluxes in soils of Taylor Valley, and our work confirms that these are driven by diel variation in subsoil CO_2 concentration gradients. These fluxes have no biological explanation, and they have a similar magnitude to the positive fluxes often attributed to heterotrophic respiration. If these negative abiotic fluxes are not converted to positive fluxes on a diel cycle, then the soil must be storing carbon in an inorganic form. To totally dismiss an abiotic efflux would require that the soil stores about 220 μmol $CaCO_3/m^2$/day according to our data. Assuming this diel variation happens over 60 days per year (the number of days during which soil temperatures oscillate above 0 °C, hence liquid water is present), and that the process has been going on for about 20,000 years (the age of the Ross Sea drift), then the soil should be about 5% $CaCO_3$ by mass. Our analyses show it is 0.4% at the most.

Furthermore, recent work by Ma et al. (2013) clearly demonstrates through a field, laboratory and modelling study that the same abiotic mechanism of CO_2 fluxes that we invoke for Dry Valley soils contributes significantly to the total soil CO_2 flux for saline/alkaline soils in an arid temperate environment. In addition, Ma et al.'s (2013) data show that the abiotically-driven soil CO_2 flux is even more dominant when soils are dry, and that the effect is enhanced with both increasing pH and electrical conductivity. This suggests that our results are applicable to an even larger proportion of Dry Valley soils than previously considered, with soils classified as Typic Anhyorthels and Typic Anhyturbels also likely to exhibit this effect. Together with the broad applicability of this mechanism to Typic Haploturbels (and Typic Haplorthels), and individual site characteristics notwithstanding, this extends the area over which abiotic CO_2 fluxes are likely to make a significant contribution to the total soil CO_2 flux to ~93% of soils in the McMurdo Dry Valleys (Bockheim and McLeod, 2008).

Finally, Elberling et al. (2013) "do not dispute that there could be an abiotic contribution to CO_2 efflux under some conditions". Consequently, Elberling et al.'s (2013) apprehension that our findings would "undermine one of the main conclusions of our [their] work" is puzzling. Their conclusion "that contemporary sources of organic carbon are sufficient to sustain current soil biological activity" is not challenged by our results. By identifying an important abiotic contribution to soil CO_2 fluxes, net heterotrophic respiration rates would be lower than those previously inferred, hence shifting the balance further towards a self-sustaining carbon economy.

In summary, Shanhun et al. (2012) present a novel, mechanistically-based approach to understanding CO_2 dynamics in soils typical of large parts of the McMurdo Dry Valleys. We

DOI of original article: http://dx.doi.org/10.1016/j.soilbio.2012.04.027.

0038-0717/$ – see front matter
http://dx.doi.org/10.1016/j.soilbio.2013.10.039

Please cite this article in press as: Shanhun, F.L., et al., Reply to Elberling et al.'s (2013) comments on "Abiotic processes dominate CO_2 fluxes in Antarctic soils" (Soil Biol. Biochem. 53, 99–111), Soil Biology & Biochemistry (2013), http://dx.doi.org/10.1016/j.soilbio.2013.10.039

maintain that our findings place an important caveat on interpretation of Dry Valley soil CO_2 fluxes – they cannot be assumed to be solely biologically driven.

References

Ball, B.A., Virginia, R.A., Barrett, J.E., Parsons, A.N., Wall, D.H., 2009. Interactions between physical and biotic factors influence CO_2 flux in Antarctic dry valley soils. Soil Biol. Biochem. 41, 1510–1517.

Bockheim, J.G., McLeod, M., 2008. Soil distribution in the McMurdo Dry Valleys, Antarctica. Geoderma 144, 43–49. http://dx.doi.org/10.1016/j.geoderma.2007.10.015.

Bockheim, J.G., Prentice, M.L., McLeod, M., 2008. Distribution of glacial deposits, soils, and permafrost in Taylor Valley, Antarctica. Arct. Antarct. Alpine Res. 40, 279–286. http://dx.doi.org/10.1657/1523-0430(06-057).

Elberling, B., Jakobsen, B.H., 2000. Soil solution pH measurements using in-line chambers with tension lysimeters. Can. J. Soil Sci. 80, 283–288.

Elberling, B., Greenfield, L.G., Gregorich, E.G., Hopkins, D.W., Novis, P., Sparrow, A.D., 2013. Comments on "Abiotic processes dominate CO_2 flux in Antarctic soils" by Shanhun et al. Soil Biology & Biochemistry 53, 99–111 (2012). Soil Biol. Biochem. (Submitted for publication).

Ma, J., Wang, Z.Y., Stevenson, B.A., Zheng, X.J., Li, Y., 2013. An inorganic CO_2 diffusion and dissolution process explains negative CO_2 fluxes in saline/alkaline soils. Sci. Rep. 3, 2025. http://dx.doi.org/10.1038/srep02025.

McLeod, M., Bockheim, J., Balks, M., Aislabie, J., 2009. Soils of western Wright Valley, Antarctica. Antarct. Sci. 21, 355–365. http://dx.doi.org/10.1017/S0954102009001965.

Parsons, A.N., Barrett, J.E., Wall, D.H., Virginia, R.A., 2004. Soil carbon dioxide flux in Antarctic Dry Valley ecosystems. Ecosystems 7, 286–295.

Shanhun, F.L., Almond, P.C., Clough, T.J., Smith, C.M.S., 2012. Abiotic processes dominate CO_2 fluxes in Antarctic soils. Soil Biol. Biochem. 53, 99–111. http://dx.doi.org/10.1016/j.soilbio.2012.04.027.

Fiona L. Shanhun*, Peter C. Almond, Tim J. Clough
Department of Soil and Physical Sciences, PO Box 85084, Lincoln University, Lincoln 7647, New Zealand

* Corresponding author. Tel.: +64 21 408 909; fax: +64 3 325 3607.
E-mail addresses: fiona.shanhun@lincoln.ac.nz (F.L. Shanhun), peter.almond@lincoln.ac.nz (P.C. Almond), timothy.clough@lincoln.ac.nz (T.J. Clough).

18 October 2013
Available online xxx